

Synthesis and Application of Triazole Containing Peptidomimetics

Dissertation

Submitted to the Department of Chemistry, Bielefeld University

In partial fulfillment of the requirements for the degree of
Doctor rerum naturalium (Dr. rer. nat.)

by

Oliver Kracker, M.Sc.

Bielefeld, May 2018

Synthesis and Application of Triazole Containing Peptidomimetics

Dissertation

Submitted to the Department of Chemistry, Bielefeld University
In partial fulfillment of the requirements for the degree of
Doctor rerum naturalium (Dr. rer. nat.)

by

Oliver Kracker, M.Sc.

Bielefeld, May 2018

1st Referee:

Prof. Dr. Norbert Sewald

Organic and Bioorganic Chemistry

University of Bielefeld, Germany

2nd Referee:

Prof. Dr. Harald Gröger

Organic Chemistry I

University of Bielefeld, Germany

Gedruckt auf alterungsbeständigem Papier – ISO 9706

Acknowledgements

First of all, I would like to express my gratitude to Prof. Dr. Norbert Sewald for the opportunity to work in his laboratories at such an interesting topic, which involved a broad and diverse spectrum of organic chemistry, for the trust and encouragement, as well as for the numerous discussions we had over the years. I am further very grateful to Prof. Dr. Harald Gröger for conducting the second opinion of this dissertation.

In respect to fruitful collaborations, I would like to thank the groups of Prof. Dr. Rafał Latajka, Prof. Dr. Iris Antes and Prof. Dr. Sandrine Onger, especially Dr. Jerzy Góra, Dr. Joanna Krzciuk-Gula, Dr. Antoine Marion, Dr. Julia Kaffy and Dr. Nicolo Tonali, for all the valuable discussions and successful experiments.

I would like to thank all the current and former members of the OC3 for providing such a friendly and collegial environment for excellent research and friendly activities, which I enjoyed a lot during the last years. Anke Nieß for her laboratory assistance in peptide synthesis and Marco Wißbrock for solving all kinds of technical issues and providing me with numerous mass spectra during the late stage of this dissertation. Dr. Sandip Jadhav for some of his secrets in compound crystallization, Isabell Kemker for performing the cell adhesion and ELISA assays in the project of RGD peptidomimetics, David Schröder for molecular modelling simulations and Matthias Wünsch for numerous discussions about the topics of peptidomimetics and propargylamines and proof-reading of some parts of this thesis. I thank all my bachelor, internship students and apprentices for their engagement in the laboratory, good teamwork and reliable results.

I would also like to thank the analytic department, Dr. Andreas Mix and Peter Mester for their support with the 600 MHz NMR device, Dr. Hans-Georg Stammer and Beate Neumann for the X-ray crystal structure analysis and Dr. Jens Sproß and the mass department for their support at the LC- and TLC-MS device.

Last but not least, I thank my parents and family, who always believed in me and supported me during the last four years and beyond, more than I could have asked and wished for.

Abbreviations

A β	Amyloid beta
CAN	Acetonitrile
Aib	Aminoisobutyric acid
AMBER	Assisted Model Building with Energy Refinement
Boc	<i>tert</i> -Butoxycarbonyl
Bzl	Benzyl
Cbz	Carboxybenzyl
chGly	Cyclohexylglycine
COMU	1-Cyano-2-ethoxy-2-oxoethylidenaminoxy)dimethylamino-morpholino-carbenium-hexafluorophosphat
CuAAC	Copper catalyzed azide alkyne cycloaddition
DBU	1,8-Diazabicyclo[5.4.0]undec-7-ene
DCC	<i>N,N'</i> -dicyclohexylcarbodiimide
DCM	Dichlormethane
DIBALH	Diisobutylaluminium hydride
DIC	<i>N,N'</i> -diisopropylcarbodiimide
DIPEA	<i>N,N</i> -diisopropylethylamine
DMF	dimethylformamide
DOP	Dimethyl 2-oxopropylphosphonate
EDC	<i>N</i> -Ethyl- <i>N'</i> -(3-dimethylaminopropyl)carbodiimide
ELISA	Enzyme-linked Immunosorbent Assay
Fmoc	Fluorenylmethoxycarbonyl
HOAt	1-Hydroxy-7-azabenzotriazole
HPLC	High performance liquid chromatography
NMR	Nuclear Magnetic Resonance
Oxyma	Ethyl cyano(hydroxyimino)acetate
<i>p</i> -ABSA	4-Acetamidobenzenesulfonyl azide
PG	Protecting Group
pK _a	Acid dissociation constant
Pmc	2,2,5,7,8-pentamethylchromane-6-sulfonyl
PyBOP	(Benzotriazol-1-yloxy)tripyrrolidinophosphonium hexafluorophosphate
ROESY	Rotating frame nuclear Overhauser effect spectroscopy
rt	room temperature
RuAAC	Ruthenium catalyzed Azide Alkyne Cycloaddition
SPPS	Solid Phase Peptide Synthesis
T3P	1-Propanephosphonic anhydride
TBAF	Tetrabutylammonium fluoride
TEA	Triethylamine
Tf	Trifluoromethanesulfonyl
TFA	Trifluoroacetic acid
THF	Tetrahydrofurane
ThT	Thioflavin T
TMS	Trimethylsilyl
Trt	Triphenylmethyl
Tz	Triazole

Table of contents

1. Abstract	- 1 -
2. Introduction	- 3 -
2.1. Amino acids, peptides and proteins.....	- 3 -
2.2. Peptide Synthesis	- 8 -
2.3. Peptidomimetics	- 16 -
2.4. Triazoles as amide bond isosters.....	- 18 -
2.5. Chiral propargylamines and α -azido acids	- 23 -
2.6. Foldamers.....	- 26 -
2.7. Amyloid- β related diseases	- 29 -
2.8. Monitoring of the A β aggregation and fibrillization process	- 30 -
2.9. Integrins and RGD-peptides	- 32 -
3. Research Objective	- 35 -
4. Results and Discussion	- 37 -
4.1. Synthesis of 1,5-disubstituted triazole containing peptidotriazolamers	- 37 -
4.2. Synthesis of 1,4-disubstituted triazole containing peptidotriazolamers	- 46 -
4.3. Conformational analysis.....	- 49 -
4.4. Synthesis of propargylamines with functional side chains	- 54 -
4.5. KLVFF aggregation inhibitors.....	- 61 -
4.6. Cyclic RGD peptidomimetics	- 76 -
5. Summary	- 81 -
6. Outlook	- 87 -
7. Experimental section	- 89 -
7.1. General Procedures.....	- 96 -
7.2. Synthesis results.....	- 99 -
7.3. X-ray crystal structure analysis.....	- 155 -
Boc-Val[5Tz]Ala-OBzl (9c).....	- 155 -
Boc-D-Leu[5Tz]Val-OBzl (9d).....	- 157 -
Boc-D-Val[5Tz]Ala-OBzl (9f)	- 161 -
Boc-Ala[5Tz]Ala-OBzl (9g).....	- 163 -
Boc-chGly[5Tz]Phe-OBzl (9h)	- 165 -
Boc-Val[5Tz]Ala-Leu[5Tz]Val-OBzl (10)	- 167 -
8. References	- 171 -

1. Abstract

In the course of this dissertation, three major topics were elaborated. Initially, the focus was placed on the synthesis and conformational analysis of 1,5-disubstituted 1*H*-1,2,3-triazole containing peptidomimetics, in which the triazole units replace every second amide bond. Such oligomers were addressed as peptidotriazolamers and might comprise of a homochiral or heterochiral alignment of residues. This topic involved the synthesis of enantiomerically pure propargylamines and α -azido acids, the ruthenium catalysed alkyne azide cycloaddition (RuAAC) and the peptide coupling of triazoles which are conversantly prone to epimerization. The conformational analysis was done utilizing X-ray crystal structure analysis and molecular modelling, taking ROESY-NMR constraints into account. The homochiral oligomer Boc-Ala[5Tz]Phe-Val[5Tz]Ala-Leu[5Tz]Val-OBzl turned out to closely resemble a β Via1 turn, while the sequence related heterochiral peptidotriazolamer Boc-D-Ala[5Tz]Phe-D-Val[5Tz]Ala-D-Leu[5Tz]Val-OBzl adopts a polyproline-like helical structure.

The second topic covered the synthesis and biological evaluation of Amyloid- β aggregation inhibitors, based on the peptide sequence KLVFF. This work included the Bestmann-Ohira reaction of trityl protected amino aldehydes and the application of deprotected triazoles, as dipeptide isosters, on solid phase peptide synthesis. The synthesized peptidomimetics were evaluated as inhibitors of Amyloid- β fibrillization by a Thioflavin-T assay. As a result, the triazole does not serve as a generic substitute for an amide bond in complex biological interactions and replacement positions ought to be carefully selected. However, the SEN304-based peptidotriazolamer H-D-[chGly[4Tz]chGly-chGly[4Tz]Tyr-(NMe)Leu]-NH₂ lead to complete inhibition of Amyloid- β oligomerization.

Lastly, the synthesis of cyclic peptidomimetics, containing one or two 1,5-disubstituted triazoles, based on cilengitide (cyclo-[RGDf(NMe)V]) was studied. Thus, the *N*-methylated peptide bond was replaced by a 1,5-disubstituted triazole. This included the synthesis of a versatile, functionalizable peptidomimetic, in which the non-essential valine was exchanged with an azidobutyl residue for a possible prodrug application. The peptidomimetic was shown to exhibit a nanomolar antagonistic activity towards the $\alpha_v\beta_3$ receptor.

Keywords: Peptidomimetics, Foldamers, Triazoles, Amyloid- β , RGD peptides.

2. Introduction

2.1. Amino acids, peptides and proteins

Proteins and peptides are constructed by the organism from amino acids as building blocks. While there are more than ~500 different amino acids conversant, only 20 of them are encoded as triplet nucleotides (codons) in the genetic code of a cell (**Figure 1**).¹ Although few bacteria incorporate D-amino acids in their cell wall, most of the amino acids exclusively occur in their L-configuration.

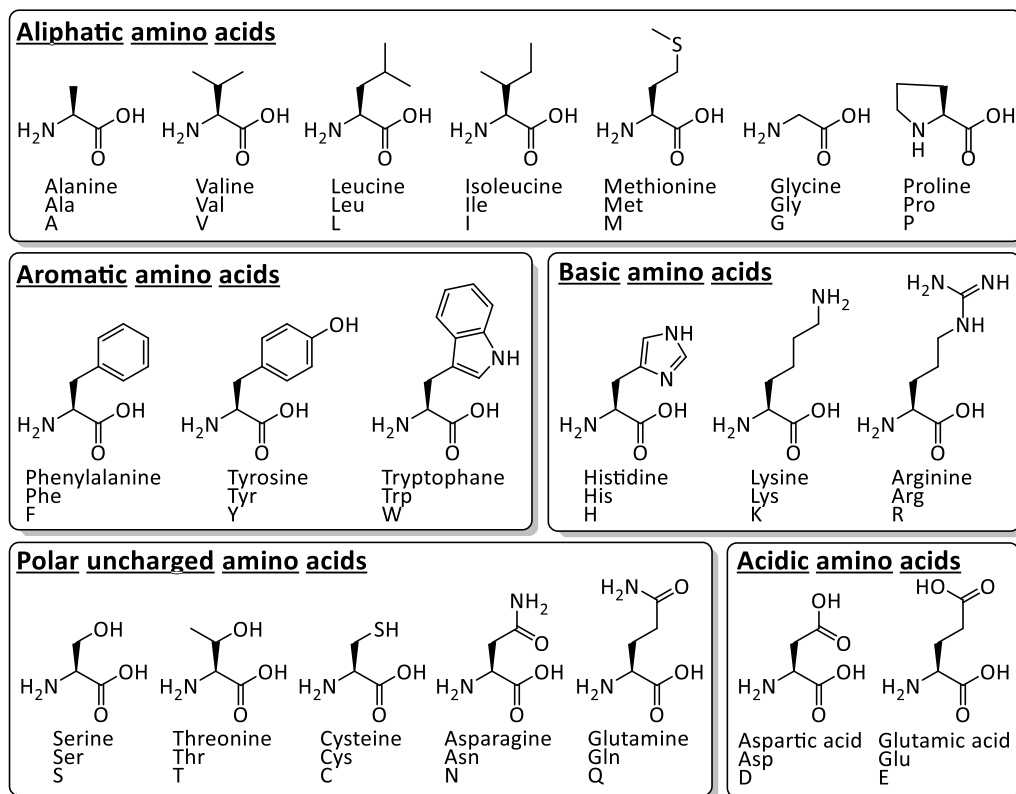


Figure 1. The 20 genetically encoded amino acids (full name, three and one letter code), grouped by their side chain functionality.

For the human body, nine of these amino acids (H, I, L, K, M, F, T, W and V) are referred to as essential amino acids, implying that they cannot be produced by its own and must be delivered via nutrition.² While some single amino acids display crucial functions in the human body in isolated form (e. g. glutamic acid and γ -aminobutyric acid (GABA) which work as neurotransmitters, therefore influencing the function of neurons by modulating trans-membrane ion flux)³, they are mainly used as structural units for the linear build-up of proteins and peptides. The biological process of protein synthesis is called translation

2. Introduction

and is a part of gene expression. The proteins are therefore gene products, which are encoded by different triplet codons on the DNA. The translation follows transcription of the DNA into single stranded m-RNA and is performed by the ribosomes in the cytoplasm of the cell. The ribosome consists of two subunits, a smaller subunit, which reads out the information on the m-RNA and a larger ribosomal subunit, which connects the related amino acids by condensation into a growing polypeptide chain.⁴

While a protein comprises only of a single-stranded, non-branched polypeptide chain, it folds, in a reproducible manner, into a distinct biologically active three-dimensional arrangement. This is predetermined by the linear sequence of the amino acid side-chains (Anfinsen's dogma),⁵ which can undergo a myriad of intramolecular correlations (*H*-bonds, hydrophobic and hydrophylic interactions, salt-bridges, disulphide bonds etc.) ultimately leading to a thermodynamic and entropic favoured global minimum. Although this process is considered a physical process, it is often aided by so called chaperons, a class of proteins which aid in the correct folding of proteins, or more precise, prevent the aggregation of several proteins during the folding stage.⁶

The structural evolvment of a protein during its translation and folding is divided and defined by four structures, the primary, secondary, tertiary and quaternary structure.⁷ The growing peptide chain is already folding during the translation process at the ribosome. The linear random coil peptide chain is considered as the primary structure but contains the information of the native protein structure in the sequence of its amino acid residues. The development of a periodic secondary structure is the first step during the folding process, its driving force is the formation of *H*-bonds, between the amide proton and the carbonyl oxygen, along the backbone of the peptide. Two common examples of secondary structure motifs are the α -helix and β -sheet, first correctly proposed by Pauling *et al.* in 1951, considering the idea of a planar amide bond (**Figure 2**).^{8, 9}

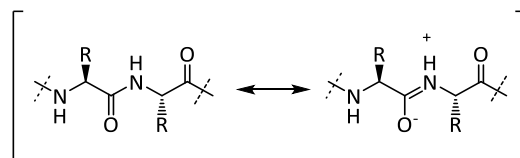


Figure 2. The resonance structure of an amide bond explains the planarity of a peptide bond. Thus, the atoms C α -CO-NH-C α' are located on the same plain. The oscillation between its constitutional isomers, where the amide proton migrates to the carbonyl oxygen is described by amide / imidic acid tautomerism.

The α -helix represents the most common secondary structure motif in peptides and proteins, it is a right-handed helix, often termed as 3.6₁₃-helix, which signifies the average number of amino acid side chains per helix turn, involving 13 atoms in the ring formed by the hydrogen bond (**Figure 3**).⁷

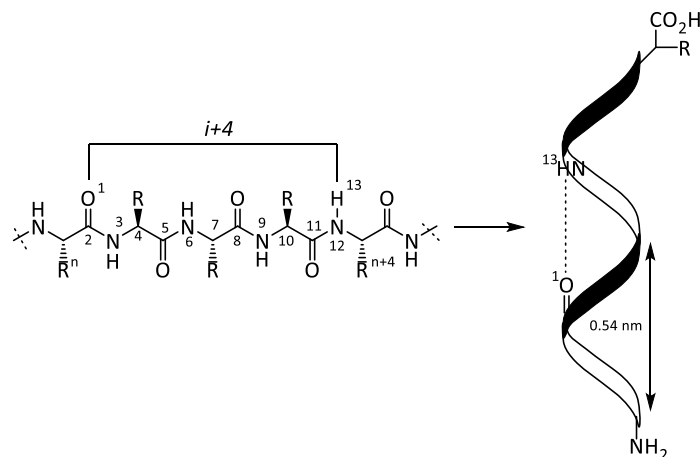


Figure 3. Schematic depiction of an α -helix. Every carbonyl oxygen of an amino acid, forms a hydrogen bond with the amide proton four amino acids further in direction of the C-terminus, forming a loop consisting of 13 atoms. This leads to the formation of a right-handed helix, where the hydrogen bonds are parallel to the helix axis. The carbonyl oxygen atoms orientate towards the C-terminus, the amino acid residues are pointing outside the helix, each repetitive turn is 3.6 amino acids long, which translates into a distance of 0.54 nm between loops.

The β -sheet on the other hand consists of so called β -strands, these are peptide chains in linear extended “zig-zag” conformation, which are aligned laterally and connected by backbone hydrogen bonds, forming a pleated peptide sheet (**Figure 4**).⁹

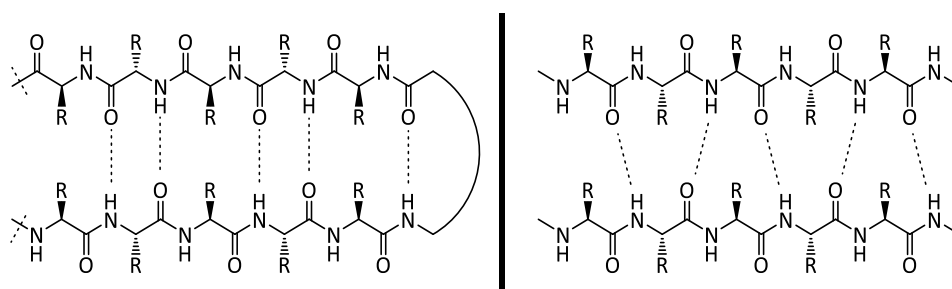


Figure 4. Two extended peptide chains form a β -sheet by connecting the parallel strands by hydrogen bonds. This is possible in antiparallel fashion (left) or parallel fashion (right), intra and intermolecularly, resulting in planar or nonplanar inter-strand hydrogen bonds, where the antiparallel alignment is the more stable form.

2. Introduction

These sheets may expand into a network of hydrogen bonds, between several antiparallel aligned β -strands, where each turn frequently consists of adjustable and or turn-inducing amino acids (Gly, Pro), which result in a flexible loop (**Figure 5 A**).

Turn motifs usually consist of two to five amide bonds, classified as followed: δ -turn (one bond, sterically unlikely); γ -turn (two bonds); β -turn (three bonds, most common); α -turn (four bonds), π -turn (five bonds) and ω -loop (longer, extended disordered loop), with diverse categories in each type, dependent on their dihedral angles.¹⁰ A β -turn between two interacting, antiparallel β -strands is defined as a β -hairpin, including all different types of turns (**Figure 5 B**).¹¹

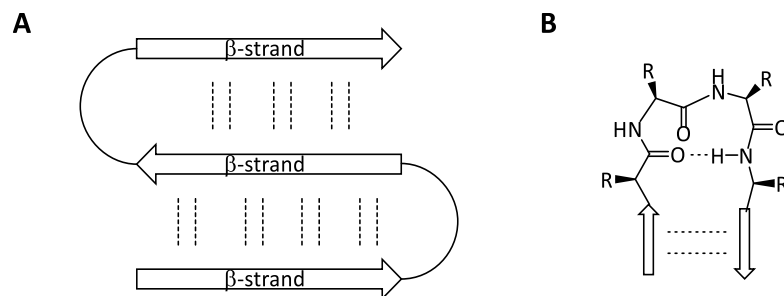


Figure 5. A) Antiparallel β -strands are connected by flexible turns, forming a β -sheet network. B) Example of a β -hairpin: a β -turn (Type II) connects two antiparallel β -strands.

Although β -sheets are common secondary structure elements in proteins and necessary for proper function, they are also related to age dependent amyloidosis diseases such as Alzheimer, resulting of off uncontrolled aggregation of β -sheets leading to insoluble fibrils and plaques, finally damaging tissue and compromising proper organ function.¹²

Despite the planarity of the peptide bond explained by its resonance structure (**Figure 2**), the polypeptide chain is quite flexible, resulting in secondary structure motifs discussed above. The flexibility is enabled by backbone rotations and thereby, a change of the dihedral angles between the amide N and C α , as well as C α and the carbonyl C. The dihedral angles are termed ϕ and ψ (**Figure 6A**)⁷ which describe the angles between two intersecting planes spanned by four different atoms (ϕ : CO-NH-C α -C'O, ψ : NH-C α -CO-N'H). The defined angle ω , which describes the rotation of the amide bond (ω : C α -CO-NH-C' α), is either 0° or 180° due to the planarity discussed above, where $\omega=180^\circ$ corresponds to a *trans* peptide bond and is favoured by 8 kJmol⁻¹ over its *cis* isomer.¹³ The assignment of the dihedral angle can be illustrated by a view alongside the central bond of the four contributing atoms (**Figure 6 B, C**)⁷.

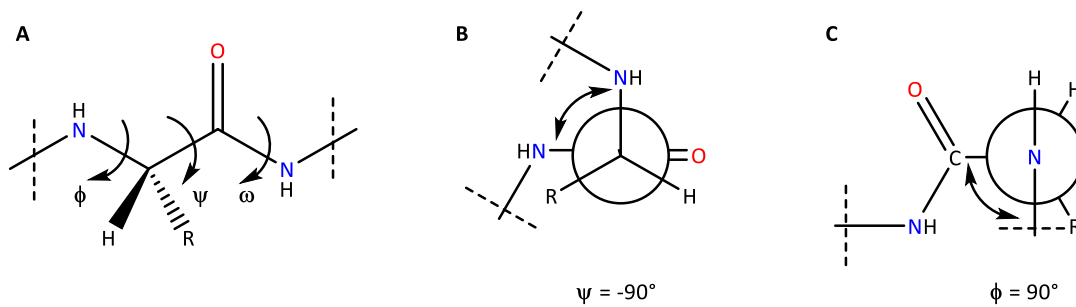


Figure 6. A) Defined dihedral angles of a peptide backbone next to the alpha carbon. B, C) Determination of both dihedral angles by a view alongside the rotating bond.⁷

Although the dihedral angles offer a free rotation along both backbone bonds, due to steric hindrance, depending on the nature of side chain residues, not all angles are equally favoured. Many dihedral angle combinations would lead to the collision of atoms and are therefore, considered as not allowed. As a consequence, the remaining possible angle combinations lead to different secondary structures discussed above.

The combinations of dihedral angles, in relation to the conformation of the peptide, were studied by Ramachandran *et al.*¹⁴ who proposed a convenient notation for this kind of peptide backbone organization principle. They came up with the idea of displaying combinations of all dihedral angles of the peptide or protein by a two-dimensional graph, highlighting possible and or favoured combinations through coloured surfaces, the Ramachandran-plot (Figure 7).⁷

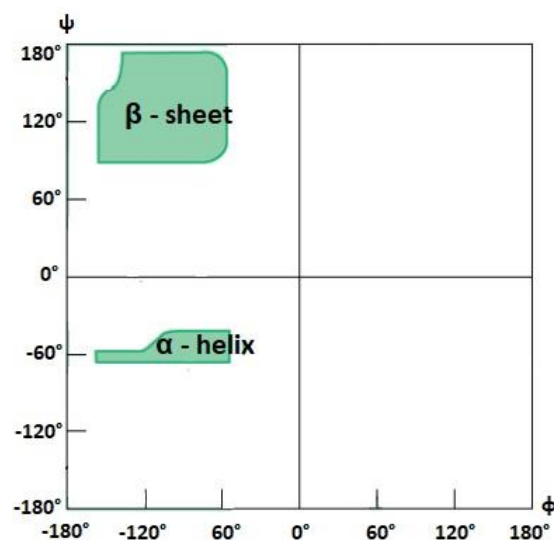


Figure 7. The Ramachandran-diagram displays allowed combinations of ψ (y-axis) and ϕ (x-axis), green surfaces. Angle combinations corresponding to the white surface are unfavoured for the particular peptide due to steric hindrance.⁷ For example around $-135/135$ lies a typical basin for β -sheets and around $-60/-60$ for α -helices.

2. Introduction

With knowledge about the structure of a peptide (e.g. by X-ray structure analysis or molecular modelling) the Ramachandran plot can be used to verify the quality of the crystallographic refinement or homology models, as it would expose disallowed torsion angle combinations or some uncommon wide distribution around secondary structure regions.

The tertiary structure is a characteristic of proteins, necessary for proper function and describes the three-dimensional shape and folding of the protein. For example, a water-soluble protein will have a polar surface around a lipophilic centre.⁷ It describes the alignment of independent secondary structure regions, within a given protein domain. The human β -tryptase for example, a serine protease expressed and released by mastcells, comprises four closely related protein subunits.¹⁵ The arrangement of this tetramer-subunit complex is defined as the quaternary structure, where the single protein domains are defined as a tertiary structure (**Figure 8**).

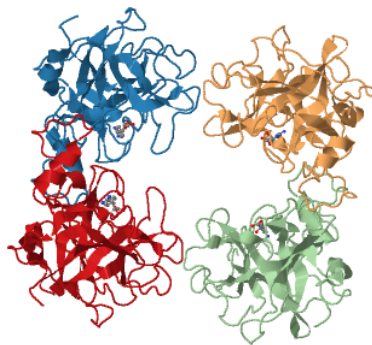
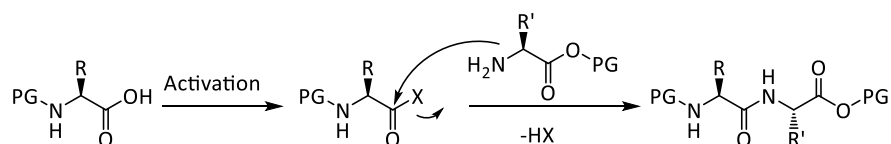


Figure 8. The quaternary structure of the human β -Tryptase is a ringlike tetramer, with active sites facing towards a central pore. It consists of four tertiary structure protein domains (blue, orange, green and red).¹⁵ (PDB 1A0L).

2.2. Peptide Synthesis

The condensation reaction between a carboxylic acid and a free amine is seemingly a simple process, which results in the formation of the peptide bond and one molecule of water. However, at room temperature the starting materials result in a deprotection of the carboxylic acid and formation of a stable salt. Laboratory strategies involve the activation of the carboxylic acid, following a nucleophilic attack of the amine moiety, resulting in elimination of the activation group and formation of the peptide bond (**Scheme 1**).¹³



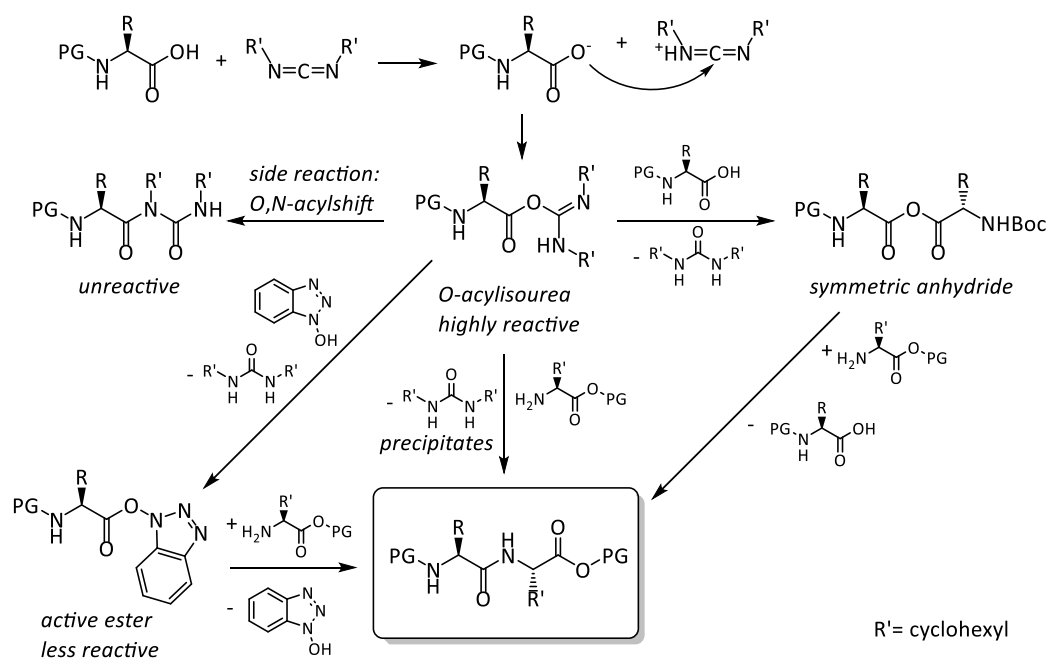
R, R' = aliphatic, aromatic or thoroughly protected

Scheme 1. Formation of a peptide bond, starting by activation of the carboxylic acid, followed by nucleophilic attack of the amine.

Although the peptide bond is one of the most abundant chemical connections in natural and biologically active compounds and despite being an object of high interest of comprehensive studies for decades, the laboratory synthesis is quite tedious. Compared to nature and its ribosomal synthesis (expressing complicated proteins and peptides starting from unprotected amino acids in minutes up to a few hours), the synthesis requires protecting groups for all functional moieties, different coupling reagents for specific couplings and, therefore, results in long reaction times and an unfavourable atom economy.

Beside the old activation methods of carboxylic acids (namely the formation of mixed anhydrides and acid chlorides), a more convenient method was published by Sheehan *et al.*¹⁶ in 1955, using *N,N'*-dicyclohexylcarbodiimide as an activation reagent, which exploits the formation of stable and precipitating dicyclohexylurea as a driving force for the reaction (**Scheme 2**). DCC reacts with carboxylic acids to form a highly reactive *O*-acylisourea, which readily reacts with free amines to form amide bonds. This highly reactive intermediate may also react with another acid molecule to form a symmetric anhydride, which delivers the amide by reaction with the amine. The main undesired side reaction observed is the *O,N*-acylshift, which results in a stable substituted urea derivative which is inaccessible to further peptide coupling.¹³

2. Introduction



Scheme 2. The reaction between a carboxylic acid and a carbodiimide leads to the formation of an *O*-acylisourea as a highly reactive species which reacts with amines to form an amide bond. A possible side reaction (especially during preactivation): the *O*-acylisourea may react with a second acid molecule to form a symmetric anhydride. Another option is the *O*, *N*-acylshift, which leads to the formation of a stable *N*-acylurea. The side reactions can be suppressed with the addition of a hydroxybenzotriazole, which captures the *O*-acylisourea and leads to the formation of a less reactive HOBt active ester.

In 1970, König and Geiger published a modified procedure of carbodiimide mediated peptide couplings, utilizing acidic alcohols (e.g. 1-hydroxybenzotriazoles) as additives.¹⁷ These alcohols act as nucleophiles which trap the reactive *O*-acylisourea and form less reactive active esters, therefore suppressing the side reactions mentioned above, consequently resulting in decreased racemization and improved yields.

Other frequently used carbodiimides are *N,N'*-diisopropylcarbodiimide (DIC), which forms soluble diisopropylurea suitable for solid phase peptide synthesis and 1-ethyl-3-(3-dimethylaminopropyl)carbodiimide (EDC) which forms a water soluble urea, removed by an acidic aqueous wash of the organic phase (**Figure 9**).

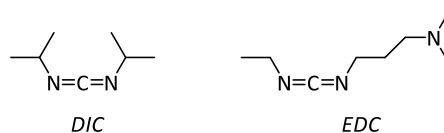


Figure 9. Commonly used carbodiimides.

In 1993, Carpino introduced 1-hydroxy-7-azabenzotriazol (HOAt) as a more efficient additive than the widely used HOBT at this time.¹⁸ HOAt has been shown to decrease reaction times and racemization compared to other additives, this has been explained with a neighbouring group effect of the aromatic nitrogen, which pre-organizes the amine for the subsequent nucleophilic attack (**Figure 10**). Another reason for the increased activity is the slightly decreased pK_a value (3.28 for HOAt compared to 4.60 of HOBT)¹⁹ which results in a more stable alcoholate anion and therefore a better leaving group.

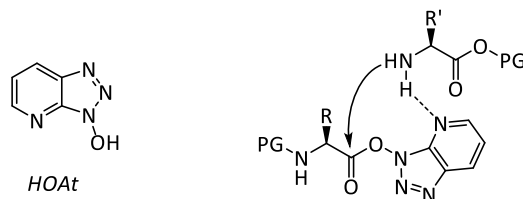


Figure 10. The *H*-bond between the aromatic nitrogen atom and a proton of the free amine pre-organizes the amine for the subsequent nucleophilic attack, by close spatial orientation. Additionally, the *H*-bond leads to increased nucleophilicity of the amine.

For a more practical usage, especially for automatized applications, stand-alone coupling reagents have been developed (**Figure 11**), the most successful based on uronium-/guanidinium salts and phosphonium salts, containing different additives introduced above and a non-nucleophilic anion as a counterion.²⁰

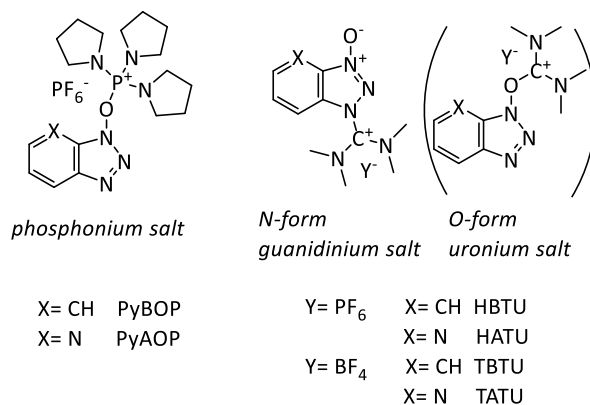
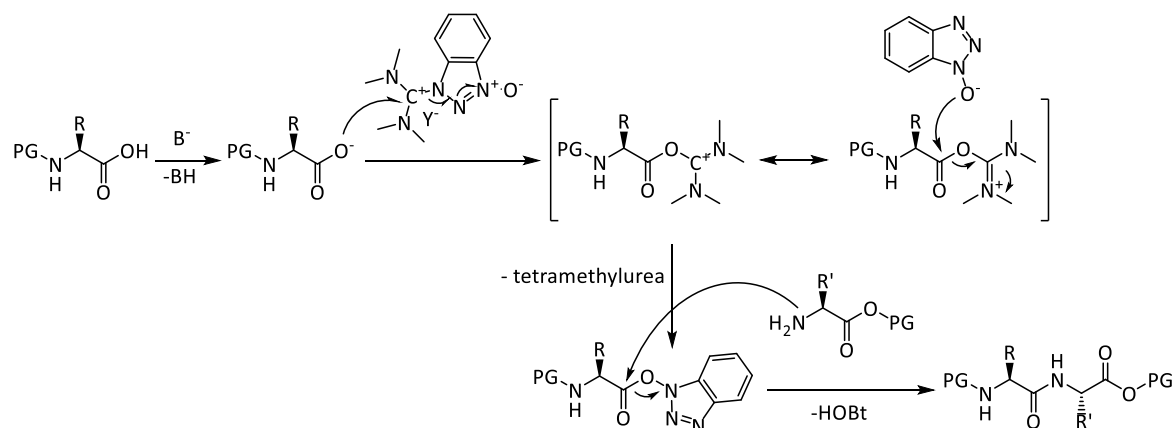


Figure 11. Stand-alone coupling reagents based on phosphonium- and iminium-salts.

In contrast to carbodiimides, these require a base to activate the carboxylic acid (**Scheme 3**).

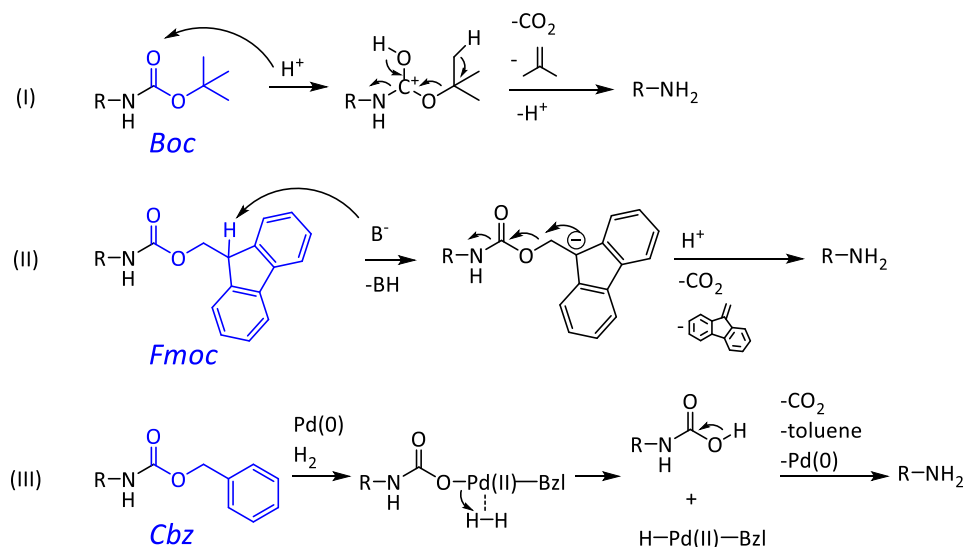
2. Introduction



Scheme 3. The stand-alone coupling reagents require a base for the initial preactivation of the carboxylic acid. The coupling itself is also facilitated by the HOBT ester as for the carbodiimide facilitated peptide coupling.

To enable a selective coupling between amines and carboxylic acids, chemists use a combination of temporary and semi-permanent protective groups, which have to be orthogonally cleaved. The temporary protecting groups, usually the amine protecting group of the activated carboxylic acid or C-terminal protecting group, depending on the direction of synthesis, is cleaved after each single coupling step. The permanent protecting groups are reserved for the sidechains. These protecting groups are cleaved when the peptide is completed.

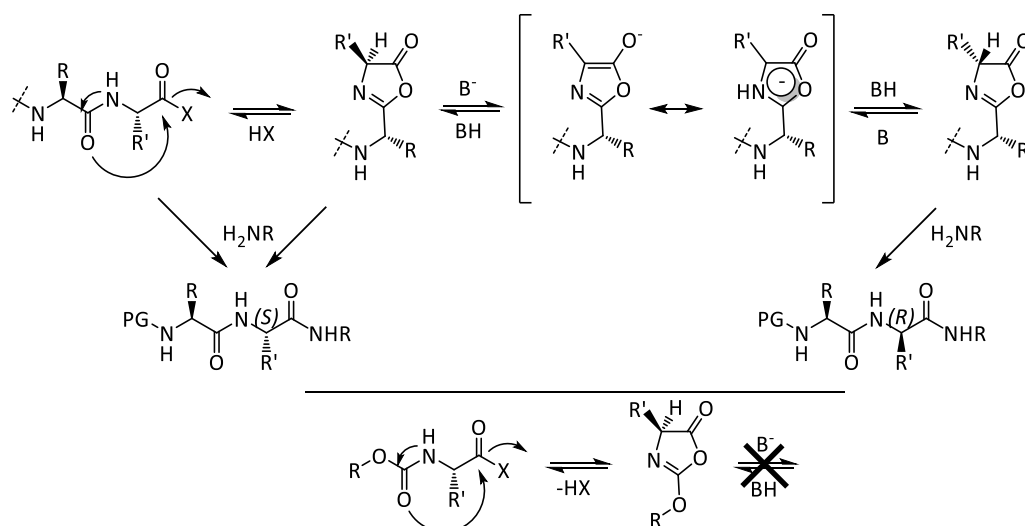
Frequently used protecting groups for amine functions are urethane based, with Boc, Fmoc and Cbz being most widely used (**Scheme 4**).



Scheme 4. The Boc, Fmoc and Cbz group are cleaved under orthogonal conditions. (I) The Boc group is cleaved under acidic conditions, resulting in the elimination of isobutene and CO_2 . (II) the Fmoc group is generally cleaved with secondary amines such as piperidine. The elimination of dibenzofulven is initiated by a deprotonation of the double benzylic proton, resulting in elimination of CO_2 . The electrophilic dibenzofulven may be trapped by an addition of secondary amine. (III) The Cbz group is cleaved hydrogenolytically, starting with an oxidative addition to the $\text{Pd}(0)$ catalyst and coordination of H_2 by a three centered σ -complex. The coordination to the $\text{Pd}(\text{II})$ center facilitates the deprotonation of hydrogen by the carboxylate, resulting in elimination of carbamic acid which releases the free amine by CO_2 elimination, the $\text{Pd}(0)$ is regenerated through reductive elimination of toluene.

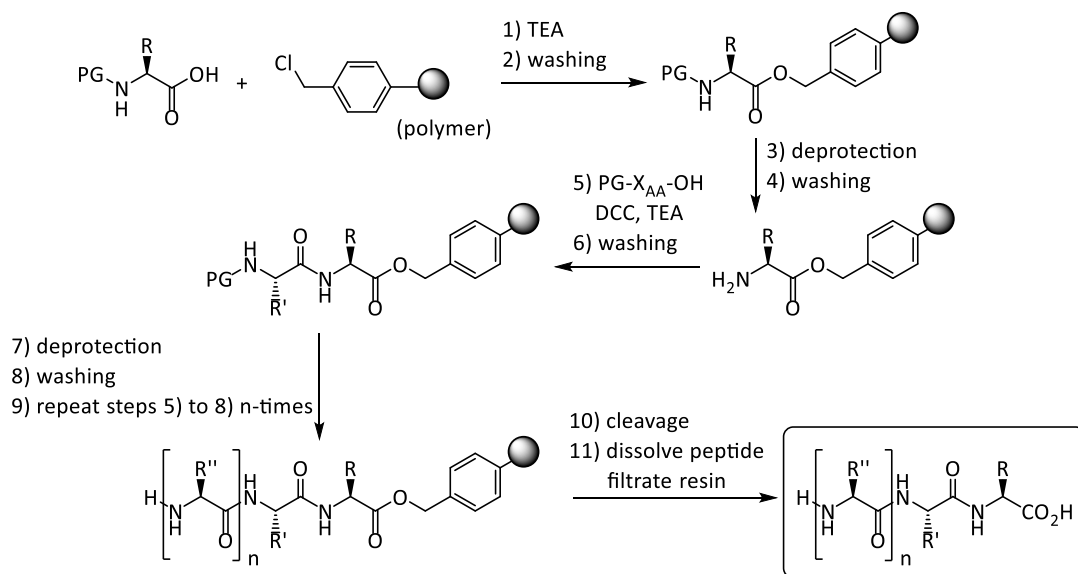
Common protecting group combinations are Fmoc/*t*Bu and Boc/Bzl, were the latter ones are the semi-permanent (ether and ester type) protecting groups for the sidechains, whose cleavage conditions are orthogonal towards the amine protecting group.

Urethane based protecting groups and the *N*-terminal synthesis direction offer the advantage, that possible epimerization is minimized, which is predominantly caused by 5(4*H*)-oxazolone formation after activation of the carboxylic acid. This oxazolone is readily deprotonated to form an aromatic enolate while losing its stereo information (**Scheme 5**).



Scheme 5. Strongly activated peptides (e.g. acid chlorides, *O*-acylisoureas) may undergo a cyclization to a 5(4*H*)-oxazolones, strong acylation agents which get readily deprotonated to form aromatic enolates. In contrast, the urethane group offers enough electron donor capacity to prevent enolate formation and loss of its stereo information.

In 1963, Merrifield revolutionized the synthesis of peptides with his approach of solid phase peptide synthesis,²¹ for which he received the Nobel Prize for chemistry in 1984. He developed a solid phase resin, a chloromethylated copolymer based on styrene and divinylbenzene, which showed suitable swelling properties in organic solvents to allow access for reagents. The chloromethylene moiety allowed the anchoring of *N*-protected amino acids in combination with triethylamine to the solid phase, by forming a covalent benzylester bond. Continuous cycles of *N*-terminal deprotection on resin and coupling of an amino acid active ester in combination with washing steps in between, allow the formation of a polypeptide chain in *N*-terminal direction on solid phase (**Scheme 6**). The finished peptide is obtained through cleavage from the resin.



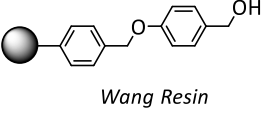
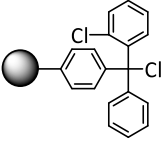
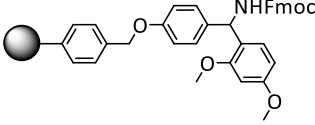
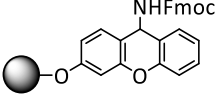
Scheme 6. General schematic work-flow of the SPPS.

In 1966, Merrifield and co-workers demonstrated the advantages of this method with the complete synthesis of the peptide hormone insulin in a matter of days and in high yields.²²

In the last decades, the SPPS found widespread application and has evolved a lot as its own industrial field and towards easier automatized handling. The Fmoc/^tBu SPPS evolved to be the method of choice for most applications, utilizing different acid labile protecting groups for the sidechains, mainly: Pbf, Trt, O^tBu, ^tBu and Boc.²³ Different and versatile linkers attached to the resin material allow for modified and mild cleavage conditions. Cleavage of side-chain protected peptides or cleavage of the peptide as carboxamides is possible. Some established linkers are presented in **Table 1** as an example.

2. Introduction

Table 1. Exemplary representation of resins (among others), which enable the synthesis of either fully protected/ deprotected peptides with a free carboxylic acid or carboxamide terminus.

	Cleavage		Cleavage	Product
 <i>Wang Resin</i>	90–95% TFA for 1-2 h.	 <i>Barlos resin</i>	1–5% TFA in DCM for 1 min.	acid
 <i>Rink amide resin</i>	90–95% TFA for 1-2 h.	 <i>Sieber resin</i>	1–5% TFA in DCM for 1 min.	amide

The mild cleavage conditions of the Barlos and Sieber resin allow the synthesis of fully protected acids or carboxamides bearing peptides, where the Wang and Rink amide resins deliver a complete deprotected peptide upon cleavage, which can be precipitated from ether to increase its purity.

Additionally, several new resin materials have been developed (e.g. PEG based ChemMatrix® resin),²⁴ which showed improved swelling properties in more polar and greener solvents.²⁵ De Marco *et al.* even demonstrated SPPS in water without conventional protecting groups, which were simultaneously protected and activated by the formation of *N*-carboxyanhydrides (Leuchs anhydrides).²⁶

2.3. Peptidomimetics

Proteins and peptides are playing an essential role in complex living organisms. While proteins are mostly constituents of tissues or engaged in biocatalytic tasks in the form of enzymes, the smaller peptides operate as hormones, neurotransmitters and regulators in signal transduction pathways.⁷ Many pathologic conditions, caused by a disorder in the interplay between enzymes and receptors with their substrates or ligands, are treated by medicinal chemists with peptides and their chemical analogues.²⁷ However, due to their pharmacologic properties, the use of peptides as therapeutic tools is often limited by low bioavailability and digestion by proteases.

In the last decades, peptidomimetics, which mimic biological effects of peptides (agonists), obtained an increased meaning in the medicinal and chemical research. In comparison to biologically active peptides, peptidomimetics possess a range of interesting benefits, which feature them as suitable candidates for drug development and for medicinal treatment. Increased potency by stabilization of active conformations and therefore decreased side effects, generation of oral bioavailability and prolonged duration of effect and prevention of metabolic degradation are objects of present research.²⁷ Progress is accompanied by improvement and development of computational methods and programs, which aid in the rational *de novo* design of novel peptidomimetics. Spectroscopic methods (NMR), X-ray crystal structure analysis and molecular modelling play a vital role to solve the bioactive conformation of peptides, for example in an enzyme-substrate complex.²⁸

The design of functional peptidomimetics should be built upon two key attributes, a favourable conformation through the installation of a rigid structure-element, and the placement of functional groups in space to enable specific interactions (hydrophobic, hydrogen-bonds, electrostatic, salt bridges). A synthetic approach, to access new peptidomimetics, is to start from the native peptide as a lead structure and to apply one or several modifications (*N*-alkylation, C^α -alkylation, incorporation of D-amino acids) to the backbone, finally leading to improved pharmaco-kinetic properties in SAR-studies (Figure 12).²⁹

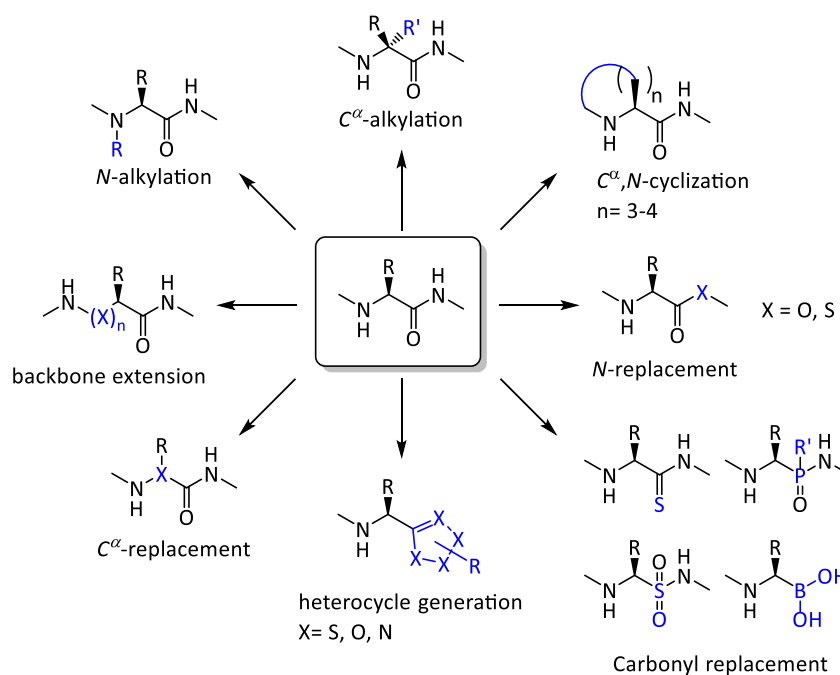


Figure 12. Backbone modification of a native peptide segment.²⁹

Modification of the peptide backbone not only increases metabolic stability but has also a substantial influence on the secondary structure and folding properties of the peptide, by changing *H*-bond patterns or through steric demands.

2.4. Triazoles as amide bond isosters

Pursuing the idea of replacing amide bonds by proteolytically stable and planar chemical groups, the triazole, which shares electronic and topologic characteristics with natural peptide bonds, emerged in the focus of peptidomimetic chemists.³⁰ The 1,2,3-triazoles represent a class of aromatic heterocycles, whose characteristics make them promising candidates for the development of bioactive peptidomimetics with improved pharmacologic properties.³¹ Like amide bonds, 1,2,3-triazoles are planar, have a strong dipole moment and are capable of accepting and donating hydrogen bonds. While the distance between the α -carbons of 1,5-disubstituted triazoles matches quite well for the *cis* amide bond (3.0 compared to 3.2 Å), the distances for the *trans* amide bond does not comply well (3.7 compared to 4.9 Å) with the 1,4-disubstituted triazole (Figure 13).³¹

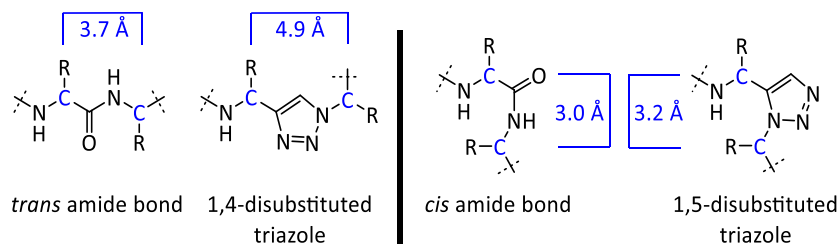
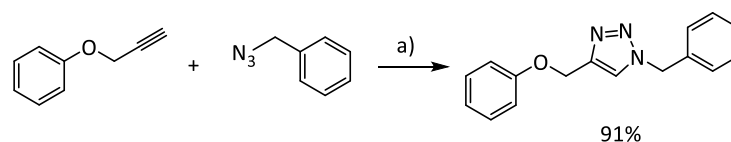


Figure 13. Comparison of *trans*- and *cis* amide bonds and their resembling 1,4- and 1,5-disubstituted triazole surrogates.

The synthesis of triazoles by a cycloaddition between mono-substituted alkynes (as dipolarophiles) and azides (as 1,3-dipolar components) was first described by Michael *et al.* in 1893 and reviewed by Huisgen.³² The thermal reaction between phenylazide and phenylacetylide gave a nearly 1:1 regioisomer-mixture of the 1,4- and 1,5-disubstituted diphenyltriazole.

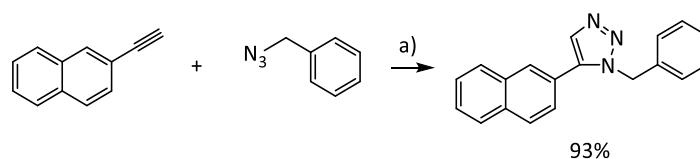
Since the independent discovery of the copper(I) catalysed azide alkyne cycloaddition (CuAAC) by the groups of Meldal and Sharpless in 2002 (Scheme 7),^{33, 34} which leads exclusively to 1,4-disubstituted 1,2,3-triazoles, the CuAAC has found wide spread use by the chemical community.³⁵



Scheme 7. CuAAC between Propargyl phenyl ether and benzylazide in aqueous media without the exclusion of oxygen. The reductive “CuSO₄/sodium ascorbate”-system serves as a regenerative Cu^I source; a) CuSO₄·5H₂O (1 mol%), sodium ascorbate (5 mol%), H₂O/^tBu (2:1), RT, 8 h.³⁴

Several key features account for the popularity of this versatile reaction. It proceeds very selectively and without side products also in aqueous media and is orthogonal towards biologically relevant functional groups. Due to its perfect atom economy and straightforward workup, Sharpless and co-workers defined the CuAAC as a prototype of a “click-reaction”.³⁶ Because the reaction mechanism is initiated by a formation of a copper acetylide derivative, the CuAAC can be only performed with terminal alkynes.³⁴

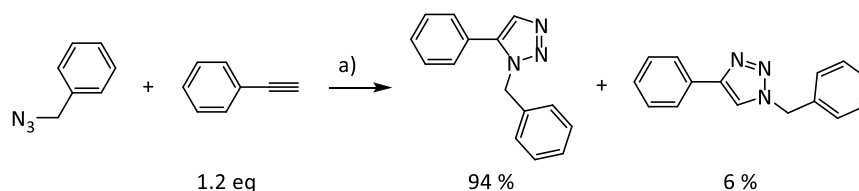
In 2005, the groups of Fokin and Jia published its counterpart, the ruthenium(II) catalysed azide alkyne cycloaddition (RuAAC) based on the complex Cp^{*}RuCl(L₂), which enabled the selective synthesis of the 1,5-disubstituted 1,2,3-triazole regioisomer (**Scheme 8**).³⁷



Scheme 8. RuAAC between 2-ethynyl naphthalene and benzylazide under elevated temperatures; a) Cp^{*}RuCl(PPh₃)₂ (1 mol%), benzene, 80 °C, 4 h.³⁷

Although the reaction does not tolerate water or protic solvents, it is quite tolerable towards functional groups like alcohols, aldehydes, alkenes, amides, amines, boronic esters, ketones and halides.³⁸ Since the reaction is initiated by a π -complex between the acetylide and the Ru(II) center, the reaction also tolerates internal alkynes as substrates, which would lead to trisubstituted triazoles with another possible regioisomeric combination.

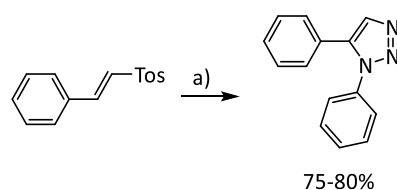
A recent publication from Kim *et al.* in 2017 describes the nickel(II) catalysed [3+2] alkyne azide cycloaddition to obtain 1,5-disubstituted triazoles in aqueous media under oxygen atmosphere, thereby addressing the disadvantages of the RuAAC (**Scheme 9**).³⁹



Scheme 9. Optimized reaction condition example of a NiAAC between benzylazide and phenylacetylide. The regioisomers 1,5-disubstituted and 1,4-disubstituted triazole were isolated in a ratio of 94% to 6%; a) Cp_2Ni (10 mol%), Xantphos (10 mol%), Cs_2CO_3 (1 eq), toluene, rt, air, 12 h.

However, the reaction conditions seem to be critical for the regioselectivity. A deviation from the standard conditions, considering temperature, amount of base and ligand, leads to varying formation of undesired 1,4-disubstituted triazole, which might be challenging to separate from its regioisomer. Even the optimized protocol leads to the formation of 6% 1,4-disubstituted triazole, and to 94% of the 1,5-disubstituted in toluene (for the specific reaction example between benzylazide and phenylacetylide), whereas a change of solvent using water as a reaction solvent leads to a 91% to 6% ratio in isolated yield. Although the authors claimed a broad substrate scope similar to the CuAAC, biocompatibility could not be proven, since the NiAAC failed with unprotected sugars as substrates, further experiments with amino acids were done with fully protected starting materials.

An interesting, alternative approach for the synthesis of 1,5-disubstituted triazoles, without the use of alkynes, was published in 2011 by Dey *et al.*⁴⁰ They described a metal-free and regioselective formation of 1,5-disubstituted triazoles in water under reflux conditions, utilizing vinyl sulfones and azides (**Scheme 10**).

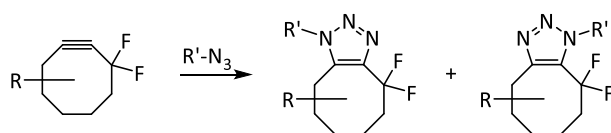


Scheme 10. Metal-free formation of 1,5-disubstituted triazoles between vinylsulfones and azides in water, both aromatic or aliphatic substrates are tolerated; a) Ph-N_3 , water or toluene, reflux, 12 h.

This approach works for either aromatic or aliphatic substrates. Furthermore, the substrate scope included several ethers, free alcohols, mesylated amines and ketals. Although, vinyl sulfones are readily available from alkenes, 1,2-diols, epoxides and aldehydes,⁴¹ to the best of our knowledge, a synthesis of 3-tosyl-prop-2-en-1-amines, starting from chiral amino aldehydes under preservation of the chiral integrity, has not been described in the

literature yet (which would be suitable starting materials for peptide-based building blocks).

If “click chemistry” is supposed to be used in living organisms and *in vivo* applications, the toxic nature of transition metals may pose a problem, this could be circumvented employing electron withdrawing substituents and by ring-strain activated alkynes, which readily react selectively with azides to form the desired disubstituted triazoles within minutes, without transition metal catalysts. The group of Bertozzi published a bioorthogonal *in vivo* ligation employing difluorinated cyclooctyne as an activated alkyne for the copper-free click chemistry,⁴² therefore combining the rate-enhancing features of ring-strain and electron-withdrawing substituents (**Scheme 11**).



Scheme 11. Difluorinated strained alkynes react readily with azides in a biological environment to form trisubstituted triazoles as “click”-product.

However, the formation of both regioisomers might impose a problem for the synthesis of smaller ligation products but is generally not considered an issue in the labelling or immobilization of larger biomolecules.

With these tools in hand, chemists started to come up with applications for both, 1,4- and 1,5-disubstituted triazoles.⁴³ A successful replacement of a backbone amide bond by a 1,4-disubstituted triazole was demonstrated by Nahrwold *et al.* in Cryptophycin-52, while preserving its bioactivity (**Figure 14**).⁴⁴

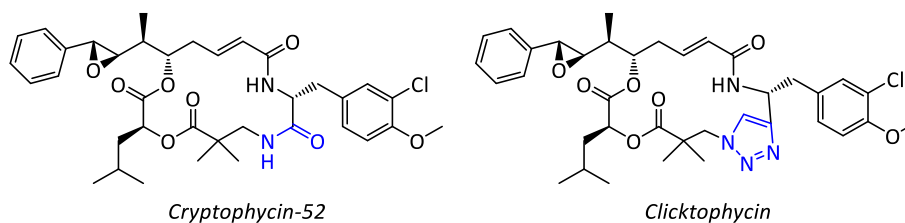


Figure 14. Schematic depiction of the cryptophycin-52 and its peptidomimetic, which contains a 1,4-disubstituted triazole between the 3-chloro-4-methoxy-phenylalanine and β -Aib moieties.

Cryptophycin-52 is a cyclic depsipeptide, which shows high *in vitro* cytotoxicity against multidrug resistant human cancer cell lines (KB-V1), after the incorporation of the 1,4-

2. Introduction

disubstituted triazole, reproducing the *trans* configured amide bond (in this position), the bioactivity was only slightly reduced ($IC_{50} = 3.2$ nM compared to 0.7 nM).⁴⁴

The 1,5-disubstituted triazole was demonstrated to be a *cis* amide bond surrogate by Tam *et al.* in 2007.⁴⁵ In this work, the dipeptide surrogate -X_{aa}[5Tz]Ala- was shown to be a general substitute for -X_{aa}-*cis*-Pro- (**Figure 15**), built into the turn region of RNase A by an expressed protein ligation (Asn₁₁₃-Pro₁₁₄ were replaced). The semisynthetic folded enzymes were compared to their wild-types, resulting in thoroughly retained catalytic activity and similar CD-spectra.⁴⁵

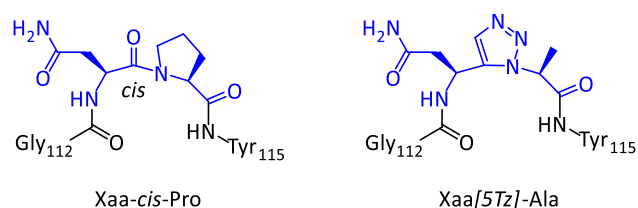


Figure 15. Comparison of the turn region -Gly-Asn-*cis*-Pro-Tyr- and its mimic -Gly-Asn[5Tz]Ala-Tyr-.⁴⁵

2.5. Chiral propargylamines and α -azido acids

Chiral propargylamines are important building blocks for the synthesis of conformationally restricted amide-bond isosters. Beside their use as precursors for dipolar cycloadditions, e.g. the 1,2,3-triazole formation in peptidomimetics³⁰ or the Diels-Alder reaction,⁴⁶ they serve as valuable starting materials for several transition metal catalysed additions, for example the Sonogashira cross-coupling,⁴⁷ allyl-transformation followed by Stille-coupling⁴⁸ and other versatile transformations⁴⁹ (**Figure 16**).

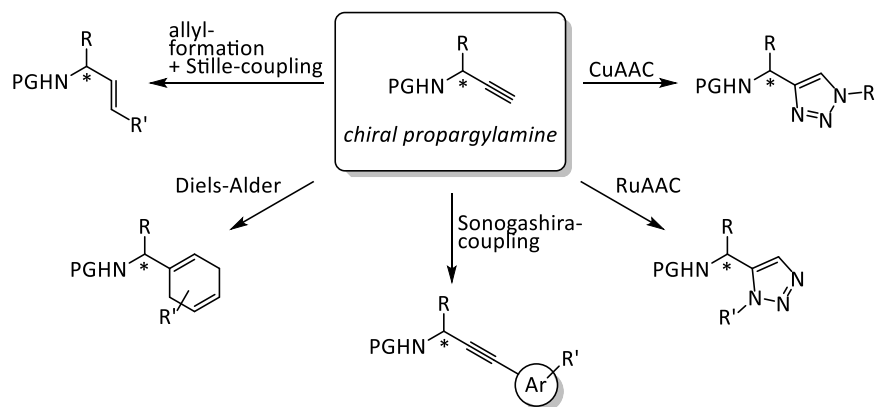
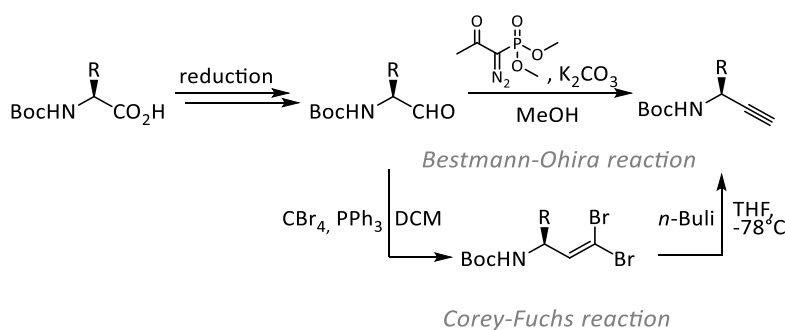


Figure 16. Several selected transformation and extension reactions of propargylamines in organic chemistry.

Besides the possible route to obtain chiral propargylamines by an asymmetric alkynylation of imines, or enzymatic racemic resolution, alkynes are commonly obtained from homologation reactions starting from aldehydes.⁵⁰ The synthesis of chiral propargylamines has been described starting from protected α -amino aldehydes converted in a Corey-Fuchs or Bestmann-Ohira reaction (Scheme 12).^{48, 51,}

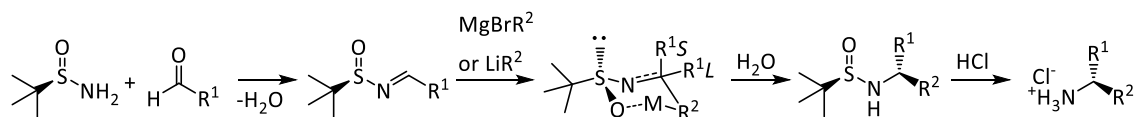
The α -amino aldehydes are accessible by either reduction of the corresponding Weinreb amide with $\text{LiAlH}_4/\text{DIBAL-H}$, or oxidation of the amino alcohol by Swern oxidation.^{53, 54} However, these α -amino aldehydes are prone to epimerization during prolonged storage or upon contact with silica and are advised to be used immediately.⁵⁵



Scheme 12. After conversion of the amino acid into an α -amino aldehyde it can be transformed, by two Wittig related homologation reactions, into chiral propargylamines.

Both methods have the advantage that the chiral pool of naturally occurring amino acids (Figure 1) is commercially available, with orthogonal protecting group combinations.

The group of Ellman engaged themselves in the asymmetric synthesis of chiral amines.⁵⁶ They applied *tert*-butanesulfinamide as a chiral auxiliary. Together with aldehydes or ketones, the sulfinamide forms chiral *N*-sulfinimines which are further susceptible towards nucleophilic attacks by metal organyls. They postulated a cyclic hexagonal transition state, formed by coordination of the oxygen to the metal ion, which explains the diastereoselective induction.⁵⁶ After the nucleophilic addition, the *N*-sulfinyl group can be cleaved under acidic conditions to release the free amine as a salt (Scheme 13).

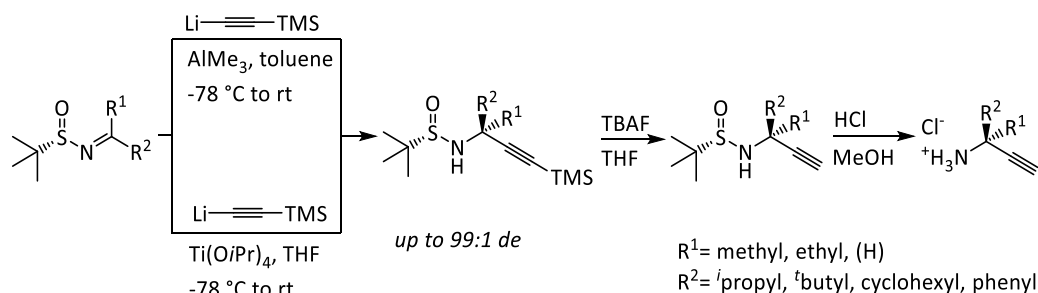


Scheme 13. Synthesis of chiral amines utilizing Ellman's auxiliary.

2. Introduction

Hence, it was argued that the *N*-sulfinyl group may be used as an alternative to the Boc-group. Moreover, after acidic cleavage it was shown that the Ellman-auxiliary can be recovered from the reaction.^{57, 58} In 2010, Chen *et al.* published an extensive report about the addition of different alkynylmagnesium chlorides to *N*-sulfinylimines. In this publication, the Grignard-addition of trimethylsilylacetylide provided several chiral propargylamines with unnatural amino acid side chains.⁵⁹

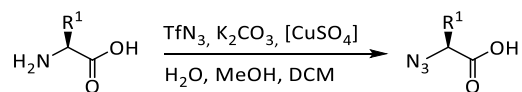
The groups of Ellman and Qing published the addition of *in situ* generated ((trimethylsilyl)ethynyl)lithium to sulfinketimines. In the presence of a Lewis acid high yields and diastereomeric excesses were afforded (**Scheme 14**).^{60, 61} Addition of a Lewis acid drastically improved the diastereomeric excess of the addition to the sulfinimine. Both groups showed that the reaction could be either performed in toluene, with AlMe₃ as a Lewis acid, or in THF, with Ti(OiPr)₄, with excellent diastereomeric purity and yields. It was furthermore demonstrated that the TMS group can be cleaved off in quantitative yields with TBAF, giving access to synthetic versatile terminal alkynes. The procedures are also applicable to sulfinylaldimines (R¹ = H).



Scheme 14. Diastereofacial addition of *in situ* generated ((trimethylsilyl)ethynyl)lithium to chiral *N*-sulfinylketimines lead to α,α -dibranched propargylamines in high purity. The TMS group could be cleaved off by the addition of TBAF in organic solvents, affording versatile terminal alkynes.

During the fluoride mediated deprotection of the TMS-group, under certain circumstances where the residue at the alkyne homologues allylic position is either electron withdrawing or aromatic, a deprotonation of the proton at the stereogenic center is observed, which results in the formation of an allene which further rearranges into an α,β -unsaturated imine.⁶² This was shown to be prevented by protodesilylation of the TMS-group catalysed by Ag(I)-salts.⁶³ The principles and scope of this method, towards the asymmetric synthesis of natural and non-natural propargylamines, were further explored in our group by Wünsch *et al.*⁶²

The synthesis of chiral α -azido acids is well established since a decade ago. Starting from the pool of 20 natural amino acids (**Figure 1**), the complementary chiral azides can be obtained by a Cu(II)-catalysed diazotransfer employing triflyl azide (**Scheme 15**).^{64, 65}



Scheme 15. Chiral α -azido acids can be obtained by a diazotransfer reaction using Tf-N₃ as a transfer reagent under basic conditions.

The mechanism was postulated by Wong and coworkers in 2002⁶⁶ and later confirmed by Pandiakumar *et al.*⁶⁷ in 2014 by isotopic ¹⁵N labelling of the diazotransferreagent. With or without the addition of copper(II) ions, the two outer nitrogen atoms of the diazo-transfer reagent are transmitted to the amine.

Regarding the safety issues of toxic NaN₃, which is used to prepare TfN₃ out of triflyl anhydride in big excess and the potential explosive nature of TfN₃, an improved method has been published by Yan *et al.* in 2005 which significantly reduces its amount.⁶⁸

The HCl-salt of imidazole sulfonyl azide was described 2007 as inexpensive and shelf-stable diazotransfer reagent,⁶⁹ which was later corrected by the authors, as safety concerns arised.⁷⁰ The hydrogen sulfate salt on the other hand, can be considered safe to handle as a solid.^{71, 72}

2.6. Foldamers

A chain-like oligomer which folds itself into a discrete conformation in solution can be applied to mimic structure features of peptides and proteins. The noncovalent interaction properties, between nonadjacent monomers of these synthetic compounds are explored in studying of molecular self-assembly and host-guest complexes. Gellman used and defined the word “foldamer” to describe any polymer which strives to adopt a specific compact conformation.⁷³ Control over polymer folding might lead to molecules with useful biological or material properties. In recent years, several foldamers have been designed, targeting protein surfaces and antagonizing protein-protein interaction binding tightly in a specific manner.⁷⁴ Protein-protein interaction is an elementary event of signal transduction pathways, the manipulation of those pathways has become a promising strategy for the treatment of several diseases and reducing of cancer growth.

2. Introduction

In the field of nonpeptidic foldamers which mimic secondary structure motifs of native peptides, the group of Arora published in 2010 a set of oligooxopiperazines as α -helix mimetics,⁷⁵ which are derived from α -amino acids and feature a chiral backbone (Figure 17 A). These mimics imitate the binding surface of an alpha helix in protein-protein interactions, therefore reproducing the arrangement of the i , $i+4$ and $i+7$ residue of a helix. Since only the arrangement of the key side chains is reproduced, those synthetic scaffolds are thought to have an increased selectivity over their natural counterpart. These oxopiperazine helix mimics were shown by Lao *et al.* in 2014 to be suitable small-molecule inhibitors of the transcriptional protein-protein interaction of HIF-p300/CBP⁷⁶ which results in modulation of gene expression and reduction of tumor growth in mice model.

In the research field of peptidomimetics for enzymatic inhibition, the extended β -sheet structure as well as its H -bonding capabilities are crucial parameters for the search of convenient non-peptidic scaffolds. In 1992 the group of Hirschmann published a peptidomimetic framework based on pyrrolinone, which mimics the conformation of a β -sheet with the residues in axial orientation to the heteroaromatic rings. The heteroaromatic ring itself was shown to fix the angles analogue to ψ and ω in a peptide, where the ϕ -angle is defined by steric interactions of a side-chain with its neighbouring heteroaromate (Figure 17 B).⁷⁷

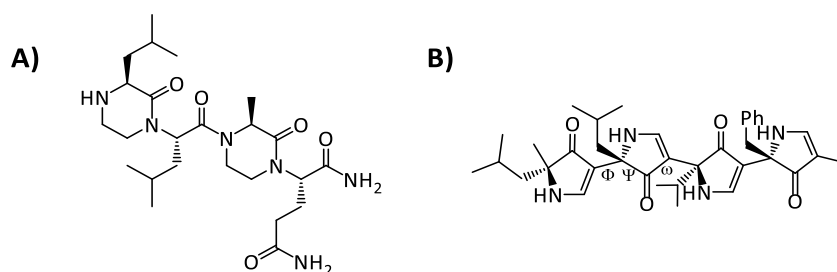


Figure 17. A) Example of an oligomer build up by oxopiperazines which mimics a section of an α -helix.⁷⁶ B) A framework based on pyrrolinone effectively mimics a β -sheet.⁷⁷

By an overlay comparison with the X-ray crystal structure of a β -sheet forming peptide the group of Hirschmann could show that the carbonyl functions of the pyrrolinone-moieties closely match the orientation of the amide-carbonyl functions of the peptide. Consequently, the peptidomimetic maintains the crucial H -bond acceptor capability which would be necessary for protease recognition.

In 2005 the group of Arora published the synthesis and conformational analysis of 1,4-disubstituted 1,2,3-triazole containing oligomers, which they termed triazolamers. In these,

every amide bond is substituted by a triazole as amide-bond isoster, but the chiral main-chain, which contains the amino-acid residues, remains preserved.⁷⁸ This distinctly folded new class of nonpeptidic oligomers adopts a *zig-zag* conformation reminiscent of peptide β -strands through the large dipole moment of single triazole moieties of ~ 5 D (**Figure 18**).

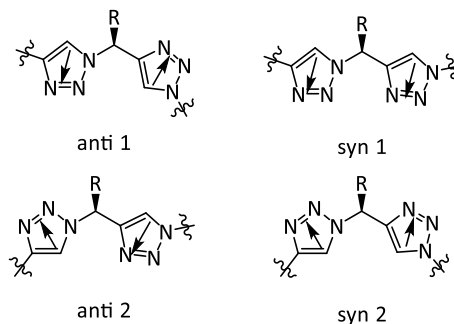


Figure 18. Comparison of both sets of *syn*- and *anti*-conformations. The dipole moment of each single triazolering is represented by an arrow. The *anti*-conformations are favoured by 4 kcal/mol over their *syn*-conformations.

The triazolamers were shown to be obtainable by solid phase or solution phase synthesis, through iterative diazotransfer of the free amine function followed by copper catalysed dipolar cycloaddition with a chiral propargylamine and a final deprotection of the amine protective group.⁷⁹

Due to their extended conformation and capability to contribute to *H*-bonding, these oligomers were examined as possible protease inhibitors. Jochim *et al.* evaluated the potential of these triazolamers as HIV-1 protease inhibitors in 2009,⁸⁰ by designing triazolamers which mimic the residual orientation of the known peptidic HIV-1 protease inhibitors (L-700,417 and A74704), which have been co-crystallized with the enzyme in their biological active conformation.⁸¹ Although docking experiments suggest that the triazolamer superimposes in good agreement with the established inhibitors, the inhibitory concentrations were only in μ M range ($IC_{50} = 25 \mu$ M for the most active triazolamer), compared to the low nanomolar inhibition constants of the leading inhibitors ($IC_{50} = 0.67$ nM for L-700,417) (**Figure 19**).

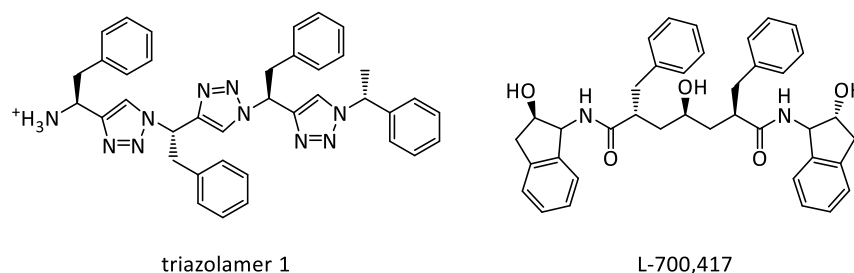


Figure 19. Structural comparison between triazolamer-1 and the known inhibitor L-700,417.

2.7. Amyloid- β related diseases

The term amyloid originally referred to protein deposits resembling those of starch, with amyloid meaning starch-like.⁸² It is nowadays specifically associated with the fibrillization process of peptides and proteins, by aggregation of β -sheet structured monomers. The aggregation of the amyloid- β peptide ($\text{A}\beta$) plays a role in Alzheimer's disease, an age dependent, neurodegenerative disease, which was first described by Alois Alzheimer in 1906.⁸³ Due to the aging society and increasing lifespan which goes along with a rising incidence of this condition, a lot of effort is performed to investigate the causes and treatment of Alzheimer's disease (AD), which is responsible for 50-80% of all dementia cases.⁸² An estimated amount of 18 million people is currently affected by AD, a number which is predicted to double within the next 20 years, causing billions of US-\$ annual medical-cost for society. Aggravatingly is the fact, that a single genetic risk-factor does not exist, but several genes associated with susceptibility to the condition are known, as well as lifestyle comprising of unfavourable diet (leading to increased IGF-1 levels), lack in exercise and mental activity.⁸² AD is usually diagnosed by cognitive testing methods supported by MRI scanning, which does not consider the fact, that the pathogenic process leading to AD, often times, start a period of one decade before obvious symptoms are observed. Until now, the progression of AD is not reversible or curable, however, several existing treatments can decelerate the progression of the disease.

The $\text{A}\beta$ -hypothesis implies Amyloid- β ($\text{A}\beta$) as a central causative of AD, which is supported by the fact, that levels of soluble $\text{A}\beta$ correlate better with the extent of cognitive degradation than simple plaque counts.⁸⁴ The two predominant variants of $\text{A}\beta$ in human have been identified as $\text{A}\beta_{40}$ and $\text{A}\beta_{42}$, with 40 or 42 residues. Although $\text{A}\beta_{40}$ is ~10 times more abundant, the more hydrophobic $\text{A}\beta_{42}$ has been shown to form fibrils more rapidly,

the early oligomers formed in the initial self-assembly process are thought to be the neurotoxic agents.⁸² A β is formed by proteolytic cleavage of the transmembrane precursor-protein APP (amyloid precursor protein), which is expressed in many tissues but concentrated in synapses of neurons, by the endoproteases β - and γ -secretase. Therefore, the β - and γ -secretase are considered to be prime targets for the development of protease inhibitors, to treat the disease at an initial stage, preventing the formation of A β and as a consequence the development of neurotoxic oligomers.⁸⁵ The role of APP in the human body is not entirely understood, it is an ancient gene encoded on chromosome-21 and has been linked as a modulator in the formation-process of synapses,⁸⁶ or in apoptosis processes by releasing a cytotoxic C-terminal fragment.⁸⁷ Consequently, low levels of soluble A β can be also detected in the plasma of healthy individuals. The accumulation and aggregation in brain tissue, however, is prevented by different clearance pathways, which allow A β to cross the blood-brain-barrier followed by subsequent degradation by proteases.⁸⁸ Hence, Alzheimer's disease is further characterized by an imbalance between production and clearance of A β .

Beside the approach to hinder the pathogenesis of Alzheimer's disease at an early stage in the cascade, by inhibiting the secretase enzymes, a physicochemical path is imaginable to prevent the aggregation of A β . The idea behind this approach is to utilize a small peptide with a specific recognition sequence for A β , which binds A β and meanwhile prevents the ability of the affected strand to form neurotoxic oligomers. Searching such a recognition sequence, chemists focused on the peptide sequence of A β itself, since it is able to selectively bind and interact intermolecularly with other A β -strands to form oligomers. This self-recognition element was discovered and limited to the A β fragment 16-20, which corresponds to the truncated amino acid sequence KLVFF. Tjernberg *et al.* showed in 1996, that the core motif KLVFF is indeed able to bind full length A β and to interrupt its polymerization, therefore envisioning KLVFF as a lead-structure for the discovery and development of novel potent aggregation inhibitors *in vivo*.⁸⁹

2.8. Monitoring of the A β aggregation and fibrillization process

Fluorescence dye binding assays are used to investigate the self-assembly process of amyloid proteins and to study the nature of early stage soluble oligomers. The fluorescence

2. Introduction

probe should exhibit distinct spectral properties, for instance a shift in emission wavelength upon binding compared to its unbound state. Thioflavin T (ThT) (**Figure 20**), a benzothiazole derivative, is widely used as a histochemical dye to quantify the amount of misfolded protein aggregates.⁹⁰ It is able to recognize and noncovalently bind β -sheet rich structures, which is accompanied by a red shift in its fluorescence spectrum.

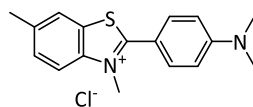


Figure 20. Structure of Thioflavin T, which is synthesized by methylation of 6-methyl-2-benzothiazolyl-4-aminophenyl with methanol in the presence of hydrochloric acid.

In presence of amyloid, ThT becomes highly fluorescent with an emission maximum at 480 nm arising from a new absorption peak at 450 nm, indicating an impact of interactions between ThT and amyloid on fluorescence. A study in 2005 by Krebs *et al.*⁹¹ examined the localisation of binding between ThT and amyloid proteins, discovering a regular and specific binding pattern of ThT, which leads to increased quantum yields during the fluorescence assay. This is explained by a 6.5 to 6.9 Å wide binding channel, typical for the extended β -sheets of amyloid fibrils, stabilizing the excited state conformation of ThT. This explains the inability of some β -sheet rich structures to increase fluorescence (e.g. transthyretin).⁹⁰ As a direct implication, Krebs *et al.* proclaimed ThT as a dye more suitable for the probing of amyloid fibrils.

Small molecular dyes, which selectively bind secondary structure motifs of A β , are of great interest in today's investigation in the formation of smaller, soluble neurotoxic oligomers, representative for the early stage of Alzheimer's disease development. 2010, Smith *et al.* published two triazole containing BODIPY dyes, which show an improved sensitivity in the recognition towards unordered soluble oligomers of A β 1-42 (**Figure 21**).⁹²

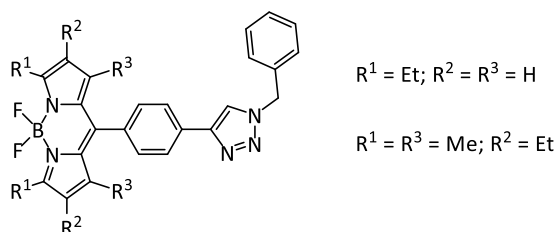


Figure 21. BODIPY derivatives, extended by a N^1 -benzyl triazole.

Whereas an excess of dye, relative to A β , is required for ThT fluorescence to receive an enhanced signal, this is not the case for the BODIPY dye, which is, therefore, not disrupting

the integrity of A β self-assembly.^{92, 93} Smith *et al.* demonstrated that small concentrations of BODIPY (2-4% compared to A β) already provide a significant enhancement of fluorescence. Additionally, the characteristic “lag-phase” of ThT assays, arising from the fact that ThT is unable to detect smaller soluble oligomers at the early stage of aggregation (which results in diminished fluorescence), is not observed for BODIPY assays. This supports the evidence that BODIPY is able to recognize smaller soluble aggregates of A β 1-42.

2.9. Integrins and RGD-peptides

RGD refers to the peptide sequence Arg-Gly-Asp which is located predominantly in the extracellular matrix (a protein-network in which the cells reside) and on certain plasma proteins. The sequence is able to bind cell surface receptors, the integrins, a class of transmembrane proteins which are important for the signal transduction between cells and their environment.⁹⁴ Integrins play a critical role in cell adhesion processes and the angiogenesis of tumor cells by regulating the activities of cytoplasmic kinases.⁹⁵ They are heterodimeric receptors, composed of noncovalently associated α - and β -subunits, the fact that they are linked with pathologic conditions have turned them into potential therapeutic targets.⁹⁶ Several types of integrins exist, composed of 18 α and eight β units giving 24 $\alpha\beta$ heterodimers in mammals. Eight of them are able to recognize the RGD sequence in their native ligands (five α_v , two β_1 (α_5 , α_8) and $\alpha_{IIb}\beta_3$).^{97, 98} All members of the integrin family adopt a large extracellular “head on two legs” resembling shape, with the head containing the ligand-binding domain, and the legs traversing the membrane and terminating in a short cytoplasmic domain. They connect the ECM with the intracellular cytoskeleton (Figure 22).^{96,99}

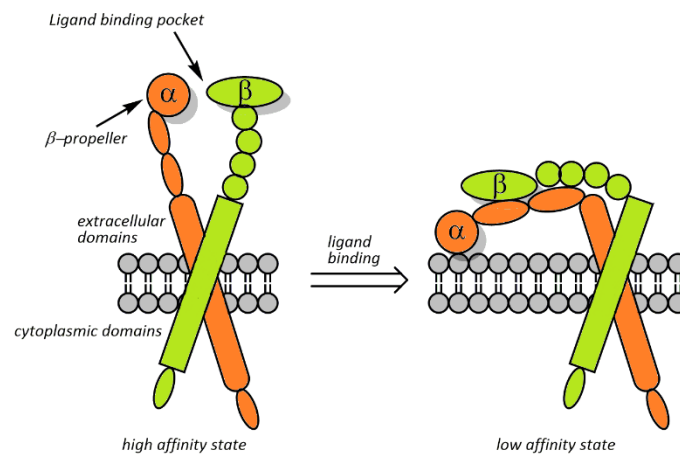


Figure 22. Schematic depiction of the bent and upright conformation of an integrin.⁹⁶

The 24 different integrins in mammals can be separated into two groups, one containing, and the other one lacking an αI domain inserted into the α subunit, which serves as a divalent cation binding site for extracellular ligands.¹⁰⁰ The binding of a ligand to a specific integrin is accompanied by a significant conformational change of the integrin, subsequently mediating the signal transduction into the cell. This is shown in **Figure 22**, where the integrin changes from an extended conformation on the left, to a bent conformation closer to the membrane in its ligand-occupied stage.

In the group of RGD binding integrins the integrins $\alpha_v\beta_3$, $\alpha_v\beta_5$, $\alpha_5\beta_1$ have been shown to be involved in angiogenesis and metastasis of solid tumors and were, therefore, considered as promising drug targets for cancer treatment, further supported by the fact that these integrins are overexpressed in tumor-cells.¹⁰¹ The group of Kessler was interested in finding ligands for the integrin $\alpha_v\beta_3$. Due to missing X-ray crystal structure of the integrin bound ligand at this time and, therefore, unknown biologically active conformation of the RGD sequence, the group focused their initial efforts on a “ligand-oriented design”. In these the RGD-sequence was optimized to develop suitable ligands. By a combinational strategy of cyclizing different peptides to restrict the conformation and a *N*-methylation scan of amide bonds, the group discovered the cyclic peptide cyclo-[RGDf(NMe)V] in 1995, which shows a sub-nanomolar antagonistic activity towards $\alpha_v\beta_3$.¹⁰¹ The peptide was called “cilengitide” and patented in collaboration with Merck, entering phase III clinical study for threatening glioblastoma in human. However, in recent years it has been shown that inhibitors targeting $\alpha_v\beta_3$ and $\alpha_v\beta_5$, although entering clinical trials, were ineffective in showing significant benefit for concerned test groups.¹⁰² Reynolds *et al.* have shown that low concentrations of RGD-mimetic integrin inhibitors paradoxically have a

proangiogenic effect, by stimulating VEGF (vascular endothelial growth factor) dependent angiogenesis in nanomolar concentrations, and therefore may increase cancer-growth, which limits their application in human.¹⁰² Cilengitide has been declined to be further developed as a single-agent anticancer drug, after failing to show significant efficiency compared to conventional chemoradiotherapy.¹⁰³

The reason for this lack of efficiency in human compared to preclinical tests is not yet resolved. Since cilengitide shows a high *in vitro* affinity towards integrin expressing glioblastoma cells, there should be a high interest to address the inefficiency towards the majority of human cancers.¹⁰² However, in the field of drug-conjugates, RGD-mimetics are still a viable option as a targeting device, combined with a potent cytotoxic drug.

3. Research Objective

The aim of this dissertation has been to develop general and convenient synthesis methods for peptidomimetics, containing 1,5-disubstituted 1,2,3-triazoles as rigid amide-bond isosters. The substitution of amide bonds should lead to increased metabolic stability and potentially to conserved defined conformations, eventually mimicking secondary structure motifs of naturally occurring peptides. The knowledge about the conformation inducing effects of nonpeptidic scaffolds would contribute to the objective to design novel peptidomimetics, which might target protein surfaces in biological systems, or mimic bioactive conformations of receptor ligands and enzymatic inhibitors.

The project was inspired by the triazolamers of the Arora workgroup,⁷⁸ which showed encouraging potential as lead structure for the development of protease inhibitors. Differently to the work of the Arora group, the effort was focused on linear compounds with an alternating sequence of amide-bonds and 1,5-disubstituted triazoles, which were termed as peptidotriazolamers in previous works of our group (Figure 23).¹⁰⁴

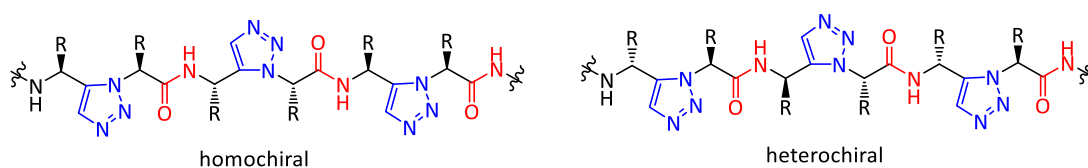
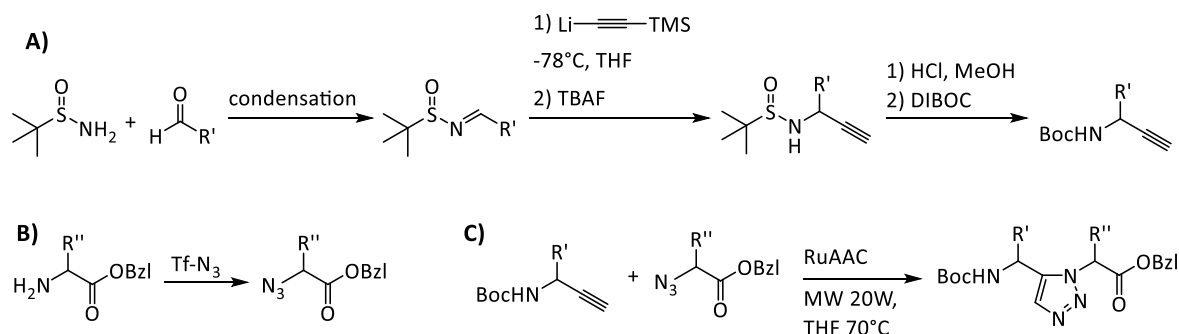


Figure 23. Two examples of peptidomimetic oligomers with an alternating sequence of amide-bonds and 1,5-disubstituted triazoles. Additionally, the compounds comprise of a homo- or heterochiral setup of proteinogenic residues.

The previous master thesis¹⁰⁵ covered the synthesis of aliphatic propargylamines from aldehydes via Ellman's auxiliary based on Xiao *et al.*,⁶¹ and later described more in depth by Wünsch *et al.*,⁶² the synthesis of benzylester protected α -azido acids by diazotransfer based on Lundquist *et al.*⁶⁵ and the microwave assisted synthesis of 1,5-disubstituted triazoles. The RuAAC utilized Boc protected propargylamines, since the sulfinyl group proved itself incompatible with the microwave conditions of the RuAAC (Scheme 16).

3. Research Objective



Scheme 16. A) formation of chiral propargylamines via Ellman's auxiliary; B) diazotransfer to form benzylester protected azido acids in high yields and C) microwave assisted RuAAC to obtain triazoles, utilizing the previously obtained starting materials.

For this dissertation and future coupling scenarios a “building block” approach would be desirable, consisting of orthogonal deprotection procedures and coupling of single triazole dipeptide isomers, instead of the “submonomer” approach applied by Fröhr.¹⁰⁴ Therefore, a suitable and epimerization free coupling procedure ought to be explored.

This research objective was likewise covered by Johansson *et al.* in 2014, who synthesized several peptidotriazolamers of various lengths, comprised of 1,5-disubstituted triazoles and peptide bonds in an alternating pattern.¹⁰⁶ Johansson *et al.* had focussed on the synthesis of achiral oligomers, comprised of glycine moieties, thus avoiding the intricate synthesis of chiral propargylamines, and the coupling of racemization prone triazole dipeptide surrogates. To prevent the issue of overlapping signals in the ¹H-NMR-spectra Johansson *et al.* had to deal with, a variety of different side chain residues should be utilized to obtain a preferable number of ROESY-NMR constraints for the following conformational analysis.

Furthermore, we were interested in the influence of stereochemistry on the adopted conformations, to understand if preferred orientations are navigated by backbone influences or the different orientation of the residues. The conformational analysis of synthesized oligomers ought to be explored by X-ray crystallography and molecular modelling. With knowledge about the foldameric properties of different peptidotriazolamers, suitable biological applications depending on protein peptide interactions should be explored.

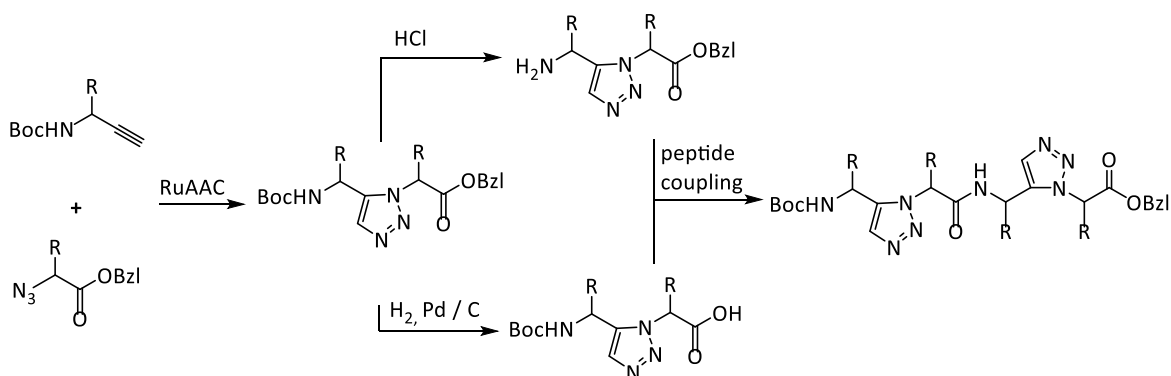
4. Results and Discussion

4.1. Synthesis of 1,5-disubstituted triazole containing peptidotriazolamers

(Part of this work was already published in “Chemistry A European Journal”:

Oliver Kracker, Jerzy Góra, Joanna Krzciuk-Gula, Antoine Marion, Beate Neumann, Hans-Georg Stammer, Anke Nieß, Iris Antes, Rafał Latajka, Norbert Sewald. (2017). 1,5-Disubstituted 1,2,3-Triazole-Containing Peptidotriazolamers: Design Principles for a Class of Versatile Peptidomimetics. *Chemistry - A European Journal*. 10.1002/chem.201704583.)¹⁰⁷

A possible synthesis route, describing the course of a “building block” approach towards peptidotriazolamers, is illustrated in **Scheme 17**.



Scheme 17. Starting with the RuAAC, the Boc/Bzl strategy allows the solution phase synthesis of peptidotriazolamers, using 1,5-disubstituted triazoles as building blocks.

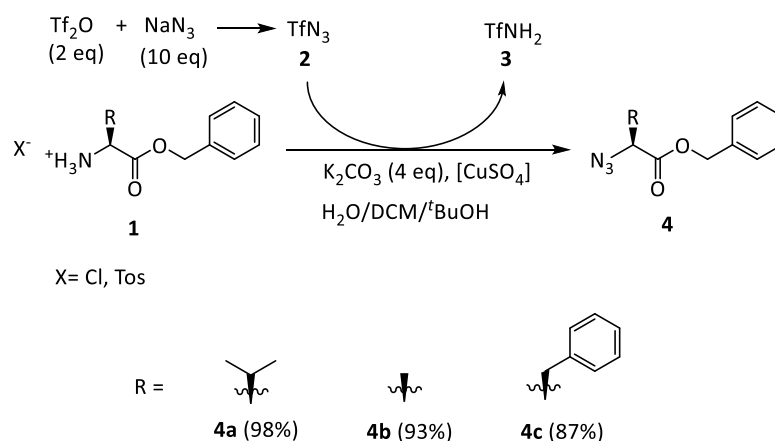
The synthesis strategy comprises of a RuAAC between Boc protected alkynes and benzelester protected azides, leading to 1,5-disubstituted triazoles in high yields without the formation of side products. Subsequent elongation of these triazoles is enabled by the orthogonal Boc/Bzl protecting group combination, which is cleavable under acidic or hydrogenolytic conditions, leading to selectively deprotected triazoles. By-products of the cleavage are removed under vacuum.

Since we were interested in peptidotriazolamers of various lengths, an oligomer synthesis in solution proved to be convenient, because each step allowed for a full characterization of the product, followed by subsequent further elongation. Previous work from our work-group¹⁰⁴ reported the elongation in a step-wise fashion in *N*-terminal direction. Coupling

4. Results and Discussion

of a free α -azido acid to a triazole, or peptidotriazolamer, followed by a cycloaddition with a propargylamine. A “building-block” approach (**Scheme 17**) offers the advantage, that single triazoles, which are valuable and interesting compounds by their own, are isolated and analysed.

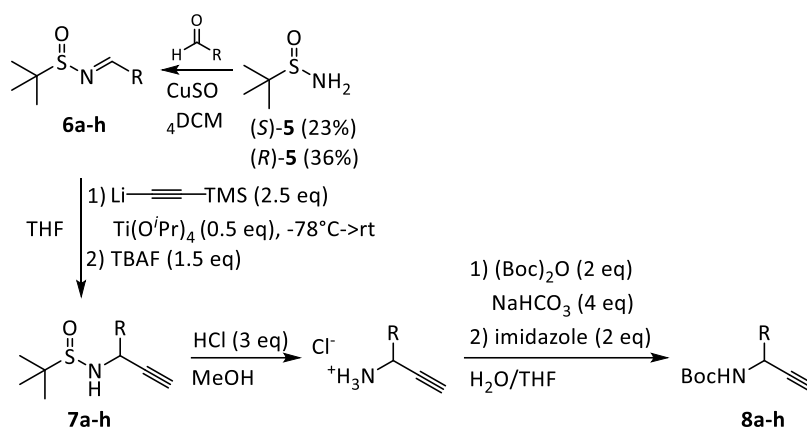
Chiral α -azido acid benzylesters **4a-c** were synthesized based on the procedure of Alper and Lundquist.^{64, 65} The azide equivalents of Val, Ala and Phe were obtained in very good yields of $\geq 87\%$ starting with commercially available amino acid benzylesters **1** by a copper(II) catalysed diazotransfer reaction with triflyl azide **2** (**Scheme 18**).



Scheme 18. The α -azido acids as analogues of Val, Ala and Phe were successfully synthesized by diazotransfer with Tf-N₃.

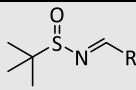
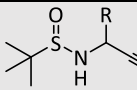
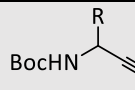
In contrast to the group of Pelletier, which established an aqueous workup to separate the trifluoromethanesulfonamide (**3**) from their free azido-acids by exploiting their different pK_a-values, a column chromatography was used to obtain the azido acid benzylesters. Moreover, a transesterification reaction from the benzylester to the methylester was noticed, facilitated by methanol under basic conditions. This could be prevented by using the less acidic and less nucleophilic *t*BuOH as a co-solvent.

The synthesis of (*R*)- and (*S*)-configured propargylamines was realized with Ellman's auxiliary as described by Wünsch *et al.* (**Scheme 19** and **Table 2**).⁶² Both enantiomers of Ellman's auxiliary were synthesized in enantiomerically pure form according to the group of Ellman, with a yield of 36% for (*R*)-**5** and 23% for the (*S*)-**5** enantiomer.¹⁰⁸



Scheme 19. Aliphatic aldehydes react with Ellman's auxiliary **5** to generate chiral sulfinamidines **6a-h**. Nucleophilic addition of ((trimethylsilyl)ethynyl)lithium followed by deprotection with TBAF affords the propargylamines **7a-h**. Acidic methanolysis of the Bus-group, followed by Boc protection lead to Boc-protected propargylamines **8a-h** in acceptable to high yields over two steps.

Table 2. Yields during the propargylamine synthesis. The synthesis of Bus protected propargylamines entails two steps (acetylide addition and TMS cleavage). As well for the Boc protected propargylamines (Bus deprotection and Boc introduction).

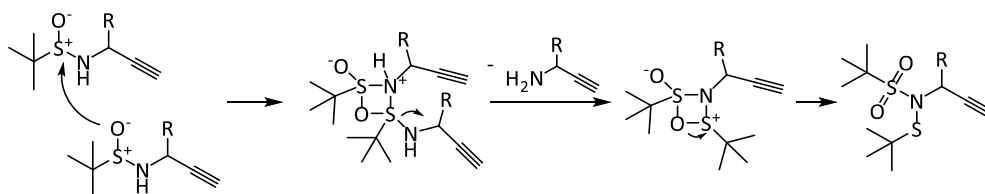
R =	 6		 7		 8	
	(R)	(S)	(R, R)	(S, S)	(R)	(S)
Methyl	6a (81%)	6b (80%)	7a (49%)	7b (46%)	8a (85%)	8b (61%)
Isopropyl	6c (90%)	6d (71%)	7c (45%)	7d (67%)	8c (90%)	8d (56%)
Isobutyl	6e (79%)	6f (93%)	7e (46%)	7f (52%)	8e (94%)	8f (82%)
Cyclohexyl	6g (93%)	6h (46%)	7g (71%)	7h (60%)	8g (84%)	8h (86%)

Utilizing different aldehydes (acetaldehyde, isovaleraldehyde, methylbutyraldehyde and formylcyclohexane), the sulfinamidines **6a-h** were synthesized in high yields, employing MgSO_4 or CuSO_4 as Lewis acids, as described by Liu *et al.*¹⁰⁹ The nucleophilic addition of ((trimethylsilyl)ethynyl)lithium was performed according to Xiao *et al.*⁶¹, utilizing $\text{Ti}(\text{O}^i\text{Pr})_4$ as a Lewis acid in THF, deprotection with TBAF lead to Bus protected propargylamines **7a-h** in diastereomerically pure form after column chromatography.

Although the Bus group was mentioned to be a feasible substitute for the Boc group in peptide synthesis, we found it to be partially unstable towards the microwave conditions during the RuAAC. Moreover, it decomposes upon standing in polar solvents. The initial low yields of the RuAAC are reasoned with a thermal rearrangement mechanism for

4. Results and Discussion

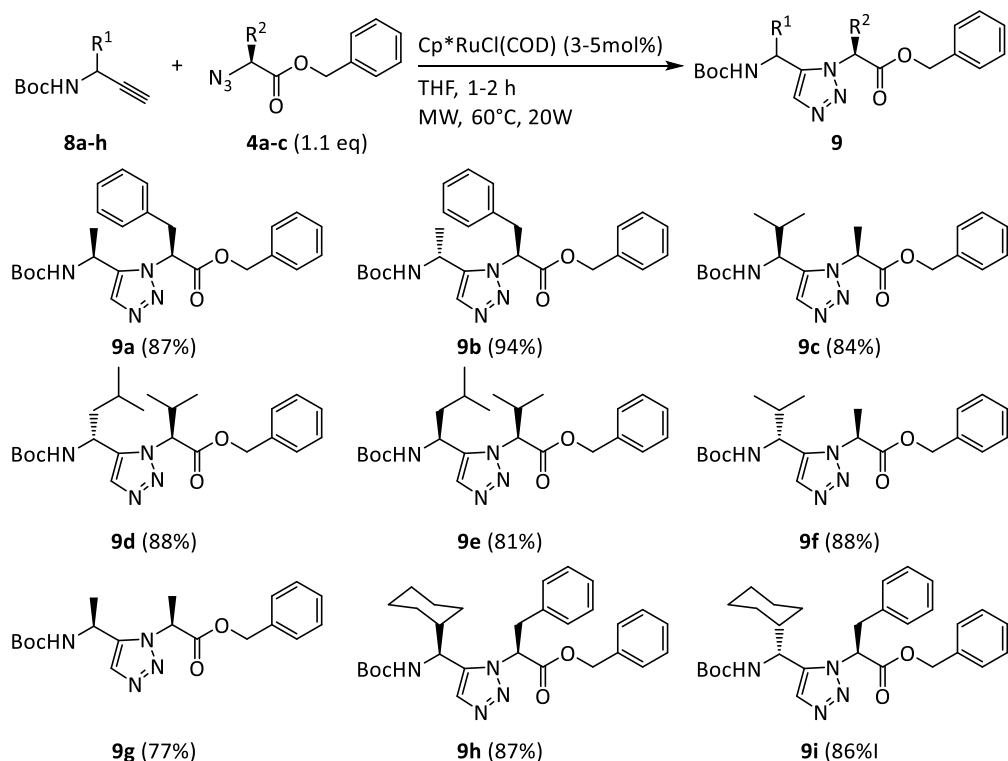
Ellman's auxiliary,¹¹⁰ which can be applied on *N*-sulfinyl protected propargylamines and triazoles. In this proposed mechanism, *N*-sulfinyl protected propargylamines react intermolecularly to form a deprotected and *N*-(*tert*-butylthio)-*tert*-butylsulfonamide linked alkyne, as the more stable forms (**Scheme 20**).¹⁰⁵



Scheme 20. The Mechanism which describes the rearrangement reaction of e.g. *N*-sulfinyl protected propargylamines, leading to an unprotected species and *N*-(*tert*-butylthio)-*tert*-butylsulfonamide linked amine.¹¹⁰

Therefore, the Bus- protected propargylamines were deprotected and the protecting group exchanged to the more stable Boc group. Based on a publication of Basel *et al.*, imidazole was used to scavenge the slight excess of (Boc)₂O, which can successively be removed by washing with diluted acid, avoiding the necessity of a column chromatography in most cases (**Scheme 19**).¹¹¹ Using this procedure, the Boc- protected (*R*)- and (*S*)-configured alkyne analogues of Ala, Val, Leu and chGly **8a-h** were successfully synthesized in enantiomerically pure form.

The RuAAC was performed under microwave conditions, where THF turned out to be a suitable solvent, regarding solubility of the starting material, boiling temperature and stability of the catalyst. In addition, degassing of the freshly distilled THF was not required. Using a slight excess of azide, the RuAAC was completed in 1-2 h in excellent yields of 77-94%, leading to different homo- and heterochiral triazoles **9a-i**, representing dipeptide isosteres (**Scheme 21**).



Scheme 21. The MW-assisted RuAAC lead to several aliphatic and aromatic 1,5-disubstituted triazoles in high to excellent yields.

The obtained triazoles proved to be highly stable, even on storing them at RT for several months. Most of them readily crystallized out of ethylacetate, methanol or isopropanol, by slow evaporation of the solvent at room temperature overnight. The obtained crystals were suitable for X-ray crystallography, once again proving the regioselectivity of the RuAAC and the configuration of the formerly propargylamines chiral centre.

The obtained crystal structures are shown in **Figure 24**, highlighting the similarity of the 1,5-disubstituted triazole with a *cis*-peptide bond, recognizable by the turn inducing properties of the triazole and distance between both α -carbons.

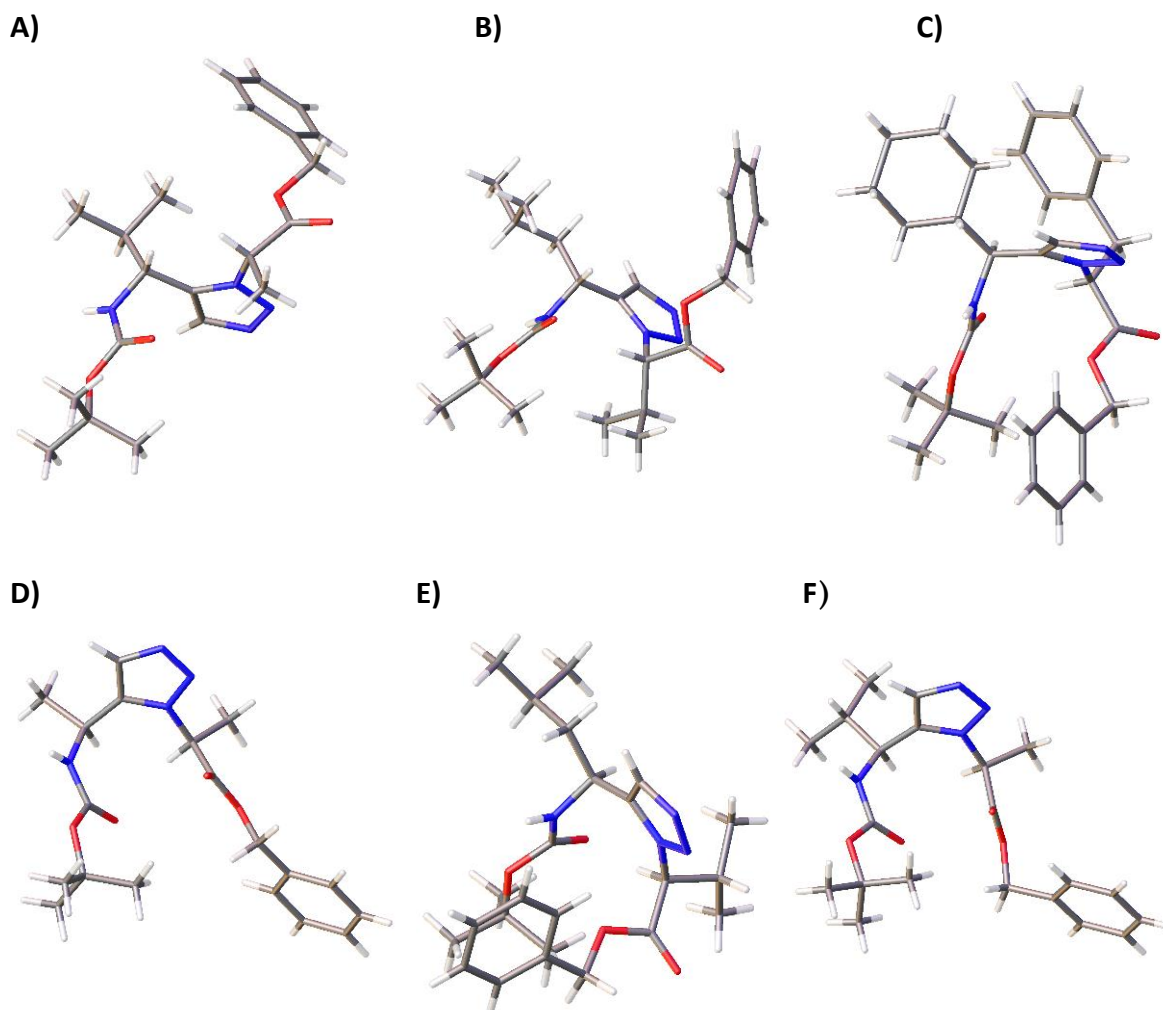


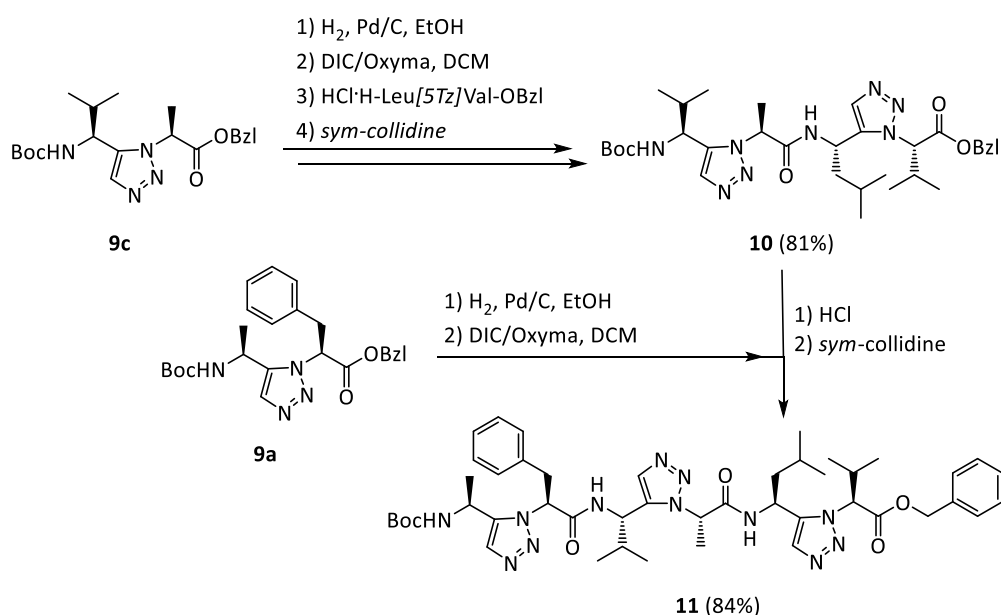
Figure 24. Obtained crystal structures of Boc protected triazoles (distance of α -carbons in Å): **A)** Boc-D-Val[5Tz]Ala-OBzl (**9f**) (3.206); **B)** Boc-D-Leu[5Tz]Val-OBzl (**9d**) (3.175); **C)** Boc-chGly[5Tz]Phe-OBzl (**9h**) (3.162); **D)** Boc-Ala[5Tz]Ala-OBzl (**9g**) (3.169); **E)** Boc-Leu[5Tz]Val-OBzl (**9e**) (3.207); **F)** Boc-Val[5Tz]Ala-OBzl (**9c**) (3.174).

Notably, in case of homochirality, the 1,5-disubstituted triazole moiety seems to result in a turn induction and reversal in direction of the peptide chain, which is not the case for both heterochiral dipeptide isomers, where the peptide chain may continue growing in the same direction, possibly leading to a more extended structure.

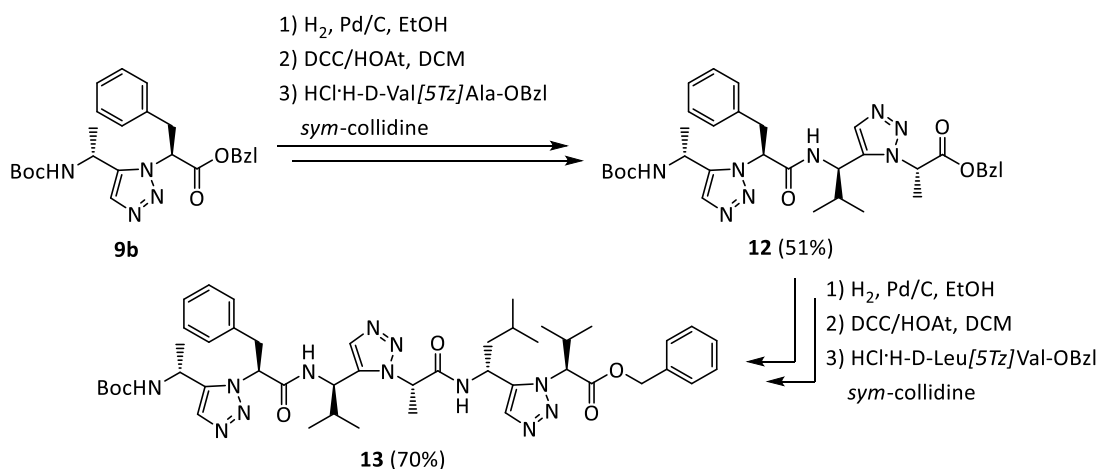
With the homo- and hetero-chiral triazole building blocks available, Boc/Bzl solution phase peptide synthesis was used for the assembly of larger oligomeric peptidotriazolamers. The acidic cleavage of the Boc- group and hydrogenolysis of the benzylester were quantitative. The deprotected derivatives were used without further purification for the peptide coupling. With TBTU or HATU as coupling reagents in DMF, either without or in combination with HOBt/HOAt and DIPEA as a base, the products were obtained in high yields, but suffered from epimerization. In contrast, a base-free carbodiimide mediated

preactivation of the carboxylic acid in DCM, in combination with OxymaPure or HOAt as an additive, followed by a *sym*-collidine facilitated coupling step, did not suffer from this shortcoming.¹⁹ A publication of Carpino and El-Faham,¹¹² which demonstrates the influence of solvent and base on the DIC/HOAt preactivation rate of amino acids, suggested to use a base-free preactivation in DCM, instead of DMF. *Sym*-collidine was used as a base for the successive coupling step, to release the free amine from the hydrochloride salt, obtained upon the Boc-cleavage and to enhance coupling efficiency.

Under these conditions, coupling proceeded in DCM without any epimerization and with high yields (**Scheme 22** and **Scheme 23**).



Scheme 22. The synthesis of the homochiral peptidotriazole tetramer **10** and hexamer **11** was performed in *N*-terminal direction, using DIC/Oxyma as coupling reagents in excellent yields.



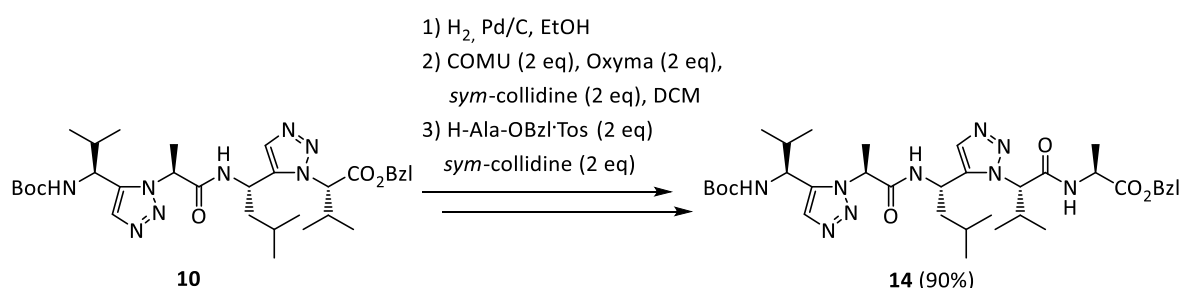
Scheme 23. The synthesis of the heterochiral peptidotriazole tetramer **12** and hexamer **13** was performed in *C*-terminal direction, employing DCC/HOAt as coupling reagents.

4. Results and Discussion

The peptidotriazolamers could be purified by either column chromatography or preparative HPLC. In contrast to Johansson *et al.*,¹⁰⁶ a drastic decrease in coupling yields between the tetramer and hexamer units was not observed. Furthermore, the carbodiimide mediated coupling seems to lead to increased coupling yields, compared to the T₃P/DIPEA system Johansson *et al.* used for their achiral oligomers. If solubility of the hydrochloride salt in DCM becomes a problem it can be dissolved in DMF and added dropwise to the preactivated acid, which is dissolved in DCM, for a final DCM/DMF ratio of 1:1 without any epimerization.

The problem of possible epimerization during the coupling of triazole dipeptide isosters was reported for 1,4-disubstituted triazoles.^{113,114} Horne *et al.* overcame this problem, by coupling with a five-fold excess of triazole/DIC/HOAt to a free amine on solid phase, without the use of any base for the coupling step. During this dissertation, a 0.1 eq excess of activated acid, in combination with *sym*-collidine as a base, proved to lead to full conversion of the amine. As a further advantage, the use of a base enables the use of synthesized and commercially available amine salts.

In addition to the homo- and heterochiral hexamer oligomers described above, which were published recently,¹⁰⁷ additional oligomers were synthesized. The peptidotriazolamer Boc-Val[5Tz]Ala-Leu[5Tz]Val-OBzl (**10**), which showed to be crystalline (CCDC 1561608) and was considered as our lead-structure for further modifications, was elongated by a simple alanine in *C*-terminal direction, however, the pentapeptide **14** failed to give any crystals (**Scheme 24**).

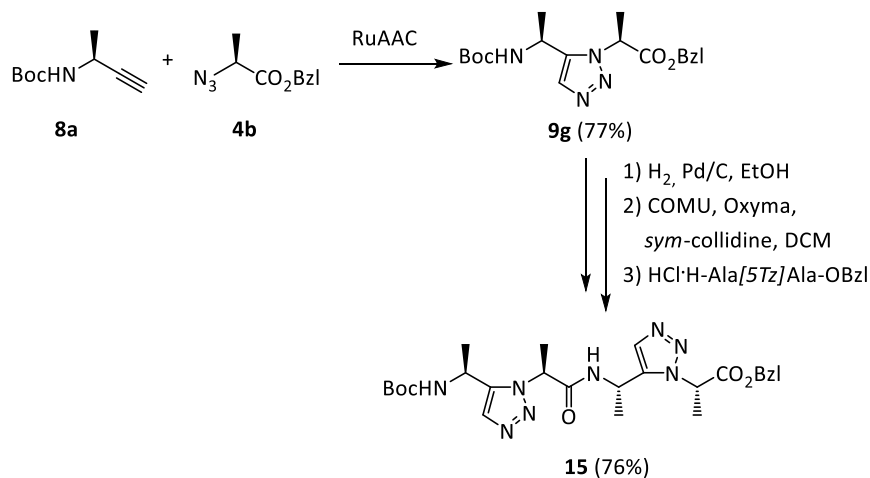


Scheme 24. Elongation of the tetramer by an alanine moiety.

Further, the possibility to analyse a simpler system, by synthesizing triazoles and oligomers based on polyalanine, was explored (**Scheme 25**).

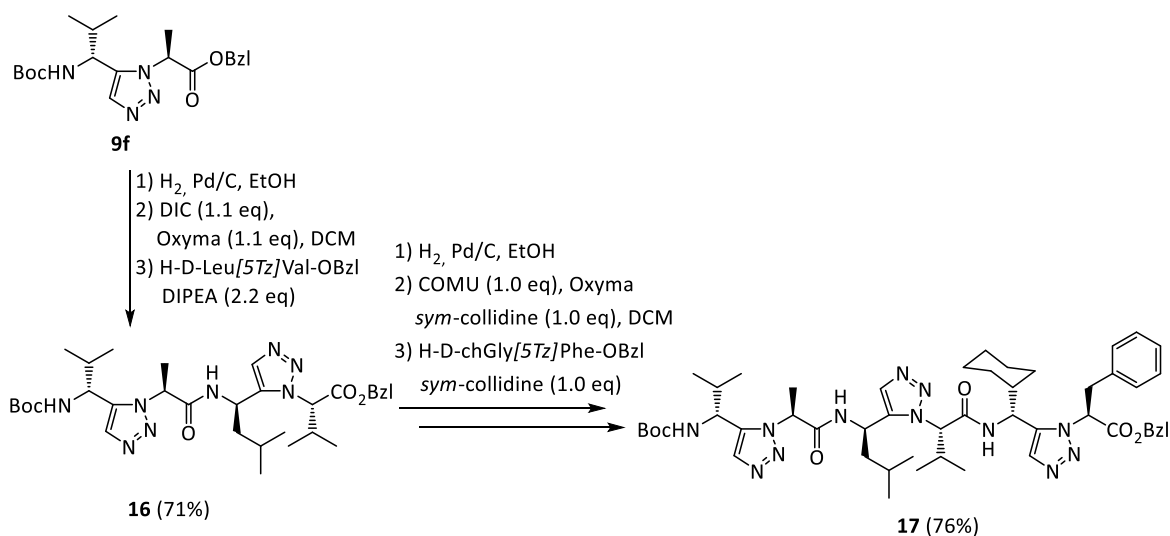
In the case of the *tetra*-alanine peptidomimetic **15**, the NMR comprised off overlapping signals, therefore the synthesis of the analogue hexamer unit was omitted. The issue of overlapping signals was also observed by Johansson *et al.* for their achiral polyglycine

oligomers, which hampers the possibility to compare calculated structures with the measured conformation in solution, by taking ROESY restraints into account. Likewise, the *tetra*-alanine peptidotriazolamer failed to give suitable crystals.



Scheme 25. Synthesis route, describing the synthesis of the *tetra*-alanine peptidotriazolamer **15**.

An additional hexameric peptidotriazolamer **17** was synthesized by solution phase peptide synthesis, however, this comprises of non-natural amino acid residues and was not addressed with comparable priority for further study (**Scheme 26**).



Scheme 26. The tetramer **16** and hexamer **17** were synthesized in *C*-terminal direction.

Noticable, some of the latter presented peptide couplings represent early modification attempts of the coupling procedure. In these, the new generation stand alone reagent COMU,¹¹⁵ in combination with Oxyma as an additive and *sym*-collidine was used in pure

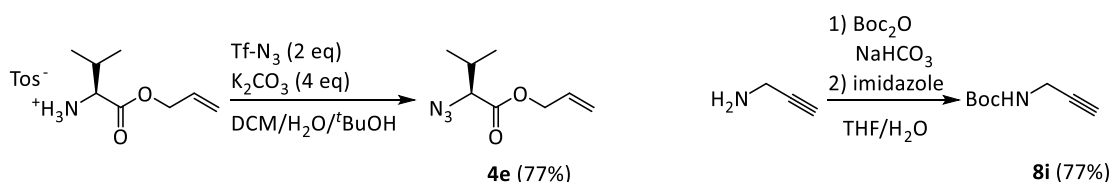
DCM, which performed without partial epimerization. However, the DIC mediated reaction, compared with stand-alone coupling reagents, scores in terms of atom economy and practical handling and proved to be highly efficient. These findings are in agreement with Fara *et al.*¹¹⁶ who demonstrated the efficiency of the DIC/HOBt system under microwave conditions for the synthesis of challenging peptide sequences on solid phase, openly questioning the necessity of more exotic coupling reagents.

In summary, a chain elongation in *N*-terminal direction, employing a slight excess of activated acid (amino acid or triazole-dipeptide in 0.1 eq excess), proved to be ideal for the synthesis of peptidotriazolamers in solution and was therefore used as a standard procedure.

4.2. Synthesis of 1,4-disubstituted triazole containing peptidotriazolamers

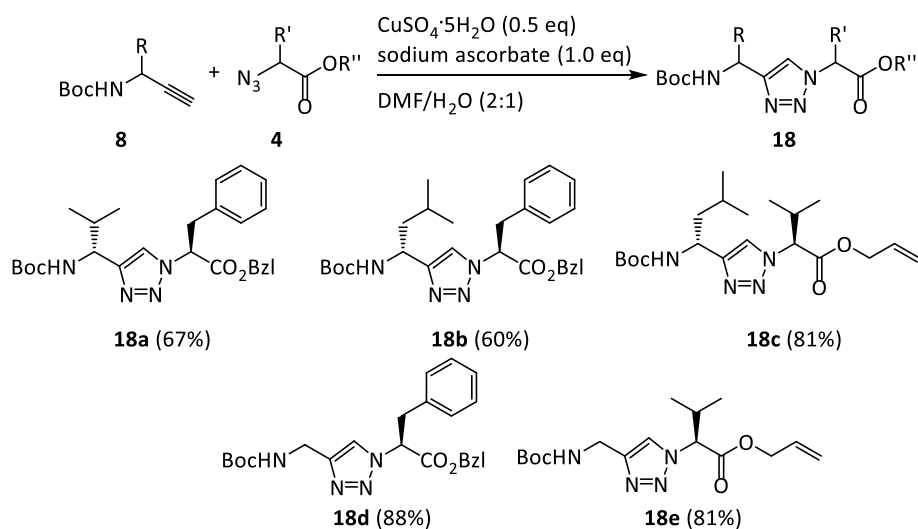
In addition to the peptidotriazolamers described above, featuring 1,5-disubstituted triazoles, two additional peptidotriazolamers were synthesized. These contain 1,4-disubstituted triazoles, to round up the set of peptidotriazolamers synthesized by Dr. Tanja Fröhr.¹⁰⁴ In contrast to the step wise synthesis strategy used by Fröhr, coupling a free azido acid in *N*-terminal direction onto the growing chain, followed by a click reaction with a Bus protected propargylamine and using the Bus/OAll protecting group pair, the synthesis strategy discussed in **Scheme 17** and demonstrated in **Scheme 22** was used.

To retain the *C*-terminal allylester of the oligomers, H-Val-OAll·TosH was converted into the α -azido acid **4e** by diazotransfer. For the oligomers with alternating stereocenter and methylene moiety, the achiral Boc protected propargylamine **8i**, was synthesized out of commercially available prop-2-yn-1-amine (**Scheme 27**).



Scheme 27. One step Synthesis of N₃-Val-OAll (**4e**) and Boc-Gly≡ (**8i**).

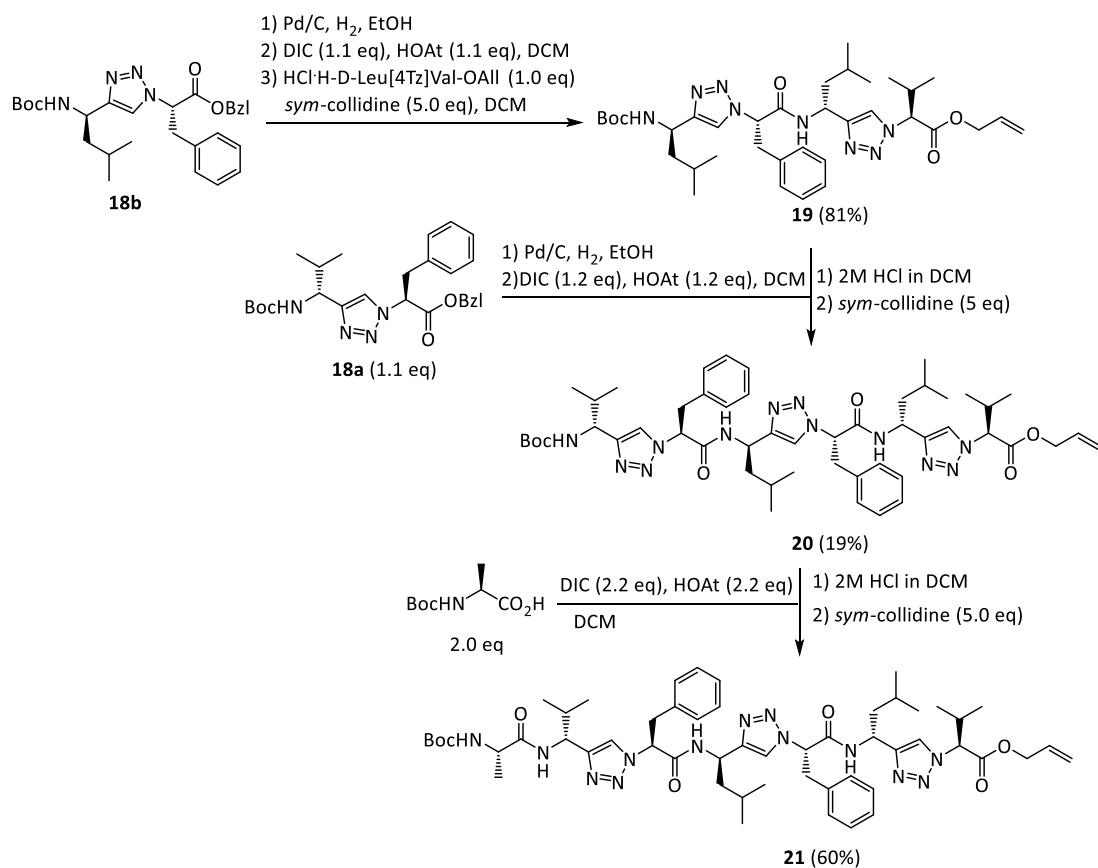
The triazoles were synthesized via CuAAC in a mixture of DMF and water, stoichiometric amounts of catalyst were required to drive the reaction to completion (**Scheme 28**).



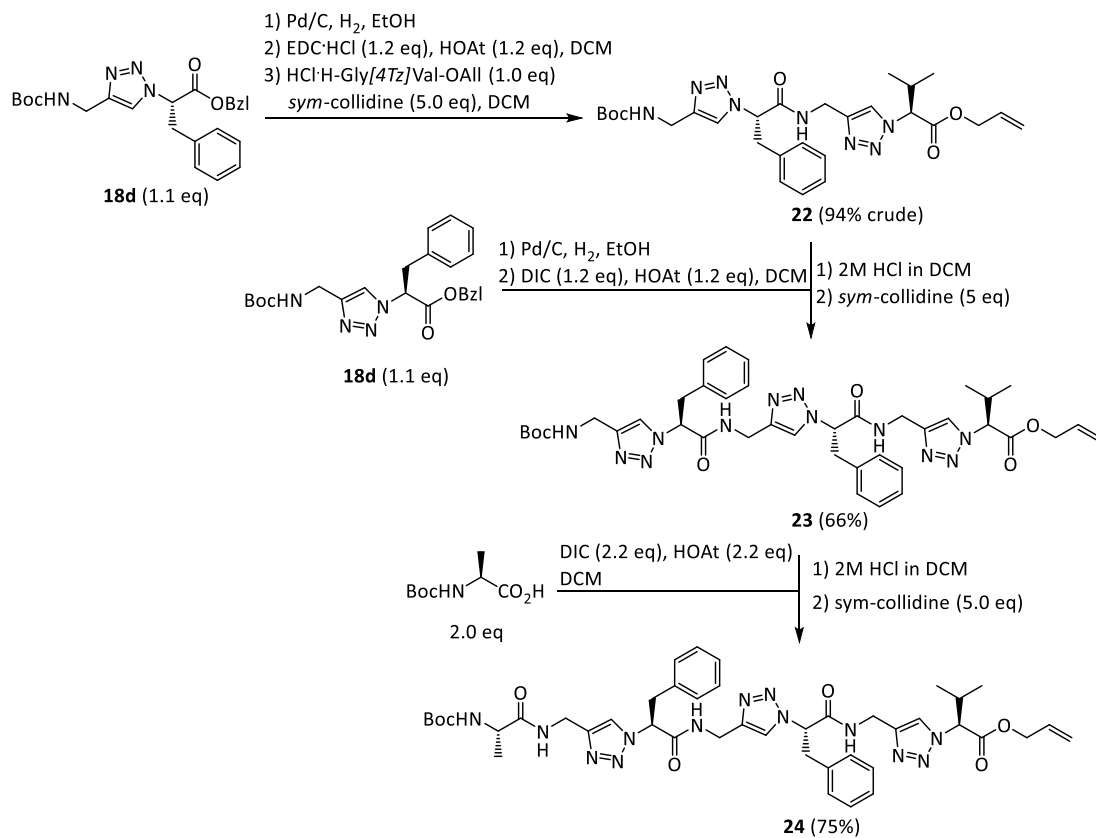
Scheme 28. The CuAAC at room temperature lead to several aliphatic and aromatic 1,4-disubstituted triazoles as benzyl- and allylestere **18a-e** in acceptable to good yields.

The triazoles obtained above were selectively deprotected with either HCl in dioxane or hydrogenolytically, the oligomer synthesis was performed with carbodiimides as described for the 1,5-disubstituted triazole containing peptidotriazolamers (**Scheme 29** and **Scheme 30**).

4. Results and Discussion



Scheme 29. Boc/Bzl solution phase synthesis of peptidotriazolamer heptamer **21**.



Scheme 30. Boc/Bzl solution phase synthesis of peptidotriazolamer heptamer **24**.

4.3. Conformational analysis

The conformational analysis of the peptidotriazolamers was done in collaboration together with the groups of Prof. Rafał Latajka and Prof. Iris Antes, by Dr. Jerzy Góra, Dr. Antoine Marión and Dr. Joanna Krzciuk-Gula,¹⁰⁷ who recently developed an AMBER based force field parametrization for 1,4- and 1,5-disubstituted triazole containing peptides, based on the triazoles and peptidotriazoles we contributed.¹¹⁷

The conformational analysis started with the *tetra*-peptidotriazolamer Boc-Val[5Tz]Ala-Leu[5Tz]Val-OBzl (**10**) and its conformation in solid state, derived from its crystal structure (Figure 25). Obtained by dissolving the compound in EtOAc (1 mg/100 μ L) and slow evaporation of the solvent overnight (CCDC 1561608).¹⁰⁷

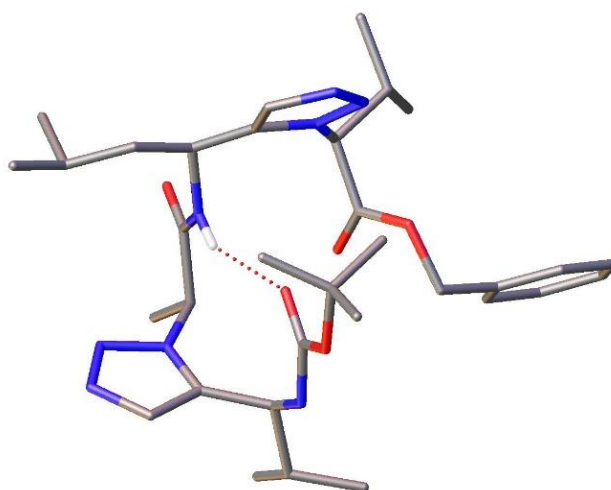


Figure 25. Solid phase conformation of Boc-Val[5Tz]Ala-Leu[5Tz]Val-OBzl (**10**).

The structure resembles a turn, induced by the 1,5-disubstituted triazoles and stabilized by an intramolecular hydrogen bond between the Boc carbonyl oxygen and the proton of the leucine amide bond, with a length of 2.08 Å.

The crystal structure offered the possibility to validate the accuracy of the developed methodology, based on the specific TZLff molecular mechanics force-field parameterization of the 1,5-disubstituted triazole based peptidomimetics. A non-restrained simulated annealing of the compound in gas phase, starting from a random conformation and performed by Dr. Antoine Marion, lead to a conformation with a nearly identical backbone orientation as the X-ray analysis (Figure 27 and Table 3).

Table 3. Torsion angles of the tetramer **10** according to X-ray analysis and molecular dynamics simulation.

Residue	$\phi_{n/c}$	$\psi_{n/c}$
	(X-ray / MD)	(X-ray / MD)
Val1	-66.4(2)° / -66.28°	132.8(1)° / 130.86°
Ala2	-112.2(2)° / -111.38°	39.8(2)° / 30.42°
Leu3	-128.6(1)° / -131.03°	57.7(2)° / 57.14°
Val4	-93.2(2)° / -100.35°	-

The torsion angles for the peptidotriazolamers are defined as followed, as the backbone differs from standard polypeptides (**Figure 26**).

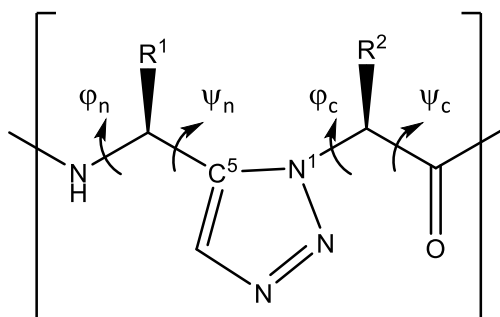


Figure 26. Defined torsion angles for this section of a peptidotriazolamer:
 $\phi_n = \text{CO-NH-C}^\alpha\text{-C}^5$; $\psi_n = \text{NH-C}^\alpha\text{-C}^5\text{-N}^1$; $\phi_c = \text{C}^5\text{-N}^1\text{-C}^\alpha\text{-CO}$; $\psi_c = \text{N}^1\text{-C}^\alpha\text{-CO-NH}$.

The similarity of both structures is expressed by the root-mean square deviation (RMSD) value, which is a measure for the average distance between atoms and was determined as RMSD= 0.37 Å for the conformational overlay (**Figure 27**).

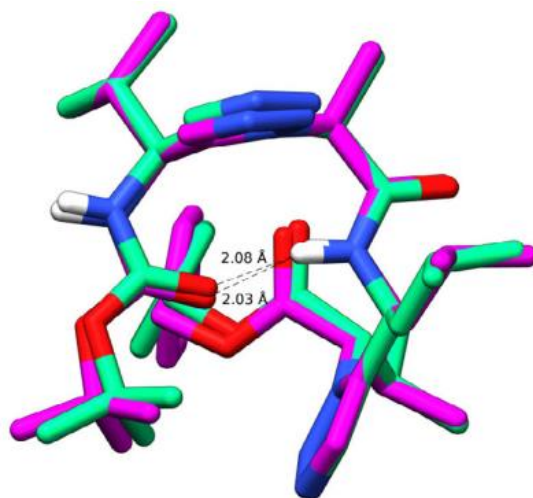


Figure 27. Overlay between the X-ray structure (green) and MD-structure (magenta) of compound **10**.

After demonstrating close agreement between X-ray analysis and the modelled conformation for the tetrameric peptidotriazolamer **10**, the methodology was used for the analysis of the hexameric structures **11** and **13**.

A comparison of torsion angles for the homochiral compound **11** between the SA calculation (gas phase) and the distance restrained MD calculation in DMSO revealed a limited number of conformations for the MD run, which oscillate around the values obtained by the simulated annealing (**Figure 28**). This confirms that the modelled structure is in close agreement to the experimental data by validating that the initial set of NMR restraints enables a similar conformational behavior.

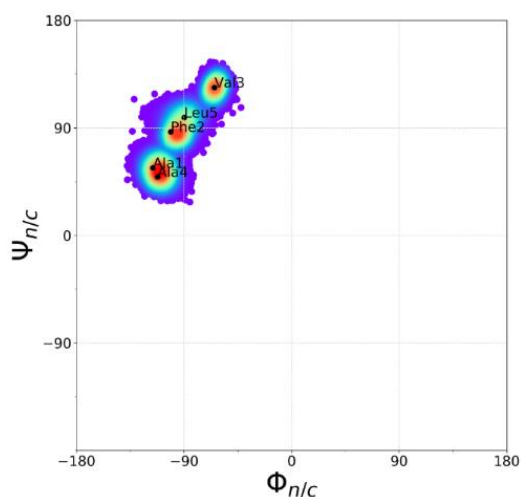


Figure 28. ψ/ϕ distribution for **11** during distance restrained MD in DMSO (values for SA represented by black dots).

The dihedral angles show close analogy to a β Vla1-turn (**Table 4**),¹¹⁸ in which the triazole backbone forms the centre and the sidechains are directed towards the solvent, this is also the case for the unrestrained MD simulations in water.¹⁰⁷

Table 4. Torsion angles for the representative structure of **11** observed during distance-restrained MD in DMSO.

	Ala1	Phe2	Val3	Ala4	Leu5	Val6
$\phi_{n/c}$	-112.9°	-92.6°	-61.1°	-108.5°	-91.3°	-166.0°
$\psi_{n/c}$	62.8°	83.1°	123.9°	52.1°	99.2°	-

The structure is stabilized by an intramolecular hydrogen bond between the carbonyl oxygen of Phe2 and the amide proton of Leu5 and shows close resemblance with its tetrameric precursor **10** (Figure 29). Interestingly, deviating from peptide chains, were the common feature between VIa1, VIa2 and VIb β turns is always a proline in position $i+3$,¹¹⁸ this is not a shared requirement for our homochiral peptidomimetics, enabling the possibility to form a β VI turn with an addressable functionality in position $i+3$ as a unique feature.

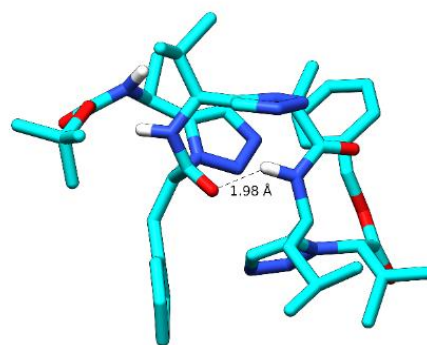


Figure 29. Representative structures for **11** derived from clustering over the last 100 ns of distance-restrained MD in DMSO.

For the heterochiral peptidotriazolamer **13** less distance restraints were found from the ROESY-NMR data (22 compared to 55 for compound **11**), indicating a more extended conformation. This is supported by the fact that the Boc group is not involved in any distance restraints.¹⁰⁷ The decreased amount of restraints and extended orientation allow for a wider variety of conformations for the sidechains and the terminal backbone, resulting in two additional basins at $-160^\circ/160^\circ$ and $160^\circ/-160^\circ$ in the Ramachandran plot compared to the simulated annealing (Figure 30).

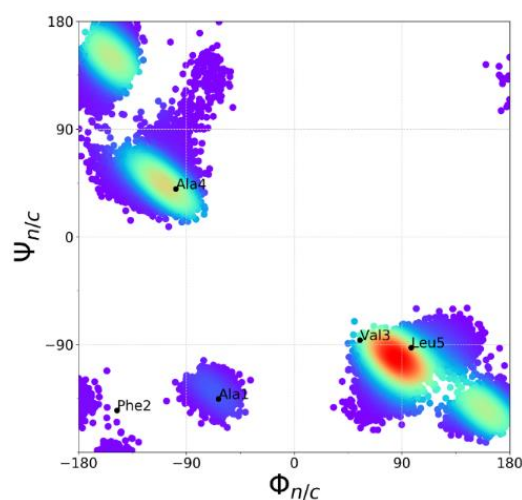


Figure 30. ψ/ϕ distribution for **13** during distance restrained MD in DMSO (values for SA represented by black dots).

The representative structure obtained from restrained MD calculations in DMSO has similarities to left-handed polyproline-I like helix, where the triazole rings are stacked on one site, and the residues are pointing towards the opposite direction (**Figure 31** and **Table 5**). In contrast to the homochiral compound, no intramolecular hydrogen bond is involved.

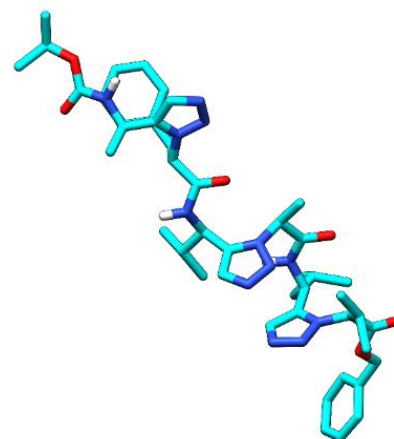


Figure 31. Representative structures for **13** derived from clustering over the last 100 ns of distance-restrained MD in DMSO.

Table 5. Torsion angles for the representative structure of **13** observed during distance-restrained MD in DMSO.

	Ala1	Phe2	Val3	Ala4	Leu5	Val6
$\phi_{n/c}$	145.6°	-135.3°	84.3°	-106.2°	92.9°	-71.9°
$\psi_{n/c}$	-140.9°	151.8°	-92.3°	43.0°	-103.3°	-

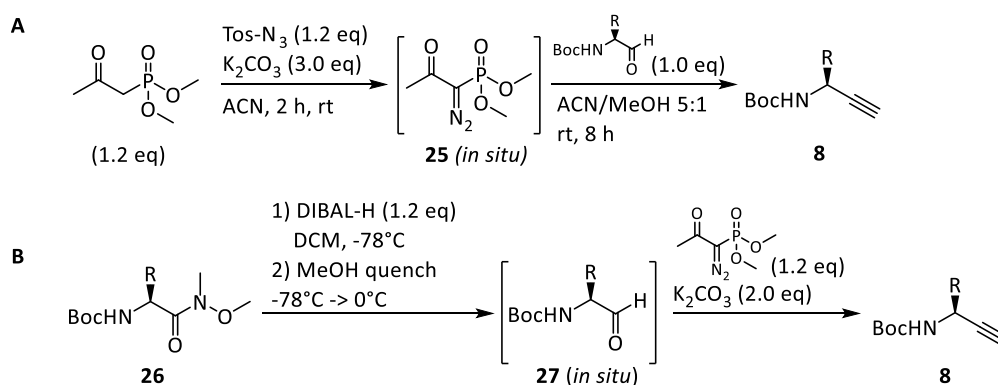
Additionally, unrestrained MD calculations in DMSO and water were performed for both compounds, to extrapolate the behaviour in a more natural environment. Although the release of the constraints resulted in more degree of freedom and the sampling of new regions in the dihedral plot, the effect was more distinct for the heterochiral compound due to its lack of intramolecular stabilization, resulting in a slightly pronounced helix in water. The overall backbone conformation for both compounds are very similar to those obtained by NMR restraint calculations.¹⁰⁷

The conformational analysis for the 1,4-disubstituted triazole containing peptidotriazolamers **21** and **24** has not been finished yet, because of encountered aggregation effects, which aggravate the ROESY-NMR assignment.

4.4. Synthesis of propargylamines with functional side chains

The propargylamines described and synthesized so far comprised of aliphatic residues, which are synthesized conveniently utilizing Ellman's auxiliary, as described in **Scheme 19** which utilizes highly reactive lithium or Grignard organyls.

For a practical synthesis of chiral propargylamines with protected functional sidechains the Bestmann-Ohira variation of the Seyferth-Gilbert homologation would be suitable.¹¹⁹ This reaction converts aldehydes into terminal alkynes by a Wittig/HWE- related reaction at mild basic conditions (**Scheme 12**). The reaction has been improved in the application by an *in situ* formation of the dimethyl 1-diazo-2-oxopropyl-phosphonate (**25**) and following addition of the aldehyde, to generate the terminal alkyne **8** (**Scheme 31 A**).^{120, 121} In 2004, Dickson *et al.* published an efficient two step one pot procedure, starting from Boc- protected amino acid methylesters or Weinreb amides **26**, followed by *in situ* reduction with DIBAL-H and subsequent Bestmann-Ohira reaction to deliver chiral propargylamines (**Scheme 31 B**).⁵²



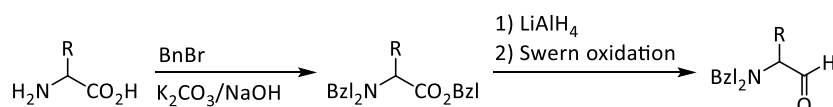
Scheme 31. Two examples of the Bestmann-Ohira reaction, where either the Bestmann-Ohira reagent **25** or the aldehyde **27** is generated *in situ*.

Although they claim that the reaction proceeds under mild conditions without loss of stereo information, if enolizable aldehydes are used, they are merely comparing the optical rotation values with former publications, which doesn't account very precisely for partial epimerization.

Applying the procedure of Dickson *et al.* starting with Boc-Phe-OMe and controlling the enantiomeric excess by chiral HPLC, Fröhr encountered partial epimerization to a changeable degree of ee= 16% and 52% after replication.¹⁰⁴ Furthermore, after triazole formation by a cycloaddition with an α -azido acid, the obtained diastereomers were not separable from each other.

A recent publication from 2017 by the group of Evans describes partial epimerization as a general feature of the Bestmann-Ohira reaction.¹²² The chiral lability of urethane protected α -amino aldehydes in aldol or Wittig reactions is further documented in the literature.¹²³

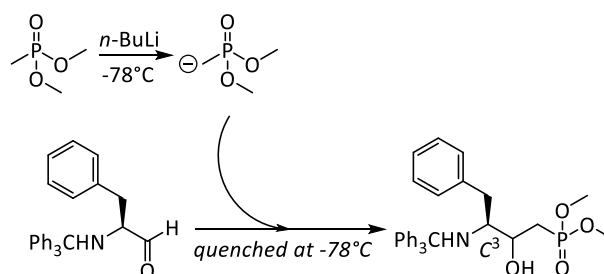
Aliphatic protecting groups, which offer a positive inductive effect, might be used as a substitute for carbamates to decrease the acidity of the alpha proton. This issue was addressed by the group of Reetz^{124, 125} with the usage of *N, N*-dibenzyl aminoaldehydes, which are accessible and isolable aldehydes and configurationally stable at room temperature (**Scheme 32**).



Scheme 32. Synthesis of dibenzyl protected α -amino aldehydes. Starting with the benzylation of free amino acids to *N, N*-dibenzyl amino benzylesters, which are reduced with LiAlH_4 to the respective dibenzylated amino alcohols, followed by a Swern oxidation to obtain the aldehydes.

These have been shown to react without loss of stereoinformation in several electrophilic reactions with organometal species, as well as aldol- and Wittig reactions.^{124, 125} However, since the benzyl group is cleaved hydrogenolytically, it cannot be cleaved on the propargylamine stage, which would result in a reduction of the triple bond. Furthermore, it would not be orthogonal to a benzylester in solution phase peptide synthesis.

The required properties are provided with the application of the acid labile *N*-trityl group, which has been successfully used by Dellaria Jr. *et al.* to add the anion of dimethyl methylphosphonate to *N*-trityl-phenylalaninal, without any racemization of the C^3 -atom of the product (**Scheme 33**).¹²⁶

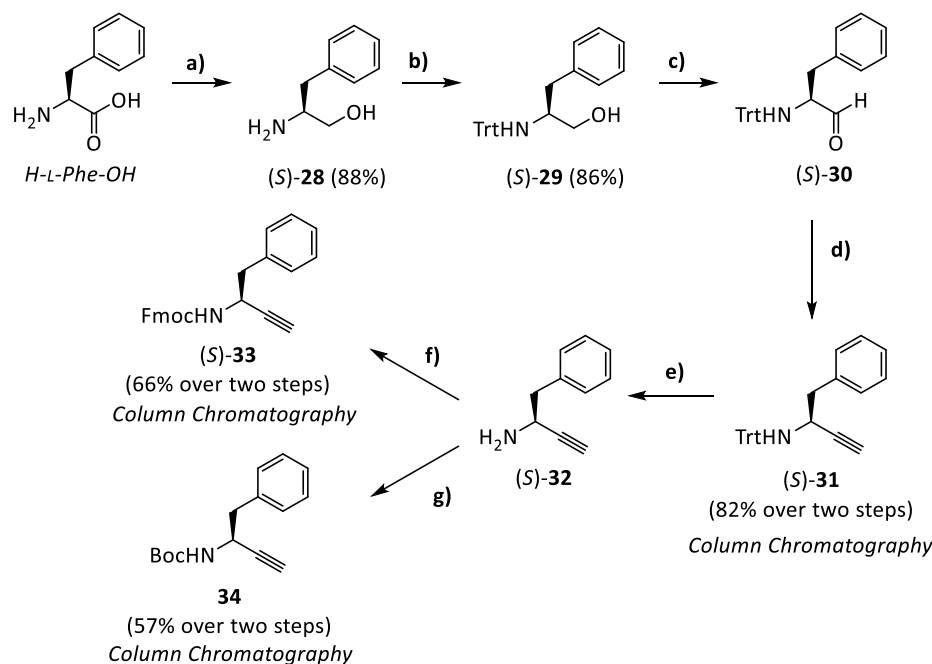


Scheme 33. The trityl protected phenylalaninal proved to be configurationally stable during nucleophilic attacks at basic conditions.

4. Results and Discussion

In a further publication they mention the comparison of the configurational stability of highly epimerization prone Boc-phenylalaninal, with *N*-trityl phenylalaninal, in presence of TEA in chloroform. The optical rotation did not change after 19 h, for the trityl protected aldehyde.¹²⁷

Since the addition of a phosphonate anion represents the first reaction step in the Seyferth-Gilbert reaction, the trityl-group was used for the Bestmann-Ohira reaction as *N*-protecting group (**Scheme 34**).

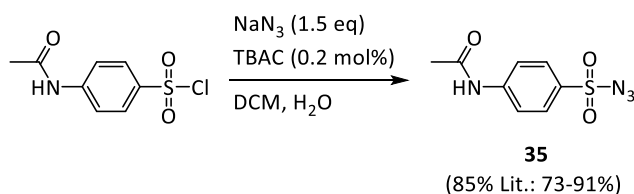


Scheme 34. Synthesis of the Boc- and Fmoc-protected propargylamine (*S*)-**33** and **34**; a) LiAlH₄ (2.0 eq), THF, 0°C 2 h, reflux, overnight; b) Trt-Cl (1.0 eq), TEA (2.0 eq), DCM, rt, overnight; c) Swern's procedure;⁵³ d) *p*-ABSA (1.2 eq), DOP (1.2 eq), K₂CO₃ (3 eq), ACN/MeOH (5:1), rt, overnight; e) DCM/MeOH/TFA (2:1:1), rt, 30 min; f) Fmoc-OSu (1.1 eq), NaHCO₃ (4 eq), THF/H₂O (1:1), rt, overnight; g) i) Boc₂O (2 eq), THF/H₂O (1:1), K₂CO₃ (4 eq), rt, overnight; ii) imidazole (3 eq), rt, 30 min.

Starting from H-Phe-OH, the phenylalaninol ((*S*)-**28**) can be obtained on multiple gram scale in good yields of 88% after reduction with LiAlH₄ and a simple extraction. On bigger scale, if desired, the inflammable LiAlH₄ can also be exchanged by the NaBH₄/I₂-system.¹²⁸ For the trityl protection step it is worthwhile to mention, that only the amino group reacts with Trt-Cl, when used in equimolar ration and the less nucleophilic alcohol moiety remains unprotected. The trityl protected amino alcohol (*S*)-**29** can be obtained in sufficient crude purity for the following Swern reaction, which likewise proceeds without side products. However, caution is advised concerning the high acid lability of the trityl group.

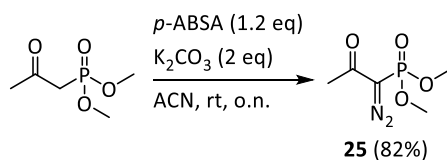
For the aqueous workup, a 10% citric acid solution is tolerated to remove residual free basic compounds, whereas commonly used dilute HCl or KHSO₄ solutions lead to a partial deprotection. If column chromatography becomes necessary, although most of the side products and remaining reagents can be removed by aqueous workup and the quantitative reaction process can be monitored by TLC, adding 1 vol% TEA into the eluent is recommended.

The Bestmann-Ohira reaction using dimethyl diazomethylphosphonate (**25**) according to the original procedure¹¹⁹ works in a very clean manner. On a bigger scale, the one-pot procedure was performed successfully, where the dimethyl diazomethylphosphonate is formed *in situ*.¹²⁰ *p*-ABSA (**35**), which is considered a safe diazo-transfer reagent, was utilized instead of Tos-N₃.¹²⁹ However, compared to Tos-N₃ it reacts more slowly, generally requiring stirring overnight, compared to the stated 2 h of the original procedure. The storable *p*-ABSA was synthesized on multi-gram scale from inexpensive starting materials (**Scheme 35**).^{129, 130}



Scheme 35. Synthesis of *p*-ABSA (**35**), starting from the sulfonyl-chloride via addition-elimination mechanism with NaN₃, the *tert*-butyl ammonium chloride serves as a phase transfer reagent.

The Bestmann-Ohira reagent **25** was obtained as a green oil after column chromatography, starting from dimethyl 2-oxopropylphosphonate and using shelf-stable *p*-ABSA as a diazotransfer reagent in high yields of 82% in acetonitrile, utilizing K₂CO₃ as a mild base by stirring overnight (**Scheme 36**).



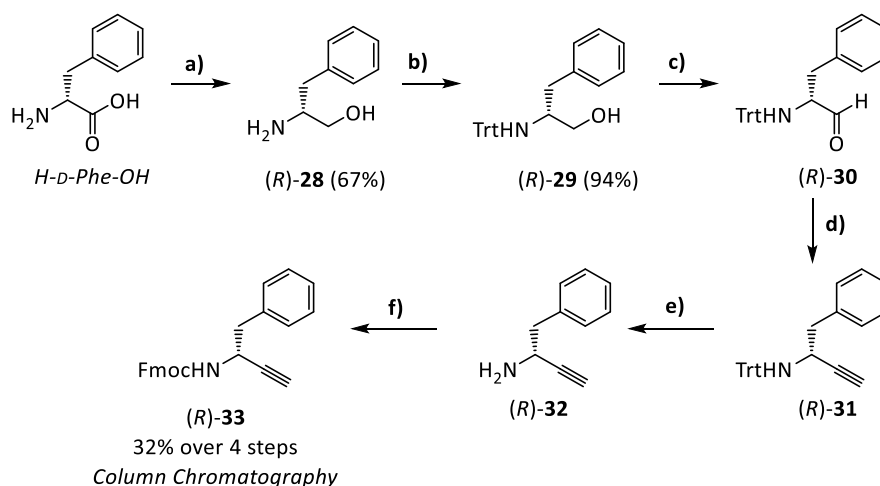
Scheme 36. Synthesis of the Bestmann-Ohira reagent (**25**), utilizing *p*-ABSA and K₂CO₃ in acetonitrile at rt.

This method avoids the usage of sodium hydride in dry THF, which is commonly used for the deprotonation of the activated methylene moiety,^{131, 132} followed by reaction with *p*-ABSA. Another advantage is the convenient nature of a one-pot process.

4. Results and Discussion

However, utilizing trityl protected propargylamines (*S*)-**31** in the RuAAC resulted in lacking conversion of the starting materials, which could be recovered after the failed reaction attempts. Therefore, the trityl group was cleaved with dilute TFA and methanol as a scavenger, followed by Boc- or Fmoc-protection without prior purification of the free amine. The Fmoc or Boc protected propargylamines (*S*)-**33** and **34** were purified by a final column chromatography and obtained in acceptable yields. Comparing the Boc-protected enantiomer via chiral HPLC with the data obtained by Fröhr,¹⁰⁴ we found it to be enantiomerically pure.

The synthesis of the D-Phenylalanine analogue propargylamine (*R*)-**33** was performed with the same method (**Scheme 37**).

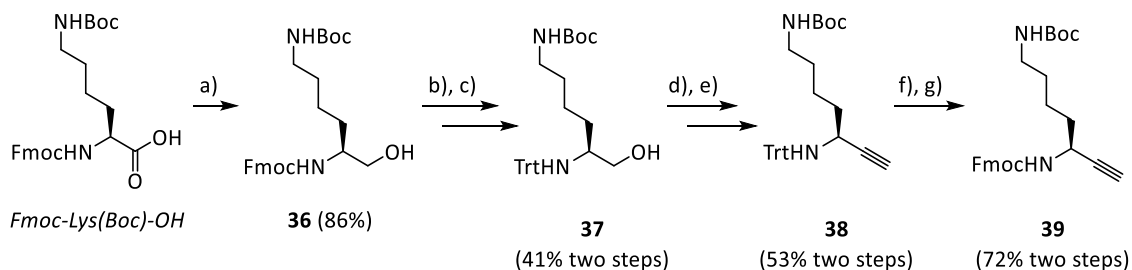


Scheme 37. Synthesis of the Fmoc-D-Phe≡ ((*R*)-**33**); a) LiAlH₄ (2.0 eq), THF, 0°C 2 h, reflux, overnight; b) Trt-Cl (1.0 eq), TEA (2.0 eq), DCM, RT, overnight; c) Swern's procedure;⁵³ d) p-ABSA (1.2 eq), DOP (1.2 eq), K₂CO₃ (3 eq), ACN/MeOH (5:1), rt, overnight; e) DCM/TFA/TES (95:2.5:2.5), rt, 30 min; f) Fmoc-OSu (1.2 eq), NaHCO₃ (4 eq), ACN/H₂O (1:1), overnight.

In contrast to the L-configured propargylamine, the column chromatography of the Trt protected propargylamine (*R*)-**33** was skipped, which resulted in an overall yield of 32% over four steps after Fmoc protection and only a single column chromatography in total (averaging 77% per step starting from D-phenylalanine).

Additionally, the possibility to apply this route for amino acids with functional side chains was investigated. Regarding solid phase peptide synthesis, a general method would be desirable, which converts commercially available Fmoc protected amino acids (bearing orthogonal sidechain protecting groups) into Fmoc protected propargylamines.

This was addressed utilizing trityl protected aminoaldehydes for Fmoc-Lys(Boc)-OH (**Scheme 38**).



Scheme 38. a) Carboxylic acid reduction.¹³³ CDI (1.3 eq), THF, rt, 10 min, NaBH₄ (1.7 eq), THF/H₂O, 0°C->rt, 30 min; b) Fmoc cleavage.¹³⁴ 1-octanethiol (10 eq), DBU (3 mol%), THF, rt, 4 h; c) Trt-Cl (1.0 eq), TEA (3.0 eq); d) Swern oxidation⁵³; e) *p*-ABSA (1.2 eq), DOP (1.2 eq), K₂CO₃ (3.0 eq), ACN/MeOH (5:1), rt, overnight; f) DCM/TFA/MeOH (92.5:2.5:5); g) Fmoc-OSu (1.2 eq), NaHCO₃ (4.0 eq), H₂O/THF (1:1), rt, overnight.

Due to the *N*-terminal Fmoc group, or ester protecting groups for several sidechain functionalities, a reduction of the weinrebamide with DIBAL-H, as described by Dickson *et al.*, is not feasible. Cleavage of the Fmoc-group followed by reduction of the carboxylic acid with LiAlH₄ under reflux condition, as in the case of the phenylalanine, would also lead to cleavage of most sidechain protecting groups. A convenient protocol of Hwang *et al.*¹³³ which converts the carboxylic acid with CDI into an activated acylimidazole and subsequently reduce it under mild conditions with NaBH₄ into the Fmoc-protected aminoalcohol **36** was used. Alternatively, an activation with DCC and *N*-hydroxysuccinimide, followed by NaBH₄ reduction would be feasible, as demonstrated by Jadhav *et al.*¹³⁵

In terms of product isolation in solution phase the cleavage of the Fmoc group is not as straightforward as for its solid phase pendant, where the free amine is immobilized on solid phase and the dibenzofulvene-adduct can be simply washed off. A procedure from Sheppeck II *et al.*¹³⁴ which cleaves the Fmoc group with catalytic amounts of DBU and uses thiols to trap the dibenzofulvene, followed by removing the dibenzofulvene-thiol adduct by trituration with petroleum ether, was used. The free amine remains as a colourless oil in sufficient crude purity.

The subsequent trityl protection is performed utilizing equimolar ratios of Trt-Cl, leaving the remaining hydroxyl group unprotected **37**. The propargylamine **38** is formed by a Bestmann-Ohira reaction of the trityl protected aminoaldehyde, which is obtained by a previous Swern oxidation.

4. Results and Discussion

Overall the Fmoc-protected propargylamine **39** was obtained in 13% yield, starting from Fmoc-Lys(Boc)-OH over seven steps (averaging 75% per step), utilizing just two column chromatographies. A possible improvement might be the application of polymer bound thiols, which would improve the execution of the Fmoc deprotection, by avoiding the trituration step and possibly, lead to improved yields at this step.

A further development and alternative to the trityl group is the phenyl fluorenyl (Pf) group, introduced in the 1980s.¹³⁶ The Pf group resembles the trityl group but is up to 6000 times more solvolytically stable towards acids and has been proven to effectively prevent racemization of α -amino acid derivatives in enantiospecific synthesis. However, stoichiometric amounts of lead are required for the introduction of the Pf group (**Scheme 39**).



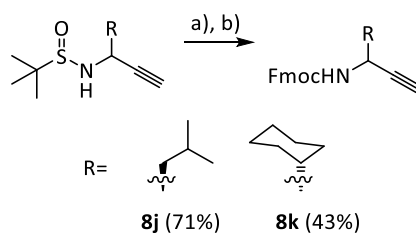
Scheme 39. The Pf group can be introduced to amino acid esters and silylesters. The lead forms a salt with the bromide to enhance its leaving group capability.

The Pf group is commonly cleaved hydrogenolytically or under strong acidic conditions. Depending on the situation, it could be used with benzyl or allyl type sidechain protecting groups.

4.5. KLVFF aggregation inhibitors

After establishing reliable and convenient procedures for the synthesis of peptidotriazolamers, this concept of peptidomimetics should be investigated in a biological context.

Based on the publication of Arai *et al.*,¹³⁷ who synthesized several derivatives of the KLVFF-sequence and quantified their ability to inhibit A β aggregation by ThT-fluorescence assay, several peptidotriazolamers were synthesized. The L[5Tz]V dipeptide isoster **18e** was already synthesized during the conformational analysis part of this dissertation. The propargylamines based on Phe **33** and **34** were synthesized utilizing trityl protected phenylalaninal in the Bestmann-Ohira reaction, as described in **Scheme 34** and **Scheme 37**. Additionally, the Fmoc protected propargylamine Fmoc-Leu \equiv (**8j**) and Fmoc-D-chGly \equiv (**8k**) were synthesized, for a convenient application on solid phase, starting from the sulfinyl protected alkyne **7f** and **7g** (**Scheme 40**).



Scheme 40. Sunfinyl cleavage and Fmoc introduction. a) 4 M HCl in dioxane (3.0 eq), MeOH, rt, 30 min; b) Fmoc-OSu (1.2 eq), NaHCO₃ (4.0 eq), H₂O/THF (1:1), overnight.

With the azides and *N*-protected propargylamines available, CuAAC and RuAAC reactions were performed, which lead to additional different triazole dipeptide isosters in good yields (**Figure 32**).

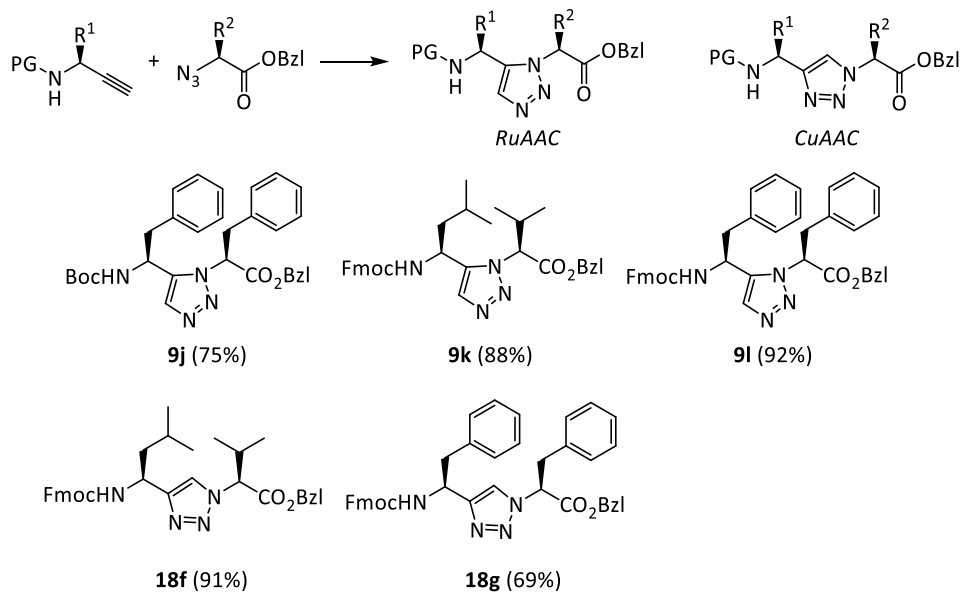


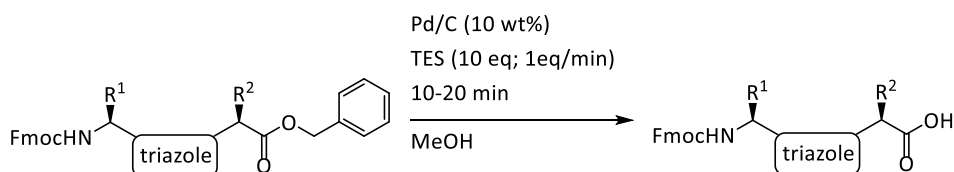
Figure 32. Several 1,4- and 1,5 disubstituted triazoles, mimicking LV and FF dipeptides, where successfully synthesized by either CuAAC or RuAAC in good to excellent yields.

The yield for the Fmoc-protected Fmoc-Phe[4Tz]Phe-OBzl (**18g**) turned out to be lower, which can be explained due to its poor solubility in the aqueous reaction mixture and the (PE/EtOAc) eluent mixture utilized for the column chromatography. Interestingly, this was not the case for the 1,5-disubstituted triazole and seemed to be a unique feature of its 1,4-disubstituted regioisomer.

The connection between both dipeptide mimetics L[Tz]V and F[Tz]F and a commercially available lysine should be tied by a peptide bond, which would result in our desired repetitive pattern of peptide bonds and triazoles. The Boc protected triazoles were deprotected at the C-terminus, using the established hydrogenolysis procedure: dissolving the triazole in EtOH and cleaving the benzylester with 1 atm of hydrogen in presence of catalytic amounts of Pd/C. After a simple filtration through a short silica plug, the Boc protected free acids were obtained in analytically pure form.

Although the Fmoc group is widely considered as orthogonal towards hydrogenolysis conditions,¹³⁸ we encountered partial deprotection of the Fmoc group, applying this procedure to the Fmoc protected triazoles. Further examples of this undesired deprotection can be found in the literature.¹³⁹ Maegawa *et al.* published the hydrogenolysis of the Fmoc group as a novel additional deprotection method,¹⁴⁰ which is accelerated in the presence of acetonitrile.

A Pd/C catalysed transfer hydrogenation with triethylsilane, as published by Mandal *et al.*,¹⁴¹ proved as a suitable and mild method (**Scheme 41**), avoiding the necessity to change the protection group strategy to Fmoc/*t*Bu. The reaction involves the *in situ* generation of H₂, which results in reduction of multiple functional groups (azides, imines, nitro groups, benzyl groups, allyl groups, unsaturated carbon bonds) by explicitly leaving the Fmoc group intact. Notably, the reaction cleaves benzyl groups as well as allyl groups, implying the formation of molecular hydrogen, as well as highlighting the hydride donor capability of the silane.



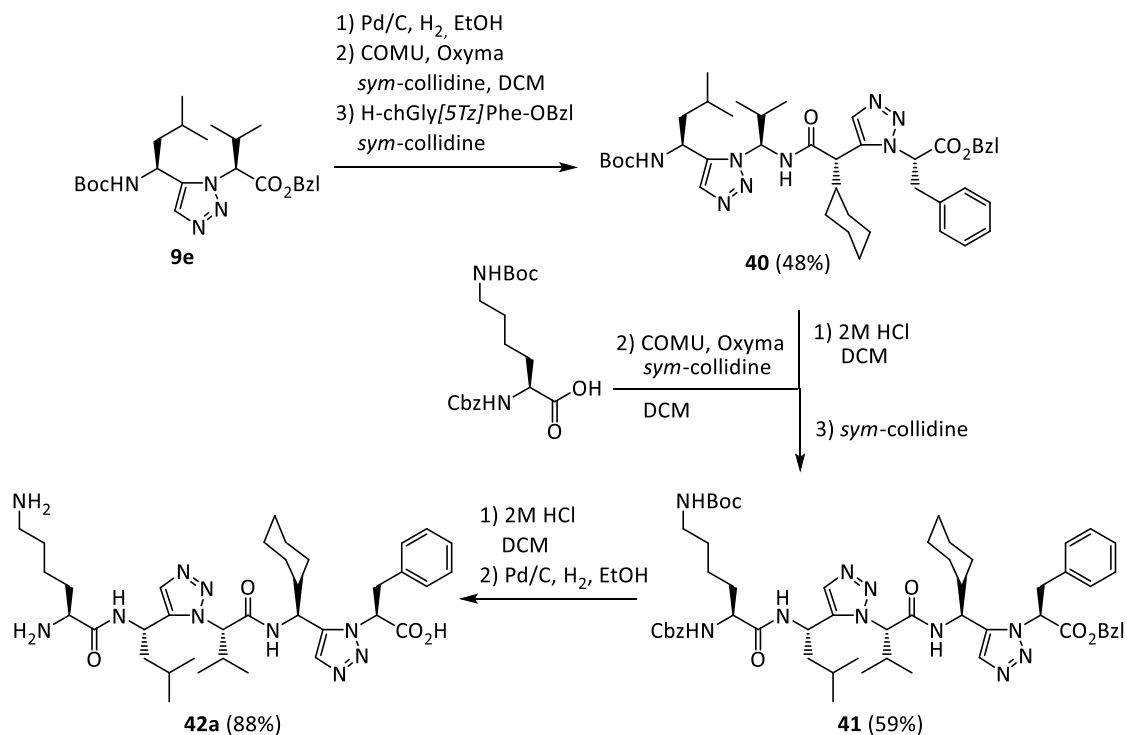
Scheme 41. The TES induced benzylester cleavage reaction consists of a Pd catalysed transfer hydrogenation, resulting in quantitative cleavage of a benzylester in presence of the *N*-terminal Fmoc group.

Standard Fmoc-SPPS protocols on Rink-amide and Barlos resin, as well as solution phase Boc/Bzl peptide synthesis were used for the generation of the compound library, in which triazoles were used as dipeptide isosters.

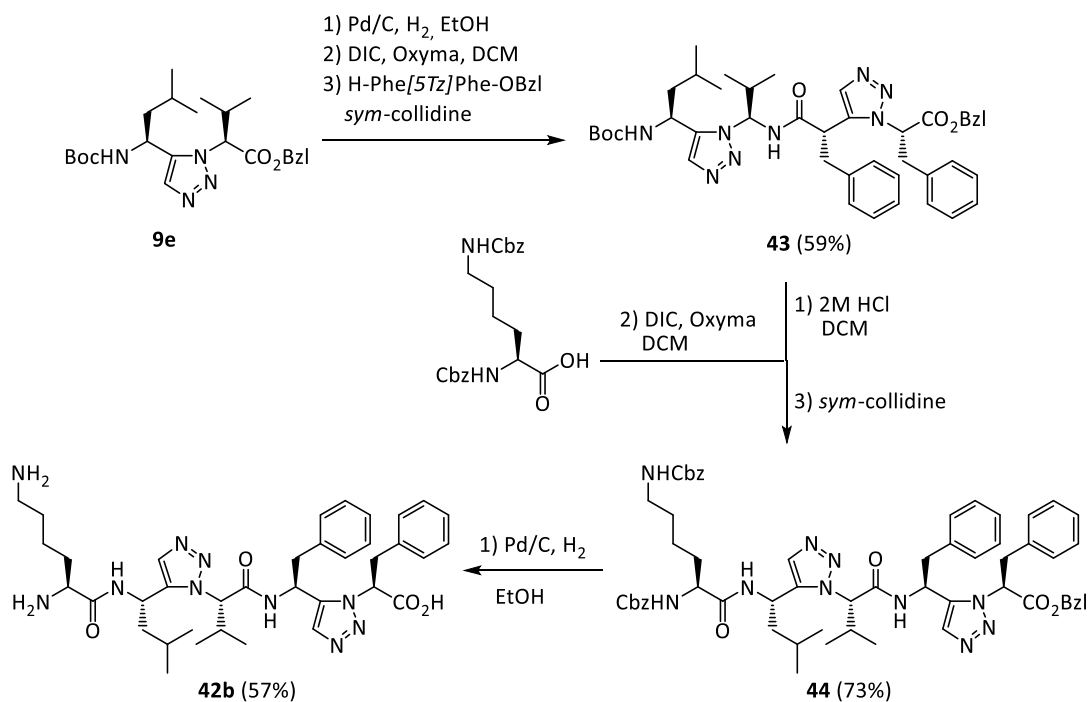
Oxyma was preferred as a coupling additive over the benzotriazoles, as it results in better solubility of the Fmoc protected active esters in DCM.

The peptidotriazolamers H-Lys-Leu[5Tz]Val-chGly[5Tz]Phe-OH (**42a**) and H-Lys-Leu[5Tz]Val-Phe[5Tz]Phe-OH (**42b**) were synthesized in solution, with minimal excess of activated carboxylic acid (**Scheme 42** and **Scheme 43**). The cyclohexyl containing oligomer **42a** was synthesized as an alternative to the usual benzyl residue, as the propargylamine is readily available by the Elman route. Cbz-Lys(Cbz)-OH was utilized for the peptidotriazolamer **42b** on the last coupling step, which offers the convenient option to cleave all protecting groups at once by hydrogenolysis.

4. Results and Discussion



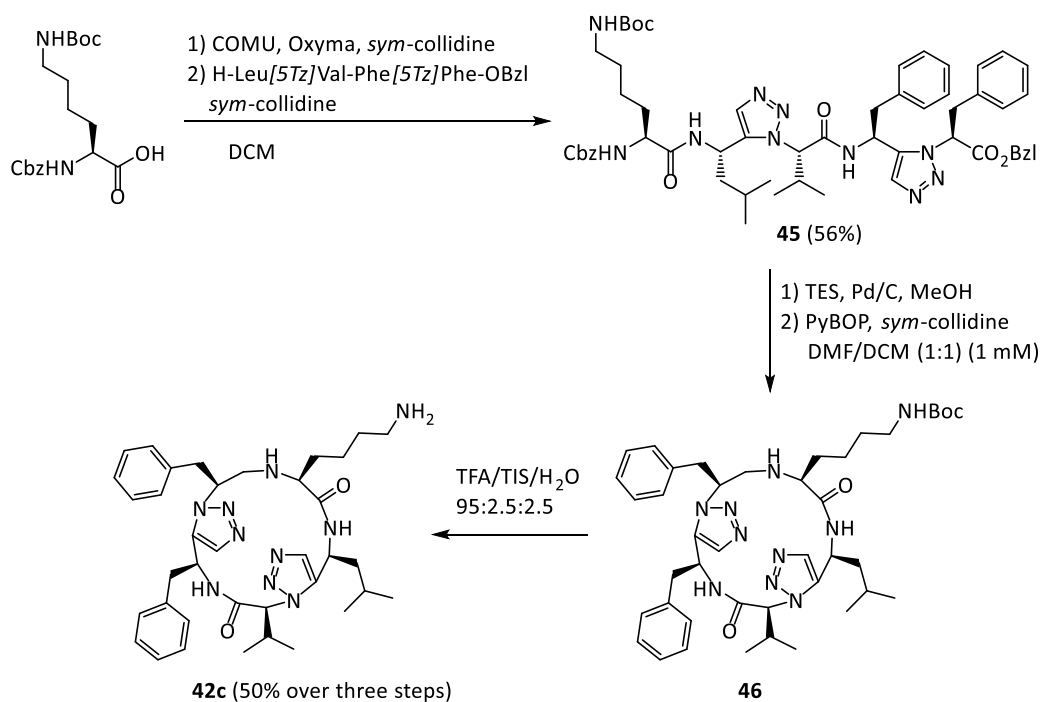
Scheme 42. Synthesis of H-Lys-Leu[5Tz]Val-chGly[5Tz]Phe-OH (**42a**) by solution phase peptide synthesis, employing COMU and using triazoles as dipeptide mimetics.



Scheme 43. Synthesis of H-Lys-Leu[5Tz]Val-chGly[5Tz]Phe-OH (**42b**) by solution phase synthesis, using DIC/Oxyma mediated preactivation and successive coupling step with *sym*-collidine as a base.

Based on the publication of Arai *et al.*¹³⁷ we were also interested in a cyclic compound, which has generally additional proteolytic stability and potentially improved pharmacophoric properties. It should be composed of 1,5-disubstituted triazoles, which might facilitate the cyclisation through their turn inducing properties.

The synthesis was once again performed by orthogonal Boc/Bzl chemistry, and based on the linear precursor Cbz-Lys(Boc)-Leu[5Tz]Val-Phe[5Tz]-OBzl (**45**) (**Scheme 44**).



Scheme 44. Synthesis of a cyclic peptidotriazolamer **42c**. PyBOP was utilized for the cyclization step, to prevent capping of the free *N*-terminus.

The three-step reaction starting from the linear precursor **45** could be monitored by analytical HPLC and worked with full conversion for all steps (**Figure 33**).

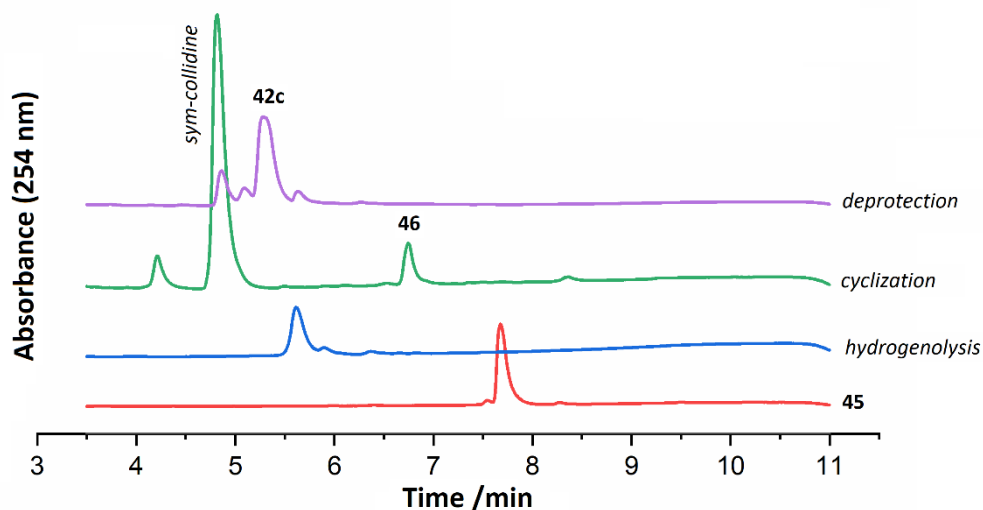


Figure 33. Chromatogram section displaying the reaction process of **Scheme 44**. Starting with the purified protected linear precursor **45** (red), the debenzylated product (blue) is obtained in pure form after hydrogenolysis and lyophilization. Cyclization is performed with full conversion (green, the chromatogram represents the reaction control, also displaying the excess of *sym*-collidine). After evaporation and lyophilization, **46** is deprotected to yield **42c** (violet), which is finally purified by preparative HPLC.

The cyclization under diluted conditions of 1 mM effectively prevented the formation of dimers or oligomers. PyBOP was utilized as a coupling reagent for the cyclization to prevent a common chain-termination reaction by guanidinylation of the free *N*-terminus, observed with uronium reagents.

The peptidotriazolamers with a *C*-terminal primary amide function were synthesized on solid phase, utilizing a polystyrene based Rink amide resin (**Figure 34**).

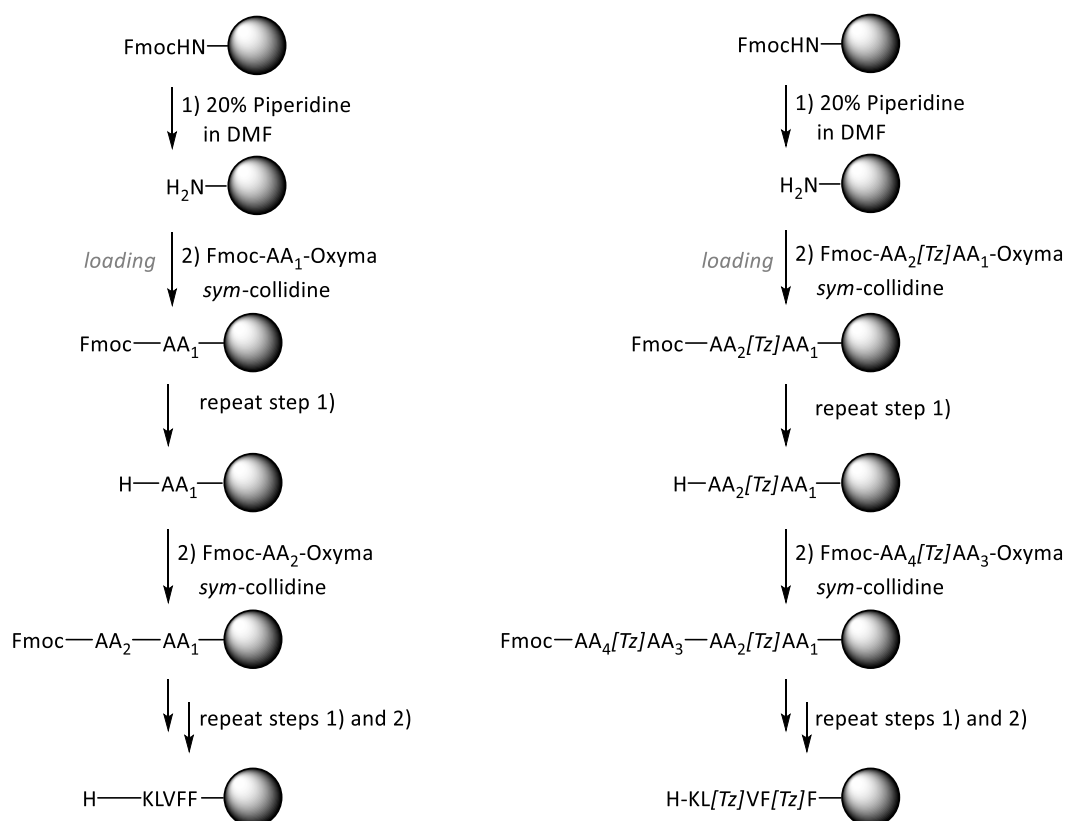


Figure 34. The Peptides were assembled by Fmoc SPPS. The activated amino acids are obtained in a separate flask, by preactivation with DIC/Oxyma in DCM for 5-10 min. The final peptide can be obtained by cleavage through concentrated TFA.

4. Results and Discussion

This led to the following additional peptides and peptidomimetics **42d-I**, which were analysed in their ability to inhibit A β -fibrillization in a ThT fluorescence assay, by Dr. Kaffy from the group of Prof. Ongeri (**Figure 35**).

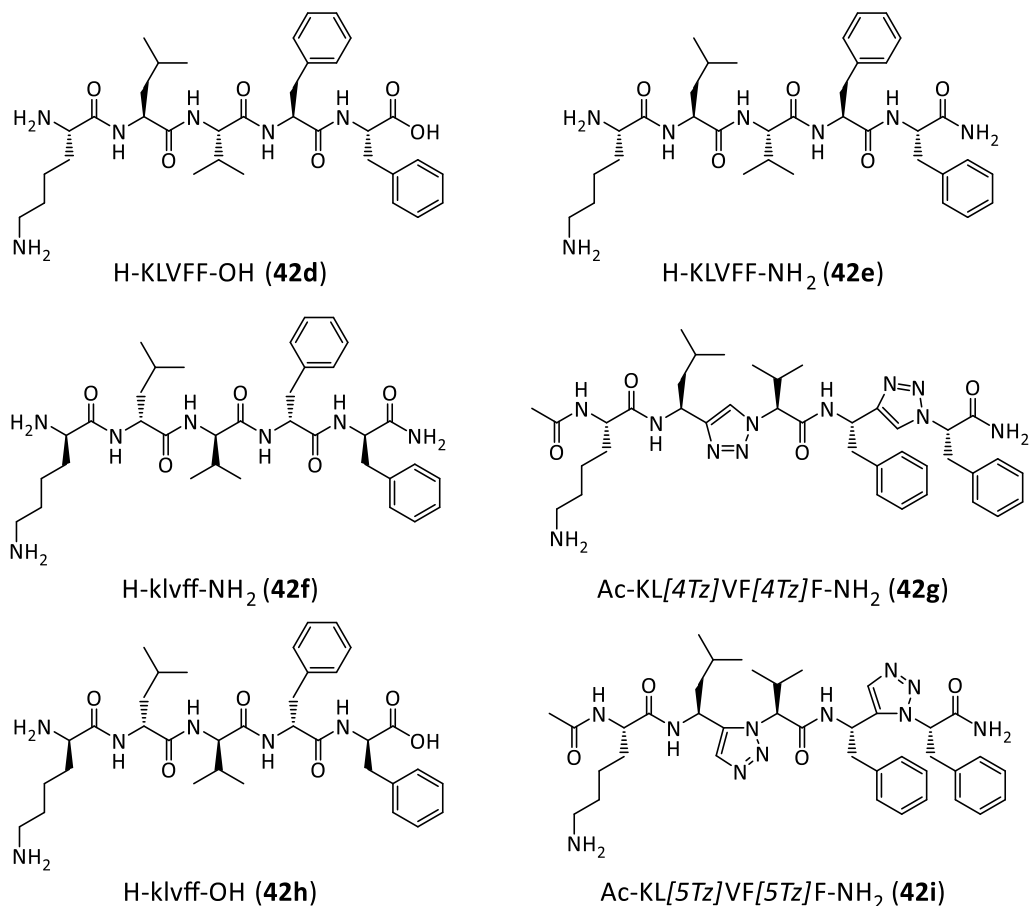


Figure 35. Peptides and Peptidotriazolamers which were obtained by SPPS, utilizing Rink amide and 2-CTC resins.

The *N*-methylated peptide SEN304 with the sequence H-D-[chGly-Tyr-chGly-chGly-(NMe)Leu]-NH₂,^{142, 143} published by Kokkoni *et al.* in 2006 as a potent A β aggregation inhibitor, was chosen as a second lead structure.

To stay as close to the original sequence as possible, the *N*-methylated amide bond between chGly and Leu was preserved, which leaves the positions one and three for a triazole replacement (**Figure 36**). Although, an exchange of the methylated amide bond with a 1,5-disubstituted triazole would be feasible, since *N*-alkylated amide bonds populate the *cis* configuration more readily.

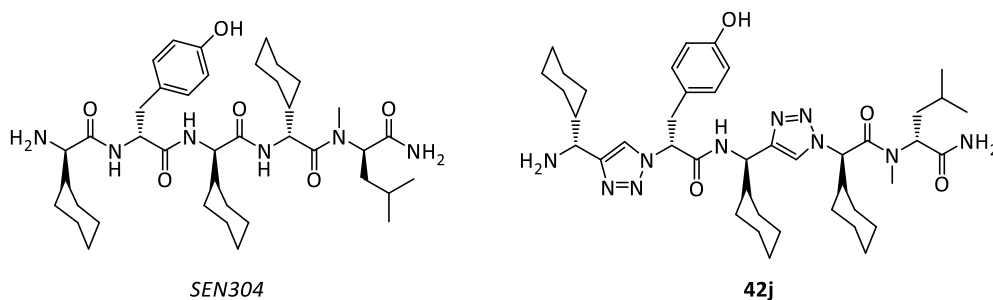
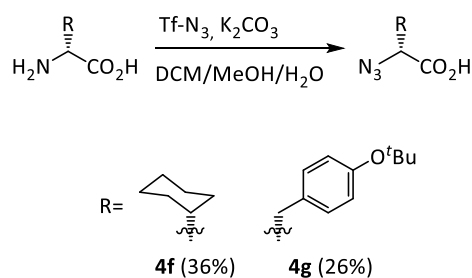


Figure 36. Comparison between SEN304 and its peptidomimetic H-D-[chGly[4Tz]Tyr-chGly[4Tz]chGly-(NMe)Leu]-NH₂ (**42j**).

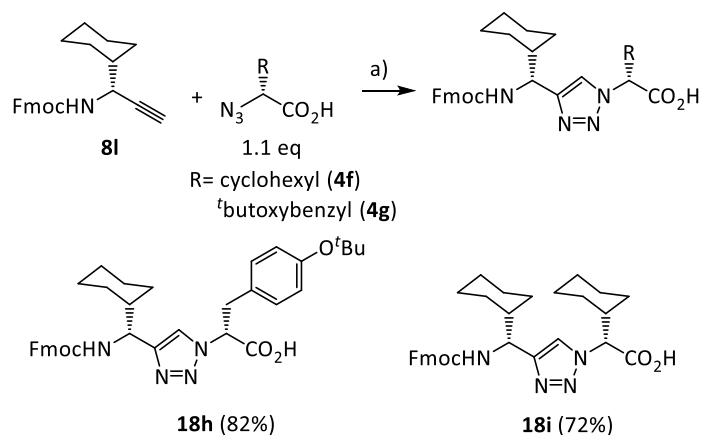
Since 1,4-disubstituted triazoles were chosen for this peptidomimetic and the CuAAC is compatible with free carboxylic acids, the azides of N₃-D-chGly-OH (**4f**) and N₃-D-Tyr(^tBu)-OH (**4g**) were prepared in their unprotected forms with the original procedure of Lundquist *et al.*⁶⁵ Instead of the column chromatography applied for the compounds **4a-e**, the procedure consists of an aqueous workup (**Scheme 45**).



Scheme 45. Synthesis of chiral azido acids.

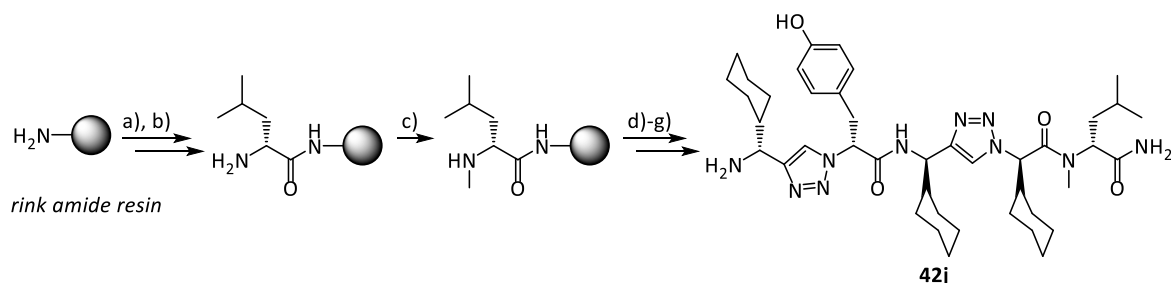
The aqueous slurry of the reaction mixture is diluted with phosphate buffer (pH 6.2) and extracted with EtOAc (4x). Since the carboxylic acid has a pK_a between 4-5, it stays deprotonated and in theory, remains in the aqueous phase, while the sulfonamide (pK_a~6.4)¹⁴⁴ remains protonated and is removed by repeated organic washing steps. Afterwards the aqueous phase is acidified to pH 2 and the product extracted with EtOAc. The yields are significantly lower than for the benzylester protected azides **4a-e**. Reasons for this might be the loss of product during the organic washing steps at pH=6.2, arising from an increased organic solubility due to the large hydrophobic residues. A column chromatography might be an alternative leading to improved yields, utilizing an eluent with 1% of AcOH as for the following triazoles **18h** and **18i**. The azides were employed in CuAAC reactions to yield Fmoc protected 1,4-disubstituted triazoles with free C-termina for subsequent coupling reactions (**Scheme 46**).

4. Results and Discussion



Scheme 46. CuAAC with the free α -azido acids **4f** and **4g** lead to 1,4-disubstituted triazoles **18h** and **18i** in good yields; a) Sodium ascorbate (1.0 eq), CuSO₄·5H₂O (0.5 eq), DMF/H₂O (2:1), rt, 1-2 days.

The solid phase synthesis was initiated with a quantitative loading of the Rink amide resin with Fmoc-D-Leucine and cleavage of the Fmoc group. The synthesis was continued with *N*-methylation according to the Chatterjee *et al.*¹⁴⁵ and coupling of the triazoles **18h** and **18i** with DIC/Oxyma/*sym*-collidine, followed by Fmoc deprotection and cleavage of the peptide with concentrated TFA. After precipitation with cold ether and purification by preparative HPLC the peptide was obtained in 14% yield (**Scheme 47**).



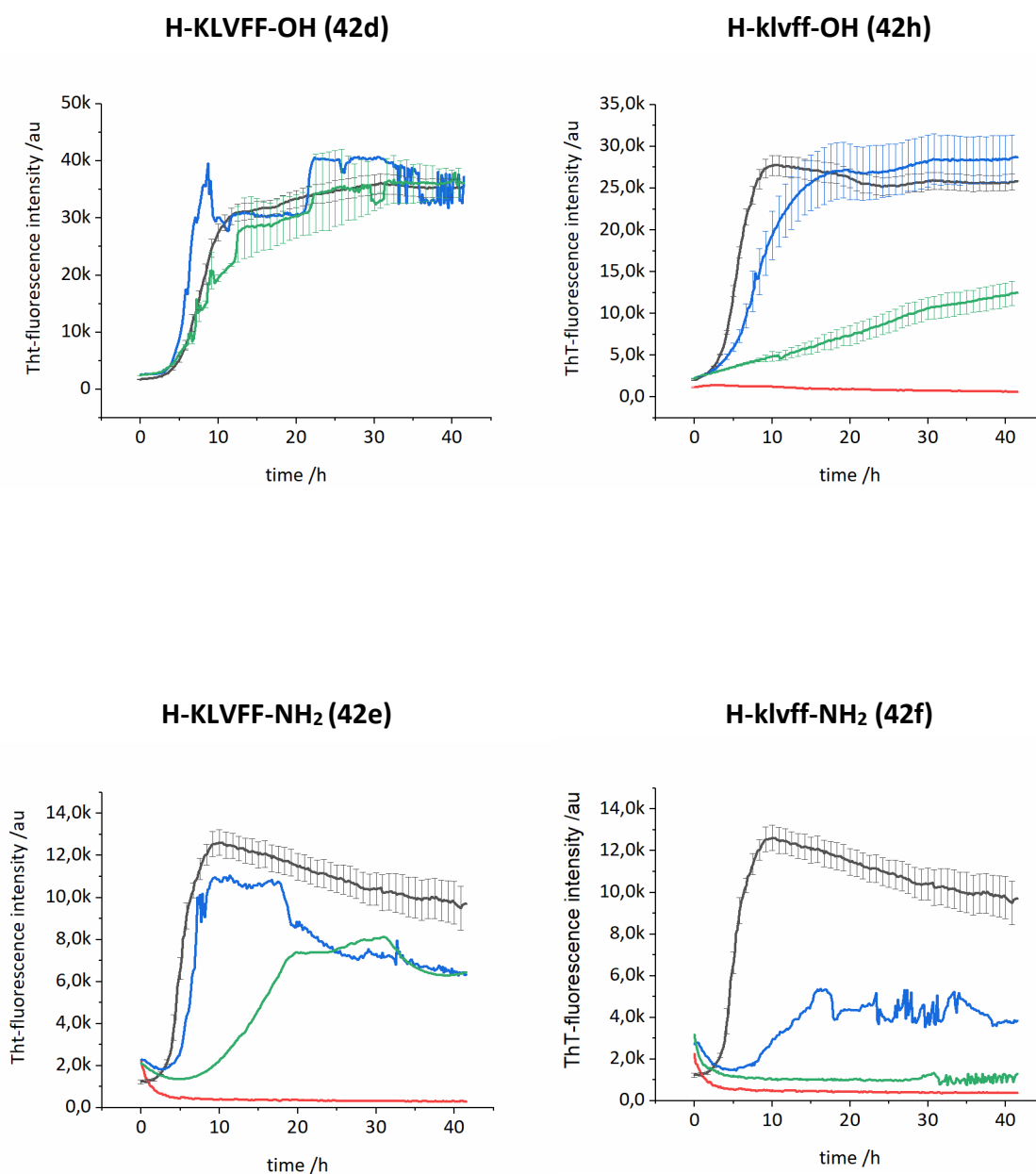
Scheme 47. a) Fmoc-D-Leu-OH (1.5 eq), Oxyma (1.65 eq), DIC (1.65 eq), DCM/DMF (1:1), rt, overnight; b) 20% piperidine in DMF; c) Methylation according to Chatterjee *et al.*¹⁴⁵; d) Fmoc-D-chGly[4Tz]-D-chGly-OH (1.5 eq), Oxyma (1.65 eq), DIC (1.65 eq), DCM/DMF (1:1), rt, overnight; e) Fmoc-D-chGly[4Tz]-D-Tyr(*t*Bu)-OH (1.5 eq), Oxyma (1.65 eq), DIC (1.65 eq), DCM/DMF (1:1), rt, overnight; f) 20% piperidine in DMF; g) TFA/H₂O/TIS (95:2.5:2.5).

The synthesized KLVFF mimetics were evaluated in their ability to inhibit early stage aggregation and later stage fibrillization of A β , using a Thioflavin-T and BODIPY fluorescence assay. These were performed by Dr. Julia Kaffy and Dr. Nicolo Tonali.

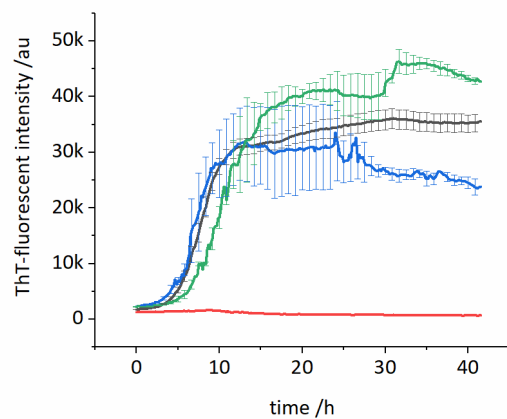
Since A β is self-aggregating over time, depending on purification and preparation protocols of the monomeric A β stock solution, the initial aggregation rate (lag phase) and kinetics may vary substantially, the comparison of fluorescence intensity values between

different publications is therefore problematic. A cautious comparison between fluorescence measurements can be achieved after identical preparations of the A β stock solution, however, it should include a control measurement with just A β and another one with the test compound to verify the integrity of the test.

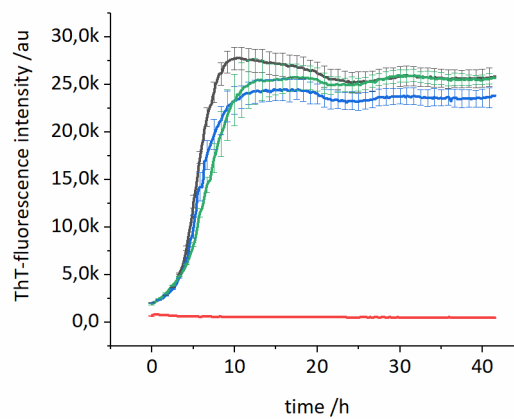
The results of the ThT-fluorescence assays are shown below (Figure 37a-j).



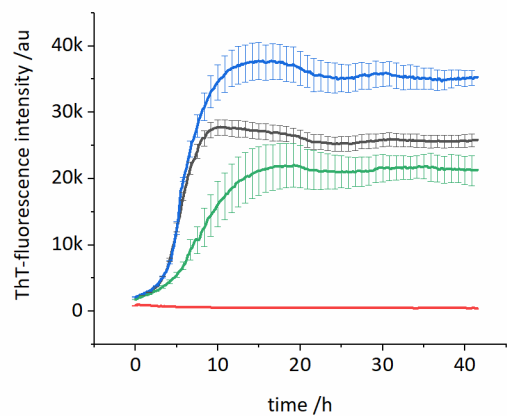
H-KL[5Tz]V-chGly[5Tz]F-OH (42a)



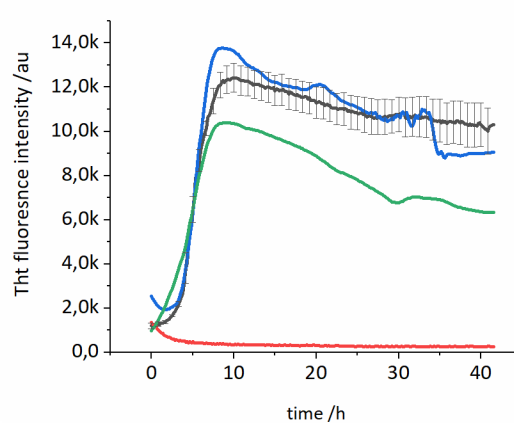
H-KL[5Tz]VF[5Tz]F-OH (42b)



Ac-KL[5Tz]VF[5Tz]F-NH₂ (42i)



Ac-KL[4Tz]VF[4Tz]F-NH₂ (42g)



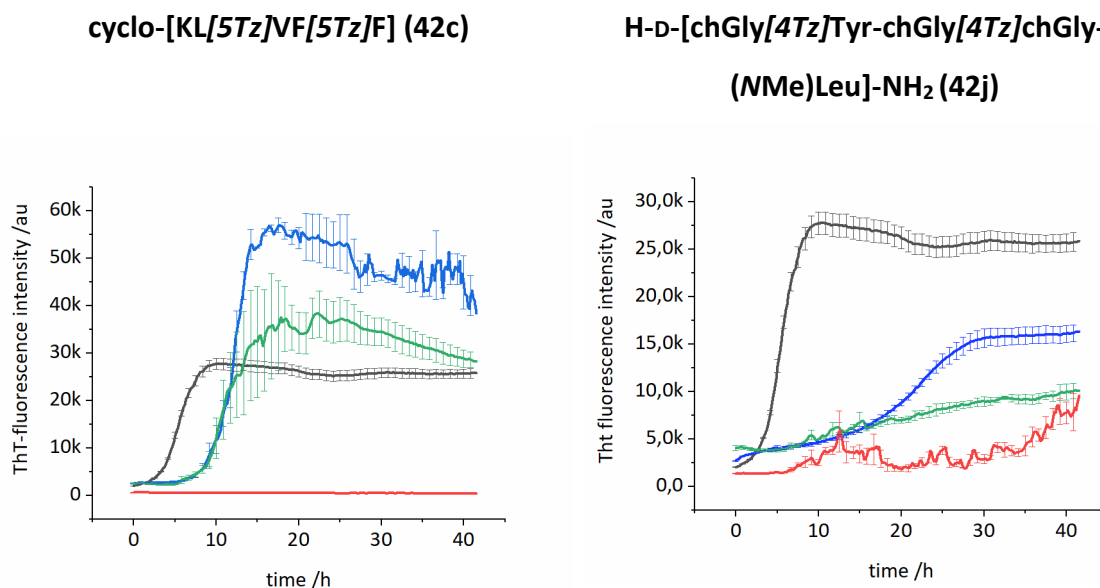


Figure 37a-j. Depicted is the ThT fluorescence progression over time, which is proportional to the amount of formed A β fibrils. Starting with a lag-phase, representing early stage oligomers which are not monitored by the ThT dye and ending in a plateau at which the fibrillization process is finished. All graphs share the same color code. Legend: [black: A β (10 μ M); red: compound (100 μ M); blue: compound (10 μ M)/A β (10 μ M) (1:1); green: compound (100 μ M)/A β (10 μ M) (10:1)]. In case of multiple measurements, the arithmetic average curve is given, complemented with the standard error of the mean.

The insignificant activity of H-KLVFF-OH (**42d**) to inhibit A β , although considered as a lead structure for development of novel A β inhibitors, is quite surprising but was also described by Arai *et al.*¹³⁷ In agreement to their structure-activity relationship studies, the activity is greatly increased for the D-configured peptide H-klvff-OH (**42h**), which decreases fibril formation by half after 40 h when applied in a tenfold excess, equimolar ratios compared to A β show a slight decrease of the slope during the aggregation phase. The activity for both peptides increases, when the carboxylic acid is exchanged with a terminal carboxamide, leading to a peptide which completely shuts down A β fibril formation in tenfold excess with H-klvff-NH₂ (**42f**).

The peptide Ac-KLVFF-NH₂ (not synthesized in this work, but used as a comparison standard by the group Prof. Onger)¹⁴⁶ is comparable in its activity to H-klvff-OH, leading to half the amount of fibrils after 40 h (plateau decrease of 46% after 40 h),¹⁴⁶ if utilized in a tenfold excess.

4. Results and Discussion

From the studies with the native peptides, it can be concluded that the D-form is always more active than the L-form, this also applies for the terminal carboxamide in comparison to the carboxylic acid, also an acetylated *N*-terminus seems to be advantageous.

Unfortunately, the exchange of amide positions two and four, with either 1,4- or 1,5-disubstituted triazoles, generally decreases its activity. As can be seen most drastically by a comparison of Ac-KLVFF-NH₂ with Ac-KL[4Tz]VF[4Tz]F-NH₂ (**42g**) and Ac-KL[5Tz]VF[5Tz]F-NH₂ (**42i**), where the latter one even increases amyloid fibril formation at an equimolar ratio. This effect was also pronounced with two other 1,5-disubstituted triazole containing peptidomimetics, H-Lys-Leu[5Tz]Val-chGly[5Tz]Phe-OH (**42b**) and the cyclic derivative cyclo-[KL[5Tz]VF[5Tz]F] (**42c**).

The SEN304 analogue H-D-[chGly[4Tz]Tyr-chGly[4Tz]chGly-(NMe)Leu]-NH₂ (**42j**) on the other hand, which bears the 1,4-disubstituted triazoles at position one and four, showed a good activity. Considering the fluorescence increase arising from the compound by itself, a tenfold excess completely inhibits A β fibril formation, while an equimolar ratio approximately decreases it by half after 40 h. A comparison with SEN304 was not performed, however, the authors describe a ~85% decreased fluorescence intensity (compared to A β control) utilizing equimolar ratios in a ThT assay after 24 h,^{142, 143} which is comparable to our results for the peptidotriazolamer **42j**.

Figure 38 shows the results of the BODIPY measurements for **42j**, confirming a good inhibition of A β early stage oligomerization in equimolar ratios and ten-fold excess.

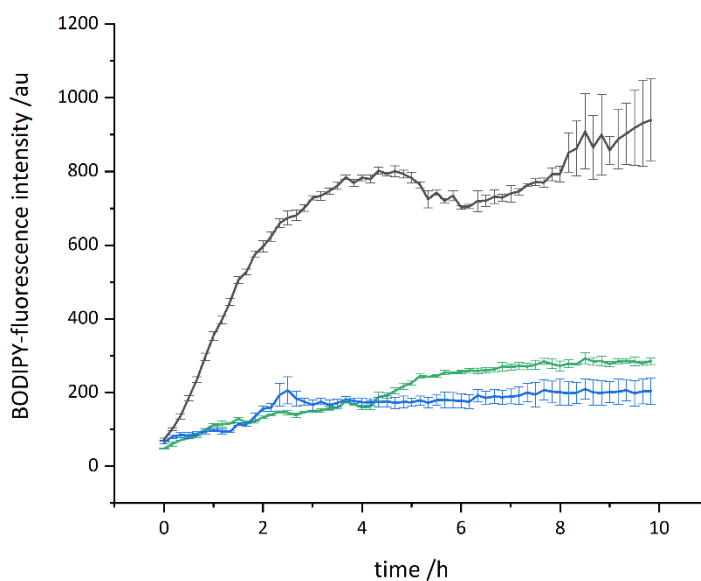


Figure 38. Representative curves of BODIPY fluorescence assays over time showing 10 μ M A β 42 oligomerization in the absence (**black curve**) and in the presence of compound **42j** at compound/A β 42 ratios 10/1 (**green curve**) and 1/1 (**blue curve**).

For this particular measurement, the control measurement with just the compound at 100 μM was not performed. However, earlier BODIPY measurements have shown that **42j**, in the absence of A β , does not increase fluorescence as it does during the ThT assay.

So far, the results from the ThT fluorescence assay imply that the triazole does not serve as a generic substitute for amide bonds. Reasons for this could be deviations in space between 1,4-disubstituted triazoles and a *trans*-amide bonds, as well as the weak hydrogen bond donor capabilities of the triazole, which might pose a crucial factor for the interaction with A β at the given position.

The 1,5-disubstituted regioisomer generally leads to a fixed turn in the peptide chain, which apparently disagrees with the concept of β -sheet recognition and binding sequence. However, Soto *et al.* reported about short synthetic peptides designed as beta sheet breakers (BSB) which purposely contain a proline moiety.¹⁴⁷ In this approach the peptide contains a sequence alike or similar to the beta sheet rich abnormal region of the deposits, it is able to recognize this region and prevent pathologic conformational changes by destabilizing the A β oligomers.¹⁴⁸ The BSB-peptide Soto developed with the sequence LPFFD was based on the hydrophobic L¹⁷VFF²⁰ sequence of A β and contains, beside the proline, an aspartate to increase solubility. As it turned out, besides inhibition of A β fibrillogenesis, the peptide showed the ability to disassemble already formed fibrils *in vitro* and reduces A β deposition in a rat brain model. Therefore, the carefully selected substitution of an amide bond with a 1,5-disubstituted triazole may pose an interesting approach towards novel BSB-peptides.

To address the unsatisfactory activity of the peptidotriazolamers in a methodical manner and to identify essential amide bonds, a triazole scan could be performed. In analogy to an alanine scan, which is widely used to identify essential residues in a peptide, the four amide bonds in the KLVFF sequence could be one by one replaced by a 1,4-disubstituted triazole, giving four different peptides.

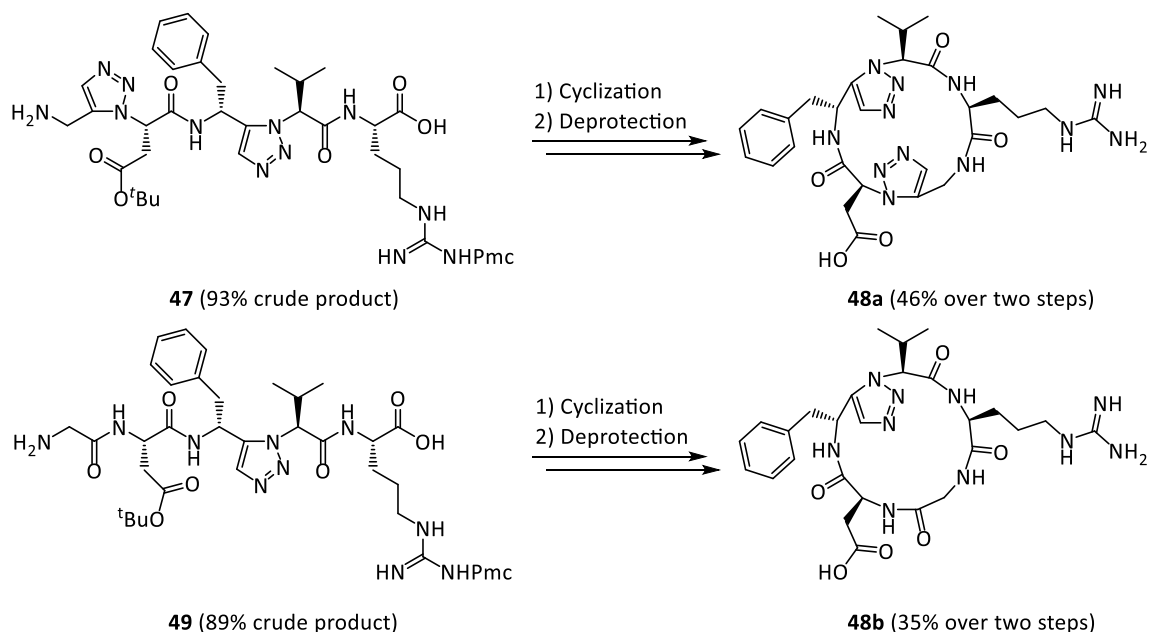
The synthesis of the necessary propargylamine for lysine was successfully addressed in our working group by Wünsch *et al.* utilizing Ellman's auxiliary.⁶² Also, the Bestmann-Ohira reaction with trityl protected α -amino aldehydes yielded Fmoc-Lys(Boc) \equiv (**39**) in good yields (**Scheme 38**).

Considering the activity-relationship of the native KLVFF peptides discussed above, also the synthesis of Ac-kl[4Tz]vf[4Tz]f-NH₂ and Ac-k[4Tz]lv[4Tz]ff-NH₂ would be promising.

4.6. Cyclic RGD peptidomimetics

Since the 1,5-disubstituted triazole, incorporated into a peptide sequence, effectively enables cyclization of pentapeptides (as demonstrated for the cyclic peptidotriazolamer **42c**), cyclic RGD peptidomimetics based on cilengitide (cyclo-[Arg-Asp-Gly-D-Phe-(NMe)Val]) ought to be developed. The *N*-methylated amide group should be replaced with a 1,5-disubstituted triazole, although Marelli *et al.* have shown that no *cis* peptide bonds are observed in the NMR structures of cilengitide.¹⁴⁹

As for the synthesis of cilengitide, the linear precursor was synthesized on solid phase, followed by a cyclization in solution.¹⁵⁰ The solid phase synthesis was done, utilizing 2-chloro trityl resin, whose mild cleavage conditions allows the synthesis of side chain protected peptides.¹⁵¹ The loading was performed with Fmoc-Arg(Pmc)-OH, to avoid the necessity to perform the loading with a triazole, which might result in decreased loading yields and loss of triazole material. In case of the second cyclic peptide **48b**, with just one triazole moiety, the loading could also begin with Fmoc-Gly-OH, to prevent racemization during the cyclization step, or side reactions between the guanidino group and the activated acid. But it was performed in analogy to the first peptide **48a** (Scheme 48).

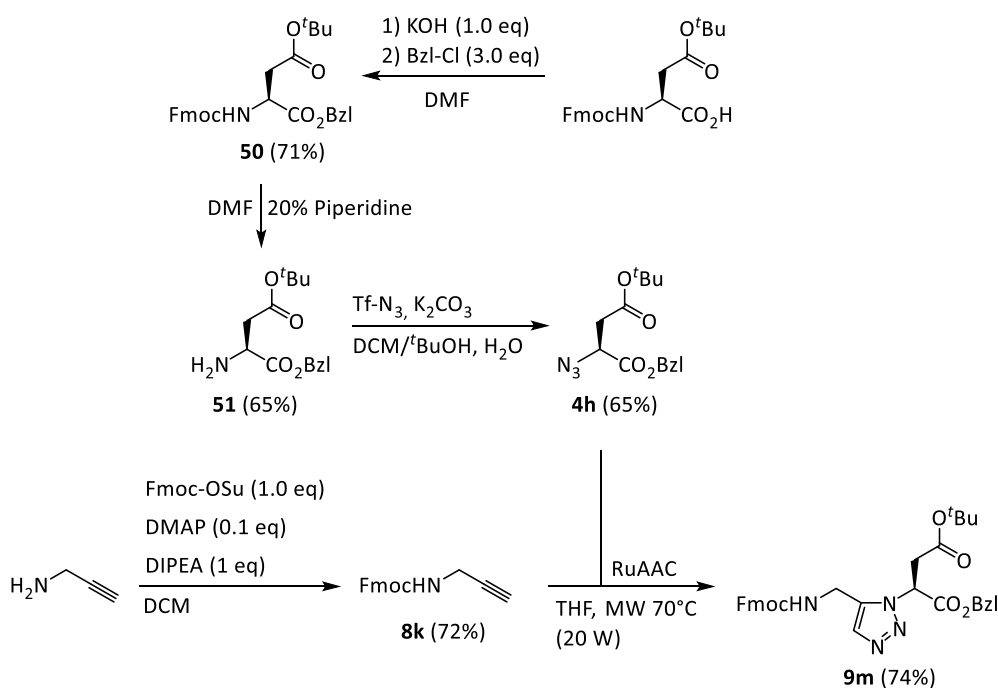


Scheme 48. Synthesis of the protected linear precursors **47** and **49** was performed on solid phase, the cyclization was done in solution under diluted conditions, to prevent the formation of oligomers. 1) *sym*-collidine (10 eq), PyBOP (1.5 eq), DCM/DMF (1:1), 1 mM; 2) Reagent "R": TFA/thioanisole/1,2-ethanedithiol/anisole (90:5:3:2).

The synthesis of the D-Phenylalanine analogue propargylamine (*R*)-**33** was performed as previously described, employing the Bestmann Ohira reaction with trityl protected α -amino aldehydes (**Scheme 37**).

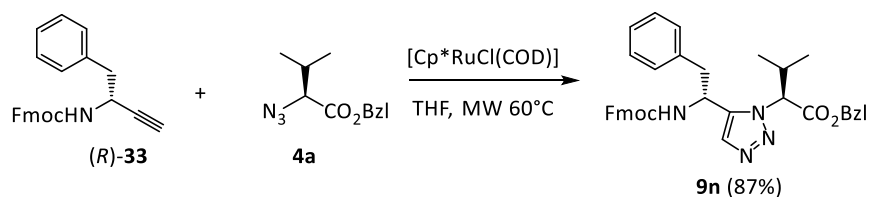
The Fmoc protected glycine analogue propargylamine **8k** was synthesized out of commercially available prop-2-yn-1-amine, through Fmoc protection with Fmoc-OSu (**Scheme 49**), providing Fmoc-Gly \equiv (**8k**) in 71% yield. The benzylester protected azide of aspartate **4f** was synthesized, starting from Fmoc-Asp(^tBu)-OH, following esterification with Bzl-Cl (thus avoiding activation of the carboxylic acid and possible epimerization of the alpha carbon), Fmoc deprotection with piperidine and subsequent diazotransfer, to obtain N₃-Asp(^tBu)-OBzl (**4f**) in 23% over three steps.

The RuAAC between both compounds yielded Fmoc-Gly[5Tz]Asp(^tBu)-OBzl (**9m**) in 74% (**Scheme 49**).



Scheme 49. Synthesis scheme for the triazole Fmoc-Gly[5Tz]Asp(^tBu)-OBzl, starting from Fmoc-Asp(^tBu)-OH and prop-2-yn-1-amine.

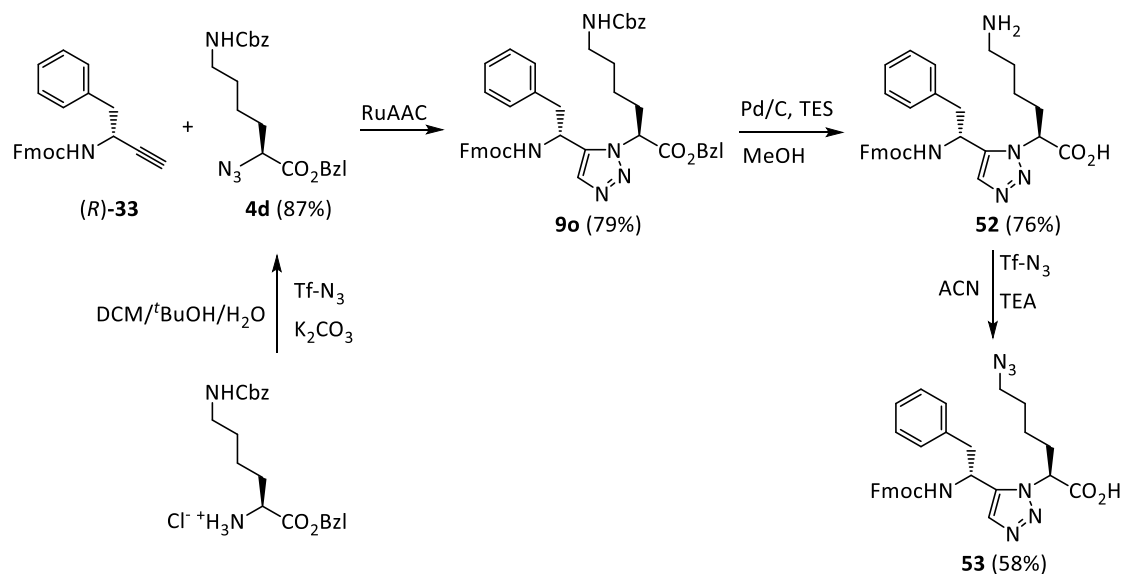
The RuACC between Fmoc-D-Phe \equiv (*R*)-**33** and N₃-Val-OBzl (**4a**) yielded Fmoc-D-Phe[5Tz]Val-OBzl (**9n**) in 87% yield (**Scheme 50**).



Scheme 50. Synthesis of Fmoc-D-Phe[5Tz]Val-OBzl (**9n**) by RuAAC.

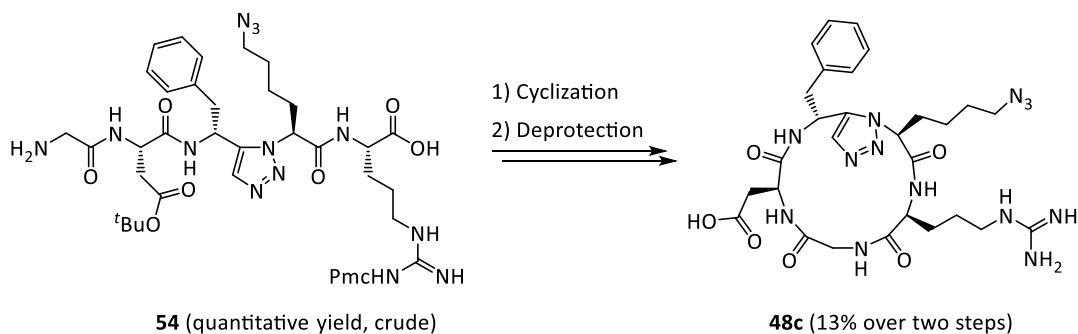
After deprotection of the benzyloxy ester, using the procedure of Mandal *et al.*¹⁴¹ (**Scheme 41**), the Fmoc protected triazoles could be used for the solid phase peptide synthesis.

Additionally, the synthesis of a functionalizable cyclic peptidomimetic would be interesting, which could be used in a prodrug application. Because the Val residue is not essential for the activity of cilengitide, it should be replaceable with an azidobutyl residue. Since the azide moiety would interfere with the *N*-terminal azido group during the RuAAC, the sidechain azido group must be introduced after the initial cycloaddition (**Scheme 51**). The synthesis was started with H-Lys(Z)-OBzl·HCl, the analogue azide (**4d**) was synthesized in 87% yield by diazotransfer with Tf-N₃. The RuAAC was performed with 79% yield, delivering triazole **9o**. The combination of Cbz group and benzyloxy ester offers a convenient deprotection of both protecting groups in one step, using the TES mediated cleavage conditions of Mandal *et al.*, which does not affect the Fmoc group. A final diazotransfer yielded the desired dipeptide-isoster **53**, for the solid phase synthesis, in 58% yield. The conditions for the final diazotransfer were based on a publication of Yan *et al.*⁶⁸ which utilizes triethylamine as a base in acetonitrile in combination with triflyl azide, which was estimated to be more compatible with the Fmoc group.



Scheme 51. Synthesis of an azidobutyl containing triazole **53**, suitable for solid-phase peptide synthesis.

The triazole was utilized in SPPS to obtain the linear protected sequence in quantitative yields from a 2-chloro trityl resin in sufficient crude purity, after loading Fmoc-Arg(Pmc)-OH with 70% yield to the resin (**Scheme 52**).



Scheme 52. After cleavage of the linear precursor **54** from the resin, the peptide was cyclized in solution followed by a cleavage of acid labile protecting groups. 1) *sym*-collidine (10 eq), PyBOP (1.5 eq), DMF/DCM (1:1) 0.1 mM; 2) Reagent “R”: TFA/thioanisole/1,2-ethanedithiol/anisole (90:5:3:2).

Reagent “R” was chosen as a cleaving cocktail, which is specifically developed for peptides containing arginine with sulfonyl based protecting groups. Although the reaction progress could be monitored by HPLC and went with full conversion, the final peptide could be only isolated in 13% yield.

The literature reveals substantial reduction of azide moieties during acidic cleavage, utilizing cleavage cocktails containing thiol scavengers.¹⁵² While cocktails lacking EDTE

4. Results and Discussion

have no influence on the artificial building block, this might explain the decreased yield compared to the cyclic peptides **48a** and **48b**.

The cyclic peptidomimetics **48a-c** were tested in their antagonistic properties towards $\alpha_v\beta_3$, compared to cilengitide as a standard, by Isabell Kemker from our workgroup. A cell adhesion assay, developed by Conradi *et al.*¹⁵³ and an ELISA-based solid phase assay, developed by the group of Kessler, were used.¹⁵⁴ The peptides **48a-b** (**48c** not tested) showed no antagonistic activity towards $\alpha_v\beta_3$ in the cell adhesion assay ($IC_{50} > 500 \mu M$).

However, the peptides **48b** and **48c** (**48a** not tested) showed a good activity in the cell free ELISA assay with an IC_{50} value of 19.7 and 18.6 nM, by comparison measurements with cilengitide (0.54 nM) against $\alpha_v\beta_3$ (**Figure 39**).

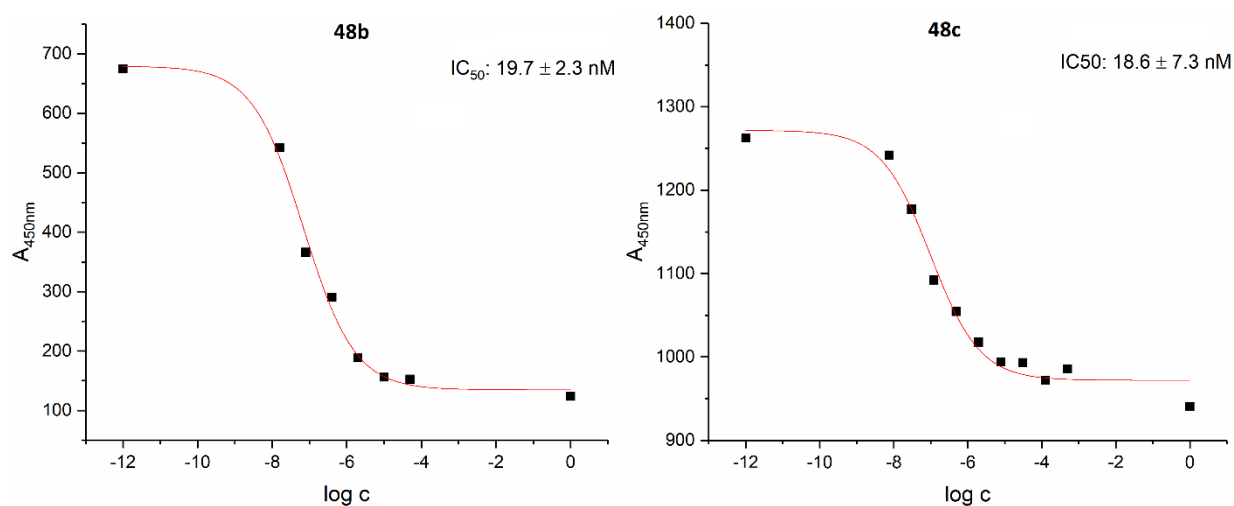
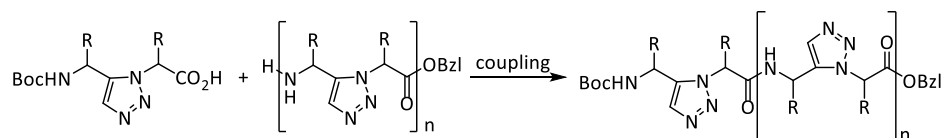


Figure 39. Dose response curve of **48b** and **48c**, the IC_{50} is determined as molar concentration at 50% inhibition.

5. Summary

In the scientific field of peptidomimetics and medicinal chemistry, the disubstituted 1,2,3-triazole evolved to be a promising surrogate for amide bonds, as they share physicochemical properties like a strong dipole moment, planarity, as well as hydrogen donor/acceptor ability. The popularity is supported by the circumstance, that both regioisomers of the triazole are selectively accessible by either copper(I) (CuAAC) or ruthenium(II) (RuAAC) catalysed azide alkyne cycloaddition, where the former leads to 1,4-disubstituted and the latter to 1,5-disubstituted triazoles.

We were interested in the synthesis and conformational behaviour of oligomeric peptidotriazolamers, consisting of amides and triazoles in an alternating fashion. Additionally, the influence of the configuration on the conformation of the oligomers was investigated by comparison of homochiral and heterochiral peptidotriazolamers. Oligopeptidotriazolamers were prepared by a building block approach in solution, exploiting the orthogonality of the Boc/Bzl protecting group pair (**Scheme 53**). In this approach, C-terminal deprotected triazoles are coupled onto the growing oligomeric chain in N-terminal direction, giving rise to different peptidotriazolamers in various lengths.



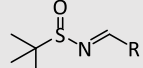
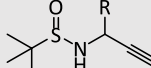
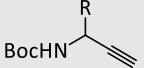
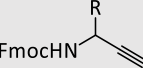
Scheme 53. The peptide coupling of a triazole as a dipeptide isoster onto the growing oligomeric chain, leads to peptidotriazolamers in various lengths.

For the synthesis of triazole building blocks, enantiomerically pure propargylamines and α -azido acids are required. The α -azido acids **4a-e**, **4h** were prepared by a diazotransfer employing Tf-N₃ based on Luindquist *et al.*⁶⁵ and benzyl-/allylester protected amino acids (Val, Ala, Phe, Lys(Boc) and Asp(^tBu)) in excellent yields of 71-98% after column chromatography. When the procedure was performed with unprotected amino acids (H-D-chGly-OH, H-D-Tyr(^tBu)-OH), the aqueous workup lead to yields of 36% (**4f**) and 26% (**4g**). The chiral propargylamines were synthesized as described by Xiao *et al.* Ellman's chiral auxiliary was condensed with aliphatic aldehydes bearing the desired sidechain (isobutyl, isopropyl, methyl, cyclohexyl) as a residue, to form *N*-sulfinylaldimines. They were reacted with *in situ* generated ((trimethylsilyl)ethynyl)lithium to give sulfinyl

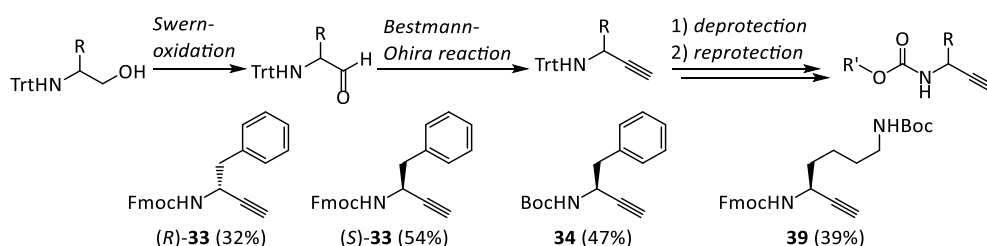
5. Summary

protected propargylamines in high diastereomeric purity. The butylsulfinyl group was cleaved off under acidic conditions and exchanged by an urethane based protecting group to prevent disproportionation at elevated temperatures. The yields for the synthesis steps are given in **Table 6**.

Table 6. Yields of intermediates in the synthesis of *N*-protected propargylamines. The yields for the Bus protected propargylamines entail two steps (acetylide addition and TMS cleavage), likewise the Boc and Fmoc protected species (Bus cleavage and urethane introduction).

R =								
	(<i>R</i>)	(<i>S</i>)	(<i>R, R</i>)	(<i>S, S</i>)	(<i>R</i>)	(<i>S</i>)	(<i>R</i>)	(<i>S</i>)
Methyl	6a (81%)	6b (80%)	7a (49%)	7b (46%)	8a (85%)	8b (61%)	-	-
Isopropyl	6c (90%)	6d (71%)	7c (45%)	7d (67%)	8c (90%)	8d (56%)	-	-
Isobutyl	6e (79%)	6f (93%)	7e (46%)	7f (52%)	8e (94%)	8f (82%)	-	8j (71%)
Cyclohexyl	6g (93%)	6h (46%)	7g (71%)	7h (60%)	8g (84%)	8h (86%)	8k (43%)	-

Additionally, the propargylamine analogues of phenylalanine and lysine were synthesized by the Bestmann-Ohira homologation. However, urethane protected α -amino aldehydes turned out to partially epimerise. Utilizing the electron donating trityl protecting group for α -amino aldehydes, the corresponding propargylamines were obtained in high enantiomeric purity (**Scheme 54**). Since they failed to give any conversion in the RuAAC they were reprotected with urethane groups like Boc or Fmoc.



Scheme 54. The trityl protected α -amino aldehydes are obtained in high yields after oxidation of the corresponding α -amino alcohols and turned out to be enantiomerically stable under the basic reaction conditions of the Bestmann-Ohira homologation.

The RuAAC was performed under MW conditions, giving rise to several 1,5-disubstituted triazoles in high yields after 1-2 h reaction times. The CuAAC was performed at room temperature overnight, providing 1,4-disubstituted triazoles (**Table 7**).

Table 7. 24 different triazoles were synthesized in good yields by RuAAC and CuAAC.

	Boc protected	Fmoc protected	
[5Tz]	Boc-Val[5Tz]Ala-OBzl (9c) (84%)	Boc-D-Val[5Tz]Ala-OBzl (9f) (88%)	Fmoc-D-Phe[5Tz]Val-OBzl (9n) (87%)
	Boc-Leu[5Tz]Val-OBzl (9e) (81%)	Boc-D-Leu[5Tz]Val-OBzl (9d) (87%)	Fmoc-D-Phe[5Tz]Lys(Cbz)-OBzl (9o) (79%)
	Boc-Ala[5Tz]Phe-OBzl (9a) (87%)	Boc-D-Ala[5Tz]Phe-OBzl (9b) (94%)	Fmoc-Phe[5Tz]Phe-OBzl (9l) (92%)
	Boc-chGly[5Tz]Phe-OBzl (9h) (87%)	Boc-D-chGly[5Tz]Phe-OBzl (9i) (86%)	Fmoc-Leu[5Tz]Val-OBzl (9k) (75%)
	Boc-Phe[5Tz]Phe-OBzl (9j) (75%)	Boc-Ala[5Tz]Ala-OBzl (9g) (77%)	Fmoc-Gly[5Tz]Asp(^t Bu)-OBzl (9m) (74%)
[4Tz]	Boc-D-Val[4Tz]Phe-OBzl (18a) (67%)	Boc-D-Leu[4Tz]Phe-OBzl (18b) (60%)	Fmoc-D-[chGly[4Tz]chGly]-OH (18i) (72%)
	Boc-Gly[4Tz]Phe-OBzl (18d) (88%)	Boc-Gly[4Tz]Val-OAll (18e) (81%)	Fmoc-D-[chGly[4Tz]Tyr(^t Bu)]-OH (18h) (82%)
	Boc-D-Leu[4Tz]Val-OAll (18c) (81%)	-	Fmoc-Leu[4Tz]Val-OBzl (18f) (91%)
	-	-	Fmoc-Phe[4Tz]Phe-OBzl (18g) (69%)
	-	-	

The Boc/Bzl protected 1,5-disubstituted triazoles were selectively deprotected by either HCl in dioxane or by palladium catalysed hydrogenolysis. The deprotected triazoles were obtained in quantitative yields and sufficient crude purity for the successive peptide coupling steps. However, the triazole dipeptide isosteres proved themselves to be highly prone to epimerization. This issue could be prevented by performing the coupling reactions in DCM, or a mixture of DCM/DMF of (1:1), with *sym*-collidine as a base. A carbodiimide mediated preactivation in DCM, followed by a *sym*-collidine facilitated coupling step, was finally favoured (**Figure 40**).

The X-ray crystal structure of the homochiral tetramer Boc-Val[5Tz]Ala-Leu[5Tz]Val-OBzl (**10**) displayed close resemblance to a β Via1 turn, which is stabilized by an intramolecular hydrogen bond between the Boc carbonyl oxygen ((CH₃)₃C-CO) and the amide proton of the leucine (NH-C ^{α ,i+3}), with a length of 2.08 Å. Additionally, the solid state conformation was supported by comparison with the gas phase structure obtained by simulated annealing, which match closely with a RMSD of 0.37 Å.

5. Summary

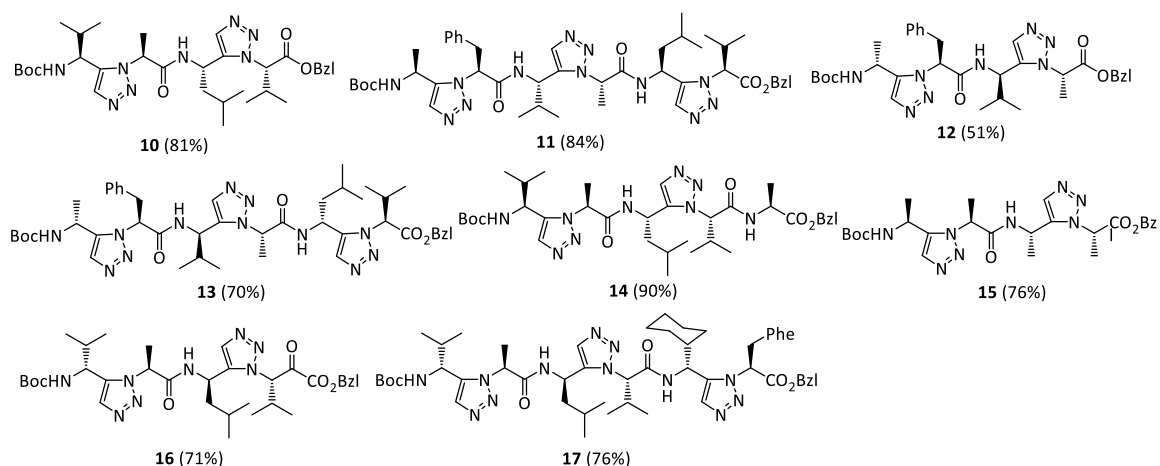


Figure 40. Boc/Bzl protected 1,5-disubstituted triazole containing peptidotriazolamers were synthesized in solution. Yields are given for the final coupling step.

The close analogy to a β VIa1 turn is preserved after elongation of the sequence to Boc-Ala[5Tz]Phe-Val[5Tz]Ala-Leu[5Tz]Val-OBzl (**11**), demonstrated by molecular modelling implying ROESY restraints. On the other hand, the heterochiral compound Boc-D-Ala[5Tz]Phe-D-Val[5Tz]Ala-D-Leu[5Tz]Val-OBzl (**13**) was shown to resemble a polyproline I reminiscent helix, where the triazoles show in the opposite direction than the residues.

Additionally, peptidotriazolamers based on 1,4-disubstituted triazoles were synthesized. These oligomers comprise of a heterochiral residue alignment and an alternating pattern of a chiral residue and a methylene moiety (**Figure 41**). The conformational analysis was not finished for these peptidotriazolamers because of encountered aggregation effects in solution.

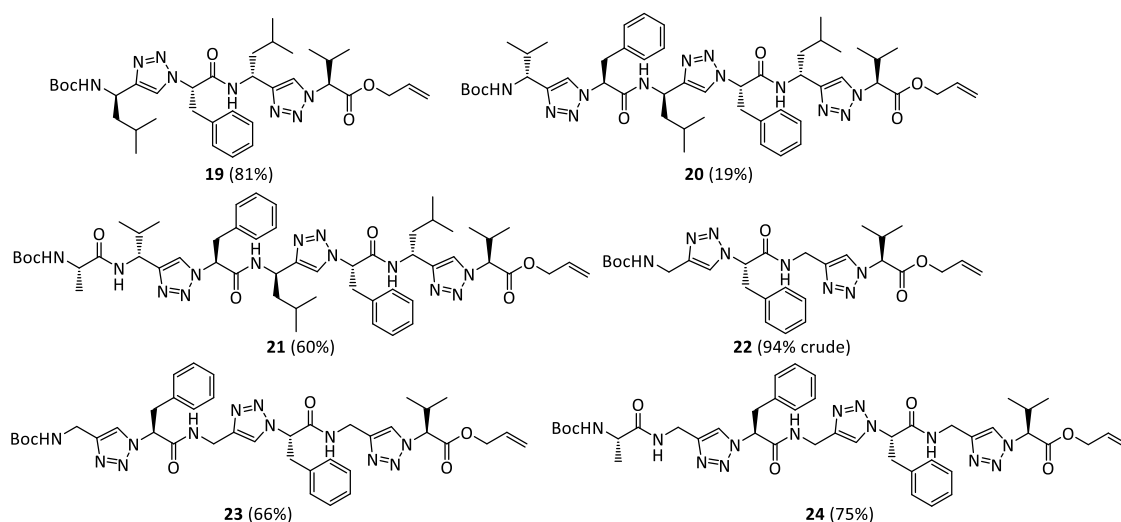


Figure 41. Boc/All protected 1,4-disubstituted triazole containing peptidotriazolamers were synthesized in solution. Yields are given for the final coupling step.

To investigate the peptidotriazolamers in a biological application, different 1,5- and 1,4-disubstituted triazole containing peptidotriazolamers were synthesized in solution and on solid phase, representing the KLVFF sequence (**Figure 42**). These novel lead compounds were investigated in their ability to inhibit neurotoxic Amyloid- β aggregation, which is responsible for neurodegenerative diseases, by ThT and BODIPY assays.

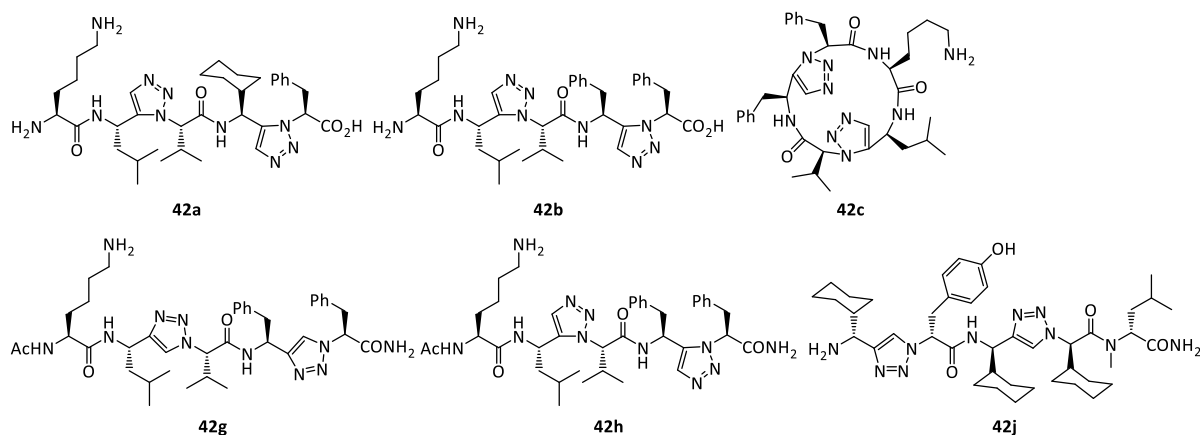


Figure 42. Linear and cyclic peptidomimetics based on the sequence KLVFF.

While the triazole containing KLVFF peptidomimetics lack the activity of their derived peptides, the SEN304 analogue **42j** turned out to completely inhibit A β fibrillization and early stage oligomerization in an equimolar ratio and tenfold excess compared to A β .

Based on the RGD-peptide cilengitide three cyclic peptidomimetics were successfully synthesized in which the *N*-methylated peptide bond was replaced by a 1,5-disubstituted triazole (**Figure 43**). Additionally, **48c** contains an azidobutyl residue for additional functionalization, which makes it readily available for a prodrug application. While the peptidomimetics **48a** and **48b** failed to show any affinity ($IC_{50} > 500 \mu M$) in a cell adhesions assay, **48b** and **48c** showed a comparable nanomolar antagonistic activity against $\alpha v \beta_3$ in an ELISA assay, with an IC_{50} of 19.7 and 18.6 nM.

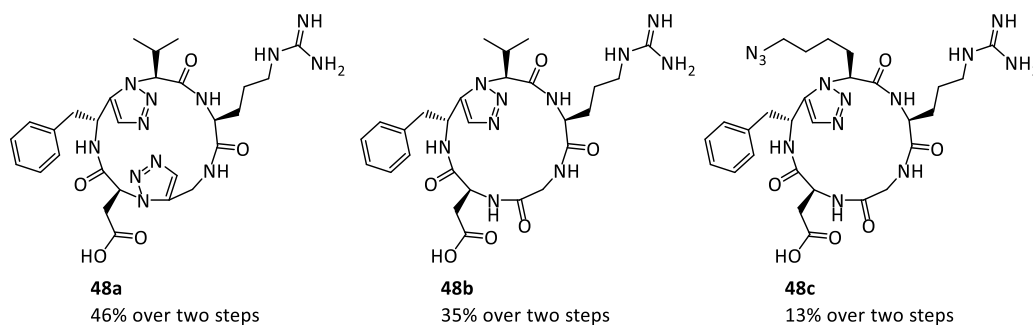


Figure 43. Cyclic peptidomimetics based on cilengitide containing one or two 1,5-disubstituted triazoles. The yields refer to the cyclization and deprotection of the linear sequence after SPPS.

6. Outlook

The results of the presented work may lay the principles and foundations for the design of future triazole containing peptidomimetics. The elaborated synthetic methods for the synthesis of enantiomerically pure propargylamines as valuable precursors for a wide variety of scaffolds, as well as solution and solid phase strategies for the obtainment of peptidotriazolamers, have been shown to be highly variable and robust.

The ability of 1,5-disubstituted triazole containing peptidotriazolamers to mimic β -turns and polyproline like helices, might represent a starting point to discover further biological applications. The direction of rotation might be additionally changed by an inversion of all stereo centres. The conformations of the 1,4-disubstituted triazole containing peptidotriazolamers Boc-Ala-D-Val[4Tz]-Phe-D-Leu[4Tz]-Phe-D-Leu[4Tz]-Val-OAll (**21**) and Boc-Ala-Gly[4Tz]-Phe-Gly[4Tz]-Phe-Gly[4Tz]-Val-OAll (**24**) still need to be confirmed by molecular modelling. Additionally, the conformation of Boc-Ala[5Tz]Ala-Ala[5Tz]Ala-OBzl (**15**), obtainable by molecular modelling, would give an insight if the conformational behaviour is controlled by the sequence of residues, or the combination of stereochemistry and triazole regioisomery.

While a *cis*- amide bond in nature is mainly facilitated by a proline in the sequence, the 1,5-disubstituted triazole enables the possibility to mimic a *cis*- peptide bond with the benefit of adding an extra residue in that position. That residue might contribute to important interactions with a protein backbone or enzymatic pocket. For clarification, Tam *et al.* identified Xaa-Pro to be efficiently mimicked by Xaa[5Tz]Ala.⁴⁵ However, the alanine moiety in the triazole might be readily exchanged with an α -azido acid bearing a functional group and thereby, the triazole would still mimic a *cis*- peptide bond.

Although it was shown that trityl protected α -aminoaldehydes are far less prone to racemization during the conditions of the Bestmann-Ohira reaction, starting from Fmoc-protected amino acids, the synthesis route contains a lot of steps resulting in overall low yields (**Scheme 38**). The Fmoc deprotection¹³⁴ might be facilitated with the usage of polymer-bound thiol groups to conveniently scavenge the dibenzofulven followed by removal through filtration. Alternatively, starting with *N*-Cbz/^tBu(side-chain) protected amino acids would be feasible, which would effectively give rise to free amino alcohols after two steps, without elaborate workup or purification procedures.

In the topic of A β aggregation inhibitors, a further peptide sequence which comes to mind is the modified Soto peptide Ac-LPFFD-NH₂, which might be modified into Ac-Leu[5Tz]Ala-Phe-Phe-Asp-NH₂ as the closest analogue.¹⁴⁷ Practically, the synthesis of the precursors Fmoc-Leu \equiv (**8j**) and N₃-Ala-OBzl (**4a**) was already presented in this dissertation. This would be an interesting model peptide for the incorporation of the 1,5-disubstituted triazole, since the other peptidomimetics synthesized so far, based on the KLVFF sequence containing 1,5-disubstituted triazoles, were inactive in inhibiting A β -fibrillization. The synthesis of Fmoc-Lys(Boc) \equiv (**39**) in this work offers the possibility to perform a triazole scan of the Ac-KLVFF-NH₂ sequence, or more promising, its enantiomer Ac-klvff-NH₂, to spot crucial amide bonds.

For the active RGD peptidomimetics **48b** and **48c**, it would be necessary to test them with other integrin receptors, for example $\alpha_{IIb}\beta_3$, to quantify the selectivity towards $\alpha_v\beta_3$. Further, the functionalizable peptide **48c** might be conjugated by “click-chemistry” with a variable linker, bearing a fluorophore or cytotoxic agent, followed by cell-based cytotoxicity assay. This could be done to determine the selectivity of the conjugate, between cells, which are highly abundant in certain integrins and cells which are not.

7. Experimental section

All chemicals were purchased from Sigma Aldrich (Taufkirchen, Germany), Acros (Geel, Belgium), Alfa Aesar (Ward Hill, USA) and VWR (Darmstadt, Germany), Chempur (Karlsruhe, Germany), Iris Biotech (Marktredwitz, Germany), Bachem (Bubendorf, Switzerland) and were employed without additional purification. Moisture- and air-sensitive reactions were conducted in flame-dried glassware and under argon atmosphere. Dichloromethane and toluene were freshly distilled from CaH₂ and Na, respectively. THF was kept over KOH before being dried with sodium/benzophenone under reflux and was freshly distilled before use.

Analytical RP-HPLC was performed on a Thermo Separation Products system equipped with a UV-6000 LP detector, a P-4000 pump, a Hypersil Gold 3 μm (C₁₈; 150 \times 2.1 mm) column. A flow rate of 0.7 ml/min using Eluent A: H₂O/CH₃CN/TFA (94.9/5.0/0.1) and Eluent B: CH₃CN/ H₂O/TFA (94.9/5.0/0.1) was employed. Gradient Elution: (A, **method 1**) 0-0.5 min (100%), 0.5-7.5 min (100% to 0%), 7.5-8.5 min (0%), 8.5-9.5 (0% to 100%), 9.5-10 min (100%). Gradient Elution: (A, **method 2**) 0-3 min (100% to 0%), 3-4 min (0%), 4-5 min (0%-100%). Gradient Elution: (A, **method 3**) 0-18 min (100% to 0%), 18-19 (0%), 19-20 min (0%-100%).

Preparative RP-HPLC was performed on a Hitachi MERCK LaChrom system equipped with a UV-Vis L-7420 detector, a L-7150 pump and a Phenomenex Jupiter 10 μm column (C₁₈; 300 \AA , 250 \times 21.1 mm). A flow rate of 10.0 ml/min using Eluent A: H₂O/CH₃CN/TFA (94.9/5.0/0.1) and Eluent B: CH₃CN/H₂O/TFA (94.9/5.0/0.1) was employed. Gradient Elution: (A, method 2) 0-35 min (100% to 0%), 35-45 min (0%), 45-50 min (0% to 100%).

Optical rotation ($[\alpha]_D^{25}$, deg $\cdot\text{cm}^3\cdot\text{g}^{-1}\cdot\text{dm}^{-1}$) was measured on a Jasco DIP-360 Digital Polarimeter at $\lambda=589$ nm. A quartz cell with a path length of 1 dm was used. The average value of ten single measurements is given. The sample concentration and solvent are mentioned in parentheses.

NMR spectra were recorded at 298 K on a DRX 500 (¹H: 500 MHz, ¹³C: 126 MHz), an Avance III 500 (¹H: 500 MHz, ¹³C: 126 MHz) and an Avance 600 spectrometer (¹H: 600 MHz, ¹³C: 151 MHz) (Bruker Biospin, Rheinstetten, Germany). Chemical shifts are reported relative

7. Experimental section

to residual solvent peaks (DMSO-*d*₆: ¹H: 2.50 ppm, ¹³C: 39.52 ppm), (CDCl₃: ¹H: 7.26 ppm, ¹³C: 77.16 ppm), (CD₃OH-*d*₃: ¹H: 3.31 ppm, ¹³C: 49.00 ppm).¹⁵⁵

ESI/APCI mass spectra were recorded using an Esquire 3000 ion trap mass spectrometer (Bruker Daltonik GmbH, Bremen, Germany) equipped with a standard ESI/APCI source. Samples were introduced directly with a syringe pump. Nitrogen served both as the nebulizer gas and the dry gas. Nitrogen was generated using a Bruker nitrogen generator NGM 11. Helium served as cooling gas for the ion trap and collision gas for MS experiments.

High-resolution ESI mass spectra are recorded using an Agilent 6220 time-of-flight mass spectrometer (Agilent Technologies, Santa Clara, CA, USA) in extended dynamic range mode equipped with a Dual-ESI source, operating with a spray voltage of 2.5 kV. Nitrogen served both as the nebulizer gas and the dry gas. Nitrogen was generated by a nitrogen generator NGM 11. Samples are introduced with a 1200 HPLC system consisting of an autosampler, degasser, binary pump, column oven and diode array detector (Agilent Technologies, Santa Clara, CA, USA) using a C₁₈ Hypersil Gold column (length: 50 mm, diameter: 2.1 mm, particle size: 1.9 μm) with a short gradient (in 4 min from 0% B to 98% B, back to 0% B in 0.2 min, total run time 7.5 min) at a flow rate of 250 μL/min and column oven temperature of 40°C. HPLC solvent A consists of 94.9% water, 5.0% acetonitrile and 0.1% formic acid, solvent B of 5.0% water, 94.9% acetonitrile and 0.1% formic acid. The mass axis was externally calibrated with ESI-L Tuning Mix (Agilent Technologies, Santa Clara, CA, USA) as calibration standard. The mass spectra are recorded in both profile and centroid mode with the Mass Hunter Workstation Acquisition B.04.00 software (Agilent Technologies, Santa Clara, CA, USA). Mass Hunter Qualitative Analysis B. 07.00 software (Agilent Technologies, Santa Clara, CA, USA) was used for processing and averaging of several single spectra.

X-Ray structure analysis of the crystals were obtained by dissolving the respective compound in EtOAc, MeOH, or ⁱPrOH (1 mg/mL), followed by slow evaporation of the solvent overnight at room temperature.

A suitable crystal was transferred to an object slide, containing a drop of paraffin-oil and taken up by a glas-fiber. The measurements were done using Cu K_α radiation with a

Supernova diffractometer at 100.0(1) K. Using Olex2¹⁵⁶ the structures were solved and refined with the ShelX program package¹⁵⁷ with direct methods and least-squares minimization. All atoms were refined anisotropically except hydrogen atoms, which were placed in calculated positions and refined using a riding model. Absolute configuration of all structures could be established by anomalous-dispersion effects in diffraction measurements on the crystal. One CH₃-group in each molecule of **9d** is disordered at two positions (ratio 76/24), one of them was restrained to have same C-C distances. Details of the X-ray investigation are given section 8. X-ray analysis.

Molecular modelling experiments were performed by Dr. Jerzy Góra and Dr. Joanna Krzciuk-Gula (Department of Bioorganic Chemistry, Wrocław University of Science and Technology) as well as Dr. Antoine Marion (Department of Chemistry, Middle East Technical University, Çankaya) and David Schröder (Organic and Bioorganic Chemistry, Department of Chemistry, University of Bielefeld) as described by Marion *et al.*¹¹⁷

The preparation of the systems and all molecular mechanics (MM) calculations were carried out using modules of the Amber16/AmberTools16 suite.¹⁵⁸ Peptidotriazolamer building blocks and protecting group parameters were adopted from the TZLff force field.¹¹⁷ The distance restraints used during molecular dynamics (MD) calculations were obtained from the analysis of ROESY spectra measured in DMSO on a Bruker 600 MHz spectrometer and calculated based on the Intensity-Ratio Method described by Ämmälähti *et al.*¹⁵⁹ All distances were restrained using a half-harmonic potential with a force constant of 32.0 kcal·mol⁻¹·Å⁻² (Amber force constant convention) for the upper boundary of the distance, while breaking of the lower limit was permitted. The upper boundary was set as +10% of the measured distance. Initially, all restraints derived from the spectra were applied. Restraints that broke an arbitrary penalty threshold (value of penalty > 5.0 kcal·mol⁻¹) during simulated annealing (SA) were removed from the calculations to produce the final set of constraints. This approach allowed to keep a large amount of constraints without introducing unnecessary strain on the system that could have been caused by assignment of distance restraints based on ROESY peaks with dubious volumetric data. The final sets of distance restraints are presented in the Supporting Information (Tables SI 2, SI 3).¹⁰⁷ The SA protocol consisted of six heat-ing (0 K to 10 K in 50 ps; 10 K to 100 K in 50 ps; 100 K to 200 K in 100 ps; 200 K to 300 K in 100 ps; 300K to 400 K in 100 ps; 400 K to 600 K in 100 ps) and six cooling stages (600 K to 400 K in 100 ps; 400 K to 300 K in 100 ps; 300 K to 200 K in 100 ps; 200 K to 100 K in 75 ps; 100 K to 10K in 20

ps; 10 K to 0 K in 5 ps) using a 1 fs time step. The temperature during the simulation was controlled by a Langevin thermostat with 2.0 ps^{-1} collision frequency. The weight of the distance restraints was gradually increased over the first 150 ps of the simulations from an initial value of 10% to 100%, which persisted for the remainder of the SA run. Structures resulting from SA were solvated using *tleap* in truncated octahedron boxes with a 15 Å buffer consisting of DMSO or TIP4PEw water. The minimization of the solvated systems was carried out using standard settings of *sander*. During the first part of the minimization the position of the solute except for its hydrogen atoms was restrained by a harmonic potential with a force constant of $3.0 \text{ kcal}\cdot\text{mol}^{-1}\cdot\text{Å}^{-2}$. These restraints were released during the final stages of minimization. The heat-up of the systems to the target temperature of 300 K was performed in a stepwise manner. First in the NVT ensemble (from 0 K to 200 K) using the Langevin thermostat,¹⁶⁰ and in NPT conditions (from 200 K to 300 K) using the Berendsen barostat.¹⁶¹ All systems reached the expected density of 0.98 g/cm^3 and 1.10 g/cm^3 for TIP4PEw water and DMSO, respectively. All molecular dynamic (MD) production runs were carried out for 200 ns with a 2 fs time step in the NPT ensemble with periodic boundary conditions and using Amber's standard pre-sets of the Particle Mesh Ewald method. Three types of MD runs were produced for each molecule: unrestrained MD in DMSO¹⁶² and TIP4PEw¹⁶³ water and restrained MD in DMSO using the previously established NMR-derived sets of distance restraints.

The ThT fluorescence assays were performed by Dr. Julia Kaffy (Fluorinated Molecules and Medicinal Chemistry, Department of Chemistry, Université Paris-Sud) as described by Kaffy *et al.*¹⁶⁴ Thioflavin T was obtained from Sigma. A β 42 was purchased from American Peptide. The peptide was dissolved in an aqueous 1% ammonia solution to a concentration of 1 mM and then, just prior to use, was diluted to 0.2 mM with 10 mM Tris-HCl, 100 mM NaCl buffer (pH 7.4). Stock solutions of compounds were dissolved in DMSO with the final concentration kept constant at 0.5% (v/v). Thioflavin T fluorescence was measured to evaluate the development of A β 42 fibrils over time using a fluorescence plate reader (Fluostar Optima, BMG labtech) with standard 96-well black microtiter plates. Experiments were started by adding the peptide (final A β 42 concentration equal to 10 μM) into a mixture containing 40 μM Thioflavin T in 10 mM Tris-HCl, 100 mM NaCl buffer (pH 7.4) with and without the tested compounds at different concentrations (100 and 10 μM) at room temperature. The ThT fluorescence intensity of each sample (performed in triplicate) was

recorded with 440/480 nm excitation/emission filters set for 42 hours performing a double orbital shaking of 10 s before the first cycle.

The BODIPY fluorescence assays were performed by Dr. Nicolo Tonali (Fluorinated Molecules and Medicinal Chemistry, Department of Chemistry, Université Paris-Sud) as described by Tonali *et al.*¹⁶⁵ BODIPY was obtained from the synthesis described in literature. A β 42 was purchased from Bachem. Milli-Q system was used to purify water that was used throughout this work. Stock solutions of the BODIPY dye for spectroscopic measurements and for time-dependent kinetics were prepared in EtOH (0.0428 mM) and subsequently diluted into the PBS buffer (5.3 μ M). The peptide was prepared, following the procedure B. Stock solutions of compounds were dissolved in DMSO (20 mM) and later diluted in PBS buffer to reach three different concentration (400 μ M, 40 μ M and 4 μ M). BODIPY fluorescence was measured to evaluate the development of A β 42 oligomers over time using a fluorescence plate reader (Fluostar Optima, BMG labtech) with standard 96-well black microtiter plates. Experiments were started by adding the peptide (final A β 42 concentration equal to 10 μ M) into a mixture containing 0.53 μ M BODIPY in 20 mM buffer (pH 7.4) with and without the tested compounds at different concentrations (100, 10 μ M and 1 μ M) at 25°C. The BODIPY fluorescence intensity of each sample (performed in triplicate) was recorded with 518/540 nm excitation/emission filters set for 9 hours performing a double orbital shaking of 10 s before the first cycle. The curves are provided as the average curves of the triplicate with error bars (+/- standard error) for each measured point (every 10 min). The ability of compounds to inhibit A β 1-42 aggregation was assessed considering the time of the half-life of aggregation ($t_{1/2}$), the intensity of the experimental fluorescence plateau (F) and the slope of the linear part of the curve. The $t_{1/2}$ extension is defined as the experimental $t_{1/2}$ in the presence of the tested compound relative to the one obtained without the compound and is evaluated as the following percentage: $t_{1/2}(\text{A}\beta 42 + \text{compound}) - t_{1/2}(\text{A}\beta 42) / t_{1/2}(\text{A}\beta 42) \times 100$. The F reduction is defined as the intensity of experimental fluorescence plateau observed with the tested compound relative to the value obtained without the compound and is evaluated as the following percentage: $(F_{\text{A}\beta 42 + \text{compound}} - F_{\text{A}\beta 42}) / F_{\text{A}\beta 42} \times 100$. The slope variation, that is correlated with the rate of the oligomerization process, was calculated by fitting the linear part of the curve between 0 and 4 hours by RMSD regression. The slope variation is defined as the slope of experimental linear curve observed with the tested compound relative to the value

7. Experimental section

obtained without the compound and is evaluated as the following percentage:
(Slope $A\beta_{42}+\text{compound}$ – Slope $A\beta_{42}$) / Slope $A\beta_{42}$ X 100.

The cell adhesions assay was performed as previously described by Conradi *et al.*¹⁵³ by Isabell Kemker (Organic and Bioorganic Chemistry, Department of Chemistry, University of Bielefeld). Competition assays were performed with WM-115 human epithelial cancer cells. Therefore, WM-115 cells were cultivated to a confluence of 70 %, detached with Trypsin-EDTA (0.05 %/0.02 % in D-PBS) (PAA, Pasching, Austria), washed with MEM medium, resuspended in MEM medium with 1 mg·mL⁻¹ fluorescein diacetate (Sigma-Aldrich, St. Louis, USA) to a cell density of 1·10⁵ cells·mL⁻¹, and incubated at 37 °C under steady shaking for 30 min. Subsequently, cells were washed two times with MEM medium, resuspended with MEM medium containing divalent cations Ca²⁺ and Mg²⁺ (2 mM) to obtain a cell density of 1·10⁵ cells·mL⁻¹ and incubated in the dark on ice for 30 min. For the cell adhesion assay CagL^{WT} was immobilized on a Nunc MaxisorpTM surface and WM-115 cells pre-incubated with varying concentrations of vitronectin were dispensed to the immobilized CagL^{WT}. Likewise, WM-115 cells were pre-incubated with different CagL^{WT} concentrations before adding to immobilized vitronectin (1 mg·mL⁻¹). The cell suspension was added to the peptide solutions to give concentrations ranging from milimolar to nanomolar and incubated 30 min at 37 °C. It was then dispensed on the coated microtiter plate (5·10⁴ cells·well⁻¹) and incubated for 1 h at 37 °C. Unbound cells were aspirated and bound cells were washed twice with MEM medium. Fluorescence was measured ($I_{\text{ex}}= 485 \text{ nm}$; $I_{\text{em}}= 514 \text{ nm}$) in an InfiniteTM 200 Microplate Reader (Tecan, Männedorf, Switzerland). IC₅₀ values (50 % cell binding inhibition) of the tested peptides were evaluated with the GraphPad Prism 4.03 software (GraphPad, San Diego, USA). In cell adhesion assays the murine monoclonal antibodies LM609 (EMD Millipore, Billerica, USA) against human integrin $\alpha_v\beta_3$, 3S3 (AbD Serotec, MorphoSys AG, Germany) against β_1 integrin, and P1F6 (EMD Millipore, Billerica, USA) against $\alpha_v\beta_5$ were used in final concentrations of 25 mg·mL⁻¹. The assay was performed as described above. Instead of staining the cells with fluorescein diacetate, they were washed with Puck's salt solution (5.4 mM KCl, 0.4 mM KH₂PO₄, 5.6 mM D-glucose, 136 mM NaCl, 2 mM MgCl₂, 2 mM MnCl₂), fixed for 30 min at rt using 5 % (w/v) glutaraldehyde, and stained with crystal violet 1 % (w/v) in 100 mM MES (pH 6.0) over 60 min at rt. After a second washing step with Puck's salt solution, 100 mM citric acid in ethanol was added and the cells were incubated 30 min at rt for visualization. Absorption at 485 nm and emission at 514 nm was

measured using the Tecan M200 Microplate Reader and the data was processed with Origin (Dose-Response).

ELISA-assay was performed by Isabell Kemker (Organic and Bioorganic Chemistry, Department of Chemistry, University of Bielefeld) according to the previously reported protocol¹⁶⁶ as adapted by Kapp *et al.*¹⁶⁷, using coated extracellular matrix proteins and soluble integrins. Cilengitide (cyclo[RGDf(NMe)V]) was used as an internal standard for $\alpha_v\beta_3$ (0.54 nM). Flat-bottom 96-well Immuno Plates (BRAND, Wertheim, Germany) were coated overnight at 4 °C with human vitronectin (1.0 mg·mL⁻¹, 100 μ L per well, R&D) in carbonate buffer (15 mM Na₂CO₃, 35 mM NaHCO₃, pH 9.6). Each well was then washed with PBS-T-buffer (phosphate-buffered saline/Tween20, 137 mM NaCl, 2.7 mM KCl, 10 mM Na₂HPO₄, 2 mM KH₂PO₄, 0.01 % Tween20, pH 7.4; 3 x 200 μ L) and blocked for 1 h at room temperature with TS-B-buffer (Tris-saline/BSA buffer, 150 μ L/well, 20 mM Tris-HCl, 150 mM NaCl, 1 mM CaCl₂, 1 mM MgCl₂, 1 mM MnCl₂, pH 7.5, 1 % BSA). In the meantime, a dilution series of the compound and internal standard was prepared in an extra plate, starting from 2000 nM to 7.1 nM (reference compound 20 nM to 0.43 nM) in 1:5 dilution steps. After washing the assay plate three times with PBS-T (200 μ L), 50 μ L of the dilution series was transferred to each well from B–G. Well A was filled with 100 μ L TSB-solution (blank) and well H was filled with 50 μ L TS-B-buffer. 50 μ L of a solution of human $\alpha_v\beta_3$ -integrin (2.0 mg·mL⁻¹, R&D) in TS-B-buffer was transferred to wells H–B and incubated for 1 h at rt. The plate was washed three times with PBS-T buffer, and then the primary antibody (2.0 mg·mL, mouse anti-human CD51/61, BD Biosciences, 100 μ L per well) was added to the plate. After incubation for 1 h at rt, the plate was washed three times with PBS-T. Then, the secondary peroxidase-labeled antibody (1.0 mg·mL⁻¹, anti-mouse IgG-POD, Sigma-Aldrich, 100 μ L/well) was added to the plate and incubated for 1 h at rt. After washing the plate three times with PBS-T, the plate was developed by quick addition of SeramunBlau (50 μ L/well, Seramun Diagnostic GmbH, Heidesee, Germany) and incubation until a colour gradient was visible. The reaction was stopped with 3 M H₂SO₄ (50 μ L/well), and the absorbance was measured at 450 nm with a plate reader (Tecan Reader). The IC₅₀ of each compound was tested in duplicate, and the resulting inhibition curves were analyzed using OriginPro 2017G (32-bit) SR1 software. The inflection point describes the IC₅₀ value. All determined IC₅₀ were referenced to the activity of the internal standard Cilengitide (0.54 nM).

7.1. General Procedures

GP1: Condensation of *tert*-Butanesulfinamide with aliphatic aldehydes. Performed as described by the group of Ellman,¹⁶⁸ utilizing CuSO₄ as Lewis acid or the MgSO₄ / PPTS pair. We found both procedures to work equally well and used them interchangeable. The analytical data was consistent with Wünsch *et al.*⁶²

GP2: α -Azido Acids. The synthesis of α -azido acids was performed based on the publication of Pelletier and Wong, without the customized workup for free carboxylic acids.^{64, 65} NaN₃ (1.78 g; 27.4 mmol) is dissolved in H₂O (4.5 mL) and DCM (7.5 mL), the solution is cooled to 0 °C. Tf₂O (930 μ L; 1.56 g; 5.53 mmol) is added dropwise at RT and stirring is continued for 2 h. The DCM phase is removed in a separatory funnel and the aqueous phase is extracted with DCM (2x4 mL). The combined organic phases, containing the Tf-N₃, are pooled and washed with saturated Na₂CO₃ solution (15 mL). Caution: The Tf-N₃ is used without further purification or concentration as a solution in DCM. The amino acid benzylester salt (2.79 mmol) and K₂CO₃ (1.55 g; 11.2 mmol; 4.0 eq) are suspended in H₂O (9 mL) and *t*BuOH (18 mL). Cu(II)SO₄·5H₂O (1 mol%; 7 mg; 0.03 μ mol) is added, followed by dropwise addition of Tf-N₃ solution (15 mL). The reaction mixture is left to react overnight. Afterwards the *t*BuOH is removed in vacuum, the aqueous slurry is diluted with brine (10 mL) and extracted with DCM (3 \times 10 mL), the combined organic phases are dried over MgSO₄ and concentrated in vacuum. The crude azide is purified by column chromatography (PE/EtOAc 10:1).

GP3: Boc Cleavage and Boc Introduction. The *N*-sulfinyl propargylamine is dissolved in MeOH (0.1 M) and 4M HCl in dioxane (3 eq) is added dropwise. Once TLC indicates complete deprotection (15-30 min), the crude HCl salt of the amine is obtained by concentrating the solution in vacuum. The residue is dissolved in H₂O/THF (1:1) (0.1 M), NaHCO₃ (4.0 eq) and Boc₂O (2.0 eq) are added portion-wise and the reaction mixture is stirred overnight. Imidazole (2.0 eq) is added and stirring is continued for 1 h. The reaction mixture is diluted with EtOAc and washed with 0.5 M aqueous HCl (3x), brine (1x) and dried over MgSO₄. If necessary, the Boc protected propargylamine can be purified by flash silica chromatography (PE/EtOAc 10:1).

GP4: RuAAC. The Boc protected propargylamine (1.0 eq) and the azide (1.1 eq) are dissolved in dry THF under an argon atmosphere to give a 0.5 M solution. Cp**Ru*Cl(COD) (3-5 mol%) is added and the reaction mixture stirred for 1-2 h under microwave irradiation (60 °C, 20 W). Once TLC indicates a full conversion of the propargylamine, the solvent is

removed under vacuum and the triazole purified by column chromatography (PE/EtOAc 2:1).

GP5: Hydrogenolysis of Boc-protected Benzyl esters. The benzyl ester protected triazole is dissolved in EtOH (0.05 M), Pd/C (20 wt%) is added and H₂ (balloon, 1 atm) is passed through the solution for 1-2 h via cannula. Once TLC indicates full conversion of the starting material, the solution is filtered through a short plug of silica, which is washed several times with EtOH. The filtrate is concentrated under vacuum and lyophilized to obtain the free acid, which is used without further purification for the coupling step.

GP6: Hydrogenolysis of Fmoc-protected Benzyl esters. The cleavage was performed according to a publication of Mandal *et al.*¹⁴¹ The filtrate is concentrated under vacuum and lyophilized to obtain the free acid, which is used without further purification for the coupling step.

GP7: Bus Cleavage and Fmoc Introduction. The *tert*-butyl sulfinamide protected propargylamine (1.0 eq) is dissolved in MeOH (0.1 M) and 4 M HCl in dioxane (3.0 eq) is added dropwise. After TLC indicates a full conversion of the starting material, usually between 15-30 min, the reaction mixture is concentrated under vacuum to obtain the crude hydrochloride-salt. THF/H₂O 1:1 (0.1 M) is added, followed by Fmoc-OSu (1.2 eq) and NaHCO₃ (4 eq) and the reaction mixture is left to react overnight. The solvent is evaporated under vacuum and the crude dissolved in EtOAc, washed with 5% aqueous KHSO₄-solution (3x), saturated NaHCO₃-solution (3x) and brine (1x), dried over MgSO₄ and concentrated under vacuum. The Fmoc protected propargylamine is purified by column chromatography.

GP8: Nucleophilic addition of lithium (trimethylsilyl)acetylide. Performed as described by Xiao *et al.*,⁶¹ utilizing Ti(O^{*i*}Pr)₄ as a lewis acid in THF. The analytical data was found to be consistent with Wünsch *et al.*⁶²

GP9: Solid phase peptide synthesis. The loading of the 2-chloro trityl resin was performed as described by Barlos *et al.*¹⁵¹ Loading of the rink-amide resin was performed as followed: swelling of the resin is performed in DMF (10 mL/g of resin) for 30 min, deprotection of the Fmoc group is performed with 20% piperidine in DMF (10 mL/g of resin) for 15 min and 30 min, with DMF washing steps in between. The amino acid or triazole (1.0 eq) is dissolved in DCM (5 mL/g of resin) and Oxyma or HOAt (1.1 eq) is added, followed by DIC (1.1 eq) with a preactivation time of 10 min. During the preactivation time, DMF (5 mL/g of resin) is given to the resin, followed by *sym*-collidine (10 eq). Afterwards, the preactivated acid in the DCM solution is given to the resin for a final ratio of DMF/DCM

7. Experimental section

(1:1), followed by stirring overnight. Remaining amine functions are capped by the addition of acetic anhydride (10 eq) and stirring for 30 min. For determination of the loading, 1 mg of loaded and dried resin is placed into a 1 cm quartz cuvette with 3 mL of a 20% piperidine solution in DMF. The absorption is measured at 290 nm which correlates with the amount of formed piperidine-dibenzofulven adduct. As a reference, the 20% piperidine in DMF solution is used. The loading is determined with **Formula 1**,¹⁶⁹ in which “A” is the absorbance at 290 nm and “m” is the amount of weighted resin.

$$\text{Loading} = \frac{A}{m \cdot 1,65} [\text{mmol} \cdot \text{g}^{-1}] \quad (\text{Formula 1})$$

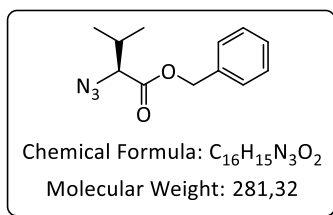
Fmoc deprotection: The loaded resin is mixed with a 20% piperidine in DMF solution (10 mL/g of resin, containing 0.1 M HOBT) and shaken for 15 and 30 min, with DMF washing steps in between. Afterwards the resin is washed (10 mL/g of resin): DMF (5x), DCM (3x), MeOH (1x), Et₂O (1x).

Coupling: The amino acid or triazole (1.5 eq) is dissolved in DCM (5 mL/g of resin), Oxyma or HOAt (1.65 eq) is added followed by DIC (1.65 eq). The mixture is stirred 10 min for preactivation. During the preactivation time, the resin is mixed with DMF (5 mL / g of resin). *Sym*-collidine (10 eq) is added to the resin, followed by the preactivated acid in the DCM solution for a final ratio of DMF/DCM (1:1), followed by stirring overnight. Afterwards the resin is washed (10 mL/g of resin): DMF (3x), DCM (3x), MeOH, Et₂O. If desired, the coupling can be verified by Kaiser test.¹⁷⁰

CCDC 1561604 to CCDC 1561608 contain supplementary crystallographic data for this dissertation already published¹⁰⁷ that can be obtained free of charge from The Cambridge Crystallographic Data Centre at www.ccdc.cam.ac.uk/data_request/cif

7.2. Synthesis results

Benzyl (S)-2-Azido-3-methylbutanoate (4a).



Prepared using general procedure **GP2**, starting from H-Val-OBzl.TsOH (1.06 g; 2.79 mmol).

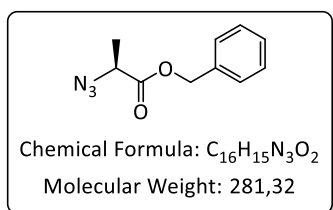
Yield: 636 mg (2.73 mmol); 98%. **R_f** (PE/EtOAc 10:1)= 0.55.

[α]_D²⁵ = -28 (CHCl₃, c = 0.2). **¹H-NMR** (500 MHz, CDCl₃):

δ [ppm]= 7.45-7.34 (m, 5H, Ph-**H**), 5.25 (d, ²J = 12.2 Hz, 1H, O-**CH**₂), 5.21 (d, ²J = 12.2 Hz, 1H, O-**CH**₂), 3.72 (d, ³J = 6.2 Hz, 1H, **H**^α), 2.24 (m, 1H, **H**^β) 1.00 (d, ³J = 7.0 Hz, 3H, **H**^γ), 0.98 (d, ³J = 6.8 Hz, 3H, **H**^γ).

¹³C{¹H}-NMR (126 MHz, CDCl₃): δ [ppm]= 170.02 (C=O), 135.11 (C^{Ar}), 128.66 (2C, CH^{Ar} meta), 128.59 (CH^{Ar}, para), 128.49 (2C, CH^{Ar}, ortho), 68.14 (O-**CH**₂-), 67.32 (C^α), 30.99 (C^β), 19.34 (C^γ), 17.96 (C^γ).

Benzyl (S)-2-Azidopropanoate (4b).



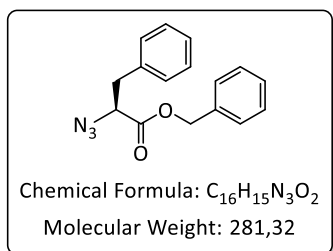
Prepared using general procedure **GP2**, starting from H-Ala-OBzl:HCl (602 mg; 2.79 mmol).

Yield: 531 mg (2.59 mmol); 93%. **R_f** (PE/EtOAc 10:1)= 0.47.

¹H-NMR (300 MHz, CDCl₃): δ [ppm]= 7.43-7.35 (m, 5H, Ar-H),

5.27-5.21 (m, 2H, O-**CH**₂), 4.00 (q, ³J = 7.1 Hz, 1H, **H**^α), 1.51 (d, ³J = 7.1 Hz, 3H, **H**^β).

Benzyl (S)-2-Azido-3-phenylpropanoate (4c).

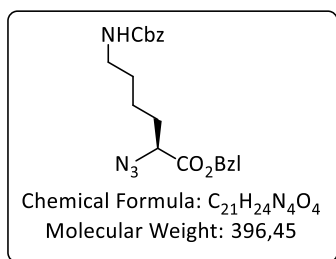


Prepared using general procedure **GP2**, starting from H-Phe-OBzl:HCl (814 mg; 2.79 mmol).

Yield: 684 mg (2.43 mmol); 87%. **R_f** (PE/EtOAc 10:1)= 0.58.

¹H-NMR (500 MHz, CDCl₃): δ [ppm]= 7.43-7.19 (m, 10H, Ph-H),

5.27-5.21 (m, 2H, O-**CH**₂), 4.12 (dd, ³J = 8.5, 5.7 Hz, 1H, **H**^α), 3.20 (dd, ²J = 14.0 Hz, ³J = 5.7 Hz, 1H, **H**^β), 3.05 (dd, ²J = 14.0 Hz, ³J = 8.5 Hz, 1H, **H**^β).

Benzyl (S)-2-azido-6-(((benzyloxy)carbonyl)amino)hexanoate (4d)

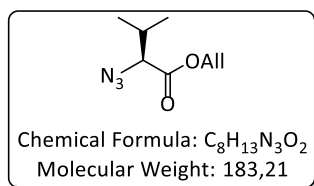
Prepared using general procedure **GP2**, starting from H-Lys(Cbz)-OBzl.HCl (1.03 g; 2.78 mmol).

Yield: 954 mg (2.41 mmol); 87%. **R_f** (PE/EtOAc 2:1)= 0.54.

MS (ESI): $m/z = 419.2 [M+Na]^+$.

¹H-NMR (500 MHz, CDCl₃): δ [ppm]= 7.41-7.32 (m, 10H, Ph-H), 5.26 (d, $^2J = 12.2$ Hz, 1H, C $^\alpha$ CO₂CHH), 5.22 (d, $^2J = 12.2$ Hz, 1H, C $^\alpha$ CO₂CHH), 5.14-5.10 (m, 2H, NCO₂CH₂), 4.78 (dd, $^3J = 6.1$ Hz, 1H, NH), 3.89 (dd, $^3J = 8.3, 5.3$ Hz, 1H, H $^\alpha$), 3.23-3.13 (m, 2H, H $^\epsilon$), 1.91-1.75 (m, 2H, H $^\beta$), 1.57-1.47 (m, 2H, H $^\delta$), 1.47-1.37 (m, 2H, H $^\gamma$).

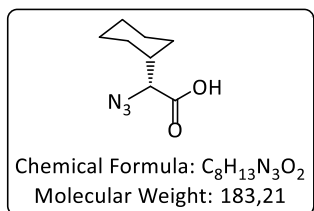
¹³C{¹H}-NMR (126 MHz, CDCl₃) δ [ppm]= 170.30 (Lys-C), 156.37 (NHCO₂), 136.57 (C Ar), 135.04 (C Ar), 128.71 (2C; CH Ar), 128.66 (2C; CH Ar), 128.54 (2C; CH Ar), 128.48 (2C; CH Ar), 128.14 (2C; CH Ar), 67.50 (C $^\alpha$ CO₂C), 66.68 (NHCO₂C), 61.83 (C $^\alpha$), 40.70 (C $^\epsilon$), 30.98 (C $^\beta$), 29.43 (C $^\delta$), 22.86 (C $^\gamma$).

(E)-Prop-1-en-1-yl (S)-2-azido-3-methylbutanoate (4e).

Prepared using general procedure **GP2**, starting from H-Val-OAll:TosH (351 mg; 1.07 mmol).

Yield: 150 mg (0.82 mmol); 77%. **R_f** (PE/EtOAc 10:1)= 0.59.

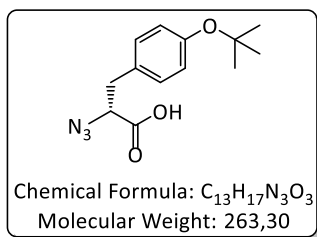
¹H-NMR (500 MHz, CDCl₃): δ [ppm]= 5.87 (dddd, $^3J = 17.4, 10.4, 5.9, 5.9$ Hz, 1H, CH₂-CH=CH₂), 5.31 (dd, $^3J = 17.4, ^2J = 1.3$ Hz, 1H, CH₂-CH=CHH E), 5.22 (dd, $^3J = 10.4, 1.3$ Hz, 1H, CH₂-CH=CH Z H), 4.67-4.59 (m, 2H, O-CH₂), 3.61 (d, $^3J = 6.2$ Hz, 1H, H $^\alpha$), 2.15 (m, 1H, H $^\beta$), 0.95 (d, $^3J = 6.8$ Hz, 3H, H $^\gamma$), 0.92 (d, $^3J = 6.8$ Hz, 3H, H $^\gamma$).

(R)-2-Azido-2-cyclohexylacetic acid (4f)

Synthesized according to the procedure of Lundquist *et al.*,⁶⁵ starting from H-D-chGly-OH (439 mg; 2.79 mmol).

Yield: 182 mg (0.99 mmol); 36%.

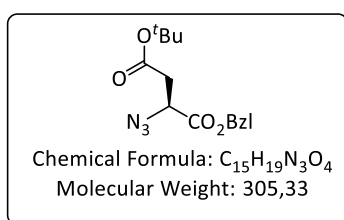
¹H-NMR (500 MHz, CDCl₃) δ [ppm]= 3.79 (d, $^3J = 6.1$ Hz, 1H, H $^\alpha$), 1.94 (m, 1H, H $^\beta$), 1.84-1.69 (m, 5H, CH₂), 1.36-1.15 (m, 5H, CH₂).

(S)-2-Azido-3-(4-(tert-butoxy)phenyl)propanoic acid (4g)

Synthesized according to the procedure of Lundquist *et al.*,⁶⁵ starting from H-D-Tyr(^tBu)-OH (662 mg; 2.79 mmol).

Yield: 191 mg (0.73 mmol); 26%.

¹H-NMR (500 MHz, CDCl₃) δ [ppm]= 7.18 (d, ³J= 7.8 Hz, 2H, **H^δ**), 6.98 (d, ³J= 7.7 Hz, 2H, **H^ε**), 4.15 (dd, ³J= 9.2, 4.9 Hz, 1H, **H^α**), 3.22 (dd, ²J= 14.3, ³J= 4.9 Hz, 1H, **H^β**), 3.03 (dd, ²J= 14.2, ³J= 8.9 Hz, 1H, **H^β**), 1.37 (s, 9H, C(CH₃)₃).

1-Benzyl 4-(tert-butyl) (S)-2-azidosuccinate (4h)

Fmoc-Asp(^tBu)-OBzl (50): Prepared according to Xu *et al.*¹⁷¹ starting from Fmoc-Asp(^tBu)-OH (1.00 g; 2.43 mmol).

Yield: 0.863 g (1.72 mmol); 71% (Lit.: 82%).

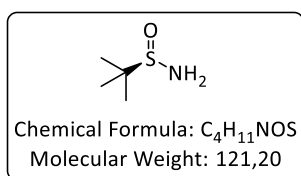
R_f (PE/EtOAc 10:1)= 0.16.

H-Asp(^tBu)-OBzl (51): Prepared according to Xu *et al.*¹⁷¹ starting from Fmoc-Asp(^tBu)-OBzl (0.863 mg; 1.72 mmol). **Yield:** 313 mg (1.12 mmol); 65% (Lit.: 91%). **R_f** (PE/EtOAc 5:1 including 1% TEA)= 0.39.

N₃-Asp(^tBu)-OBzl (4h): Prepared using general procedure **GP2**, starting from H-Asp(^tBu)-OBzl (313 mg; 1.12 mmol). **Yield:** 0.17 mg (0.56 mmol); 50%.

R_f (PE/EtOAc 5:1)= 0.39. **MS (ESI):** m/z= 328.2 [M+Na]⁺.

¹H-NMR (500 MHz, CDCl₃): δ [ppm]= 7.40-7.31 (m, 5H, Ph-**H**), 5.26-5.21 (m, 2H, O-**CH**₂), 4.35 (dd, ³J= 7.6, 5.4 Hz, 1H, **H^α**), 2.79 (dd, ²J= 16.5, ³J= 5.4 Hz, 1H, **H^β**), 2.66 (dd, ²J= 16.5, ³J= 7.6 Hz, 1H, **H^β**), 1.44 (s, 9H, C(CH₃)₃).

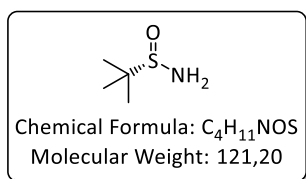
(R)-2-Methylpropane-2-sulfonamide ((R)-5)

Synthesized according to the literature procedure of the Ellman group¹⁰⁸ starting from di-*tert*-Butyldisulfid (30.0 g; 168 mmol).

Yield: 7.32 g (60.4 mmol); 36% over two steps (Lit.: 75% over two steps). **[α]_D²⁵** = +2.4 (c = 1, CHCl₃). (Lit.: **[α]_D²³** = +4.9 (c = 1, CHCl₃).

Chiral HPLC: ee ≥ 99%, t_R = 7.1 min. **R_f** (PE/EtOAc 4:3)= 0.4.

¹H-NMR (500 MHz, CDCl₃): δ [ppm]= 1.23 (s, 9H, S-C(CH₃)₃), 3.69 (s, 2H, -NH₂).

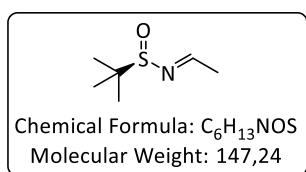
(S)-2-Methylpropane-2-sulfinamide ((S)-5)

Synthesized according to the literature procedure of the Ellman group¹⁰⁸ starting from di-*tert*-Butyldisulfid (18.9 g; 106 mmol).

Yield: 3.01 g (24.8 mmol); 23% over two steps (Lit.: 75% over two steps). **Chiral HPLC:** ee ≥ 99%, t_R = 9.2 min.

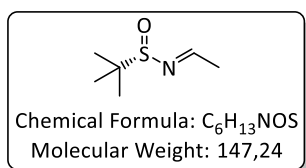
R_f (PE/EtOAc 4:3) = 0.4.

¹H-NMR (500 MHz, CDCl₃): δ [ppm] = 1.23 (s, 9H, S-C(CH₃)₃), 3.66 (s, 2H, -NH₂).

(R, E)-N-Ethylidene-2-methylpropane-2-sulfinamide (6a)

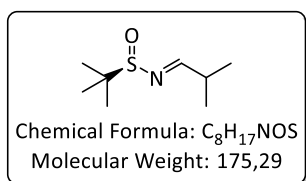
Synthesized according to **GP1** starting from (*R*)-2-methylpropane-2-sulfinamide (1.00 g; 8.25 mmol).

Yield: quant. (Lit.: 81%). The analytical data was found to be consistent with the literature.⁶²

(S, E)-N-Ethylidene-2-methylpropane-2-sulfinamide (6b)

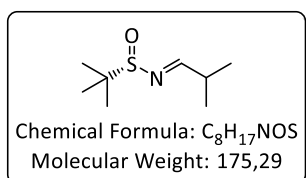
Synthesized according to **GP1** starting from (*S*)-2-methylpropane-2-sulfinamide (1.00 g; 8.25 mmol).

Yield: 967 mg (6.56 mmol); 80% (Lit.: 81%). The analytical data was found to be consistent with the literature.⁶²

(R, E)-2-Methyl-N-(2-methylpropylidene)propane-2-sulfinamide (6c)

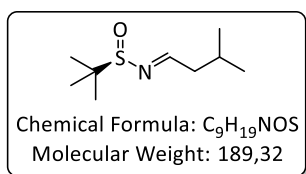
Synthesized according to **GP1** starting from (*R*)-2-methylpropane-2-sulfinamide (1.00 g; 8.25 mmol).

Yield: 1.41 g (8.04 mmol); 97% (Lit.: 90%). The analytical data was found to be consistent with the literature.⁶²

(S, E)-2-Methyl-N-(2-methylpropylidene)propane-2-sulfinamide (6d)

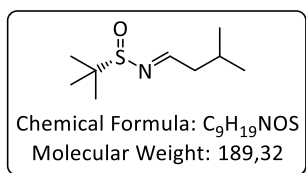
Synthesized according to **GP1** starting from (*S*)-2-methylpropane-2-sulfinamide (1.00 g; 8.25 mmol).

Yield: 1.02 g (5.82 mmol); 71% (Lit.: 90%). The analytical data was found to be consistent with the literature.⁶²

(R, E)-2-Methyl-N-(3-methylbutylidene)propane-2-sulfinamide (6e)

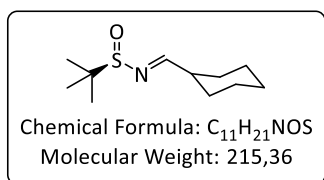
Synthesized according to **GP1** starting from (*R*)-2-methylpropane-2-sulfinamide (1.00 g; 8.25 mmol).

Yield: 1.23 g (6.50 mmol); 79% (Lit.: 92%). The analytical data was found to be consistent with the literature.⁶²

(S, E)-2-Methyl-N-(3-methylbutylidene)propane-2-sulfinamide (6f)

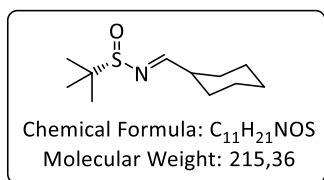
Synthesized according to **GP1** starting from (*S*)-2-methylpropane-2-sulfinamide (2.00 g; 16.5 mmol).

Yield: 2.90 g (15.3 mmol); 93% (Lit.: 92%). The analytical data was found to be consistent with the literature.⁶²

(R, E)-N-(Cyclohexylmethylene)-2-methylpropane-2-sulfinamide (6g)

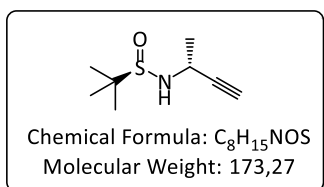
Synthesized according to **GP1** starting from (*R*)-2-methylpropane-2-sulfinamide (2.00 g; 16.5 mmol).

Yield: 3.32 g (15.4 mmol); 93% (Lit.: 96%). The analytical data was found to be consistent with the literature.⁶²

(S, E)-N-(Cyclohexylmethylene)-2-methylpropane-2-sulfinamide (6f)

Synthesized according to **GP1** starting from (*R*)-2-methylpropane-2-sulfinamide (1.00 g; 8.25 mmol).

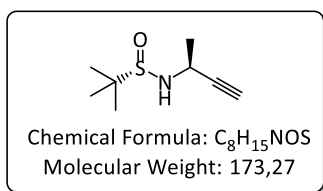
Yield: 824 mg (3.83 mmol); 46% (Lit.: 96%). The analytical data was found to be consistent with the literature.⁶²

(R)-N-((R)-But-3-yn-2-yl)-2-methylpropane-2-sulfinamide (7a)

Synthesized according to **GP8** starting (*R,E*)-*N*-ethylidene-2-methylpropane-2-sulfinamide (1.21 g; 8.25 mmol).

Yield: 696 mg (4.02 mmol); 49% over two steps (Lit.: 47%).

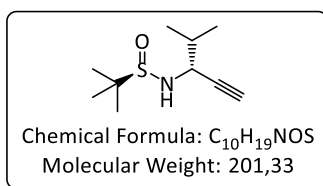
The analytical data was found to be consistent with the literature.⁶²

(S)-N-((S)-But-3-yn-2-yl)-2-methylpropane-2-sulfinamide (7b)

Synthesized according to **GP8** starting (*S, E*)-*N*-Ethylidene-2-methylpropane-2-sulfinamide (967 mg; 6.57 mmol).

Yield: 522 mg (3.01 mmol); 46% over two steps (Lit.: 47%).

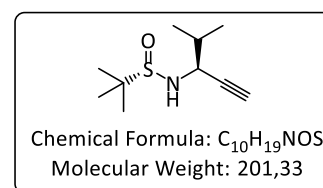
The analytical data was found to be consistent with the literature.⁶²

(R)-2-Methyl-N-((R)-4-methylpent-1-yn-3-yl)propane-2-sulfinamide (7c)

Synthesized according to **GP8** starting (*R, E*)-2-Methyl-*N*-(2-methylpropylidene)propane-2-sulfinamide (1.18 g;

6.73 mmol). **Yield:** 617 mg (3.06 mmol); 45% over two steps (Lit.: 61%). The analytical data was found to be consistent with

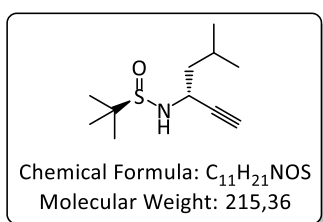
the literature.⁶²

(S)-2-Methyl-N-((S)-4-methylpent-1-yn-3-yl)propane-2-sulfinamide (7d)

Synthesized according to **GP8** starting (*S, E*)-2-Methyl-*N*-(2-methylpropylidene)propane-2-sulfinamide (1.02 g;

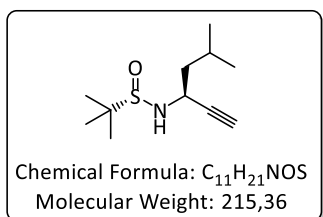
5.82 mmol). **Yield:** 782 mg (3.88 mmol); 67% over two steps (Lit.: 61%). The analytical data was found to be consistent with

the literature.⁶²

(R)-2-Methyl-N-((R)-5-methylhex-1-yn-3-yl)propane-2-sulfinamide (7e)

Synthesized according to **GP8** starting from (*R, E*)-2-Methyl-*N*-(3-methylbutylidene)propane-2-sulfinamide

Yield: 824 mg (3.83 mmol); 46% over two steps (Lit.: 53%). The analytical data was found to be consistent with the literature.⁶²

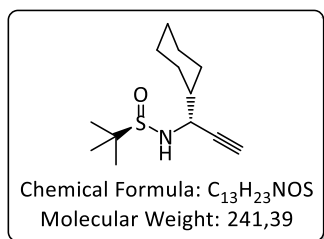
(S)-2-Methyl-N-((S)-5-methylhex-1-yn-3-yl)propane-2-sulfinamide (7f)

Synthesized according to **GP8** starting from (*S, E*)-2-Methyl-*N*-(3-methylbutylidene)propane-2-sulfinamide (1.33 g;

7.03 mmol). **Yield:** 793 mg (3.68 mmol); 52% over two steps

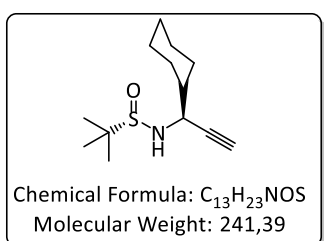
(Lit.: 53%). The analytical data was found to be consistent with the literature.⁶²

(R)-N-((R)-1-Cyclohexylprop-2-yn-1-yl)-2-methylpropane-2-sulfinamide (7g)



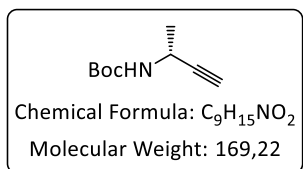
Synthesized according to **GP8** starting from (*R,E*)-*N*-(Cyclohexylmethylene)-2-methylpropane-2-sulfinamide (1.71 g; 7.94 mmol). **Yield:** 1.36 g (5.63 mmol); 71% over two steps (Lit.: 65%). The analytical data was found to be consistent with the literature.⁶²

(S)-N-((S)-1-Cyclohexylprop-2-yn-1-yl)-2-methylpropane-2-sulfinamide (7h)



Synthesized according to **GP8** starting from (*S,E*)-*N*-(Cyclohexylmethylene)-2-methylpropane-2-sulfinamide (1.60 g; 7.43 mmol). **Yield:** 1.07 g (4.43 mmol); 60% over two steps (Lit.: 65%). The analytical data was found to be consistent with the literature.⁶²

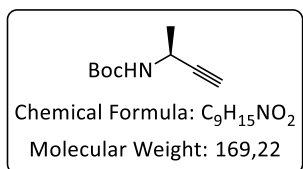
O-tert-Butyl N-(R)-But-3-yn-2-ylcarbamate (8a).



Prepared using general procedure **GP3**, starting from (*R*)-Bus-D-Ala≡ (680 mg; 3.92 mmol). **Yield:** 567 mg (3.35 mmol); 85%. **R_f** (PE/EtOAc 10:1)= 0.32. **MS** (ESI): *m/z*= 192.0 [M+Na]⁺.

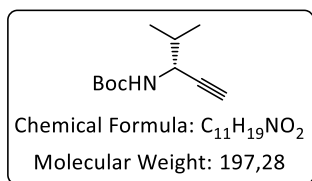
¹H-NMR (500 MHz, DMSO-*d*₆): δ [ppm]= 7.30 (d, ³*J*= 8.3 Hz, 1H, **NH**), 4.27 (dq, ³*J*= 8.3, 6.9 Hz, ⁴*J*= 2.2 Hz, **H^α**), 3.10 (d, ⁴*J*= 2.2 Hz, 1H, -**CCH**), 1.39 (s, 9H, -C(**CH**₃)₃), 1.25 (d, ³*J*= 6.9 Hz, 3H, **H^β**).

O-tert-Butyl N-(S)-But-3-yn-2-ylcarbamate (8b).

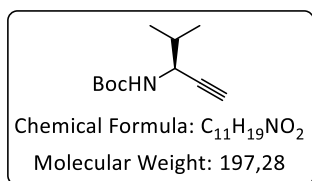


Prepared using general procedure **GP3**, starting from (*S*)-Bus-Ala≡ (522 mg; 3.01 mmol). **Yield:** 313 mg (1.85 mmol); 61%. **R_f** (PE/EtOAc 10:1)= 0.32. **¹H-NMR** (500 MHz, CDCl₃): δ [ppm]= 4.72 (m, 1H, **NH**), 4.50 (m, 1H, **H^α**), 2.27 (d, ⁴*J*= 2.3 Hz, 1H, -**CCH**),

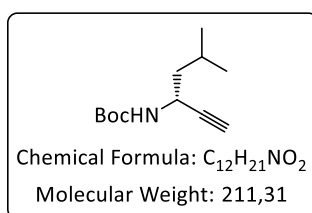
1.47 (s, 9H, -C(**CH**₃)₃), 1.42 (d, ³*J*= 6.9 Hz, 3H, **H^β**).

***O*-tert-Butyl *N*-(*R*)-(4-Methylpent-1-yn-3-yl)carbamate (8c).**

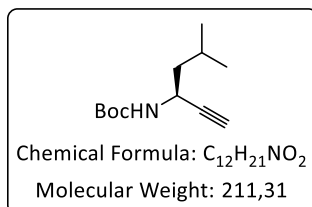
Prepared using general procedure **GP3**, starting from (*R*)-Bus-D-Val≡ (610 mg; 3.03 mmol). **Yield:** 538 mg (2.73 mmol); 90%. **R_f** (PE/EtOAc 10:1)= 0.40. **MS (ESI):** *m/z*= 220.1 [M+Na]⁺. **¹H-NMR** (500 MHz, DMSO-*d*₆): δ [ppm]= 7.28 (d, ³*J*= 9.0 Hz, 1H, **NH**), 4.02 (m, 1H, **H^α**), 3.13 (d, ⁴*J*= 2.3 Hz, 1H, -**CCH**), 1.75 (m, 1H, **H^β**), 1.39 (s, 9H, -C(**CH**₃)₃), 0.93 (d, ³*J*= 6.7 Hz, 3H, **H^γ**), 0.88 (d, ³*J*= 6.6 Hz, 3H, **H^γ**).

***O*-tert-Butyl *N*-(*S*)-(4-Methylpent-1-yn-3-yl)carbamate (8d).**

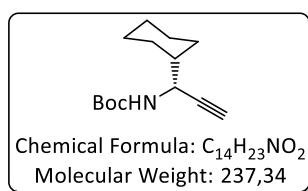
Prepared using general procedure **GP3**, starting from (*S*)-Bus-Val≡ (217 mg; 1.08 mmol). **Yield:** 121 mg (0.61 mmol); 56%. **R_f** (PE/EtOAc 10:1)= 0.40. **¹H-NMR** (500 MHz, CDCl₃): δ [ppm]= 4.75 (m, 1H, **NH**), 4.34 (m, 1H, **H^α**), 2.27 (d, ⁴*J*= 2.7 Hz, 1H, -**CCH**), 1.92 (m, 1H, **H^β**), 1.47 (s, 9H, -C(**CH**₃)₃), 1.00 (d, ³*J*= 6.5 Hz, 6H, **H^γ**).

***O*-tert-Butyl *N*-(*R*)-(5-Methylhex-1-yn-3-yl)carbamate (8e).**

Prepared using general procedure **GP3**, starting from (*R*)-Bus-D-Leu≡ (415 mg; 1.93 mmol). **Yield:** 385 mg (1.82 mmol); 94%. **R_f** (PE/EtOAc 10:1)= 0.45. **MS (ESI):** *m/z*= 234.1 [M+Na]⁺. **¹H-NMR** (500 MHz, DMSO-*d*₆): δ [ppm]= 7.26 (d, ³*J*= 8.8 Hz, 1H, **NH**), 4.21 (m, 1H, **H^α**), 3.11 (d, ⁴*J*= 2.3 Hz, 1H, -**CCH**), 1.67 (m, 1H, **H^γ**), 1.44 (m, 2H, **H^β**), 1.39 (s, 9H, -C(**CH**₃)₃), 0.88-0.86 (m, 6H, **H^δ**).

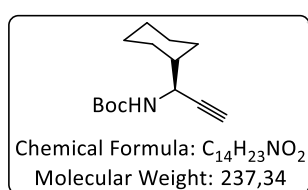
***O*-tert-Butyl *N*-(*S*)-(5-Methylhex-1-yn-3-yl)carbamate (8f).**

Prepared using general procedure **GP3**, starting from (*S*)-Bus-Leu≡ (520 mg; 2.41 mmol). **Yield:** 417 mg (1.97 mmol); 82%. **R_f** (PE/EtOAc 10:1)= 0.45. **¹H-NMR** (500 MHz, CDCl₃): δ [ppm]= 4.56 (m, 1H, **NH**), 4.37 (m, 1H, **H^α**), 2.18 (d, ⁴*J*= 2.2 Hz, 1H, -**CCH**), 1.74 (m, 1H, **H^γ**), 1.47-1.44 (m, 2H, **H^β**), 1.38 (s, 9H, -C(**CH**₃)₃), 0.88 (d, ³*J*= 6.6 Hz, 3H, **H^δ**), 0.87 (d, ³*J*= 6.6 Hz, 3H, **H^δ**).

O-tert-Butyl (S)-(1-cyclohexylprop-2-yn-1-yl)carbamate (8g).

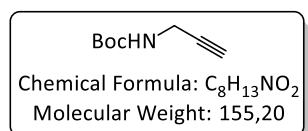
Prepared using general procedure **GP3**, starting from (*R*)-Bus-D-chGly≡ (892 mg; 3.70 mmol). **Yield:** 735 mg (3.09 mmol); 84%. **R_f** (PE/EtOAc 10:1)= 0.52.

¹H-NMR (300 MHz, CDCl₃): δ [ppm]= 4.74 (d, ³J= 6.6 Hz, 1H, **NH**), 4.32 (m, 1H, **H^α**), 2.27 (d, ⁴J= 2.4 Hz, 1H, -C**CH**), 1.47 (s, 9H, -C(**CH**₃)₃), 1.86-1.55 (m, 5H, **CH**, **CH**₂), 1.32-1.06 (m, 6H, **CH**₂).

O-tert-Butyl (S)-(1-cyclohexylprop-2-yn-1-yl)carbamate (8h).

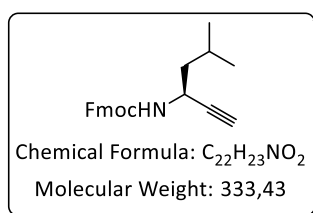
Prepared using general procedure **GP3**, starting from (*S*)-Bus-chGly≡ (209 mg; 0.87 mmol). **Yield:** 178 mg (0.75 mmol); 86%. **R_f** (PE/EtOAc 10:1)= 0.52.

¹H-NMR (300 MHz, DMSO-*d*₆): δ [ppm]= 7.26 (d, ³J= 9.0 Hz, 1H, **NH**), 3.13 (d, ⁴J= 2.4 Hz, 1H, C**CH**), 4.02 (ddd, ³J= 9.0, 8.3, ⁴J= 2.4 Hz, 1H, **H^α**), 1.88-1.53 (m, 5H, **CH**, **CH**₂), 1.38 (s, 9H, C(**CH**₃)₃), 1.26-0.81 (m, 6H, **CH**₂).

O-tert-Butyl prop-2-yn-1-ylcarbamate (8i).

Prop-2-yn-1-amine (1.00 g; 18.15 mmol; 1.0 eq) is dissolved in H₂O/THF 1:1 (20 mL). After the addition of NaHCO₃ (6.1 g; 72.6 mmol; 4 eq) and Boc₂O (8.3 mL; 36 mmol; 2 eq) the reaction mixture stirred overnight at rt. Imidazole (3.1 g; 45 mmol; 2.5 eq) is added and the reaction mixture stirred for 2 h. The THF is removed under vacuum, the aqueous slurry extracted with EtOAc (3x10 mL). The combined organic phases are washed with 5% KHSO₄ solution (3x10 mL), brine (10 mL) and dried over MgSO₄. Evaporation of the solvent gives the product in analytically pure form. **Yield:** 2.17 g (14.0 mmol); 77%.

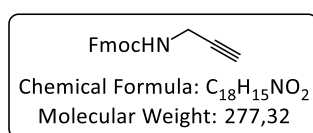
H-NMR (500 MHz, CDCl₃): δ [ppm] = 4.66 (m, 1H, **NH**), 3.89-3.78 (m, 2H, **H^α**), 2.15 (t, ³J= 2.5 Hz, 1H, C**CH**), 1.39 (s, 9H, C(**CH**₃)₃).

(9H-Fluoren-9-yl)methyl (S)-(5-methylhex-1-yn-3-yl)carbamate (8j).

Prepared according to general procedure **GP7**, starting from (S)-Bus-Leu≡ (560 mg; 2.60 mmol).

Yield: 615 mg (1.84 mmol); 71%. **R_f** (PE/EtOAc 10:1)= 0.29.

¹H-NMR (500 MHz, $CDCl_3$): δ [ppm]= 7.81-7.78 (m, 2H, H^{Ar}), 7.64-7.61 (m, 2H, H^{Ar}), 7.45-7.51 (m, 2H, H^{Ar}), 7.36-7.32 (m, 2H, H^{Ar}), 4.90 (d, $^3J= 8.8$ Hz, 1H, **NH**), 4.54 (m, 1H, H^α), 4.48-4.43 (m, 2H, CH- CH_2 -O), 4.25 (dd, $^3J= 7.0, 7.0$ Hz, 1H, CH- CH_2 -O) 2.31 (d, $^4J= 2.3$ Hz, 1H, **CCH**), 1.82 (m, 1H, H^γ), 1.62-1.58 (m, 2H, H^β), 1.01-0.9 (m, 6H, H^δ).

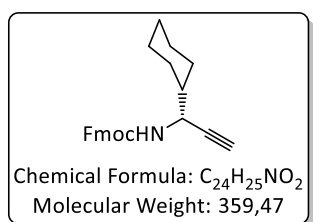
(9H-Fluoren-9-yl)methyl prop-2-yn-1-ylcarbamate (8k).

Propargylamine (0.64 mL; 10 mmol) and DIPEA (1.7 mL; 10 mmol; 1.0 eq) are dissolved in DCM (30 mL; dry) and cooled to 0°C, after the addition of Fmoc-OSu (3.4 g; 10 mmol; 1.0 eq)

and DMAP (0.12 g; 1.0 mmol; 0.1 eq) the solution is left to stir overnight. The solution is diluted with DCM (50 mL) and washed: 5% $KHSO_4$ (2x50 mL), saturated $NaHCO_3$ (2x50 mL) and brine (2x50 mL), dried over $MgSO_4$ and concentrated under vacuum. The product is purified by column chromatography (PE/EtOAc 5:1). **Yield:** 2.00 g (7.21 mmol); 72%.

R_f (PE/EtOAc 5:1)= 0.38. **MS (ESI):** m/z= 300.1 $[M+Na]^+$.

¹H-NMR (500 MHz; $CDCl_3$): δ [ppm]= 7.79-7.76 (m, 2H, H^{Ar}), 7.62-7.57 (m, 2H, H^{Ar}), 7.43-7.38 (m, 2H, H^{Ar}), 7.34-7.30 (m, 2H, H^{Ar}), 4.96 (d, 1H, $^3J= 6.9$ Hz, **NH**), 4.43 (d, $^3J= 6.9, ^4J= 2.5$ Hz, 2H, H^α), 4.23 (dd, $^3J= 6.8, 6.6$ Hz, CH CH_2 O), 4.03-3.95 (m, 2H, CH CH_2 O), 2.26 (t, $^4J= 2.5$ Hz, 1H, **CCH**).

(9H-Fluoren-9-yl)methyl (R)-(1-cyclohexylprop-2-yn-1-yl)carbamate (8l).

Prepared using general procedure **GP4**, starting from (R)-Bus-D-chGly≡ (700 mg; 2.90 mmol). **Yield:** 450 mg (1.25 mmol); 43% over two steps. **R_f** (PE/EtOAc 10:1)= 0.20.

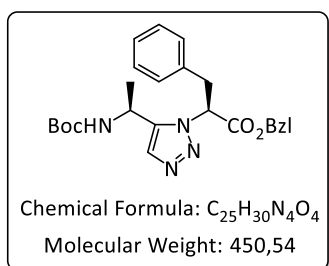
HR-MS (ESI): m/z= 360.1940 $[M+H]^+$ (calc. 360.19581).

¹H-NMR (600 MHz, $DMSO-d_6$) δ [ppm]= 7.90-7.87 (m, 2H, CH^{Ar}), 7.81 (d, $^3J= 8.9$ Hz, 1H, **NH**), 7.74-7.70 (m, 2H, CH^{Ar}), 7.44-7.39 (m, 2H, CH^{Ar}), 7.35-7.30 (m, 2H, CH^{Ar}), 4.34 (dd, $^2J= 10.4, ^3J= 7.2$ Hz, 1H, CH H -O), 4.28 (dd, $^2J= 10.4, ^3J= 7.0$ Hz, 1H, CH H -O), 4.21 (dd, $^3J= 7.2, 7.0$ Hz, CH CH_2 O), 4.09 (ddd, $^3J= 8.9$ Hz, 7.1, $^4J= 2.4$ Hz, H^α),

3.20 (d, $^4J = 2.4$ Hz, 1H, CCH), 1.86 (m, 1H, CH₂), 1.75-1.57 (m, 4H, CH₂), 1.46 (m, 1H, H^β), 1.21-0.92 (m, 5H, CH₂).

¹³C{¹H}-NMR (151 MHz, DMSO) δ [ppm] = 156.13 (CO), 144.33 (C^{Ar}), 144.24 (C^{Ar}), 141.21 (C^{Ar}), 141.19 (C^{Ar}), 128.10 (CH^{Ar}), 128.07 (CH^{Ar}), 127.49 (2C, CH^{Ar}), 125.76 (CH^{Ar}), 125.70 (CH^{Ar}), 120.58 (CH^{Ar}), 120.55 (CH^{Ar}), 83.44 (CCH), 74.49 (CCH), 66.00 (CHCH₂O), 48.23 (C^α), 47.19 (CHCH₂O), 42.04 (C^β), 29.27 (CH₂), 29.06 (CH₂), 26.29 (CH₂), 25.78 (CH₂), 25.76 (CH₂).

Boc-Ala[5Tz]Phe-OBzl (9a).



Prepared according to general procedure **GP4**, starting from **8b** (100 mg; 0.591 mmol). **Yield:** 232 mg (0.515 mmol); 87%.

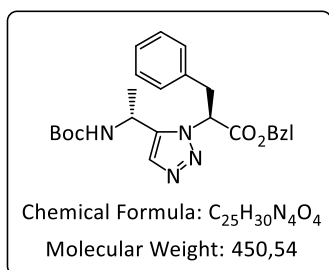
R_f (PE/EtOAc 2:1) = 0.41. **Analytical RP-HPLC:** t_R = 6.2 min (method 1, 220 nm).

HR-MS (ESI): m/z = 451.2344 [M+H]⁺ (calc. 451.23398).

¹H-NMR (600 MHz, DMSO-*d*₆): δ [ppm] = 7.50 (s, 1H, Tz-H), 7.39 (d, $^3J = 8.9$ Hz, 1H, NH), 7.36-6.96 (m, 10H, Ph-H), 5.87 (dd, $^3J = 11.3$, 4.6 Hz, 1H, Phe-H^α), 5.19 (m, 2H, O-CH₂-Ph), 4.35 (dq, $^3J = 8.9$, 7.0 Hz, 1H, Ala-H^α), 3.66 (dd, $^2J = 13.8$, $^3J = 4.6$ Hz, 1H, Phe-H^β), 3.43 (dd, $^2J = 13.8$, $^3J = 11.3$ Hz, 1H, Phe-H^β), 1.29 (s, 9H, C(CH₃)₃), 0.94 (d, $^3J = 7.0$ Hz, 3H, Ala-H^β).

¹³C{¹H}-NMR (151 MHz, DMSO-*d*₆): δ [ppm] = 168.18 (Phe-C), 155.25 (tBuO-C), 142.13 (Tz-C), 136.49 (Phe-C^{Ar}), 135.82 (C^{Ar}), 130.98 (Tz-CH), 129.41 (2C; CH^{Ar}), 128.81 (2C; CH^{Ar}), 128.78 (2C; CH^{Ar}), 128.46 (CH^{Ar}), 127.90 (2C; CH^{Ar}), 127.29 (CH^{Ar}), 78.80 (-C(CH₃)₃), 67.22 (O-CH₂-Ph), 61.32 (Phe-C^α), 39.46 (Ala-C^α), 38.00 (Phe-C^β), 28.49 (-C(CH₃)), 20.27 (Ala-C^β).

Boc-D-Ala[5Tz]Phe-OBzl (9b).



Prepared according to general procedure **GP4**, starting from **8a** (100 mg; 0.59 mmol). **Yield:** 251 mg (0.56 mmol); 94%.

R_f (PE/EtOAc 2:1) = 0.42.

HR-MS (ESI): m/z = 451.23571 [M+H]⁺ (calc. 451.23398).

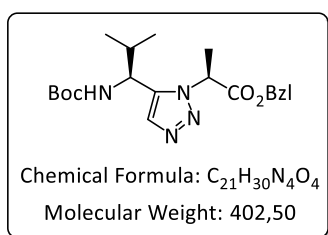
¹H-NMR (500 MHz; DMSO-*d*₆): δ [ppm] = 7.60 (s, 1H, Tz-H), 7.39 (d, $^3J = 8.5$ Hz, 1H, Ala-NH), 7.37-7.31 (m, 3H, Ph-H), 7.24-7.14 (m, 7H, Ph-H), 5.91 (dd, $^3J = 9.2$, 6.2 Hz, 1H, Phe-H^α), 5.18 (d, $^2J = 12.7$ Hz, 1H, O-CH₂), 5.15 (d, $^2J = 12.7$ Hz, 1H, O-CH₂), 4.79 (dq, $^3J = 8.5$, 6.9 Hz, 1H, Ala-H^α), 3.71 (dd, $^2J = 14.4$ Hz,

7. Experimental section

$^3J = 6.2$ Hz, 1H, Phe- H^β), 3.64 (dd, $^2J = 14.4$ Hz, $^3J = 9.3$ Hz, 1H, Phe- H^β), 1.36 (s, 9H, $-C(CH_3)_3$)
1.23 (d, $^3J = 6.9$ Hz, 3H, Ala- H^β).

$^{13}C\{^1H\}$ -NMR (126 MHz; DMSO- d_6): δ [ppm] = 168.36 (Phe-C), 155.29 (t BuO-C), 141.71 (Tz-C), 136.61 (Phe- C^{Ar}), 135.69 (C^{Ar}), 131.69 (Tz-CH), 129.36 (2C, CH^{Ar}), 128.85 (2C, CH^{Ar}), 128.68 (2C, CH^{Ar}), 128.63 (1C, CH^{Ar}), 128.09 (2C, CH^{Ar}), 127.10 (CH^{Ar}), 78.92 ($-C(CH_3)_3$), 67.46 (O-CH₂), 60.67 (Phe- C^α), 49.07 (Ala- C^α), 36.30 (Phe- C^β), 28.60 ($-C(CH_3)_3$), 20.80 (Ala- C^β).

Boc-Val[5Tz]Ala-OBzl (9c).



Prepared according to general procedure **GP4**, starting from **8d** (100 mg; 0.507 mmol). **Yield:** 171 mg (0.425 mmol); 84%. **R_f** (PE/EtOAc 1:1) = 0.50.

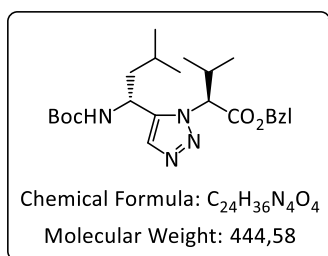
Analytical RP-HPLC: $t_R = 5.5$ min (method 1, 220 nm).

HR-MS (ESI): $m/z = 403.2351$ [M+H]⁺ (calc. 403.23398).

1H -NMR (600 MHz, DMSO- d_6): δ [ppm] = 7.63 (s, 1H, Tz- H), 7.41 (d, $^3J = 9.1$ Hz, 1H, NH), 7.36–7.25 (m, 5H, Ph H), 5.74 (q, $^3J = 7.1$ Hz, 1H, Ala- H^α), 5.16–5.10 (m, 2H, $-O-CH_2$), 4.53 (dd, $^3J = 9.2$ Hz, 1H, Val- H^α), 2.00 (m, 1H, Val- H^β), 1.76 (d, $^3J = 7.1$ Hz, 3H, Ala- H^β), 1.33 (s, 9H, $-C(CH_3)_3$), 0.92 (d, $^3J = 6.6$ Hz, 3H, Val- H^γ), 0.71 (d, $^3J = 6.7$ Hz, 3H, Val- H^γ).

$^{13}C\{^1H\}$ -NMR (151 MHz, DMSO- d_6): δ [ppm] = 169.29 (Ala-C), 155.67 (t BuO-C), 139.60 (Tz-C), 135.89 (C^{Ar}), 132.03 (Tz-CH), 128.81 (2C; CH^{Ar}), 128.48 (CH^{Ar}), 127.93 (2C; CH^{Ar}), 78.61 ($-C(CH_3)_3$), 67.08 (O-CH₂-), 55.59 (Ala- C^α), 50.44 (Val- C^α), 32.35 (Val- C^β), 28.56 ($C(CH_3)_3$), 19.88 (Val- C^γ), 19.27 (Val- C^γ), 18.03 (Ala- C^β). **Crystal structure:** CCDC 1561604.

Boc-D-Leu[5Tz]Val-OBzl (9d).



Prepared according to general procedure **GP4**, starting from **8e** (50 mg; 0.24 mmol). **Yield:** 96 mg (0.20 mmol); 88%.

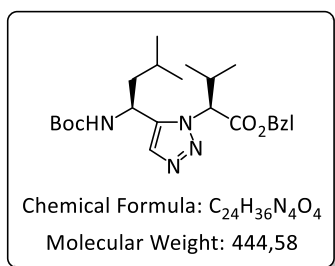
R_f (PE/EtOAc 2:1) = 0.40.

HR-MS (ESI): $m/z = 445.28273$ [M+H]⁺ (calc. 445.28093).

1H -NMR (500 MHz; DMSO- d_6): δ [ppm] = 7.64 (s, 1H, Tz- H), 7.49 (d, $^3J = 9.0$ Hz, 1H, Leu- NH), 7.33 (m, 3H, Ph- H), 7.20 (m, 2H, Ph- H), 5.21 (d, $^3J = 9.5$ Hz, 1H, Val- H^α), 5.16–5.13 (m, 2H, O-CH₂), 4.76 (m, 1H, Leu- H^α), 2.84 (m, 1H, Val- H^β), 1.74 (ddd, $^2J = 13.2$ Hz, $^3J = 9.7$, 5.1 Hz, 1H, Leu- H^β), 1.51–1.39 (m, 2H, Leu- H^β , Leu- H^γ), 1.35 (s, 9H, $-C(CH_3)_3$), 1.05 (d, $^3J = 6.7$ Hz, 3H, Val- H^γ), 0.80–0.72 (m, 9H, Leu- H^δ , Val- H^γ).

$^{13}\text{C}\{^1\text{H}\}$ -NMR (126 MHz; DMSO- d_6): δ [ppm]= 168.04 (Val-C), 155.71 ($^t\text{BuO-C}$), 141.58 (Tz-C), 135.66 (C^{Ar}), 131.36 (Tz-CH), 128.88 (2C, CH^{Ar}), 128.73 (CH^{Ar}), 128.29 (2C, CH^{Ar}), 79.06 ($-\text{C}(\text{CH}_3)_3$), 67.26 (O- CH_2), 65.09 (Val- C^α), 42.68 (Leu- C^β), 41.98 (Leu- C^α), 30.00 (Val- C^β), 28.58 ($-\text{C}(\text{CH}_3)_3$), 24.72 (Leu- C^γ), 22.86 (Leu- C^δ), 21.75 (Leu- C^δ), 19.64 (Val- C^γ), 18.76 (Val- C^γ). **Crystal structure:** CCDC 1561605.

Boc-Leu[5Tz]Val-OBzl (9e).



Prepared according to general procedure **GP4**, starting from **8f** (120 mg; 0.568 mmol). **Yield:** 205 mg (0.461 mmol); 81%.

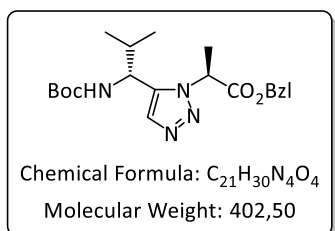
R_f (PE/EtOAc 1:1)= 0.71. **Analytical RP-HPLC:** t_R = 6.2 min (method 1, 220 nm). $[\alpha]_D^{21} = -72$ (CHCl_3 , $c = 0.12$).

HR-MS (ESI): $m/z = 445.2818$ [$\text{M}+\text{H}$] $^+$ (calc. 445.28093).

^1H -NMR (500 MHz, DMSO- d_6): δ [ppm]= 7.64 (s, 1H, Tz-**H**), 7.46 (d, $^3J = 8.7$ Hz, 1H, **NH**), 7.37–7.25 (m, 5H, Ph-**H**), 5.31 (d, $^3J = 8.1$ Hz, 1H, Val- H^α), 5.20–5.10 (m, 2H, O- CH_2), 4.79 (m, 1H, Leu- H^α), 2.75 (dq, $^3J = 8.1, 6.8, 6.7$ Hz, 1H, Val- H^β), 1.79 (m, 1H, Leu- H^γ), 1.54–1.46 (m, 2H, Leu- H^β), 1.30 (s, 9H, $\text{C}(\text{CH}_3)_3$), 0.96 (d, $^3J = 6.7$ Hz, 3H, Val- H^γ), 0.87 (d, $^3J = 6.2$ Hz, 3H, Leu- H^δ), 0.84 (d, $^3J = 6.0$ Hz, 3H, Leu- H^δ), 0.79 (d, $^3J = 6.8$ Hz, 3H, Val- H^γ).

$^{13}\text{C}\{^1\text{H}\}$ -NMR (125 MHz, DMSO- d_6): δ [ppm]= 168.09 (Val-C), 155.58 ($^t\text{BuO-C}$), 141.01 (Tz-C), 135.81 (C^{Ar}), 131.71 (Tz-CH), 128.85 (2C; CH^{Ar}), 128.57 (CH^{Ar}), 128.16 (2C; CH^{Ar}), 78.75 ($-\text{C}(\text{CH}_3)_3$), 67.10 (O- CH_2 -), 65.28 (Val- C^α), 42.69 (Leu- C^β), 42.56 (Leu- C^α), 31.06 (Val- C^β), 28.48 ($-\text{C}(\text{CH}_3)_3$), 24.79 (Leu- C^γ), 23.07 (Leu- C^δ), 21.98 (Leu- C^δ), 19.59 (Val- C^γ), 19.03 (Val- C^γ). **Crystal structure:** CCDC 1561606.

Boc-D-Val[5Tz]Ala-OBzl (9f).



Prepared according to general procedure **GP4**, starting from **8c** (100 mg; 0.51 mmol). **Yield:** 180 mg (0.45 mmol); 88%.

R_f (PE/EtOAc 2:1)= 0.39.

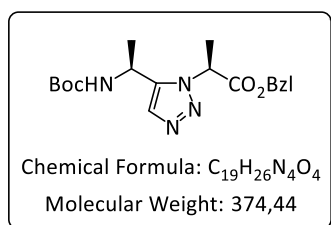
HR-MS (ESI): $m/z = 403.23560$ [$\text{M}+\text{H}$] $^+$ (calc. 403.23398).

^1H -NMR (500 MHz; DMSO- d_6): δ [ppm]= 7.65 (s, 1H, Tz-**H**), 7.52 (d, $^3J = 8.9$ Hz, 1H, Val-**NH**), 7.43–7.28 (m, 5H, Ph-**H**), 5.82 (q, $^3J = 7.0$ Hz, 1H, Ala- H^α), 5.21 (d, $^2J = 12.8$ Hz, 1H, -O- CH_2 -), 5.19 (d, $^2J = 12.8$ Hz, 1H, -O- CH_2 -), 4.47 (dd, $^3J = 8.9, 8.9$ Hz, 1H, Val- H^α), 2.07 (m, 1H, Val- H^β), 1.81 (d, $^3J = 7.0$ Hz, 3H, Ala- H^β), 1.41 (s, 9H, $-\text{C}(\text{CH}_3)_3$), 0.94 (d, $^3J = 6.6$ Hz, 3H, Val- H^γ), 0.71 (d, $^3J = 6.7$ Hz, 3H, Val- H^γ).

7. Experimental section

$^{13}\text{C}\{^1\text{H}\}$ -NMR (126 MHz; DMSO- d_6): δ [ppm]= 169.24 (Ala-C), 155.97 ($^t\text{BuO-C}$), 140.36 (Tz-C), 135.83 (C^{Ar}), 131.29 (Tz-CH), 128.81 (2C, CH^{Ar}), 128.57 (CH^{Ar}), 128.11 (2C, CH^{Ar}), 78.87 ($-\text{C}(\text{CH}_3)_3$), 67.23 ($-\text{O}-\text{CH}_2-$), 55.45 (Ala- C^α), 50.52 (Val- C^α), 31.75 (Val- C^β), 28.55 ($-\text{C}(\text{CH}_3)_3$), 19.95 (Val- C^γ), 19.32 (Val- C^γ), 17.83 (Ala- C^β). **Crystal structure:** CCDC 1561607.

Boc-Ala[5Tz]Ala-OBzl (9g).



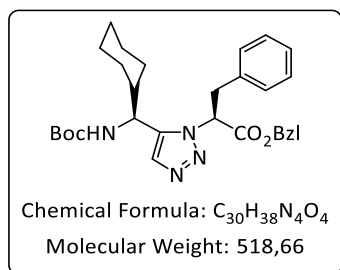
Prepared according to general procedure **GP4**, starting from **8b** (100 mg; 0.591 mmol). **Yield:** 170 mg (0.454 mmol); 77%.

R_f (PE/EtOAc 1:1)= 0.47. **MS** (ESI): m/z = 397.3 [$\text{M}+\text{Na}$] $^+$.

^1H -NMR (500 MHz, DMSO- d_6): δ [ppm]= 7.63 (s, 1H, Tz-**H**), 7.42 (d, 3J = 8.8 Hz, 1H, **NH**), 7.38-7.27 (m, 5H, Ar-**H**), 5.70 (q, 3J = 7.1 Hz, 1H, Ala2- H^α), 5.17-5.13 (m, 2H, O- CH_2-), 4.93 (dq, 3J = 8.8, 7.2 Hz, 1H, Ala1- H^α), 1.78 (d, 3J = 7.2 Hz, 3H, Ala2- H^β), 1.39 (d, 3J = 7.0 Hz, 3H, Ala1- H^β), 1.33 (s, 9H, $\text{C}(\text{CH}_3)_3$).

$^{13}\text{C}\{^1\text{H}\}$ -NMR (126 MHz, DMSO- d_6): δ [ppm]= 169.41 (Ala2-C), 155.23 ($^t\text{BuO-C}$), 141.08 (Tz-C), 135.90 (Ar-C), 131.51 (Tz-CH), 128.86 (2C, CH^{Ar}), 128.52 (CH^{Ar}), 127.96 (2C, CH^{Ar}), 78.74 ($\text{C}(\text{CH}_3)_3$), 67.11 (O- CH_2-), 55.75 (Ala2- C^α), 39.98 (Ala1- C^α), 28.55 ($\text{C}(\text{CH}_3)_3$), 20.92 (Ala1- C^β), 18.03 (Ala2- C^β).

Boc-chGly[5Tz]Phe-OBzl (9h).



Prepared according to general procedure **GP4**, starting from **8h** (50 mg; 0.21 mmol). **Yield:** 98 mg (0.19 mmol); 90%. R_f (PE/EtOAc 2:1)= 0.46.

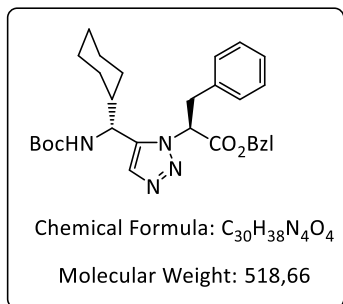
HR-MS (ESI): m/z = 519.2988 [$\text{M}+\text{H}$] $^+$ (519.29658).

^1H -NMR (500 MHz; DMSO- d_6): δ [ppm]= 7.39 (s, 1H, Tz-**H**), 7.26-7.20 (m, 3H, Ph-**H**), 7.19 (d, 3J = 9.1 Hz, 1H, chGly1-**NH**), 7.16-7.13 (m, 2H, Ph-**H**), 7.08-7.01 (m, 3H, Ph-**H**), 6.98-6.94 (m, 2H, Ph-**H**), 5.69 (dd, 3J = 11.5, 4.3 Hz, 1H, Phe2- H^α), 5.09 (d, 2J = 12.8 Hz, 1H, -O CHH -), 4.99 (d, 2J = 12.9 Hz, 1H, -O CHH -), 4.04 (dd, 3J = 9.4, 9.1 Hz, 1H, chGly1- H^α), 3.55 (dd, 2J = 13.9, 3J = 4.3 Hz, 1H, Phe2- H^β), 3.43 (dd, 2J = 13.9, 3J = 11.5 Hz, 1H, Phe2- H^β), 1.57-1.34 (m, 4H, CH_2), 1.25 (m, 1H, chGly1- H^β), 1.18 (s, 9H, $\text{C}(\text{CH}_3)_3$), 0.89-0.76 (m, 3H, CH_2), 0.70-0.52 (m, 2H, CH_2), 0.01 (m, 1H, CH_2).

$^{13}\text{C}\{^1\text{H}\}$ -NMR (126 MHz, DMSO- d_6) δ [ppm]= 168.24 (Phe2-C), 155.73 ($^t\text{BuO-C}$), 140.36 (Tz-C), 136.55 (Ar-C), 135.81 (Ar-C), 131.54 (Tz-CH), 129.62 (2C; CH^{Ar}), 128.83 (2C; CH^{Ar}), 128.75 (CH^{Ar}), 128.45 (CH^{Ar}), 127.81 (3C; CH^{Ar}), 127.18 (CH^{Ar}), 78.56 ($\text{C}(\text{CH}_3)_3$), 67.18 (O-

CH₂), 61.36 (Phe2-C^α), 49.03 (chGly1-C^α), 40.54 (chGly1-C^β), 37.44 (Phe2-C^β), 29.68 (CH₂), 28.85 (CH₂), 28.50 (C(CH₃)₃), 26.13 (CH₂), 25.59 (CH₂), 25.56 (CH₂).

Boc-D-chGly[5Tz]Phe-OBzl (9i).



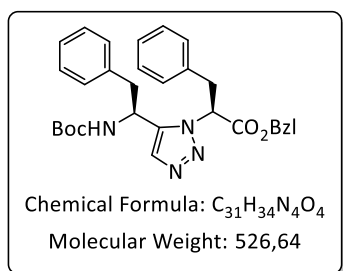
Prepared according to general procedure **GP4**, starting from **8g** (100 mg; 0.42 mmol). **Yield:** 189 mg (0.36 mmol); 86%. **R_f** (PE/EtOAc 2:1)= 0.47.

HR-MS (ESI): *m/z*= 519.2978 [M+H]⁺ (calc. 519.29658).

¹H-NMR (500 MHz; DMSO-*d*₆): δ [ppm]= 7.53 (s, 1H, Tz-**H**), 7.36-7.31 (m, 3H, Ph-**H**), 7.28 (d, ³*J*= 9.1 Hz, 1H, **NH**), 7.25-7.13 (m, 7H, Ph-**H**), 5.86 (dd, ³*J*= 9.3, 6.1 Hz, 1H, Phe-**H**^α), 5.17 (d, ²*J*= 12.7 Hz, 1H, O-**CHH**-), 5.14 (d, ²*J*= 12.7 Hz, O-**CHH**-), 4.39 (d, ³*J*= 9.4, 9.1 Hz, 1H, chGly-**H**^α), 3.70 (dd, ²*J*= 14.1, ³*J*= 6.1 Hz, 1H, Phe-**H**^β), 3.60 (dd, ²*J*= 14.3, ³*J*= 9.3 Hz, 1H, Phe-**H**^β), 1.80-1.43 (m, 5H, chGly-**H**^β, CH₂), 1.36 (s, 9H, C(CH₃)₃), 1.10-0.88 (m, 4H, CH₂), 0.81 (m, 1H, CH₂), 0.5 (m, 1H, CH₂).

¹³C{¹H}-NMR (126 MHz, DMSO-*d*₆): δ [ppm]= 168.40 (Phe-C), 155.79 (^tBuO-C), 139.95 (Tz-C), 136.48 (C^{Ar}), 135.58 (C^{Ar}), 132.01 (Tz-CH), 129.40 (2C; CH^{Ar}), 128.83 (2C; CH^{Ar}), 128.68 (2C; CH^{Ar}), 128.30 (2C; CH^{Ar}), 127.12 (2C; CH^{Ar}), 78.78 (C(CH₃)₃), 67.50 (O-CH₂-), 60.66 (Phe-C^α), 49.36 (chGly-C^α), 40.85 (chGly-C^β), 36.76 (Phe-C^β), 29.94 (CH₂), 29.16 (CH₂), 28.60 (C(CH₃)₃), 26.07 (CH₂), 25.60 (CH₂), 25.55 (CH₂).

Boc-Phe[5Tz]Phe-OBzl (9j).



Prepared according to general procedure **GP4**, starting from Boc-Phe≡ (**34**) (200 mg; 0.815 mmol).

Yield: 318 mg (0.718 mmol); 88%. **R_f** (PE/EtOAc 2:1)= 0.28.

HR-MS (ESI): *m/z*= 527.2663 [M+H]⁺ (calc. 527.26528).

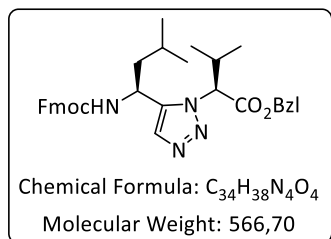
¹H-NMR (600 MHz, DMSO-*d*₆): δ [ppm]= 7.60 (s, 1H, Tz-**H**), 7.38 (d, ³*J*= 9.2 Hz, 1H, **NH**), 7.34-6.97 (m, 15H, Ph-**H**), 5.85 (dd, ³*J*= 11.1, 4.7 Hz, 1H, Phe2-**H**^α), 5.20-5.14 (m, 2H, O-**CH**₂-), 4.48 (ddd, ³*J*= 11.0, 9.2, 4.5 Hz, 1H, Phe1-**H**^α), 3.66 (dd, ²*J*= 13.8, ³*J*= 4.7 Hz, 1H, Phe2-**H**^β), 3.42 (dd, ²*J*= 13.8, ³*J*= 11.1 Hz, 1H, Phe2-**H**^β), 2.81 (dd, ²*J*= 13.8, ³*J*= 11.0 Hz, 1H, Phe1-**H**^β), 2.29 (dd, ²*J*= 13.8, ³*J*= 4.5 Hz, 1H, Phe1-**H**^β), 1.17 (s, 9H, -C(CH₃)₃).

¹³C{¹H}-NMR (151 MHz; DMSO-*d*₆): δ [ppm]= 168.14 (Phe2-C), 155.43 (^tBuO-C), 141.10 (Tz-C), 137.67 (C^{Ar}), 136.52 (C^{Ar}), 135.79 (C^{Ar}), 131.43 (Tz-CH), 129.51 (2C, CH^{Ar}), 129.43

7. Experimental section

(2C, CH^{Ar}), 128.87 (2C, CH^{Ar}), 128.81 (2C, CH^{Ar}), 128.46 (CH^{Ar}), 128.44 (2C, CH^{Ar}), 127.86 (2C, CH^{Ar}), 127.37 (CH^{Ar}), 126.72 (CH^{Ar}), 78.66 (-C(CH₃)₃), 67.24 (O-CH₂), 61.34 (Phe2-C^α), 45.06 (Phe1-C^α), 39.26 (Phe1-C^β), 37.93 (Phe2-C^β), 28.38 (-C(CH₃)₃).

Fmoc-Leu[5Tz]Val-OBzl (9k).



Prepared according to general procedure **GP4**, starting from Fmoc-Leu≡ (413 mg; 1.24 mmol).

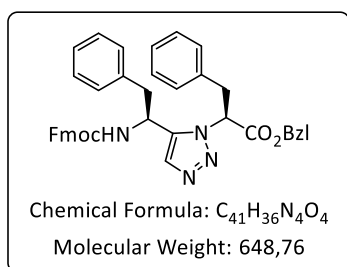
Yield: 621 mg (1.10 mmol); 89%. **R_f** (PE/EtOAc 3:1)= 0.27.

MS (ESI): *m/z*= 589.3 [M+Na]⁺. [α]_D²⁵ = -70 (CHCl₃, c= 1).

¹H-NMR (600 MHz; DMSO-*d*₆): δ [ppm]= 7.90-7.83 (m, 3H, H^{Ar}, NH), 7.64-7.61 (m, 2H, H^{Ar}), 7.42-7.38 (m, 2H, H^{Ar}), 7.31-7.27 (m, 2H, H^{Ar}), 7.27-7.16 (m, 5H, Ph-H), 7.69 (s, 1H, Tz-H), 5.22 (d, ³*J*= 8.4 Hz, 1H, Val2-H^α), 5.08 (d, ²*J*= 12.6 Hz, 1H, O-CHH-), 4.98 (d, ²*J*= 12.6 Hz, 1H, O-CHH-), 4.84 (m, 1H, Leu1-H^α), 4.37 (dd, ²*J*= 10.4, ³*J*= 6.7 Hz, 1H, CH-CHH-O), 4.14 (dd, ³*J*= 7.0, 6.7 Hz, 1H), 4.08 (dd, ²*J*= 10.4, ³*J*= 7.0 Hz, 1H, CH-CHH-O), 2.74 (m, 1H, Val2-H^β), 1.82 (m, 1H, Leu1-H^β), 1.55-1.44 (m, 2H, Leu1-H^β, Leu1-H^γ), 0.96 (d, ³*J*= 6.7 Hz, 3H, Val2-H^γ), 0.87 (d, ³*J*= 6.1 Hz, 3H, Leu1-H^δ), 0.85 (d, ³*J*= 5.9 Hz, 3H, Leu1-H^δ), 0.76 (d, *J*= 6.7 Hz, 3H, Val2-H^γ).

¹³C{¹H}-NMR (151 MHz, DMSO-*d*₆) δ [ppm]= 168.10 (Val-C), 156.12 (OCON), 144.18 (C^{Ar}), 144.10 (C^{Ar}), 141.21 (C^{Ar}), 141.20 (C^{Ar}), 140.63 (Tz-C), 135.72 (C^{Ar}), 131.84 (Tz-CH), 128.76 (2C; CH^{Ar}), 128.51 (CH^{Ar}), 128.10 (2C; CH^{Ar}), 128.07 (CH^{Ar}), 127.45 (2C; CH^{Ar}), 127.43 (CH^{Ar}), 125.65 (CH^{Ar}), 125.49 (CH^{Ar}), 120.57 (CH^{Ar}), 120.54 (CH^{Ar}), 67.06 (CH₂-Ph), 65.99 (C-CH₂-O), 65.48 (Val2-C^α), 47.07 (CH-CH₂O), 43.10 (Leu1-C^α), 42.71 (Leu1-C^β), 31.00 (Val2-C^β), 24.71 (Leu1-C^γ), 23.14 (Leu1-C^δ), 21.95 (Leu1-C^δ), 19.56 (Val1-C^γ), 19.14 (Val1-C^γ).

Fmoc-Phe[5Tz]Phe-OBzl (9l).



Prepared according to general procedure **GP4**, starting from Fmoc-Phe≡ (300 mg; 0.816 mmol). **Yield:** 482 mg

(0.743 mmol); 91%. [α]_D²⁵ = -95 (CHCl₃, c= 1).

R_f (PE/EtOAc 1:1)= 0.54.

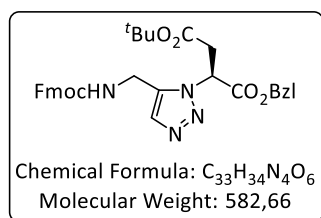
HR-MS (ESI): *m/z*= 671.2629 [M+Na]⁺ (calc. 671.26288).

¹H-NMR (600 MHz; CDCl₃): δ [ppm]= 7.77-7.75 (m, 2H, H^{Ar}), 7.46 (s, 1H, Tz-H), 7.43-7.34 (m, 4H, H^{Ar}), 7.30-7.17 (m, 11H, H^{Ar}), 7.14-7.10 (m, 2H, H^{Ar}), 7.05-7.01 (m, 2H, H^{Ar}), 6.92-6.88 (m, 2H, H^{Ar}), 5.54 (dd, ³*J*= 11.2, 4.5 Hz, 1H, Phe2-H^α), 5.11 (d, ²*J*= 12.4 Hz, 1H, O-CHH-

Ph), 5.05 (d, $^2J = 12.4$ Hz, 1H, O-CHH-Ph), 4.84 (d, $^3J = 9.4$ Hz, 1H, NH), 4.62 (ddd, $^3J = 9.4$, 9.4, 5.5 Hz, 1H, Phe1- H^α), 4.30 (m, 1H, CH-CHHO), 4.03-3.97 (m, 2H, CH-CH₂O, CH-CHHO), 3.76-3.60 (m, 2H, Phe2- H^β), 2.81 (dd, $^2J = 14.3$, $^3J = 9.4$ Hz, 1H, Phe1- H^β), 2.73 (dd, $^2J = 14.3$, $^3J = 5.5$ Hz, 1H, Phe1- H^β).

$^{13}\text{C}\{^1\text{H}\}$ -NMR (151 MHz, CDCl₃) δ [ppm]= 167.55 (Phe2-C), 155.53 (OCON), 143.60 (C^{Ar}), 143.47 (C^{Ar}), 141.23 (2C; C^{Ar}), 138.97 (Tz-C), 136.00 (C^{Ar}), 135.55 (C^{Ar}), 134.83 (C^{Ar}), 131.13 (Tz-CH), 129.08 (2C; CH^{Ar}), 128.93 (2C; CH^{Ar}), 128.79 (2C; CH^{Ar}), 128.59 (2C; CH^{Ar}), 128.48 (2C; CH^{Ar}), 128.32 (CH^{Ar}), 127.84 (CH^{Ar}), 127.78 (2C; CH^{Ar}), 127.75 (CH^{Ar}), 127.25 (2C; CH^{Ar}), 127.07 (2C; CH^{Ar}), 125.05 (CH^{Ar}), 124.92 (CH^{Ar}), 119.99 (CH^{Ar}), 119.98 (CH^{Ar}), 67.70 (O-CH₂-Ph), 67.05 (CH-CH₂O), 62.15 (Phe2- C^α), 46.96 (CH-CH₂O), 45.24 (Phe1- C^α), 39.79 (Phe1- C^β), 37.93 (Phe2- C^β).

Fmoc-Gly[5Tz]Asp(^tBu)-OBzl (9m).



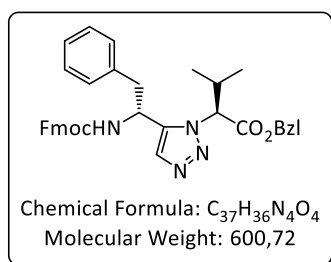
Prepared according to general procedure **GP4**, starting from Fmoc-Gly≡ (0.15 g; 0.54 mmol).

Yield: 0.23 g (0.40 mmol); 74%. **Rf** (PE/EtOAc 2:1)= 0.20.

MS (ESI): m/z= 605.3 [M+Na]⁺.

^1H -NMR (500 MHz, DMSO-*d*₆) δ [ppm]= 7.94 (dd, $^3J = 6.1$, 6.0 Hz, 1H, NH), 7.91-7.88 (m, 2H, H^{Ar}), 7.68-7.64 (m, 2H, H^{Ar}), 7.56 (s, 1H, Tz-H), 7.44-7.40 (m, 2H, H^{Ar}), 7.34-7.23 (m, 7H, H^{Ar} , Ph-H), 5.85 (dd, $^3J = 8.2$, 6.1 Hz, 1H, Asp- H^α), 5.15-5.09 (m, 2H, CH₂Ph), 4.39-4.36 (m, 2H, Gly- H^α), 4.33 (dd, $^2J = 10.5$, $^3J = 6.9$ Hz, CHCHHO), 4.30 (dd, $^2J = 10.5$, $^3J = 6.7$ Hz, 1H, CHCHHO), 4.21 (dd, $^3J = 6.9$, 6.7 Hz, 1H, CH-CH₂O), 3.36-3.26 (m, 2H, Asp- H^β), 1.28 (s, 9H).

$^{13}\text{C}\{^1\text{H}\}$ -NMR (151 MHz, CDCl₃) δ [ppm]= 168.59 (CO₂tBu), 167.81 (Asp-C), 156.68 (OCON), 144.21 (2C; CAr), 141.21 (2C; CAr), 137.07 (Tz-C), 135.62 (C^{Ar}), 132.96 (Tz-CH), 128.83 (2C; CH^{Ar}), 128.58 (CH^{Ar}), 128.10 (2C; CH^{Ar}), 128.01 (2C; CH^{Ar}), 127.50 (2C; CH^{Ar}), 125.55 (2C; CH^{Ar}), 120.59 (2C; CH^{Ar}), 81.43 (C(CH₃)₃), 67.54 (CO₂CH₂Ph), 66.15 (CHCH₂O), 56.62 (Asp- C^α), 47.10 (CHCH₂O), 36.99 (Asp- C^β), 33.52 (Gly- C^α), 27.93 (C(CH₃)₃).

Fmoc-D-Phe[5Tz]/Val-OBzl (9n).

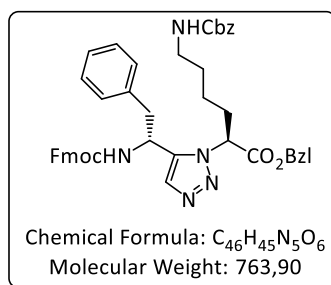
Prepared according to general procedure **GP4**, starting from Fmoc-D-Phe= (100 mg; 0.28 mmol).

Yield: 142 mg (0.24 mmol); 86%. **Rf** (PE/EtOAc 2:1)= 0.22.

MS (ESI): $m/z = 623.3 [M+Na]^+$.

1H -NMR (600 MHz; DMSO- d_6): δ [ppm]= 8.06 (d, $^3J = 8.8$ Hz, 1H, **NH**), 7.88-7.84 (m, 2H, **H^{Ar}**), 7.79 (s, 1H, **Tz-H**), 7.57-7.52 (m, 2H, **H^{Ar}**), 7.41-7.38 (m, 2H, **H^{Ar}**), 7.33-7.18 (12H, **H^{Ar}**, **Ph-H**), 5.21 (d, $^3J = 9.0$ Hz, 1H, Val-**H^{\alpha}**), 5.13 (d, $^2J = 12.6$ Hz, 1H, CO₂**CHHPh**), 5.10 (d, $^2J = 12.6$ Hz, 1H, CO₂**CHHPh**), 4.97 (ddd, $^3J = 10.0, 8.8, 5.2$ Hz, 1H, Phe-**H^{\alpha}**), 3.08 (dd, $^2J = 13.8, ^3J = 10.0$ Hz, 1H, Phe-**H^{\beta}**), 2.97 (dd, $^2J = 13.8, 5.2$ Hz, 1H, Phe-**H^{\beta}**), 4.23 (dd, $^2J = 10.6, ^3J = 7.0$ Hz, 1H, CH-**CHHO**), 4.18 (dd, $^2J = 10.5, ^3J = 6.9$ Hz, 1H, CH-**CHHO**), 4.10 (dd, $^3J = 7.0, 6.9$ Hz, 1H, CH-**CH₂O**), 2.76 (m, 1H, Val-**H^{\beta}**), 0.97 (d, $^3J = 6.7$ Hz, 3H, Val-**H^{\gamma}**), 0.67 (d, $^3J = 6.7$ Hz, 3H, Val-**H^{\gamma}**).

$^{13}C\{^1H\}$ -NMR (151 MHz, DMSO) δ [ppm]= 167.93 (Val2-C), 156.00 (OCON), 144.08 (**C^{Ar}**), 143.98 (**C^{Ar}**), 141.14 (**C^{Ar}**), 141.10 (**C^{Ar}**), 140.78 (Tz-C), 137.68 (**C^{Ar}**), 135.75 (**C^{Ar}**), 131.77 (Tz-CH), 129.60 (2C; **CH^{Ar}**), 128.86 (2C; **CH^{Ar}**), 128.67 (**CH^{Ar}**), 128.57 (2C; **CH^{Ar}**), 128.28 (2C; **CH^{Ar}**), 128.07 (2C; **CH^{Ar}**), 127.48 (**CH^{Ar}**), 127.45 (**CH^{Ar}**), 126.93 (**CH^{Ar}**), 125.55 (**CH^{Ar}**), 125.43 (**CH^{Ar}**), 120.55 (2C; **CH^{Ar}**), 67.24 (CO₂CH₂Ph), 66.09 (CHCH₂O), 65.13 (Val-**C^{\alpha}**), 46.97 (CHCH₂O), 46.39 (Phe-**C^{\alpha}**), 39.63 (Phe-**C^{\beta}**), 30.24 (Val-**C^{\beta}**), 19.55 (Val-**C^{\gamma}**), 18.86 (Val-**C^{\gamma}**).

Fmoc-D-Phe[5Tz]/Lys(Cbz)-OBzl (9o).

Prepared according to general procedure **GP4**, starting from Fmoc-D-Phe= (250 mg; 0.68 mmol).

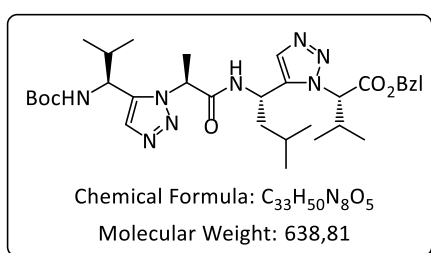
Yield: 411 mg (0.54 mmol); 79%. **Rf** (PE/EtOAc 2:1)= 0.15.

HR-MS (ESI): $m/z = 764.3409 [M+H]^+$ (calc. 764.34426).

1H -NMR (600 MHz; DMSO- d_6): δ [ppm]= 8.03 (d, $^3J = 8.8$ Hz, 1H, Fmoc**NH**), 7.89-7.83 (m, 2H, **H^{Ar}**), 7.79 (s, 1H, **Tz-H**), 7.56-7.51 (m, 2H, **H^{Ar}**), 7.40-7.37 (m, 2H, **H^{Ar}**), 7.33-7.15 (m, 17H, **H^{Ar}**, **Ph-H**), 7.11 (t, $^3J = 5.6$ Hz, 1H, **NH₂**), 5.51 (dd, $^3J = 9.0, 5.9$ Hz, 1H, Lys-**H^{\alpha}**), 5.13 (d, $^2J = 12.6$ Hz, 1H, **CHHPh**), 5.09 (d, $^2J = 12.7$ Hz, 1H, **CHHPh**), 4.96 (ddd, $^3J = 10.0, 8.8, 5.2$ Hz, 1H, Phe-**H^{\alpha}**), 4.94-4.89 (m, 2H, NCO₂**CH₂**), 4.22 (dd, $^2J = 10.6, ^3J = 7.1$ Hz, 1H, CH-**CHHO**), 4.16 (dd, $^2J = 10.7, ^3J = 7.0$ Hz, 1H, CH-**CHHO**), 4.07 (dd, $^3J = 7.1, 7.0$ Hz, 1H, CH-**CH₂O**), 3.07 (dd, $^2J = 13.8, ^3J = 10.0$ Hz, 1H, Phe-**H^{\beta}**), 2.97 (dd, $^2J = 13.8, ^3J = 5.2$ Hz, 1H, Phe-**H^{\beta}**), 2.88-2.81 (m, 2H, Lys-**H^{\epsilon}**), 2.32-2.23 (m, 2H, Lys-**H^{\delta}**), 1.40-1.23 (m, 2H, Lys-**H^{\delta}**), 1.19 (m, 1H, Lys-**H^{\gamma}**), 0.98 (m, 1H, Lys-**H^{\gamma}**).

$^{13}\text{C}\{^1\text{H}\}$ -NMR (151 MHz, DMSO- d_6) δ [ppm]= 168.61 (Lys-C), 156.45 (NCO₂Bzl), 156.05 (CHCH₂OC), 144.06 (C^{Ar}), 143.99 (C^{Ar}), 141.13 (C^{Ar}), 141.10 (C^{Ar}), 140.64 (Tz-C), 137.65 (2C; C^{Ar}), 135.78 (C^{Ar}), 132.06 (Tz-CH), 129.64 (2C; CH^{Ar}), 129.39 (CH^{Ar}), 128.86 (2C; CH^{Ar}), 128.75 (2C; CH^{Ar}), 128.62 (CH^{Ar}), 128.57 (2C; CH^{Ar}), 128.15 (2C; CH^{Ar}), 128.09 (CH^{Ar}), 128.07 (CH^{Ar}), 127.75 (CH^{Ar}), 127.45 (CH^{Ar}), 126.93 (CH^{Ar}), 125.53 (CH^{Ar}), 125.45 (CH^{Ar}), 121.84 (CH^{Ar}), 120.54 (CH^{Ar}), 120.48 (CH^{Ar}), 110.22 (CH^{Ar}), 67.32 (OCH₂Ph), 66.06 (CHCH₂O), 65.52 (NCO₂CH₂Ph), 59.97 (Lys-C ^{α}), 47.01 (CHCH₂O), 46.49 (Phe-C ^{α}), 40.22 (Lys-C ^{ϵ}), 30.44 (Lys-C ^{β}), 29.21 (Lys-C ^{δ}), 22.88 (Lys-C ^{γ}).

Boc-Val[5Tz]Ala-Leu[5Tz]Val-OBzl (10).



Boc-Leu[5Tz]Val-OBzl (**9e**) (58 mg; 0.13 mmol; 1.2 eq) is dissolved in DCM/(4 M HCl in dioxane) 1:1 (1 mL) and stirred overnight at rt. After evaporation of the solvent, the ammonium salt is used without further purification. Boc-Val[5Tz]Ala-OH (35 mg; 0.11 mmol; synthesized from **9c** according to **GP5**) and Oxyma (17 mg; 0.12 mmol; 1.1 eq) are dissolved in DCM (dry; 1 mL) under an argon atmosphere. After addition of DIC (18 μL ; 15 mg; 0.12 mmol; 1.1 eq) the solution is stirred 5 min at rt for preactivation. After preactivation of the carboxylic acid, the ammonium salt is dissolved in DCM (dry; 1 mL) and added dropwise to the reaction mixture, followed by *sym*-collidine (22 μL ; 17 mg; 0.13 mmol; 1.2 eq). After 5 min, another amount of *sym*-collidine (22 μL) is added and the reaction mixture left to stir overnight. After evaporation of the solvent, the product is purified by preparative HPLC.

Yield: 57 mg (89 μmol); 81%. **Analytical RP-HPLC:** t_{R} = 6.0 min (method 1, 220 nm). $[\alpha]_{\text{D}}^{21}$ = -55 (CHCl₃, c = 0.1). **HR-MS (ESI):** m/z = 639.3996 [M+H]⁺ (calc. 639.39769). **^1H -NMR** (600 MHz; MeOH- d_3): δ [ppm] = 7.91 (d, 3J = 9.3 Hz, 1H, Leu-NH), 7.69 (s, 1H, Tz2-H), 7.64 (d, 3J = 6.1 Hz, 1H, Val1-NH), 7.58 (s, 1H, Tz1-H), 7.39-7.23 (m, 5H, Ph-H), 5.32 (dt, 3J = 9.3, 4.7 Hz, 1H, Leu-H ^{α}), 5.26 (d, 2J = 12.6 Hz, 1H, O-CH₂-), 5.17 (d, 2J = 12.6 Hz, 1H, O-CH₂-), 5.13 (d, 3J = 9.3 Hz, 1H, Val4-H ^{α}), 5.10 (q, 3J = 6.9 Hz, 1H, Ala-H ^{α}), 4.14 (dd, 3J = 8.7, 6.1 Hz, 1H, Val1-H ^{α}), 2.91 (m, 1H, Val4-H ^{β}), 1.98 (m, 1H, Val1-H ^{β}), 1.72 (ddd, 2J = 13.9 Hz, 3J = 10.7, 4.7 Hz, 1H, Leu-H ^{β}), 1.63 (d, 3J = 6.9 Hz, 3H, Ala-H ^{β}), 1.56 (ddd, 2J = 13.9, 3J = 9.4, 4.7 Hz, 1H, Leu-H ^{β}), 1.35 (s, 9H, -C(CH₃)₃), 1.25 (m, 1H, Leu-H ^{γ}), 1.11 (d, 3J = 6.7 Hz, 3H, Val4-

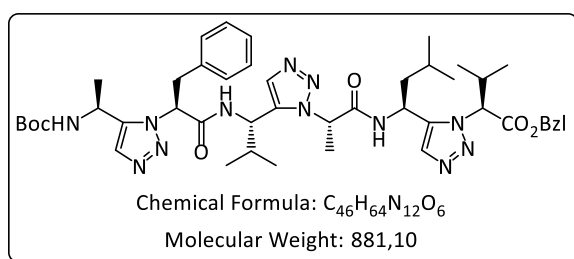
7. Experimental section

H), 1.04 (d, $^3J = 6.6$ Hz, 3H, Val1-**H** $^{\gamma}$), 0.88 (d, $^3J = 6.5$ Hz, 3H, Leu-**H** $^{\delta}$), 0.85 (d, $^3J = 6.7$ Hz, 3H, Val4-**H** $^{\gamma}$), 0.78 (d, $^3J = 6.6$ Hz, 3H, Leu-**H** $^{\delta}$), 0.77 (d, $^3J = 7.4$ Hz, 3H, Val1-**H** $^{\gamma}$).

$^{13}\text{C}\{^1\text{H}\}$ -NMR (151 MHz, MeOH- d_3): δ [ppm] = 167.86 (Val4-**C**), 167.63 (Ala-**C**), 156.97 (tBuO-**C**), 140.62 (Tz1-**C**), 140.54 (Tz2-**C**), 135.33 (**C** $^{\text{Ar}}$), 131.10 (Tz2-**CH**), 130.15 (Tz1-**CH**), 128.28 (2C, **CH** $^{\text{Ar}}$), 128.05 (**CH** $^{\text{Ar}}$), 127.49 (2C, **CH** $^{\text{Ar}}$), 79.66 (-**C**(CH $_3$) $_3$), 67.03 (O-**CH** $_2$ -), 66.45 (Val-**C** $^{\alpha}$), 55.46 (Ala-**C** $^{\alpha}$), 42.22 (Leu-**C** $^{\beta}$), 40.84 (Leu-**C** $^{\alpha}$), 32.50 (Val1-**C** $^{\beta}$), 30.78 (Val4-**C** $^{\beta}$), 27.41 (3C, -**C**(CH $_3$) $_3$), 23.78 (Leu-**C** $^{\gamma}$), 21.99 (Leu-**C** $^{\delta}$), 20.35 (Leu-**C** $^{\delta}$), 18.66 (Val1-**C** $^{\gamma}$), 18.40 (Val4-**C** $^{\gamma}$), 18.05 (Val1-**C** $^{\gamma}$), 17.89 (Val4-**C** $^{\gamma}$), 16.20 (Ala-**C** $^{\beta}$).

Crystal structure: CCDC 1561608.

Boc-Ala[5Tz]Phe-Val[5Tz]Ala-Leu[5Tz]Val-OBzl (11).



10 (40 mg; 63 μmol) is dissolved in DCM/(4 M HCl in dioxane) 1:1 (2 mL) and stirred for 3 h at rt. After evaporation of the solvent, the ammonium salt is used without further purification. Boc-Ala[5Tz]Phe-OH

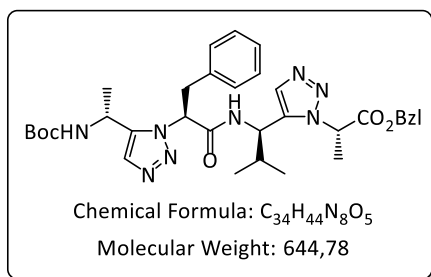
(25 mg; 69 μmol ; 1.1 eq; synthesized from **9a** according to **GP5**), Oxyma (11 mg; 76 μmol ; 1.2 eq) are dissolved in DCM (dry; 0.7 mL), after the addition of DIC (12 μL ; 76 μmol ; 1.2 eq) the mixture is stirred 5 min for preactivation. The ammonium salt is dissolved in DCM (dry; 0.7 mL) together with *sym*-collidine (84 μL ; 0.63 mmol; 10 eq) and stirred at rt. The activated acid is added dropwise to the amine solution, after this the combined mixture is stirred overnight. After evaporation of the solvent, the product is purified by preparative RP-HPLC. **Yield:** 47 mg (53 μmol); 84%. **Analytical RP-HPLC:** $t_{\text{R}} = 6.4$ min (method 1, 220 nm). **HR-MS (ESI):** $m/z = 881.5162$ [$\text{M} + \text{H}$] $^+$ (calc. 881.51445).

^1H -NMR (600 MHz; MeOH- d_3): δ [ppm] = 8.28 (d, $^3J = 6.6$ Hz, 1H, Val3-NH), 8.17 (d, $^3J = 8.7$ Hz, 1H, Leu-NH), 7.80 (s, 1H, Tz3-**H**), 7.61 (s, 1H, Tz2-**H**), 7.54 (s, 1H, Tz1-**H**), 7.47 (d, $^3J = 5.2$ Hz, 1H, Boc-NH), 7.37-7.27 (m, 5H, Ph-**H**), 7.19-7.16 (m, 3H, Ph-**H**), 6.91-6.89 (m, 2H, Ph-**H**), 5.54 (dd, $^3J = 7.8, 7.8$ Hz, 1H, Phe-**H** $^{\alpha}$), 5.32 (m, 1H, Leu-**H** $^{\alpha}$), 5.27 (d, $^2J = 12.5$ Hz, 1H, O-**CH** $_2$ -), 5.25-5.22 (m, 2H, Ala4-**H** $^{\alpha}$, Val6-**H** $^{\alpha}$), 5.20 (d, $^2J = 12.5$ Hz, 1H, O-**CH** $_2$ -), 4.48 (dd, $^3J = 10.0, 6.6$ Hz, 1H, Val3-**H** $^{\alpha}$), 4.37 (qd, $^3J = 6.9, 5.2$ Hz, 1H, Ala1-**H** $^{\alpha}$), 3.42-3.41 (m, 2H, Phe2-**H** $^{\beta}$), 2.93 (m, 1H, Val6-**H** $^{\beta}$), 2.04 (m, 1H, Val3-**H** $^{\beta}$), 1.91 (ddd, $^2J = 14.5$ Hz, $^3J = 9.9, 5.4$ Hz, 1H, Leu-**H** $^{\beta}$), 1.64 (m, 1H, Leu-**H** $^{\beta}$), 1.63 (d, $^3J = 7.0$ Hz, 3H, Ala4-**H** $^{\beta}$), 1.39 (s, 9H, -**C**(CH $_3$) $_3$), 1.31 (m, 1H, Leu-**H** $^{\gamma}$), 1.13 (d, $^3J = 6.7$ Hz, 3H, Val6-**H** $^{\gamma}$), 0.91 (d, $^3J = 6.5$ Hz, 3H, Val6-**H** $^{\gamma}$), 0.88

(d, $^3J = 6.7$ Hz, 6H, Leu-**H^δ**), 0.78 (d, $^3J = 6.5$ Hz, 3H, Val3-**H^γ**), 0.72 (d, $^3J = 6.7$ Hz, 3H, Val3-**H^γ**), 0.60 (d, $^3J = 6.9$ Hz, 3H, Ala1-**H^β**).

¹³C-NMR (151 Mhz; MeOH-*d*₃): δ [ppm]= 168.59 (Phe-**C**), 167.65 (Ala4-**C**), 167.56 (Val6-**C**), 156.67 (^tBuO-**C**), 143.89 (Tz1-**C**), 140.45 (Tz3-**C**), 139.76 (Tz2-**C**), 136.29 (Phe-**C^{Ar}**), 135.41 (**C^{Ar}**), 131.28 (Tz3-**CH**), 130.30 (Tz2-**CH**), 129.46 (Tz1-**CH**), 128.90 (2C, **CH^{Ar}**), 128.40 (2C, **CH^{Ar}**), 128.32 (2C, **CH^{Ar}**), 128.09 (2C, **CH^{Ar}**), 127.71 (**CH^{Ar}**), 126.78 (**CH^{Ar}**), 79.48 (-**C(CH₃)₃**), 67.16 (O-**CH₂-Ph**), 66.47 (Val6-**C^α**), 61.79 (Phe-**C^α**), 55.84 (Ala4-**C^α**), 50.87 (Val3-**C^α**), 42.29 (Leu-**C^β**), 41.41 (Leu-**C^α**), 40.67 (Ala1-**C^α**), 37.31 (Phe-**C^β**), 32.64 (Val3-**C^β**), 30.83 (Val6-**C^β**), 27.30 (3C, -**C(CH₃)₃**), 24,16 (Leu-**C^γ**), 20.64 (Val6-**C^γ**), 18.88 (Ala1-**C^β**), 18.49 (Val3-**C^γ**), 18.46 (Val6-**C^γ**), 18.27 (Val3-**C^γ**), 17.94 (2C, Leu-**C^δ**), 16.43 (Ala4-**C^β**).

Boc-D-Ala[5Tz]Phe-D-Val[5Tz]Ala-OBzl (**12**).



Boc-D-Val[5Tz]Ala-OBzl (**9f**) (41 mg; 0.10 mmol; 1.0 eq) is dissolved in 1 mL DCM/(4 M HCl in dioxane) 1:1 and stirred for 2 h at RT. The solvent is removed under vacuum to obtain the crude ammonium salt. Boc-D-Ala[5Tz]Phe-OH (37 mg; 0.10 mmol; 1.0 eq; synthesized from **9b** according to GP5), HOAt (15 mg;

0.11 mmol; 1.1 eq) and DCC (23 mg; 0.11 mg; 1.1 eq) are dissolved in DCM (1.5 mL; dry) and stirred for 10 min at RT. The ammonium salt is dissolved in DCM (1 mL; dry) and added dropwise to the activated acid, followed by *sym*-collidine (66 μ L; 61 mg; 0.50 mmol; 5.0 eq), the reaction mixture is stirred overnight. The reaction mixture is diluted with DCM (10 mL) and filtered to remove dicyclohexylurea. The filtrate is concentrated in vacuum, the crude products purified by preparative HPLC. **Yield:** 33 mg (0.051 mmol); 51%.

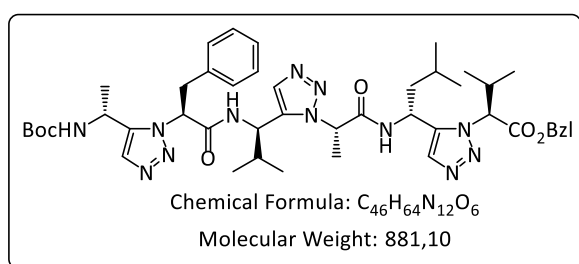
MS (ESI): $m/z = 667.4$ [$M+Na$]⁺. **Analytical RP-HPLC:** $t_R = 5.9$ (method 1, 220 nm).

¹H-NMR (600 MHz; DMSO-*d*₆): δ [ppm]= 8.89 (d, $^3J = 8.5$ Hz, 1H, Val3-**NH**), 7.66 (s, 1H, Tz2-**H**), 7.55 (s, 1H, Tz1-**H**), 7.47 (d, $^3J = 8.2$ Hz, 1H, Ala1-**NH**), 7.35-7.15 (m, 10H, Ph-**H**), 5.62 (q, $^3J = 7.0$ Hz, 1H, Ala4-**H^α**), 5.56 (dd, $^3J = 8.0, 7.4$ Hz, 1H, Phe2-**H^α**), 5.12 (d, $^2J = 12.7$ Hz, 1H, -O-**CH₂-**), 5.10 (d, $^2J = 12.7$ Hz, 1H, -O-**CH₂-**), 4.73 (dq, $^3J = 8.2, 7.0$ Hz, 1H, Ala1-**H^α**), 4.61 (dd, $^3J = 8.5, 8.5$ Hz, 1H, Val3-**H^α**), 3.66 (dd, $^2J = 13.9$ Hz, $^3J = 8.0$ Hz, 1H, Phe2-**H^β**), 3.49 (dd, $^2J = 13.9$ Hz, $^3J = 7.4$ Hz, 1H, Phe2-**H^β**), 2.03 (m, 1H, Val3-**H^β**), 1.57 (d, $^3J = 7.0$ Hz, 3H, Ala4-**H^β**), 1.36 (s, 9H, -**C(CH₃)₃**), 1.04 (d, $^3J = 7.0$ Hz, 3H, Ala1-**H^β**), 0.64 (d, $^3J = 6.6$ Hz, 3H, Val3-**H^γ**), 0.58 (d, $^3J = 6.6$ Hz, 3H, Val3-**H^γ**).

7. Experimental section

$^{13}\text{C}\{^1\text{H}\}$ -NMR (151 MHz; DMSO- d_6): δ [ppm]= 169.19 (Ala4-C), 167.34 (Phe2-C), 155.50 ($t\text{BuO-C}$), 141.44 (Tz1-C), 139.35 (Tz2-C), 136.84 (Phe2-C^{Ar}), 135.78 (C^{Ar}), 131.42 (Tz1-CH), 131.24 (Tz2-CH), 129.45 (2C, CH^{Ar}), 128.79 (2C, CH^{Ar}), 128.58 (CH^{Ar}), 128.56 (2C, CH^{Ar}), 128.10 (2C, CH^{Ar}), 127.04 (CH^{Ar}), 78.96 (-C(CH₃)₃), 67.25 (-O-CH₂-), 61.92 (Phe2-C ^{α}), 55.42 (Ala4-C ^{α}), 49.00 (Val3-C ^{α}), 39.88 (Ala1-C ^{α}), 37.01 (Phe2-C ^{β}), 31.36 (Val3-C ^{β}), 28.59 (-C(CH₃)₃), 20.64 (Ala1-C ^{β}), 19.82 (Val3-C ^{γ}), 18.90 (Val3-C ^{γ}), 17.34 (Ala4-C ^{β}).

Boc-D-Ala[5Tz]Phe-D-Val[5Tz]Ala-D-Leu[5Tz]Val-OBzl (13).



Boc-D-Leu[5Tz]Val-OBzl (**9d**) (18 mg; 0.040 mmol; 1.0 eq) is dissolved in 2 mL DCM/(4 M HCl in dioxane) 1:1 and stirred for 2 h at RT. The solvent is removed under vacuum to obtain the crude ammonium

salt. Boc-D-Ala[5Tz]Phe-D-Val[5Tz]Ala-OH (22 mg; 0.040 mmol; 1.0 eq; synthesized from **12** according to **GP5**), HOAt (6 mg; 0.04 mmol; 1.0 eq) and DCC (9 mg; 0.04 mg; 1.0 eq) are dissolved in DCM (1 mL; dry) and stirred for 10 min at RT. The ammonium salt is dissolved in DCM (1 mL; dry) and added dropwise to the activated acid, followed by *sym*-collidine (29 μL ; 27 mg; 0.22 mmol; 5.5 eq), the reaction mixture is stirred overnight. The solvent is removed under vacuum, the residue dissolved in EtOAc (10 mL) and filtered to remove insoluble dicyclohexylurea. After washing with 5% KHSO₄ solution (3x5 mL), 5% NaHCO₃ solution (3x5 mL), brine (1x5 mL), and drying over MgSO₄ the triazole is purified by flash chromatography. **Yield**: 25 mg (0.028 mmol); 70%. **R_f** (PE/EtOAc 1:3)= 0.50.

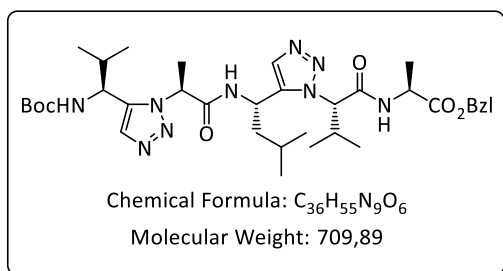
HR-MS (ESI): m/z = 881.51325 [$\text{M}+\text{H}$]⁺ (calc. 881.51445).

^1H -NMR (600 MHz; DMSO- d_6): δ [ppm]= 8.91 (d, 3J = 8.1 Hz, 1H, Leu5-NH), 8.87 (d, 3J = 8.5 Hz, 1H, Val3-NH), 7.72 (s, 1H, Tz3-H), 7.61 (s, 1H, Tz2-H), 7.54 (s, 1H, Tz1-H), 7.48 (d, 3J = 8.1 Hz, 1H, BocNH), 7.35-7.16 (m, 10H, Ph-H), 5.55 (dd, 3J = 7.9, 7.5 Hz, 1H, Phe2-H ^{α}), 5.25 (q, 3J = 7.1 Hz, 1H, Ala4-H ^{α}), 5.17 (d, 2J = 12.4 Hz, 1H, O-CH₂-), 5.11 (d, 2J = 12.4 Hz, 1H, O-CH₂-), 5.05 (d, 3J = 8.7 Hz, 1H, Val6-H ^{α}), 4.91 (ddd, 3J = 10.4, 8.1, 4.8 Hz, 1H, Leu5-H ^{α}), 4.69 (dq, 3J = 8.1, 6.9 Hz, 1H, Ala1-H ^{α}), 4.39 (dd, 3J = 8.9, 8.5 Hz, Val3-H ^{α}), 3.65 (dd, 2J = 14.0 Hz, 3J = 7.9 Hz, 1H, Phe2-H ^{β}), 3.52 (dd, 2J = 13.9, 3J = 7.5 Hz, 1H, Phe2-H ^{β}), 2.76 (dq, 3J = 8.7, 6.7, 6.7 Hz, 1H, Val6-H ^{β}), 1.86 (m, 1H, Val3-H ^{β}), 1.72 (ddd, 2J = 13.6, 3J = 10.4, 5.0 Hz, 1H, Leu5-H ^{β}), 1.62 (d, 3J = 7.1 Hz, 3H, Ala4-H ^{β}), 1.51 (m, 1H, Leu5-H ^{γ}), 1.36 (s, 9H, C(CH₃)₃), 1.32 (ddd, 2J = 13.6 Hz, 3J = 8.9, 4.8 Hz, 1H, Leu5-H ^{β}), 0.99 (d, 3J = 6.9 Hz, 3H, Ala1-H ^{β}) 0.96 (d, 3J = 6.7

Hz, 3H, Val6-**H^γ**), 0.75 (d, $^3J = 6.6$ Hz, 3H, Leu5-**H^δ**), 0.72 (d, $^3J = 6.6$ Hz, 3H, Leu5-**H^δ**), 0.67 (d, $^3J = 6.7$ Hz, 3H, Val6-**H^γ**), 0.54 (d, $^3J = 6.6$ Hz, 3H, Val3-**H^γ**), 0.34 (d, $^3J = 6.6$ Hz, 3H, Val3-**H^γ**).

¹³C-NMR (151 MHz; DMSO-*d*₆): δ [ppm] = 168.92 (Ala4-**C**), 168.08 (Val6-**C**), 167.45 (Phe2-**C**), 155.49 (*t*BuO-**C**), 141.54 (Tz1-**C**), 141.21 (Tz3-**C**), 139.01 (Tz2-**C**), 136.79 (Phe2-**C^γ**), 135.61 (**C^{Ar}**), 131.41 (2C, Tz2-**CH**, Tz3-**CH**), 131.14 (Tz1-**CH**), 129.42 (2C, **CH^{Ar}**), 128.86 (2C, **CH^{Ar}**), 128.75 (**CH^{Ar}**), 128.59 (2C, **CH^{Ar}**), 128.50 (2C, **CH^{Ar}**), 127.06 (**CH^{Ar}**), 78.98 (-**C(CH₃)₃**), 67.34 (O-**CH₂-**), 65.37 (Val6-**C^α**), 61.89 (Phe2-**C^α**), 56.64 (Ala4-**C^α**), 48.86 (Val3-**C^α**), 42.96 (Leu5-**C^β**), 41.66 (Leu5-**C^α**), 40.07 (Ala1-**C^α**), 36.97 (Phe2-**C^β**), 31.25 (Val3-**C^β**), 30.20 (Val6-**C^β**), 28.60 (-**C(CH₃)₃**), 24.75 (Leu5-**C^γ**), 23.05 (Leu5-**C^δ**), 21.39 (Leu5-**C^δ**), 20.60 (Ala1-**C^β**), 19.70 (Val3-**C^γ**), 19.54 (Val6-**C^γ**), 18.95 (Val6-**C^γ**), 18.75 (Val3-**C^γ**), 17.82 (Ala4-**C^β**).

Boc-Val[5Tz]Ala-Leu[5Tz]Val-Ala-OBzl (14).



Boc-Val[5Tz]Ala-Leu[5Tz]Val-OH (32 mg; 58 μ mol; synthesized from **10** according to **GP5**), COMU (50 mg; 0.12 mmol; 2.0 eq) and Oxyma (16 mg; 0.12 mmol; 2.0 eq) are dissolved in DCM (2 mL; dry), after addition of *sym*-collidine (15 μ L; 0.12 mmol; 2.0 eq), the mixture is stirred

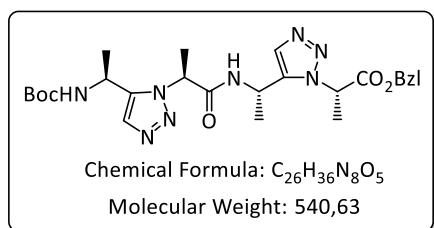
for 10 min at RT for preactivation. H-Ala-OBzl-Tos (41 mg; 0.12 mmol; 2.0 eq) is added, followed by *sym*-collidine (15 μ L; 0.12 mmol; 2.0 eq) and the reaction mixture is left to stir overnight. Afterwards the solvent is removed under vacuum and the peptidotriazolamer purified by preparative HPLC. **Yield:** 37 mg (52 μ mol); 90%. **Analytical RP-HPLC:** $t_R = 3.4$ min (method 2, 254 nm). **HR-MS** (ESI): $m/z = 710.4340$ (calc. 710.43481).

¹H-NMR (600 MHz; DMSO-*d*₆): δ [ppm] = 8.66 (d, $^3J = 6.5$ Hz, 1H, Ala5-**NH**), 7.92 (d, $^3J = 8.6$ Hz, 1H, Leu3-**NH**), 7.76 (d, $^3J = 7.2$ Hz, 1H, Boc-**NH**), 7.70 (s, 1H, Tz2-**H**), 7.57 (s, 1H, Tz1-**H**), 7.39-7.30 (m, 5H, Ph-**H**), 5.43 (q, $^3J = 6.7$ Hz, 1H, Ala2-**H^α**), 5.13 (s, 2H, O-**CH₂-**), 5.34 (m, 1H, Leu3-**H^α**), 4.91 (d, $^3J = 10.4$ Hz, 1H, Val4-**H^α**), 4.52 (dd, $^3J = 7.8, 7.2$ Hz, 1H, Val1-**H^α**), 4.28 (qd, $^3J = 7.3$ Hz, 6.5 Hz, Ala5-**H^α**), 2.82 (dq, $^3J = 10.4, 6.6, 6.5$ Hz, 1H, Val4-**H^β**), 1.91 (dq, $^3J = 7.8, 6.8, 6.5$ Hz, 1H, Val1-**H^β**), 1.62 (m, 1H, Leu3-**H^β**), 1.58 (d, $^3J = 6.8$ Hz, 3H, Ala2-**H^β**), 1.43 (m, 1H, Leu3-**H^β**), 1.37 (s, 9H, C(**CH₃)₃**), 1.33 (d, $^3J = 7.3$ Hz, 3H, Ala5-**H^β**), 1.24 (m, 1H, Leu3-**H^γ**), 0.98 (d, $^3J = 6.6$ Hz, 3H, Val4-**H^β**), 0.93 (d, $^3J = 6.5$ Hz, 3H, Val1-**H^γ**), 0.79 (d, $^3J = 6.5$ Hz, 3H, Leu3-**H^δ**), 0.71 (d, $^3J = 6.7$ Hz, 3H, Leu3-**H^δ**), 0.69 (d, $^3J = 6.8$ Hz, 3H, Val1-**H^γ**), 0.63 (d, $^3J = 6.5$ Hz, 3H, Val4-**H^β**).

7. Experimental section

$^{13}\text{C}\{^1\text{H}\}$ -NMR (151 MHz, DMSO- d_6): δ [ppm]= 172.40 (Phe6-C), 167.75 (Ala2-C), 167.13 (Val4-C), 156.53 ($^t\text{BuO-C}$), 140.75 (Tz2-C), 140.30 (Tz1-C), 136.28 (C^{Ar}), 132.33 (Tz2-CH), 131.17 (Tz1-CH), 128.86 (2C, CH^{Ar}), 128.49 (CH^{Ar}), 128.26 (2C, CH^{Ar}), 79.26 ($\text{C}(\text{CH}_3)_3$), 68.21 (Val4- C^α), 66.49 (O- CH_2 -), 55.67 (Ala3- C^α), 51.10 (Val1- C^α), 48.62 (Ala5- C^α), 44.05 (Leu3- C^β), 41.91 (Leu3- C^α), 32.93 (Val1- C^β), 30.18 (Val4- C^β), 28.59 ($\text{C}(\text{CH}_3)_3$), 24.61 (Leu3- H^γ), 23.17 (CH_3), 22.07 (CH_3), 19.45 (2C, CH_3), 19.40 (CH_3), 19.15 (CH_3), 17.72 (Ala3- C^β), 17.04 (Ala5- C^β).

Boc-Ala[5Tz]Ala-Ala[5Tz]Ala-OBzl (15).



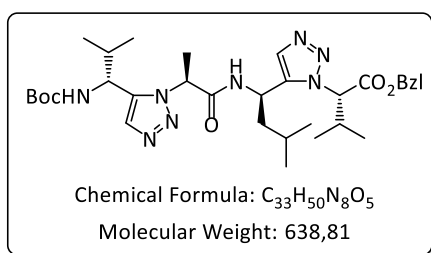
Boc-Ala[5Tz]Ala-OBzl (**9g**) (52 mg; 0.14 mmol; 1.1 eq) is dissolved in DCM/(4 M HCl in dioxane) 1:1 (1.5 mL) and stirred overnight at rt. After evaporation of the solvent, the ammonium salt is used without further purification. Boc-Ala[5Tz]Ala-OH (36 mg; 0.13 mmol; synthesized from **9g** according to **GP5**), Oxyma (20 mg; 0.14 mmol; 1.1 eq) and COMU (60 mg; 0.14 mmol; 1.1 eq) are dissolved in DCM (dry; 1 mL) under an argon atmosphere, after the addition of *sym*-collidine (34 μL ; 0.26 mmol; 2.0 eq) the mixture is preactivated for 5 min at RT. After preactivation of the carboxylic acid, the ammonium salt is dissolved in DCM (dry; 1 mL) and added dropwise to the reaction mixture, followed by *sym*-collidine (34 μL ; 0.26 mmol; 2.0 eq). The reaction mixture left to stir overnight. After evaporation of the solvent, the product is purified by preparative HPLC.

Yield: 52 mg (0.10 mmol); 77%. **Analytical RP-HPLC:** t_{R} = 2.9 min (method 2, 220 nm).

HR-MS (ESI): m/z = 541.2897 [$\text{M}+\text{H}$] $^+$ (calc. 541.28814).

^1H -NMR (600 MHz; DMSO- d_6): δ [ppm]= 8.45 (d, 3J = 8.4 Hz, 1H, Ala3- NH), 7.73 (s, 1H, Tz2- H), 7.61 (s, 1H, Tz1- H), 7.46 (d, 3J = 7.5 Hz, 1H, Boc- NH), 7.39-7.30 (m, 5H, Ph- H), 5.64 (q, 3J = 7.2 Hz, 1H, Ala4- H^α), 5.23 (dq, 3J = 8.4, 6.9 Hz, Ala3- H^α), 5.18 (q, 3J = 7.1 Hz, Ala2- H^α), 5.19-5.16 (m, 2H, O- CH_2 -), 4.81 (dq, 3J = 7.5, 7.0 Hz, 1H, Ala1- H^α), 1.78 (d, 3J = 7.2 Hz, 3H, Ala4- H^β), 1.61 (d, 3J = 7.1 Hz, 3H, Ala2- H^β), 1.40 (d, 3J = 6.9 Hz, 3H, Ala3- H^β) 1.35 (s, 9H, $\text{C}(\text{CH}_3)_3$), 1.34 (d, 3J = 7.0 Hz, 3H, , Ala1- H^β).

$^{13}\text{C}\{^1\text{H}\}$ -NMR (151 MHz, DMSO- d_6): δ [ppm]= 168.91 (Ala4-C), 167.41 (Ala2-C), 154.95 ($^t\text{BuO-C}$), 140.80 (Tz1-C), 139.80 (Tz2-C), 135.43 (C^{Ar}), 131.33 (Tz2-CH), 131.04 (Tz1-CH), 128.42 (2C, CH^{Ar}), 128.12 (CH^{Ar}), 127.74 (2C, CH^{Ar}), 78.46 ($\text{C}(\text{CH}_3)_3$), 66.85 (O- CH_2 -), 56.26 (Ala2- C^α), 55.41 (Ala4- C^α), 40.33 (Ala1- C^α), 38.24 (Ala3- C^α), 28.13 ($\text{C}(\text{CH}_3)_3$), 21.18 (Ala1- C^β), 19.90 (Ala3- C^β), 17.49 (2C, Ala2- C^β , Ala4- C^β).

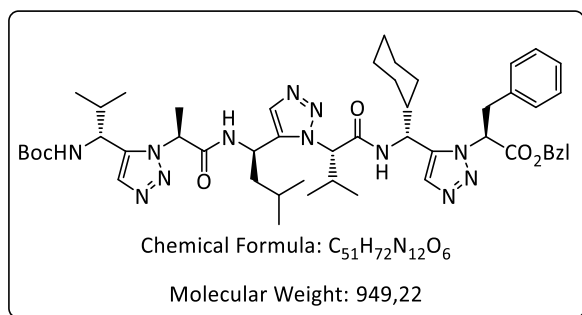
Boc-D-Val[5Tz]Ala-D-Leu[5Tz]Val-OBzl (16).

Boc-D-Leu[5Tz]Val-OBzl (**9d**) (71 mg; 0.16 mmol; 1.1 eq) is dissolved in DCM/(4 M HCl in dioxane) 1:2 (1.5 mL) and stirred overnight at rt. After evaporation of the solvent, the ammonium salt is used without further purification. Boc-D-Val[5Tz]Ala-OH (45 mg;

0.14 mmol; synthesized from **9f** according to **GP5**) and Oxyma (23 mg; 0.16 mmol; 1.1 eq) are dissolved in DCM (dry; 1 mL) under an argon atmosphere. After addition of DIC (25 μ L; 0.16 mmol; 1.1 eq) the solution is stirred 5 min at rt for preactivation. After preactivation of the carboxylic acid, the ammonium salt is dissolved in DCM (dry; 1 mL) and added dropwise to the reaction mixture, followed by DIPEA (56 μ L; 0.32 mmol; 2.2 eq). After evaporation of the solvent, the product is purified by preparative HPLC. **Yield:** 66 mg (0.10 mmol); 71%. **R_f** (ethylacetate)= 0.60. **MS (ESI):** m/z = 661.4 [M+Na]⁺.

¹H-NMR (600 MHz; DMSO-*d*₆): δ [ppm]= 8.86 (d, ³*J*= 8.2 Hz, 1H, Leu3-NH), 7.73 (s, 1H, Tz2-H), 7.52 (s, 1H, Tz1-H), 7.39 (d, ³*J*= 9.0 Hz, 1H, Boc-NH), 7.35-7.31 (m, 3H, Ph-H), 7.25-7.21 (m, 2H, Ph-H), 5.37 (q, ³*J*= 7.0 Hz, 1H, Ala2-H ^{α}), 5.17 (d, ²*J*= 12.2 Hz, 1H, O-CHH), 5.11 (d, ²*J*= 12.2 Hz, 1H, O-CHH), 5.10 (d, ³*J*= 9.0 Hz, 1H, Val4-H ^{α}), 4.94 (m, 1H, Leu3-H ^{α}), 4.25 (dd, ³*J*= 9.0, 8.9 Hz, 1H, Val1-H ^{α}), 2.76 (m, 1H, Val4-H ^{β}), 1.85-1.74 (m, 2H, Val1-H ^{β} , Leu3-H ^{β}), 1.76 (d, ³*J*= 7.0 Hz, 3H, Ala2-H ^{β}), 1.51 (m, 1H, Leu3-H ^{γ}), 1.32 (m, 1H, m, 1H, Leu3-H ^{β}), 0.97 (d, ³*J*= 6.7 Hz, 3H, Val4-H ^{γ}), 0.73 (d, ³*J*= 6.6 Hz, 3H, Leu3-H ^{δ}), 0.77 (d, ³*J*= 6.6 Hz, 6H, Leu3-H ^{δ} , Val1-H ^{γ}), 0.66 (d, ³*J*= 6.7 Hz, 3H, Val4-H ^{γ}), 0.43 (d, ³*J*= 6.7 Hz, 3H, Val1-H ^{γ}).

¹³C{¹H}-NMR (126 MHz; DMSO-*d*₆): δ [ppm]= 168.81 (Ala2-C), 168.14 (Val4-C), 156.01 (^tBuO-C), 140.98 (Tz2-C), 140.09 (Tz1-C), 135.62 (C^{Ar}), 131.57 (Tz2-CH), 131.19 (Tz1-CH), 128.87 (CH^{Ar}; 2C), 128.75 (CH^{Ar}), 128.51 (CH^{Ar}; 2C), 78.81 (C(CH₃)₃), 67.34 (OCH₂), 65.35 (Val4-C ^{α}), 56.50 (Ala2-C ^{α}), 50.30 (Val1-C ^{α}), 42.93 (Leu3-C ^{β}), 41.45 (Leu3-C ^{α}), 31.68 (Val1-C ^{β}), 30.11 (Val4-C ^{β}), 28.56 (C(CH₃)₃), 24.75 (Leu3-C ^{γ}), 23.03 (Val1-C ^{γ}), 21.45 (Leu3-C ^{δ}), 19.83 (Val1-C ^{γ}), 19.53 (Val4-C ^{γ}), 18.98 (Leu3-C ^{δ}), 18.93 (Val4-C ^{γ}), 18.38 (Ala2-C ^{β}).

Boc-D-Val[5Tz]Ala-D-Leu[5Tz]Val-D-chGly[5Tz]Phe-OBzl (17).

Boc-D-chGly[5Tz]Phe-OBzl (**9i**) (32 mg; 61 μ mol; 1.1 eq) is dissolved in DCM/(4 M HCl in dioxane) 1:1 (2 mL) and stirred overnight at rt. After evaporation of the solvent, the ammonium salt is used without further purification. Boc-D-

Val[5Tz]Ala-D-Leu[5Tz]Val-OH (30 mg; 55 μ mol; synthesized from **16** according to **GP5**), COMU (24 mg; 55 μ mol; 1.0 eq) and Oxyma (8 mg; 0.06 mmol; 1.0 eq) are dissolved in DCM (1 mL; dry), after addition of *sym*-collidine (7.3 μ L; 55 μ mol; 1.0 eq), the mixture is stirred for 5 min at RT for preactivation. After preactivation of the carboxylic acid, the ammonium salt is dissolved in DCM (dry; 0.5 mL) and added dropwise to the reaction mixture, followed by *sym*-collidine (7.3 μ L; 55 μ mol; 1.0 eq). The reaction mixture left to stir overnight. After evaporation of the solvent, the product is purified by preparative HPLC.

Yield: 40 mg (42 μ mol); 76%. **Analytical RP-HPLC:** t_R = 3.6 min (method 2, 254 nm).

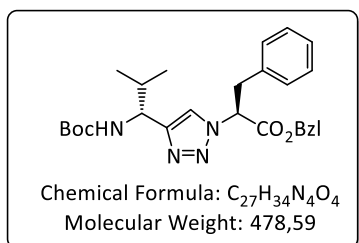
HR-MS (ESI): m/z = 475.2933 [$M+2H$] $^{2+}$ (calc. 475.29216).

1H -NMR (600 MHz; DMSO- d_6): δ [ppm] = 8.84 (d, 3J = 8.0 Hz, 1H, Leu3-NH), 8.69 (d, 3J = 8.5 Hz, 1H, chGly5-NH), 7.66 (s, 1H, Tz2-H), 7.63 (s, 1H, Tz3-H), 7.51 (s, 1H, Tz1-H), 7.37 (d, 3J = 8.9 Hz, 1H, Boc-NH), 5.97 (dd, 3J = 7.9, 7.3 Hz, 1H, Phe6- H^α), 5.35 (q, 3J = 7.0 Hz, 1H, Ala2- H^α), 5.09 (d, 2J = 12.5 Hz, 1H, -O-CHH-), 5.05 (d, 2J = 12.5 Hz, 1H, -O-CHH-), 4.88 (ddd, 3J = 10.7, 8.0, 4.9 Hz, 1H, Leu3- H^α), 4.77 (d, 3J = 9.9 Hz, 1H, Val4- H^α), 4.68 (dd, 3J = 8.8, 8.5 Hz, 1H, chGly5- H^α), 4.22 (dd, 3J = 8.9, 8.8 Hz, 1H, Val1- H^α), 3.64 (dd, 2J = 14.0, 3J = 7.9 Hz, 1H, Phe6- H^β), 3.28 (dd, 2J = 14.0, 3J = 7.3 Hz, 1H, Phe6- H^β), 2.83 (dq, 3J = 9.9, 6.8 6.5 Hz, 1H, Val4- H^β), 1.77 (d, 3J = 7.0 Hz, 3H, Ala2- H^β), 1.77-1.71 (m, 2H, Val1- H^β , chGly5- H^β), 1.66-1.59 (m, 2H, Leu3- H^β , CH $_2$), 1.58-1.44 (m, 3H, CH $_2$), 1.36 (m, 1H, Leu3- H^γ), 1.35 (s, 9H, C(CH $_3$) $_3$), 1.12 (m, 1H, CH $_2$), 1.04-0.87 (m, 4H, Leu3- H^β , CH $_2$), 0.80 (d, 3J = 6.8 Hz, 3H, Val4- H^γ), 0.72 (d, 3J = 6.7 Hz, 3H, Val1- H^γ), 0.69 (d, 3J = 6.6 Hz, 6H, Leu3- H^δ), 0.67 (m, 1H, CH $_2$), 0.56 (d, 3J = 6.5 Hz, 3H, Val4- H^γ), 0.50 (m, 1H, CH $_2$), 0.39 (d, 3J = 6.7 Hz, 3H, Val1- H^γ).

$^{13}C\{^1H\}$ -NMR (126 MHz, DMSO- d_6): δ [ppm] = 168.78 (Ala2-C), 168.37 (Phe6-C), 167.48 (Val4-C), 156.02 (t BuO-C), 141.01 (Tz2-C), 140.07 (Tz1-C), 139.37 (Tz3-C), 136.12 (C Ar), 135.54 (C Ar), 131.78 (Tz3-CH), 131.38 (Tz2-CH), 131.16 (Tz1-CH), 129.56 (2C; CH Ar), 128.76(2C; CH Ar), 128.63(CH Ar), 128.51(2C; CH Ar), 128.31(2C; CH Ar), 127.02(CH Ar), 78.81 (C(CH $_3$) $_3$), 67.60 (Val4-C $^\alpha$), 67.39 (-OCH $_2$ -), 60.45 (Phe6-C $^\alpha$), 56.43 (Ala2-C $^\alpha$), 50.37 (Val1-C $^\alpha$), 47.97 (chGly5-C $^\alpha$), 43.33 (Leu3-C $^\beta$), 41.57 (Leu3-C $^\alpha$), 40.71 (chGly5-C $^\beta$), 37.27 (Phe6-

C^{β}), 31.70 (Val1- C^{β}), 30.08 (Val4- C^{β}), 29.74 (CH_2), 28.92(CH_2), 28.57 ($C(CH_3)_3$), 25.97 (CH_2), 25.57 (CH_2), 25.54 (CH_2), 24.85 (Leu3- C^{γ}), 23.07 (Leu3- C^{δ}), 21.41 (Leu3- C^{δ}), 19.80 (Val1- C^{γ}), 19.36 (Val4- C^{γ}), 18.90 (Val4- C^{γ}), 18.81 (Val1- C^{γ}), 18.42 (Ala2- C^{β}).

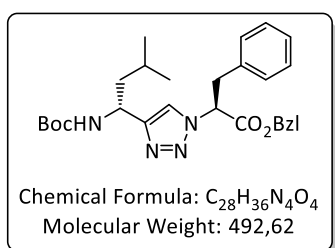
Boc-D-Val[4Tz]Phe-OBzl (18a).



Boc-D-Val≡ (**8c**) (85 mg; 0.43 mmol) and N_3 -Phe-OBzl (**4c**) (133 mg; 0.47 mmol; 1.1 eq) are dissolved in DMF/ H_2O 2:1 (1.5 mL), $CuSO_4 \cdot 5H_2O$ (54 mg; 0.22 mmol; 0.5 eq) and sodium ascorbate (85 mg; 0.43 mmol; 1.0 eq) are added and the reaction mixture left to stir overnight. The solvent is removed by rotary evaporator and the triazole purified by flash chromatography (PE/EtOAc 3:1). **Yield:** 138 mg (0.29 mmol); 67%. **R_f** (PE/EtOAc 3:1)= 0.40.

1H -NMR (500 MHz, $DMSO-d_6$): δ [ppm]= 7.92 (s, 1H, Tz-**H**), 7.38-7.31 (m, 3H, BocNH, Ph-**H**), 7.28-7.24 (m, 2H, Ph-**H**), 7.20-7.15 (m, 3H, Ph-**H**), 7.13-7.08 (m, 3H, Ph-**H**), 5.91 (dd, $^3J=10.7$, 5.3 Hz, 1H, Phe-**H $^{\alpha}$**), 5.21-5.18 (m, 2H, OCH_2), 4.43 (dd, $J=9.3$, 7.3 Hz, 1H, Val-**H $^{\alpha}$**), 3.58 (dd, $^2J=14.2$, $^3J=5.3$ Hz, 1H, Phe-**H $^{\beta}$**), 3.48 (dd, $^2J=14.2$, $^3J=10.7$ Hz, 1H, Phe-**H $^{\beta}$**), 1.89 (m, 1H, Val-**H $^{\beta}$**), 1.37 (s, 9H, $C(CH_3)_3$), 0.77 (d, $^3J=6.7$ Hz, 3H, Val-**H $^{\gamma}$**), 0.62 (d, $^3J=6.8$ Hz, 3H, Val-**H $^{\gamma}$**).

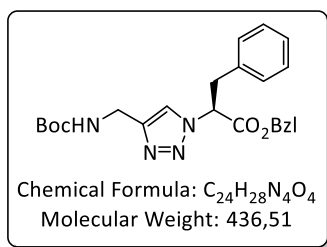
Boc-D-Leu[4Tz]Phe-OBzl (18b).



Boc-D-Leu≡ (**8e**) (90 mg; 0.43 mmol) and N_3 -Phe-OBzl (**4c**) (133 mg; 0.47 mmol; 1.1 eq) are dissolved in DMF/ H_2O 2:1 (1.5 mL), $CuSO_4 \cdot 5H_2O$ (54 mg; 0.22 mmol; 0.5 eq) and sodium ascorbate (85 mg; 0.43 mmol; 1.0 eq) are added and the reaction mixture left to stir overnight. The solvent is removed by rotary evaporator and the triazole purified by flash chromatography (PE/EtOAc 3:1).

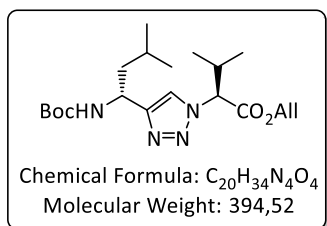
Yield: 130 mg (0.26 mmol); 60%. **R_f** (PE/EtOAc 3:1)= 0.42. **MS (ESI):** $m/z=515.3$ [$M+Na$] $^+$.

1H -NMR (500 MHz, $DMSO-d_6$): δ [ppm]= 7.94 (s, 1H, Tz-**H**), 7.39-7.30 (m, 3H, Boc-NH, Ph-**H**), 7.28-7.23 (m, 2H, Ph-**H**), 7.21-7.15 (m, 4H, Ph-**H**), 7.12-7.09 (m, 2H, Ph-**H**), 5.89 (dd, $^3J=10.4$, 5.6 Hz, 1H, Phe-**H $^{\alpha}$**), 5.20-5.18 (m, 2H, OCH_2), 4.67 (m, 1H, Leu-**H $^{\alpha}$**), 3.57 (dd, $^2J=14.2$, $^3J=5.6$ Hz, 1H, Phe-**H $^{\beta}$**), 3.50 (dd, $^2J=14.2$, $^3J=10.4$ Hz, 1H, Phe-**H $^{\beta}$**), 1.56-1.47 (m, 2H, Leu-**H $^{\beta}$**), 1.37 (s, 9H, $C(CH_3)_3$), 1.30 (m, 1H, Leu-**H $^{\gamma}$**), 0.86 (d, $^3J=6.6$ Hz, 3H, Leu-**H $^{\delta}$**), 0.83 (d, $^3J=6.6$ Hz, 3H, Leu-**H $^{\delta}$**).

Boc-Gly[4Tz]Phe-OBzl (18d).

Boc-Gly≡ (200 mg; 1.27 mmol) and N₃-Phe-OBzl (**4c**) (394 mg; 1.40 mmol; 1.1 eq) are dissolved in DMF/H₂O 2:1 (4.5 mL), CuSO₄·5H₂O (160 mg; 0.64 mmol; 0.5 eq) and sodium ascorbate (252 mg; 1.27 mmol; 1.0 eq) are added and the reaction mixture left to stir overnight. The solvent is removed by rotary evaporator and the triazole purified by flash chromatography (PE/EtOAc 2:1). **Yield:** 490 mg (1.12 mmol); 88%. **R_f** (PE/EtOAc 3:1)= 0.36.

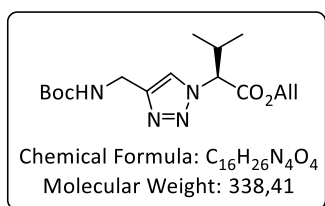
¹H-NMR (500 MHz, DMSO-*d*₆): δ [ppm]= 8.04 (s, 1H, Tz-**H**), 7.45-7.29 (m, 6H, Boc-N**H**, Phe-**H**), 7.28-7.17 (m, 5H, Phe-**H**), 5.97 (dd, ³*J*= 10.1, 5.8 Hz, 1H, Phe-**H**^α), 5.25-5.23 (m, 2H, OCH₂), 4.18 (m, 2H, Gly-**H**^α), 3.63 (dd, ²*J*= 14.5, ³*J*= 5.8 Hz, 2H, Phe-**H**^β), 3.58 (dd, ²*J*= 14.5, ³*J*= 10.1 Hz, 1H, Phe-**H**^β), 1.44 (s, 9H, C(CH₃)₃).

Boc-D-Leu[4Tz]Val-OAll (18c).

Boc-D-Leu≡ (**8e**) (88 mg; 0.42 mmol) and N₃-Val-OAll (**4d**) (86 mg; 0.47 mmol; 1.1 eq) are dissolved in DMF/H₂O 2:1 (1.5 mL), CuSO₄·5H₂O (54 mg; 0.22 mmol; 0.5 eq) and sodium ascorbate (85 mg; 0.43 mmol; 1.0 eq) are added and the reaction mixture left to stir overnight. The solvent is removed by rotary evaporator and the triazole purified by flash chromatography (PE/EtOAc 3:1).

Yield: 136 mg (0.34 mmol); 81%. **R_f** (PE/EtOAc 3:1)= 0.50. **MS (ESI):** *m/z*= 417.3 [M+Na]⁺, 811.4 [2M+Na]⁺.

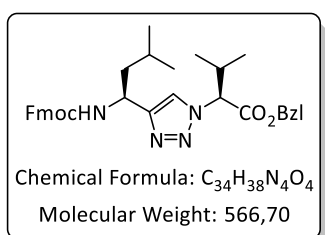
¹H-NMR (500 MHz, DMSO-*d*₆): δ [ppm]= 7.96 (s, 1H, Tz-**H**), 7.22 (d, ³*J*= 8.8 Hz, 1H, BocNH), 5.90 (dddd, ³*J*= 17.2, 10.7, 5.4, 5.4 Hz, 1H, CH₂-CH=CH₂), 5.31 (d, ³*J*= 8.4 Hz, 1H, Val-**H**^α), 5.27 (dd, ³*J*= 17.2, ²*J*= 1.6 Hz, 1H, CH₂-CH=CH**H**^ε), 5.23 (dd, ³*J*= 10.7, 1.6 Hz, 1H, CH₂-CH=CH^δH), 4.74 (m, 1H, Leu-**H**^α), 4.71-4.63 (m, 2H, CH₂-CH=CH₂), 2.54 (m, Val-**H**^β), 1.68-1.48 (m, 3H, Leu-**H**^β, Leu-**H**^γ), 1.38 (s, 9H, C(CH₃)₃), 0.95 (d, ³*J*= 6.7 Hz, 3H, Val-**H**^γ), 0.89 (d, ³*J*= 6.5 Hz, 3H, Leu-**H**^δ), 0.89 (d, ³*J*= 6.3 Hz, 3H, Leu-**H**^δ), 0.78 (d, ³*J*= 6.7 Hz, 3H, Val-**H**^γ).

Boc-Gly[4Tz]Val-OAll (18e).

Boc-Gly≡ (100 mg; 0.64 mmol) and N₃-Val-OAll (**4d**) (129 mg; 0.70 mmol; 1.1 eq) are dissolved in DMF/H₂O 2:1 (2.25 mL), CuSO₄·5H₂O (80 mg; 0.32 mmol; 0.5 eq) and sodium ascorbate (126 mg; 0.64 mmol; 1.0 eq) are added and the reaction mixture left to stir overnight. The solvent is removed by rotary evaporator and the triazole purified by flash chromatography (PE/EtOAc 2:1).

Yield: 176 mg (0.34 mmol); 81%. **R_f** (PE/EtOAc 2:1)= 0.35.

¹H-NMR (500 MHz, DMSO-*d*₆): δ [ppm]= 8.03 (s, 1H, Tz-**H**), 7.39 (dd, ³J= 5.9, 5.9 Hz, 1H, Boc-**NH**), 5.96 (dddd, ³J= 17.3, 10.7, 5.5, 5.5 Hz, 1H, CH₂-CH=CH₂), 5.37 (d, ³J= 8.7 Hz, 1H, Val-**H^α**), 5.34 (dd, ³J= 17.3, ²J= 1.5 Hz, 1H, CH₂-CH=CH^E), 5.29 (dd, ³J= 10.5, ²J= 1.5 Hz, 1H, CH₂-CH=CH^ZH), 4.76-4.68 (m, 2H, CH₂-CH=CH₂), 4.27-4.23 (m, 2H, Gly-**H^α**), 2.61 (m, 1H, Val-**H^β**), 1.44 (s, 9H, C(CH₃)₃), 1.00 (d, *J* = 6.7 Hz, 3H, Val-**H^γ**), 0.84 (d, *J* = 6.7 Hz, 3H, Val-**H^γ**).

Fmoc-Leu[4Tz]Val-OBzl (18f).

Fmoc-Leu≡ (142 mg; 426 μmol) and N₃-Val-OBzl (109 mg; 469 μmol; 1.1 eq) are suspended in DMF/H₂O (2:1) (4.3 mL). CuSO₄·5H₂O (54 mg; 0.22 mmol; 0.5 eq) and sodium ascorbate (85 mg; 0.43 mmol; 1.0 eq) are added and the reaction stirred at rt overnight. The solvent is co-evaporated with toluene and the crude triazole purified by column chromatography (PE/EtOAc 2:1). **Yield:** 222 mg (392 μmol); 92%. **R_f** (PE/EtOAc 2:1)= 0.21. **HR-MS (ESI):** *m/z*= 567.2987 (calc. 567.29658).

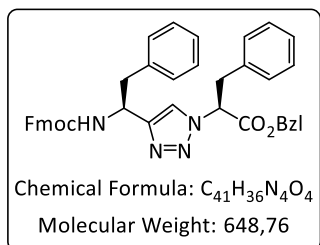
¹H-NMR (600 MHz; DMSO-*d*₆): δ [ppm]= 7.99 (s, 1H, Tz-**H**), 7.90-7.86 (m, 2H, **H^{Ar}**), 7.75 (d, ³J= 9.0 Hz, 1H, **NH**), 7.72-7.67 (m, 2H, **H^{Ar}**), 7.43-7.38 (m, 2H, **H^{Ar}**), 7.37-7.28 (m, 7H, **H^{Ar}**), 5.32 (d, ³J= 8.3 Hz, 1H, Val2-**H^α**), 5.22 (d, ²J= 12.4 Hz, 1H, O-CH^H-Ph), 5.17 (d, ²J= 12.4 Hz, 1H, O-CH^H-Ph), 4.80 (ddd, ³J= 9.0, 5.9, 5.9 Hz, 1H, Leu1-**H^β**), 4.35 (dd, ²J= 10.5, ³J= 7.2 Hz, 1H, CH-CH^HO), 4.28 (dd, ²J= 10.5, ³J= 6.9 Hz, 1H, CH-CH^HO), 4.21 (dd, ³J= 7.2, 6.9 Hz, 1H, CH-CH₂O), 2.54 (m, 1H, Val2-**H^β**), 1.68 (m, 1H, Leu1-**H^β**), 1.62 (m, 1H, Leu1-**H^β**), 1.54 (m, 1H, Leu1-**H^γ**), 0.93-0.85 (m, 9H, Val2-**H^γ**, Leu1-**H^δ**), 0.75 (d, ³J= 6.7 Hz, 3H, Val2-**H^γ**).

¹³C{¹H}-NMR (151 MHz, DMSO) δ [ppm]= 168.58 (Val2-**C**), 156.12 (OCON), 149.96 (Tz-**C**), 144.39 (**C^{Ar}**), 144.21 (**C^{Ar}**), 141.20 (**C^{Ar}**), 141.18 (**C^{Ar}**), 135.70 (**C^{Ar}**), 128.90 (2C; **CH^{Ar}**), 128.73 (**CH^{Ar}**), 128.50 (2C; **CH^{Ar}**), 128.06 (**CH^{Ar}**), 128.04 (**CH^{Ar}**), 127.47 (**CH^{Ar}**), 127.46 (**CH^{Ar}**), 125.66 (**CH^{Ar}**), 125.63 (**CH^{Ar}**), 122.28 (Tz-**CH**), 120.57 (**CH^{Ar}**), 120.54 (**CH^{Ar}**), 67.92 (Val2-**C^α**), 67.33

7. Experimental section

(O-CH₂-Ph), 65.74 (CH-CH₂-O), 47.25 (CH-CH₂-O), 46.09 (Leu1-C^α), 44.42 (Leu1-C^β), 31.18 (Val2-C^β), 24.74 (Leu1-C^γ), 23.23 (Leu1-C^δ), 22.25 (Leu1-C^δ), 19.24 (Val2-C^γ), 18.69 (Val2-C^γ).

Fmoc-Phe[4Tz]Phe-OBzl (18g).

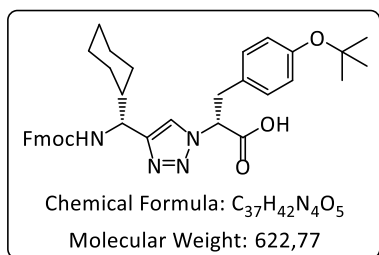


Fmoc-Phe≡ (156 mg; 425 μmol) and N₃-Phe-OBzl (132 mg; 468 μmol; 1.1 eq) are suspended in H₂O/^tBuOH (1:1) (4 mL). CuSO₄·5H₂O (21 mg; 84 μmol; 0.2 eq) and sodium ascorbate (34 mg; 0.17 μmol; 0.4 eq) are added and the reaction stirred at 60°C for 1 h under microwave condition (20W). The solvent is co-evaporated with toluene and the crude triazole purified by column chromatography (PE/EtOAc 2:1). **Yield:** 205 mg (316 μmol); 74%. **R_f** (PE/EtOAc 2:1)= 0.35. **HR-MS (ESI):** m/z= 649.2803 [M+H]⁺ (calc. 649.28093).

¹H-NMR (500 MHz; DMSO-*d*₆): δ [ppm]= 8.02 (s, 1H, Tz-**H**), 7.91-7.83 (3H, NH, **H^{Ar}**), 7.66-7.60 (2H, **H^{Ar}**), 7.44-7.39 (m, 2H, **H^{Ar}**), 7.37-7.07 (m, 17H, **H^{Ar}**, Ph-**H**), 5.90 (dd, ³J= 10.2, 5.6 Hz, 1H, Phe2-**H^α**), 5.18 (s, 2H, O-CH₂-Ph), 4.88 (ddd, J= 9.4, 9.0, 5.8 Hz, 1H, Phe1-**H^α**), 4.23 (m, 1H, CH-CHH-O), 4.17-4.10 (m, 2H, CH-CHH-O, CH-CHH-O), 3.58 (dd, ²J= 14.2, ³J= 5.6 Hz, 1H, Phe2-**H^β**), 3.51 (dd, ²J= 14.3, ³J= 10.2 Hz, 1H, Phe2-**H^β**), 3.13 (dd, ²J= 13.6, ³J= 5.8 Hz, 1H, Phe1-**H^β**), 3.01 (dd, ²J= 13.6, ³J= 9.4 Hz, 1H, Phe1-**H^β**).

¹³C{¹H}-NMR (126 MHz, DMSO) δ [ppm]= 168.61 (Phe2-C), 155.92 (OCON), 148.90 (C^{Ar}), 144.27 (C^{Ar}), 144.24 (C^{Ar}), 141.15 (C^{Ar}), 138.71 (Tz-C), 136.20 (C^{Ar}), 135.73 (2C; C^{Ar}), 129.70 (2C; CH^{Ar}), 129.39 (2C; CH^{Ar}), 128.89 (3C; CH^{Ar}), 128.76 (2C; CH^{Ar}), 128.62 (CH^{Ar}), 128.52 (2C; CH^{Ar}), 128.16 (3C; CH^{Ar}), 128.07 (CH^{Ar}), 127.51 (CH^{Ar}), 127.30 (CH^{Ar}), 126.62 (CH^{Ar}), 125.75 (CH^{Ar}), 125.67 (CH^{Ar}), 122.93 (Tz-CH), 120.56 (2C; CH^{Ar}), 67.37 (O-CH₂-Ph), 65.93 (CH-CH₂-O), 63.39 (Phe2-C^α), 49.59 (CH-CH₂-O), 47.10 (Phe1-C^α), 39.50 (Phe1-C^β), 37.11 (Phe2-C^β).

Fmoc-D-chGly[4Tz]-D-Tyr(^tBu)-OH (18h).



Fmoc-D-chGly≡ (100 mg; 0.28 mmol; 1.0 eq) and N₃-Tyr(^tBu)-OH (81 mg; 0.31 mmol; 1.1 eq) are suspended in 2.8 mL DMF/H₂O 2:1, after the addition of sodium ascorbate (55 mg; 0.28 mmol; 1.0 eq) and CuSO₄·5H₂O (35 mg; 0.14 mmol; 0.5 eq) the reaction mixture is left to stir overnight. EtOAc (50 mL) and 5% KHSO₄-solution (50 mL) are added and the phases

separated. The aqueous layer is extracted with EtOAc (50 mL x 1), the combined organic layers dried over MgSO₄ and concentrated under vacuum. The crude triazole is purified by column chromatography (gradient: PE/EtOAc 2:1 to 1:1, containing 1% AcOH).

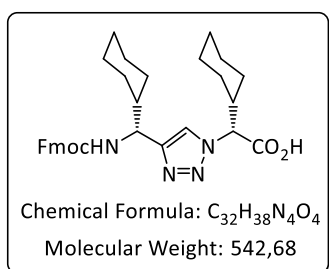
Yield: 142 mg (0.23 mmol); 82%. **R_f** (PE/EtOAc 1:1, 1% AcOH)= 0.14.

HR-MS (ESI): *m/z*= 623.3212 [M+H]⁺ (calc. 623.32280).

¹H-NMR (600 MHz, DMSO) δ [ppm]= 7.90 (s, 1H, Tz-**H**), 7.90-7.88 (m, 2H, **H^{Ar}**), 7.74-7.67 (m, 3H, **NH**, **H^{Ar}**), 7.42-7.39 (m, 2H, **H^{Ar}**), 7.33-7.29 (m, 2H, **H^{Ar}**), 6.96 (d, ³*J*= 8.4 Hz, 2H, Tyr2-**H^δ**), 6.72 (d, ³*J*= 8.4 Hz, 2H, Tyr2-**H^ε**), 5.62 (dd, ³*J*= 11.0, 4.8 Hz, 1H, Tyr2-**H^α**), 4.48 (m, 1H, chGly1-**H^α**), 4.34 (dd, ²*J*= 10.1, ³*J*= 6.9 Hz, 1H, **CHH-O**), 4.26-4.18 (m, 2H, **CH-CH₂O**, **CHH-O**), 3.46 (dd, ²*J*= 14.3, ³*J*= 4.8 Hz, 1H, Tyr2-**H^β**), 3.34 (dd, ²*J*= 14.3, ³*J*= 11.0 Hz, 1H), 1.71-1.52 (m, 5H, chGly1-**H^β**, **CH₂**), 2.30 (m, 1H, **CH₂**), 1.18 (s, 9H, C(**CH₃**)₃), 1.15-1.02 (m, 3H, **CH₂**), 0.87 (m, 1H, **CH₂**), 0.74 (m, 1H, **CH₂**).

¹³C{¹H}-NMR (151 MHz, DMSO-*d*₆) δ [ppm]= 170.26 (Tyr2-**C**), 156.22 (O-**CO**), 154.22 (Tyr2-**C^ξ**), 147.85 (Tz-**C**), 144.44 (**C^{Ar}**), 144.18 (**C^{Ar}**), 141.20 (**C^{Ar}**), 141.17 (**C^{Ar}**), 131.05 (Tyr2-**C^γ**), 129.90 (2C, Tyr2-**C^δ**), 128.06 (**CH^{Ar}**), 128.04 (**CH^{Ar}**), 127.48 (2C, **CH^{Ar}**), 125.71 (2C, **CH^{Ar}**), 123.72 (2C, Tyr2-**C^ε**), 122.74 (Tz-**CH**), 120.56 (**CH^{Ar}**), 120.52 (**CH^{Ar}**), 78.11 (C(**CH₃**)₃), 65.77 (CH-**CH₂-O**), 63.80 (Tyr2-**C^α**), 52.87 (chGly1-**C^α**), 47.25 (CH-**CH₂-O**), 42.37 (chGly1-**C^β**), 36.86 (Tyr2-**C^β**), 29.65 (**CH₂**), 28.99 (**CH₂**), 28.92 (3C, C(**CH₃**)₃), 26.37 (**CH₂**), 25.96 (**CH₂**), 25.92 (**CH₂**).

Fmoc-D-chGly[4Tz]-D-chGly-OH (**18i**).



Fmoc-D-chGly= (50 mg; 0.14 mmol; 1.0 eq) and N₃-chGly-OH (28 mg; 0.15 mmol; 1.1 eq) are suspended in 1.4 mL DMF/H₂O 2:1, after the addition of sodium ascorbate (28 mg; 0.14 mmol; 1.0 eq) and CuSO₄·5H₂O (17 mg; 0.07 mmol; 0.5 eq) the reaction mixture is left to stir for two days. EtOAc (25 mL) and 5% KHSO₄-solution (25 mL) are added and the phases

separated. The aqueous layer is extracted with EtOAc (1x25 mL), the combined organic layers are washed with brine (25 mL), dried over MgSO₄ and concentrated under vacuum. The crude triazole is purified by column chromatography (gradient: PE/EtOAc 2:1 to 1:1, both containing 1% AcOH). **Yield:** 55 mg (0.10 mmol); 72%. **R_f** (PE/EtOAc 1:1, 1% AcOH)= 0.20. **HR-MS** (ESI): *m/z*= 543.2966 [M+H]⁺ (calc. 543.29658).

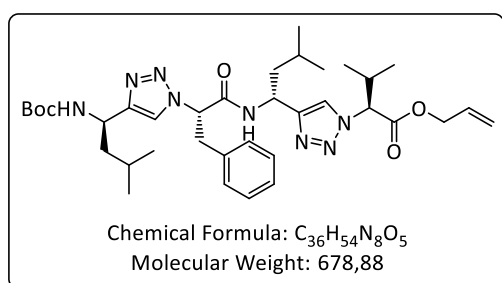
¹H-NMR (600 MHz, DMSO-*d*₆) δ [ppm]= 7.99 (s, 1H, Tz-**H**), 7.74 (d, ³*J*= 9.5 Hz, 1H, **NH**), 5.14 (d, ³*J*= 8.3 Hz, 1H, chGly2-**H^α**), 4.59 (dd, ³*J*= 9.5, 7.4 Hz, 1H, chGly1-**H^α**), 4.35 (dd, ²*J*=

7. Experimental section

10.5, $^3J = 7.2$ Hz, 1H, CH-CHH-O), 4.27 (dd, $^2J = 10.5$, $^3J = 6.9$ Hz, 1H, CH-CHH-O), 4.21 (dd, $^3J = 7.2$, $^3J = 6.9$ Hz, 1H, CH-CH₂-O), 2.15 (m, 1H, chGly2-H^β), 1.79-1.46 (m, 8H, chGly1-H^β, CH₂), 1.43 (m, 1H, CH₂), 1.29-0.61 (m, 12H, CH₂).

¹³C{¹H}-NMR (151 MHz, DMSO) δ [ppm] = 170.06 (chGly2-C), 156.31 (O-CO), 148.13 (Tz-C), 144.41 (C^{Ar}), 144.18 (C^{Ar}), 141.20 (C^{Ar}), 141.17 (C^{Ar}), 128.06 (CH^{Ar}), 128.03 (CH^{Ar}), 127.46 (2C, CH^{Ar}), 125.69 (2C, CH^{Ar}), 122.57 (Tz-CH), 120.57 (CH^{Ar}), 120.53 (CH^{Ar}), 67.61 (chGly2-C^α), 65.78 (CH₂-O), 52.88 (chGly1-C^α), 47.25 (CH-CH₂-O), 42.45 (chGly1-C^β), 40.09 (chGly2-C^β), 29.80 (CH₂), 29.61 (CH₂), 28.87 (CH₂), 28.53 (CH₂), 26.41 (CH₂), 25.96 (CH₂), 25.92 (CH₂), 25.91 (CH₂), 25.59 (CH₂), 25.53 (CH₂).

Boc-D-Leu[4Tz]Phe-D-Leu[4Tz]Val-OAll (19).



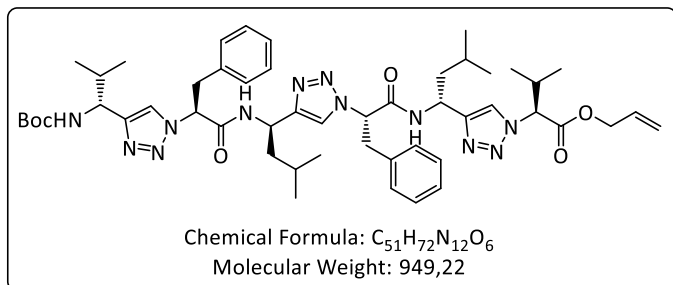
Boc-D-Leu[4Tz]Val-OAll (**18c**) (87 mg; 0.22 mmol; 1.0 eq) is dissolved in 3 mL of a 1:1 mixture of DCM and HCl (4 M in dioxane) and stirred for 2 h at rt. After complete cleavage of the Boc-group, the free amine is evaporated to dryness. In a second flask, Boc-D-Leu[4Tz]Phe-

OH (93 mg; 0.23 mmol; 1.0 eq; synthesized from **18b** according to **GP5**) and HOAt (34 mg; 0.25 mmol; 1.1 eq) are dissolved in DCM (4 mL, dry). After addition of DIC (39 μL; 0.25 mmol; 1.1 eq), the mixture is stirred 5 min at RT for preactivation and is then added to the free amine, followed by TMP (155 μL; 1.17 mmol; 5.0 eq). This solution is left stirring over night at rt. After evaporation of the solvent, the crude product is dissolved in EtOAc (50 mL) and washed: 5% KHSO₄ (3x25 mL), saturated NaHCO₃ (3x25 mL), brine (1x25 mL) and dried over MgSO₄. The organic phase is concentrated under vacuum and the crude product purified by column chromatography (PE/EtOAc 1:3). **Yield:** 127 mg (187 μmol); 81%. **R_f** (PE/EtOAc 1:3) = 0.81. **MS (ESI):** m/z = 701.4 [M+Na]⁺.

¹H-NMR (500 MHz, DMSO-*d*₆): δ [ppm] = 8.98 (d, $^3J = 8.6$ Hz, 1H, Leu3-NH), 8.10 (s, 1H, Tz1-H), 8.05 (s, 1H, Tz2-H), 7.32-7.24 (m, 5H, Ph-H), 7.19 (d, $^3J = 9.0$ Hz, 1H, Boc-NH), 5.94 (dddd, $^3J = 17.3$, 10.8, 5.5, 5.5 Hz, 1H, CH₂-CH=CH₂), 5.66 (dd, $^3J = 8.0$, 7.4 Hz, 1H, Phe2-H^α), 5.33 (d, $^3J = 8.5$ Hz, 1H, Val4-H^α), 5.30 (dd, $^3J = 17.3$, $^2J = 1.4$ Hz, 1H, CH₂-CH=CH^EH), 5.25 (dd, $^3J = 10.4$, $^2J = 1.4$ Hz, 1H, CH₂-CH=CH^ZH), 5.06 (m, 1H, Leu3-H^α), 4.75 (m, 1H, Leu1-H^α), 4.74-4.66 (m, 2H, CH₂-CH=), 3.44 (dd, $^2J = 13.7$, $^3J = 7.4$ Hz, 1H, Phe2-H^β), 3.40 (dd, $^2J = 13.7$, $^3J = 8.0$ Hz, 1H, Phe2-H^β), 2.50 (m, 1H, Val4-H^β), 1.64-1.57 (m, 4H, Leu1-H^β, Leu3-H^β), 1.50 (m, 1H, Leu1-H^γ), 1.44 (s, 9H, C(CH₃)₃), 1.30 (m, 1H, Leu3-H^γ), 0.98 (d, $^3J = 6.7$ Hz, 3H,

Val4-**H^γ**), 0.93 (d, $^3J = 6.5$ Hz, 3H, Leu1-**H^δ**), 0.91 (d, $^3J = 6.5$ Hz, 3H, Leu1-**H^δ**), 0.87 (d, $^3J = 6.8$ Hz, 3H, Leu3-**H^δ**), 0.86 (d, $^3J = 6.9$ Hz, 3H, Leu3-**H^δ**) 0.78 (d, $^3J = 6.7$ Hz, 3H, Val4-**H^γ**).

Boc-D-Val[4Tz]Phe-D-Leu[4Tz]Phe-D-Leu[4Tz]Val-OAll (20).



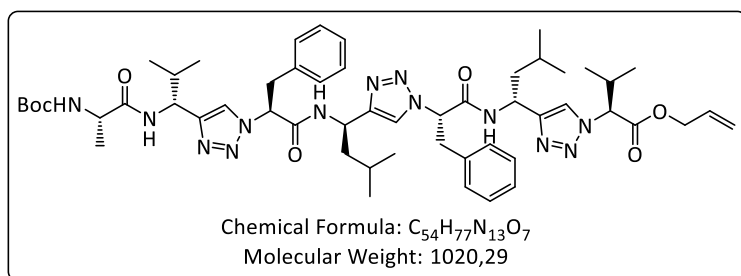
Boc-D-Leu[4Tz]Phe-D-Leu[4Tz]Val-OAll (**19**) (110 mg; 162 μmol; 1.0 eq) is dissolved in 2 mL of a 1:1 mixture of DCM and HCl (4 M in dioxane) and stirred for 2 h at rt. After complete cleavage of

the Boc-group, the free amine is evaporated to dryness. In a second flask, Boc-D-Val[4Tz]Phe-OH (68 mg; 0.18 mmol; 1.1 eq; synthesized from **18a** according to **GP5**) and HOAt (26 mg; 0.19 mmol; 1.2 eq) are dissolved in DCM (4 mL, dry). After addition of DIC (30 μL; 0.19 mmol; 1.2 eq), the mixture is stirred 5 min at RT for preactivation and is then added to the free amine, followed by TMP (106 μL; 0.800 mmol; 5.0 eq). This solution is left stirring over night at rt. After evaporation of the solvent, the crude product is purified by preparative HPLC.

Yield: 29 mg (31 μmol); 19%. **Analytic RP-HPLC:** $t_R = 6.96$ min (method 1, 220 nm).

The product was characterized after the last step, the coupling of Boc-Ala-OH to the *N*-terminus.

Boc-Ala-D-Val[4Tz]Phe-D-Leu[4Tz]Phe-D-Leu[4Tz]Val-OAll (21).



Boc-D-Val[4Tz]Phe-D-Leu[4Tz]Phe-D-Leu[4Tz]Val-OAll (**20**) (23.3 mg; 25.0 μmol; 1.0 eq) is dissolved in 1 mL of a 1:1 mixture of DCM and HCl (4 M in dioxane) and stirred

for 2 h at rt. After complete cleavage of the Boc-group, the free amine is evaporated to dryness. In a second flask, Boc-Ala-OH (9.5 mg; 50 μmol; 2.0 eq) and HOAt (7.5 mg; 55 μmol; 2.2 eq) are dissolved in DCM (2 mL, dry). After addition of DIC (8.5 μL; 55 μmol; 2.2 eq), the mixture is stirred 5 min at RT for preactivation and is then added to the free amine, followed by TMP (16.5 μL; 125 μmol; 5.0 eq). This solution is left stirring over night

7. Experimental section

at rt. After evaporation of the solvent, the crude product is purified by preparative HPLC.

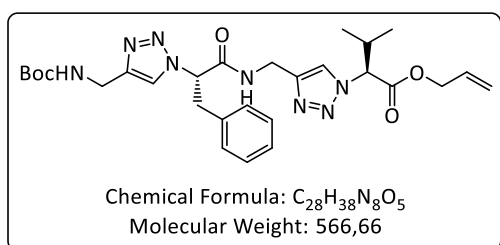
Yield: 15.4 mg (15.1 μmol); 60%. **Analytic RP-HPLC:** t_{R} = 6.6 min (method 1, 220 nm).

HR-MS (ESI): m/z^{-1} = 1020.6126 $[\text{M}+\text{H}]^+$ (calc. 1020.6142).

$^1\text{H-NMR}$ (600 MHz, $\text{DMSO-}d_6$): δ [ppm] = 8.92 (d, 3J = 8.6 Hz, 1H, **NH**), 8.89 (d, 3J = 8.7 Hz, 1H, **NH**) 8.19 (s, 1H, **Tz2-H**), 8.14 (s, 1H, **Tz1-H**), 8.00 (s, 1H, **Tz3-H**), 7.88 (d, 3J = 9.2 Hz, 1H, **Val2-NH**), 7.23–7.14 (m, 10H, **Ph-H**) 6.89 (d, 3J = 7.6 Hz, 1H, **Boc-NH**), 5.86 (ddt, 3J = 17.2, 10.6, 5.5 Hz, 1H, **-CH=C**), 5.63–5.58 (m, 2H, **Phe3+Phe5-H $^{\alpha}$**), 5.26 (d, 3J = 8.4 Hz, 1H, **Val7-H $^{\alpha}$**), 5.23 (dd, 3J = 17.2, 2J = 1.7 Hz, 1H, **=CH E**), 5.18 (dd, 3J = 10.6, 2J = 1.5 Hz, 1H, **=CH Z**), 5.01–4.96 (m, 2H, **Leu4+Leu6-H $^{\alpha}$**), 4.81 (dd, 3J = 9.2, 6.4 Hz, 1H, **Val2-H $^{\alpha}$**), 4.68–4.61 (m, 2H, **O-CH $_2$ -**), 4.03 (dq, 1H, 3J = 7.6, 7.2 Hz, **Ala1-H $^{\alpha}$**), 3.40–3.26 (m, 4H, **Bzl-H**), 2.50 (m, 1H, **Val7-CH(Me) $_2$**), 2.01 (m, 1H, **Val2-CH(Me) $_2$**), 1.58–1.50 (m, 4H, **Leu4+Leu6-CH $_2$**), 1.36 (s, 9H, **tBu-H**), 1.28–1.14 (m, 2H, **Leu4+Leu6-CH(Me) $_2$**), 1.18 (d, 3J = 7.2 Hz, 1H, **Ala1-H $^{\beta}$**), 0.91 (d, 3J = 6.7 Hz, 3H, **Val7-CH $_3$**), 0.82–0.78 (m, 12H, **Leu4+Leu6-CH $_3$**), 0.75 (d, 3J = 6.7 Hz, 3H, **Val2-CH $_3$**), 0.72 (d, 3J = 6.8 Hz, 3H, **Val7-CH $_3$**), 0.70 (d, 3J = 6.8 Hz, 3H, **Val2-CH $_3$**).

$^{13}\text{C}\{^1\text{H}\}$ -NMR (151 MHz, $\text{DMSO-}d_6$): δ [ppm] = 172.77 (**Ala1-C**), 168.32 (**Val7-C**), 166.96 (**Phe-C**), 166.94 (**Phe-C**), 155.42 (**tBuOC**), 148.53 (**Tz3-C $^{\text{quart}}$**), 148.04 (**Tz1-C $^{\text{quart}}$**), 147.33 (**Tz2-C $^{\text{quart}}$**), 136.27 (**Phe-C $^{\gamma}$**), 136.22 (**Phe-C $^{\gamma}$**), 132.16 (**CH $_2$ -C=**), 129.50 (**Phe-C $^{\alpha\gamma}$**), 129.48 (**Phe-C $^{\alpha\gamma}$**), 128.62 (**Phe-C $^{\alpha\gamma}$**), 127.20 (**Phe-C $^{\alpha\gamma}$**), 122.46 (**Tz3-CH**), 122.28 (**Tz2-CH**), 121.82 (**Tz1-CH**), 118.91 (**=CH $_2$**), 78.49 (**-C(Me) $_3$**), 67.96 (**Val7-C $^{\alpha}$**), 66.14 (**O-CH $_2$ -**), 64.17 (**Phe3+Phe5-C $^{\alpha}$**), 50.82 (**Val2-C $^{\alpha}$**), 50.38 (**Ala1-C $^{\alpha}$**), 44.21 (**Leu-C $^{\beta}$**), 44.05 (**Leu-C $^{\beta}$**), 43.90 (**Leu4+Leu6-C $^{\alpha}$**), 38.81 (**Bzl-C**), 38.41 (**Bzl-C**), 32.80 (**Val2-CH(Me) $_2$**), 31.08 (**Val7-CH(Me) $_2$**), 28.63 (**-C(CH $_3$) $_3$**), 24.56 (**Leu4-CH(CH $_3$) $_2$**), 24.46 (**Leu6-CH(CH $_3$) $_2$**), 23.09 (**Leu4-CH $_3$**), 22.97 (**Leu4-CH $_3$**), 22.37 (**Leu6-CH $_3$**), 22.26 (**Leu6-CH $_3$**), 19.34 (**Val2-CH $_3$**), 19.24 (**Val7-CH $_3$**), 18.84 (**Ala1-C $^{\beta}$**), 18.68 (**Val7-CH $_3$**), 18.41 (**Val2-CH $_3$**).

Boc-Gly[4Tz]Phe-Gly[4Tz]Val-OAll (22).



Boc-Gly[4Tz]Val-OAll (**18e**) (170 mg; 0.502 mmol; 1.0 eq) is dissolved in 4 mL of a 1:1 mixture of DCM and HCl (4 M in dioxane) and stirred for 2 h at rt. After complete cleavage of the Boc-group, the free amine is evaporated to dryness. In

a second flask, Boc-Gly[4Tz]Phe-OH (0.19 g; 0.55 mmol; 1.1 eq; synthesized from **18d** according to **GP5**) and HOAt (82 mg; 0.60 mmol; 1.2 eq) are dissolved in DCM (5 mL, dry). After addition of EDCxHCl (115 mg; 0.600 mmol; 1.2 eq), the mixture is stirred 5 min at RT

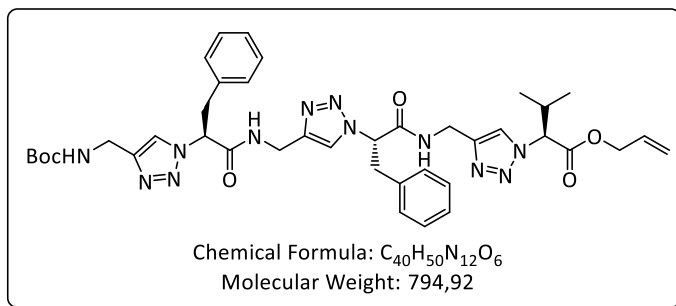
for preactivation and is then added to the free amine, followed by TMP (0.33 mL; 2.5 mmol; 5.0 eq). This solution is left stirring over night at rt. After evaporation of the solvent, the crude product is dissolved in EtOAc (100 mL) and washed: 5% KHSO₄ (3x50 mL), saturated NaHCO₃ (3x50 mL), brine (1x50 mL) and dried over MgSO₄. The organic phase is concentrated under vacuum, the crude product obtained as a colourless solid.

Yield: 269 mg (187 μmol); 94% crude. **R_f** (PE/EtOAc 1:3)= 0.16.

MS (ESI): m/z= 589.3 [M+Na]⁺.

¹H-NMR (600 MHz, DMSO-d₆): δ [ppm]= 9.02 (dd, ³J= 5.5, 5.5 Hz, 1H, Gly3-NH), 8.04 (s, 1H, Tz1-H), 7.91 (s, 1H, Tz2-H), 7.26 (dd, ³J= 6.0, 6.0 Hz, 1H, Boc-NH), 7.23-7.11 (m, 5H, Ph-H), 5.89 (dddd, ³J= 17.2, 10.7, 5.5, 5.5 Hz, 1H, CH₂-CH=), 5.58 (dd, ³J= 9.4, 6.2 Hz, 1H, Phe2-H^α), 5.29 (d, ³J= 8.4 Hz, 2H, Val4-H^α), 5.28 (dd, ³J= 17.2, ²J= 1.4 Hz, CH=CH^H), 5.22 (dd, ³J= 10.5, ²J= 1.4 Hz, 1H, CH=CH^H), 4.69-4.61 (m, 2H, O-CH₂), 4.40-4.30 (m, 2H, Gly3-H^α), 4.16-4.10 (m, 2H, Gly1-H^α), 3.40 (dd, ²J= 14.1, ³J= 6.2 Hz, Phe2-H^β), 3.32 (dd, ²J= 14.1, ³J= 9.4 Hz, 1H, Phe2-H^β), 2.53 (m, 1H, Val4-H^α), 1.39 (s, 9H, C(CH₃)₃), 0.94 (d, ³J= 6.7 Hz, 3H, Val4-H^γ), 0.76 (d, ³J= 6.7 Hz, 3H, Val4-H^γ).

Boc-Gly[4Tz]Phe-Gly[4Tz]Phe-Gly[4Tz]Val-OAll (23).



Boc-Gly[4Tz]Phe-Gly[4Tz]Val-OAll (22) (130 mg; 0.229 mmol; 1.0 eq) is dissolved in 2 mL of a 1:1 mixture of DCM and HCl (4 M in dioxane) and stirred for 2 h at rt. After complete cleavage of the Boc-

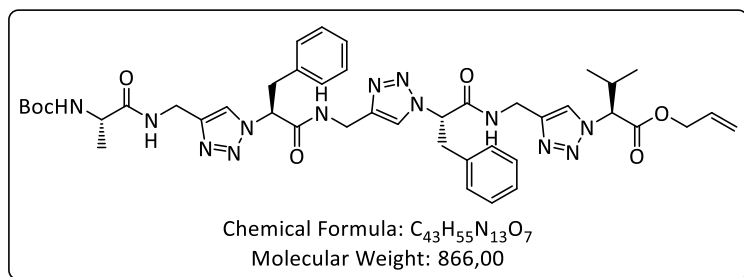
group, the free amine is evaporated to dryness. In a second flask, Boc-Gly[4Tz]Phe-OH (88 mg; 0.25 mmol; 1.1 eq; synthesized from **18d** according to **GP5**) and HOAt (38 mg; 0.28 mmol; 1.2 eq) are dissolved in DCM (5 mL, dry). After addition of EDCxHCl (54 mg; 0.28 mmol; 1.2 eq), the mixture is stirred 5 min at RT for preactivation and is then added to the free amine, followed by TMP (152 μL; 1.15 mmol; 5.0 eq). This solution is left stirring over night at rt. After evaporation of the solvent, the crude product is dissolved in EtOAc (100 mL) and washed: 5% KHSO₄ (3x50 mL), saturated NaHCO₃ (3x50 mL), brine (1x50 mL) and dried over MgSO₄. The organic phase is concentrated under vacuum, the crude product is purified by preparative HPLC. **Yield:** 120 mg (0.151 mmol); 66%.

Analytic RP-HPLC: t_R= 5.52 min (method 1, 220 nm). **MS (ESI):** m/z= 817.3 [M+Na]⁺.

7. Experimental section

The product was characterized after the last step, the coupling of Boc-Ala-OH to the *N*-terminus.

Boc-Ala-Gly[4Tz]-Phe-Gly[4Tz]-Phe-Gly[4Tz]-Val-OAll (24).



Boc-Gly[4Tz]-Phe-Gly[4Tz]-Phe-Gly[4Tz]-Val-OAll (23) (50 mg; 63 μmol; 1.0 eq) is dissolved in 2 mL of a 1:1 mixture of DCM and HCl (4 M in dioxane) and stirred for 2 h

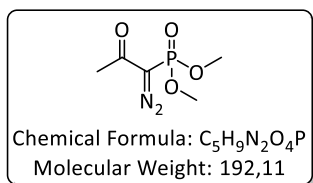
at rt. After complete cleavage of the Boc-group, the free amine is evaporated to dryness. In a second flask, Boc-Ala-OH (24 mg; 126 μmol; 2.0 eq) and HOAt (19 mg; 140 μmol; 2.2 eq) are dissolved in DCM (5 mL, dry). After addition of DIC (22 μL; 140 μmol; 2.2 eq), the mixture is stirred 5 min at RT for preactivation and is then added to the free amine, followed by TMP (42 μL; 0.32 μmol; 5.0 eq). This solution is left stirring over night at rt. After evaporation of the solvent, the crude product is purified by preparative HPLC.

Yield: 41 mg (47 μmol); 75%. **Analytic RP-HPLC:** t_R = 5.3 min (method 1, 220 nm).

HR-MS (ESI): m/z^1 = 866.4413 [M+H]⁺ (calc. 866.44202).

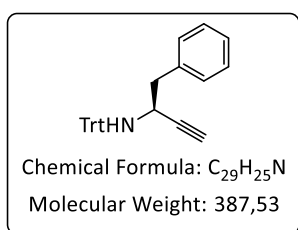
¹H-NMR (600 MHz, DMSO-*d*₆): δ [ppm] = 9.04 (dd, 1H, ³*J* = 5.6, 5.6 Hz, Gly6-NH), 9.00 (dd, 1H, ³*J* = 5.6, 5.4 Hz, Gly4-NH), 8.26 (dd, 1H, ³*J* = 6.0, 5.9 Hz, Gly2-NH), 8.08 (s, 1H, Tz1-H), 8.04 (s, 1H, Tz2-H), 7.94 (s, 1H, Tz3-H), 7.25-7.08 (m, 10H, PhH), 6.91 (d, ³*J* = 7.4 Hz, 1H, Boc-NH), 5.90 (m, 1H, -CH=CH₂), 5.62-5.57 (m, 2H, Phe3+Phe5-H^α), 5.30 (d, ³*J* = 8.4 Hz, 1H, Val-H^α), 4.70-4.62 (m, 2H, CH₂-CH=), 4.41-4.24 (m, 6H, Gly-H^α), 3.97 (dq, 1H, ³*J* = 7.4, 7.2 Hz, Ala1-H^α), 3.42-3.27 (m, 4H, Phe-H^β) 2.54 (dq, ³*J* = 8.4, 6.7, 6.5 Hz, 1H, Val-H^β), 1.38 (s, 9H, C(CH₃)₃), 1.17 (d, ³*J* = 7.2 Hz, 3H, Ala1-H^β), 0.94 (d, ³*J* = 6.5 Hz, 3H, Val-H^γ), 0.77 (d, ³*J* = 6.7 Hz, 3H, Val-H^γ).

¹³C{¹H}-NMR (151 MHz, DMSO-*d*₆): δ [ppm] = 173.15 (Ala1-C), 168.33 (Val7-C), 167.73 (2C, Phe3+Phe5-C), 155.51 (^tBuO-C), 145.26 (Tz1-C), 144.25 (Tz3-C), 144.03 (Tz2-C), 136.52 (Phe-C^γ), 136.49 (Phe-C^γ), 132.21 (CH₂-CH=), 129.25 (Phe-C), 128.24 (Phe-C), 127.24 (Phe-C), 123.49 (Tz3-CH), 122.66 (Tz2-CH), 122.40 (Tz1-CH), 119.06 (=CH₂), 78.44 (-C(Me)₃), 67.98 (Val7-C^α), 66.23 (O-CH₂-), 64.16 (2C, Phe3+Phe5-C^α), 50.13 (Ala1-C^α), 38.29 (Phe-C^β), 38.08 (Phe-C^β), 34.84 (Gly-C^α), 34.83 (Gly-C^α), 34.80 (Gly-C^α), 31.12 (Val7-C^β), 28.68 (C(CH₃)₃), 19.26 (Val7-C^γ), 18.71 (Ala1-C^β).

Dimethyl (1-diazo-2-oxopropyl)phosphonate (25).

p-ABSA (**35**) (10.5 g; 43.7 mmol; 1.2 eq) is suspended in ACN (360 mL). After addition of DOP (5.03 mL; 36.4 mmol; 1.0 eq) and K₂CO₃ (10.1 g; 72.8 mmol; 2.0 eq) the reaction mixture is left to stir overnight. After filtration, the filtrate is concentrated and the product purified by flash chromatography (gradient: PE/EtOAc 2:1 to 1:2 to 0:1). **Yield:** 5.71 g (29.7 mmol); 82%. **R_f** (EtOAc)= 0.43.

¹H-NMR (500 MHz, CDCl₃): δ [ppm]= 3.88 (s, 3H, OCH₃), 3.85 (s, 3H, OCH₃), 2.29 (s, 3H, CH₃).

(S)-1-Phenyl-N-tritylbut-3-yn-2-amine ((S)-31).

L-Phenylalaninol (28): H-L-Phe-OH (5.00 g; 30.3 mmol) is suspended in THF (60 mL; dry) and cooled to 0°C. LiAlH₄ (2.1 eq; 64.0 mmol; 2.43 g) is added portion-wise. After stirring the reaction mixture for 2 h at 0°C, it is stirred at reflux overnight. Afterwards the suspension is diluted with Et₂O (50 mL) and cooled to 0°C. Water (50 mL) is added dropwise to quench remaining LiAlH₄. The salts are removed by filtration and the filtrate concentrated under vacuum. The basic aqueous slurry is extracted with EtOAc (3x50 mL). The combined organic phases are dried over MgSO₄ and concentrated to obtain (S)-Phenylalaninol as a yellow solid. **Yield:** 4.02 g (26.6 mmol); 88%.

¹H-NMR (500 MHz; CDCl₃): δ [ppm]= 7.28-7.09 (m, 5H, Ph-**H**), 3.57 (dd, ²J=10.6, ³J= 3.9 Hz, 1H, CHH-OH), 3.31 (dd, ²J= 10.6, ³J= 7.2 Hz, 1H, CHH-OH), 3.05 (dddd, ³J= 8.6, 7.2, 5.2, 3.9 Hz, 1H, H^α), 2.73 (dd, ²J= 13.5, ³J= 5.3 Hz, 1H, H^β), 2.46 (dd, ²J= 13.5, ³J= 8.6 Hz, 1H, H^β).

Trt-L-Phenylalaninol ((S)-29): L-Phenylalaninol ((S)-28) (1.00 g; 6.61 mmol) is dissolved in DCM (13 mL) and cooled to 0°C. After the addition of DIPEA (1.2 mL; 6.6 mmol; 1.0 eq) and Trt-Cl (1.84 g; 6.61 mmol; 1.0 eq; dissolved in 7 mL DCM) the solution is left to stir overnight at rt. The reaction mixture is diluted with DCM (100 mL) and washed with H₂O (3x50 mL), brine (1x50 mL), dried over MgSO₄ and concentrated under vacuum. **Yield:** 2.23 g (5.67 mmol); 86%. **R_f** (PE/EtOAc 10:1)= 0.13.

¹H-NMR (300 MHz; CDCl₃): δ [ppm]= 7.63-7.54 (m, 5H, Ph-**H**), 7.37-7.14 (m, 13H, Ph-**H**), 6.99-6.91 (m, 2H, Ph-**H**), 3.15 (dd, ²J= 10.9, ³J= 2.8 Hz, 1H, CHHOH) 2.96 (dd, ²J= 10.9, ³J= 4.1 Hz, 1H, CHHOH), 2.84 (dddd, ³J= 9.5, 4.7, 4.1, 2.8 Hz, 1H, H^α), 2.54 (dd, ²J= 13.1, ³J= 9.5 Hz, 1H, H^β), 2.31 (dd, ²J= 13.0, ³J= 4.7 Hz, 1H, H^β).

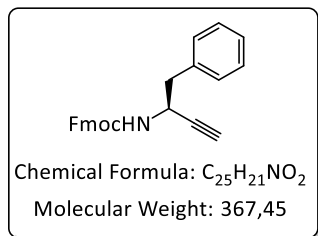
Trt-I-Phe≡ **((S)-31)**: The aldehyde **((S)-30)** was synthesized utilizing Swern's procedure,⁵³ starting from Trt-Phenylalaninol **((S)-29)** (2.23 g; 5.67 mmol). R_f (PE/EtOAc 10:1)= 0.43.

The crude aldehyde was immediately used for the following Bestmann-Ohira reaction: DOP (940 μ L; 1.13 g; 6.80 mmol; 1.2 eq), K_2CO_3 (17 mmol; 2.4 g; 3 eq) and p-ABSA (1.63 g; 6.80 mmol; 1.2 eq) are dissolved in acetonitrile (85 mL; dry) and stirred at rt overnight. The aldehyde **(30)** obtained above is dissolved in DCM (3 mL; dry) and added to the suspension, followed by MeOH (17 mL; dry), the reaction mixture is once more stirred overnight. The solvent is removed by rotary evaporator, the crude product dissolved in EtOAc (100 mL) and washed with H_2O (3x50 mL), brine (1x50 mL), dried over $MgSO_4$ and concentrated under vacuum. The crude propargylamine is purified by silica chromatography (PE/EtOAc 20:1, containing 1% TEA).

Yield: 1.81 g (4.67 mmol); 82% over two steps. R_f (PE/EtOAc 10:1)= 0.63.

1H -NMR (300 MHz; $CDCl_3$): δ [ppm]= 7.62-7.53 (m, 8H, Ph-**H**), 7.37-7.17 (m, 12H, Ph-**H**), 3.55 (ddd, $^3J= 7.7, 5.8, ^4J= 2.2$ Hz, 1H, **H a**), 2.76-2.72 (m, 2H, **H b**), 1.87 (d, $^4J= 2.1$ Hz, 1H, **CCH**).

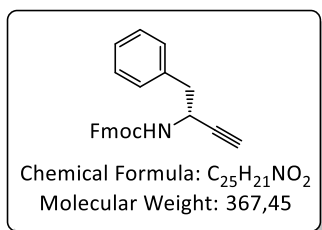
(9H-Fluoren-9-yl)methyl (S)-(1-phenylbut-3-yn-2-yl)carbamate ((S)-33)



Trt-Phe≡ **((S)-31)** (370 mg; 0.955 mmol) is dissolved in DCM/TFA/MeOH (92.5/2.5/5) (10 mL) and stirred for 1.5 h at rt. After full conversion of the starting material, the solvent is removed under vacuum, by co-evaporation with toluene. The residual free amine is Fmoc protected using **GP7**, starting the procedure by dissolving the residual material in THF/ H_2O (1:1) (10 mL).

Yield: 232 mg (0.631 mmol); 66% over two steps. R_f (PE/EtOAc 10:1)= 0.26.

1H -NMR (500 MHz; $CDCl_3$): δ [ppm]= 7.79-7.75 (m, 2H, **H Ar**), 7.59-7.54 (m, 2H, **H Ar**), 7.43-7.38 (m, 2H, **H Ar**), 7.34-7.23 (m, 7H, **H Ar** , Ph-**H**), 4.92 (d, $^3J= 7.5$ Hz, 1H, **NH**), 4.76 (m, 1H, **H a**), 4.46 (dd, $^2J= 10.6, ^3J= 7.1$ Hz, 1H, CH-**CHH**), 4.37 (dd, $^2J= 10.6, ^3J= 6.9$ Hz, 1H, CH-**CHH**), 4.21 (dd, $^3J= 7.1, 6.9$ Hz, 1H, **CHCH $_2$**), 3.06-2.92 (m, 2H, **H b**), 2.31 (d, $^4J= 2.4$ Hz, 1H, **CCH**).

(9H-Fluoren-9-yl)methyl (R)-(1-phenylbut-3-yn-2-yl)carbamate ((R)-33).

D-Phenylalaninol ((R)-28): H-D-Phe-OH (5.00 g; 30.3 mmol) is suspended in THF (60 mL; dry) and cooled to 0°C. $LiAlH_4$ (2.1 eq; 64.0 mmol; 2.43 g) is added portion-wise. After stirring the reaction mixture for 2 h at 0°C, it is stirred at reflux overnight. Afterwards the suspension is diluted with Et_2O (50 mL) and cooled to 0°C. Water (50 mL) is added dropwise to quench remaining $LiAlH_4$. The salts are removed by filtration and the filtrate concentrated under vacuum. The basic aqueous slurry is extracted with $EtOAc$ (3x50 mL). The combined organic phases are dried over $MgSO_4$ and concentrated to obtain (R)-Phenylalaninol as a yellow solid.

Yield: 3.09 g (20.4 mmol); 67%.

1H -NMR (500 MHz; $CDCl_3$): δ [ppm]= 7.35-7.31 (m, 2H, Ph-**H**), 7.27-7.20 (m, 3H, Ph-**H**), 3.68 (dd, $^2J= 10.7$, $^3J= 3.8$ Hz, 1H, **CHH**-OH), 3.43 (dd, $^2J= 10.7$, $^3J= 7.2$ Hz, 1H, **CHH**-OH), 3.18 (dddd, $^3J= 8.5$, 7.2, 5.5, 3.8 Hz, 1H, **H α**), 2.83 (dd, $^2J= 13.5$, $^3J= 5.5$ Hz, 1H, **H β**), 2.60 (dd, $^2J= 13.5$, $^3J= 8.5$ Hz, 1H, **H β**).

Trt-D-Phenylalaninol ((R)-29): D-Phenylalaninol (1.50 g; 9.92 mmol) is dissolved in DCM (15 mL) and cooled to 0°C. After the addition of TEA (2.75 mL; 19.8 mmol; 2.0 eq) and Trt-Cl (2.77 g; 9.92 mmol; 1.0 eq) the solution is left to stir overnight at rt. The reaction mixture is diluted with DCM (15 mL) and washed with H_2O (2x20 mL), brine (1x20 mL), dried over $MgSO_4$ and concentrated under vacuum.

Yield: 3.67 g (9.33 mmol); 94%. **R_f** (PE/ $EtOAc$ 10:1)= 0.13.

1H -NMR (500 MHz; $CDCl_3$): δ [ppm]= 7.58-7.55 (m, 5H, Ph-**H**), 7.31-7.25 (m, 6H, Ph-**H**), 7.22-7.12 (m, 7H, Ph-**H**), 6.95-6.92 (m, 2H, Ph-**H**), 3.12 (dd, $^2J= 10.9$, $^3J= 2.7$ Hz, 1H, **CHH**-OH), 2.93 (dd, $^2J= 10.9$, $^3J= 4.1$ Hz, 1H, **CHH**-OH), 2.82 (dddd, $^3J= 9.6$, 4.7, 4.1, 2.7 Hz, 1H, **H α**), 2.52 (dd, $^2J= 13.1$, $^3J= 9.6$ Hz, 1H, **H β**), 2.29 (dd, $^2J= 13.1$, $^3J= 4.7$ Hz, 1H, **H β**).

Trt-D-Phe≡ ((R)-31): The aldehyde ((R)-30) was synthesized utilizing Swern's procedure,⁵³ starting from Trt-Phenylalaninol (3.66 g; 9.30 mmol). **R_f** (PE/ $EtOAc$ 10:1)= 0.44. The crude aldehyde (3.37 g; 8.61 mmol; 93%) was immediately used for the following Bestmann-Ohira reaction: DOP (1.4 mL; 10 mmol; 1.2 eq), K_2CO_3 (3.6 g; 26 mmol; 3 eq) and *p*-ABSA (2.48 g; 10.3 mmol; 1.2 eq) are dissolved in acetonitrile (103 mL; dry) and stirred at rt overnight. The aldehyde obtained above is dissolved in DCM (10 mL; dry) and added to the suspension, followed by MeOH (20 mL; dry), the reaction mixture is once more stirred overnight. The solvent is removed by rotary evaporator, the

7. Experimental section

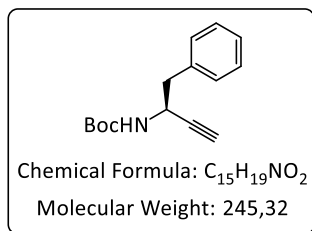
crude product dissolved in EtOAc (100 mL) and washed with H₂O (3x50 mL), brine (1x50 mL), dried over MgSO₄ and concentrated under vacuum. R_f (PE/EtOAc 10:1) = 0.64.

Fmoc-D-Phe \equiv ((**R**)-**33**): The crude propargylamine is dissolved in DCM/TFA/TES 95:2.5:2.5 (100 mL) and stirred 30 min at rt. Saturated NaHCO₃ solution (50 mL) is added and the organic phase dried over MgSO₄ and concentrated under vacuum. The crude amine is dissolved in ACN/H₂O 1:1 (60 mL), Fmoc-OSu (3.4 g; 10 mmol; 1.2 eq) and NaHCO₃ (2.89 g; 34.4 mmol; 4 eq) are added and the reaction mixture left to stir overnight at rt. The acetonitrile is removed by rotary evaporator and the aqueous slurry extracted with Et₂O (1x50 mL), the organic phase is dried over MgSO₄ and concentrated in vacuum, the crude propargylamine is purified by column chromatography (PE/EtOAc 10:1).

Yield: 32% over four steps. R_f (PE/EtOAc 10:1) = 0.13.

¹H-NMR (500 MHz; CDCl₃): δ [ppm] = 7.82-7.78 (m, 2H, **H^{Ar}**), 7.62-7.57 (m, 2H, **H^{Ar}**), 7.45-7.41 (m, 2H, **H^{Ar}**), 7.36-7.24 (m, 7H, **H^{Ar}**, Ph-**H**), 4.94 (d, ³*J* = 6.8 Hz, 1H, **NH**), 4.79 (m, 1H, **H^α**), 4.50 (m, 1H, **CHHO**), 4.40 (m, 1H, **CHHO**), 4.23 (dd, ³*J* = 6.9, 6.9 Hz, 1H, **CH-CH₂O**), 3.11-2.94 (m, 2H, **H^β**), 2.34 (d, ⁴*J* = 2.3 Hz, 1H, **CCH**).

O-tert-Butyl (S)-(1-phenylbut-3-yn-2-yl)carbamate (34).

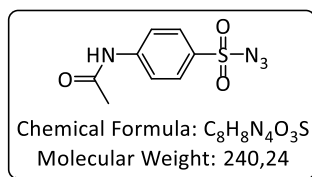


Trt-Phe \equiv ((**S**)-**31**) (1.15 g; 2.97 mmol) is dissolved in DCM/TFA/MeOH (2/1/1) (16 mL) and stirred for 30 min at rt. After full conversion of the starting material, the solvent is removed under vacuum, by co-evaporation with toluene. The residual free amine is Boc protected using **GP3**, starting the procedure by dissolving the residual material in THF/ H₂O (1:1) (30 mL).

Yield: 415 mg (1.69 mmol); 57% over two steps. R_f (PE/EtOAc 10:1) = 0.31.

¹H-NMR (500 MHz; CDCl₃): δ [ppm] = 7.33-7.25 (m, 5H, Ph-**H**), 4.74-4.61 (m, 2H, **H^α**, **NH**), 3.04-2.91 (m, 2H, **H^β**), 2.28 (m, 1H, **CCH**), 1.43 (s, 9H, C(**CH**)₃).

4-Acetamidobenzenesulfonyl azide (35).

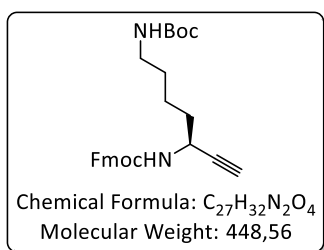


4-Acetamidobenzenesulfonyl chloride (11.7 g; 50.0 mmol) is dissolved in DCM (90 mL; dry) and cooled to 0°C. Tetrabutylammoniumchloride (28 mg; 0.1 mmol; 0.2 mol%) is added followed by a solution of sodium azide (4.9 g; 75 mmol; 1.5 eq) in H₂O (20 mL), the reaction mixture is left to stir overnight. After separation of the

phases, the organic phase is washed: H₂O (3x90 mL), brine (1x90 mL), dried over Na₂SO₄ and concentrated in vacuum. **Yield:** 10.8 g (44.9 mmol); 90%.

¹H-NMR (500 MHz; CDCl₃): δ [ppm]= 7.91 (d, ³J= 8.9 Hz, 2H, **H^{Ar}**), 7.80 (d, ³J= 8.9 Hz, 2H, **H^{Ar}**), 7.77 (s, 1H, **NH**), 2.27 (s, 3H, **CH₃**).

(9H-Fluoren-9-yl)methyl tert-butyl hept-6-yne-1,5-diyl(S)-dicarbamate (39).



Fmoc-Lys(Boc)-ol (36): Prepared according to Hwang *et al.*¹³³ starting from Fmoc-Lys(Boc)-OH (1.4 g; 3.0 mmol). **Yield:** 1.2 g (2.6 mmol); 87% (Lit.: 88%).

Trt-Lys(Boc)-ol (37): The Fmoc deprotection was realised according to Sheppeck II *et al.*¹³⁴ with octanethiol, starting from Fmoc-Lys(Boc)-ol (1.07 g; 2.35 mmol), the product was isolated by trituration as described in the literature and used without purification for the next step. Trityl protection: The residual oil is dissolved in DCM (20 mL; dry), TEA (0.98 mL; 7.1 mmol; 3.0 eq) is added followed by Tritylchloride (655 mg; 2.35 mmol; 1.0 eq) and the reaction mixture stirred for 2 h at rt. Afterwards it is concentrated under vacuum and the product purified by column chromatography (PE/EtOAc 5:1, containing 1% TEA).

Yield: 461 mg (0.97 mmol); 41% over two steps. **R_f** (PE/EtOAc 5:1)= 0.17

Trt-Lys(Boc)-al: The aldehyde was synthesized utilizing Swern's procedure,⁵³ starting from Trt-Lys(Boc)-ol (37) (455 mg; 0.96 mmol) and used without further purification for the next step.

Trt-Lys(Boc)≡ (38): DOP (159 μL; 1.15 mmol; 1.2 eq), K₂CO₃ (398 mg; 2.88 mmol; 3 eq) and *p*-ABSA (277 mg; 1.15 mmol; 1.2 eq) are dissolved in acetonitrile (15 mL; dry) and stirred at rt overnight. The aldehyde obtained above is dissolved in DCM (3 mL; dry) and added to the suspension, followed by MeOH (3 mL; dry), the reaction mixture is once more stirred overnight. The solvent is removed by rotary evaporator, the crude product dissolved in EtOAc (50 mL) and washed with H₂O (3x25 mL), brine (1x25 mL), dried over MgSO₄, concentrated under vacuum and purified by column chromatography (PE/EtOAc 20:1, containing 1% TEA). **Yield:** 239 mg (0.51 mmol), 53% over two steps.

R_f (PE/EtOAc 10:1 containing 1% TEA)= 0.25.

¹H-NMR (500 MHz, CDCl₃): δ [ppm]= 7.50-7.45 (m, 5H, Ph-**H**), 7.23-7.17 (m, 7H, Ph-**H**), 7.14-7.09 (m, 3H), 4.37 (m, 1H, Boc-**NH**), 3.17 (m, 1H, **H^α**), 3.00-2.93 (m, 2H, **H^β**), 1.76 (d, ⁴J= 2.1 Hz, 1H, C**H**), 1.37 (s, 9H, C(**CH₃**)₃), 1.33-1.15 (m, 6H, **CH₂**).

7. Experimental section

Fmoc-Lys(Boc)≡ (39): The trityl protected propargylamine (239 mg; 0.51 mmol) is dissolved in DCM/TFA/MeOH 92.5:2.5:5 (100 mL) and stirred 1.5 h at rt. After full conversion, the reaction mixture is concentrated under vacuum by co-evaporation with toluene. The crude amine is dissolved in THF/H₂O 1:1 (5.5 mL), Fmoc-OSu (258 mg; 0.77 mmol; 1.5 eq) and NaHCO₃ (171 mg; 2.04 mmol; 4 eq) are added and the reaction mixture left to stir overnight at rt. The reaction mixture is diluted with EtOAc (50 mL) and washed: 5% KHSO₄ (3x25 mL); NaHCO₃ (3x25 mL) and brine (1x25 mL). The organic phase is dried over MgSO₄ and concentrated under vacuum, the crude propargylamine is purified by column chromatography (PE/EtOAc 3:1).

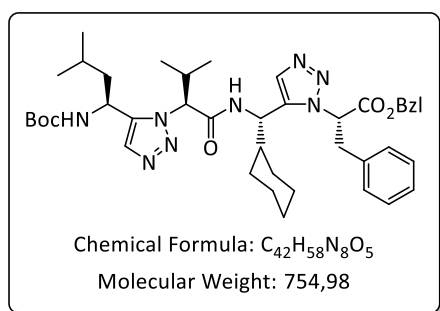
Yield: 164 mg (0.37 mmol), 73% over two steps. **R_f** (PE/EtOAc 3:1)= 0.36.

MS (ESI): m/z= 471.2 [M+Na]⁺.

¹H-NMR (500 MHz, CDCl₃): δ [ppm]= 7.80-7.77 (m, 2H, **H^{Ar}**), 7.63-7.60 (m, 2H, **H^{Ar}**), 7.44-7.40 (m, 2H, **H^{Ar}**), 7.36-7.31 (m, 2H, **H^{Ar}**), 5.09 (d, ³J= 8.6 Hz, 1H, Fmoc-**NH**), 4.60 (m, 1H, Boc-**NH**), 4.48 (m, 1H, **H^α**), 4.46-4.42 (m, 2H, CHCH₂O), 4.24 (dd, ³J= 6.9, 6.9 Hz, 1H, CHCH₂O), 3.18-3.07 (m, 2H, **H^ε**), 2.32 (d, ⁴J= 2.3 Hz, 1H, CCH), 1.76-1.69 (m, 2H, **H^β**), 1.57-1.41 (m, 13H, C(CH₃)₃), **H^γ**, **H^δ**).

¹³C{¹H}-NMR (151 MHz, CDCl₃) δ [ppm]= 156.01 (NCO₂^tBu), 155.44 (NCO₂CH₂), 143.85 (**C^{Ar}**), 143.78 (**C^{Ar}**), 141.32 (2C; **C^{Ar}**), 127.71 (2C; CH^{Ar}), 127.06 (2C; CH^{Ar}), 125.04 (CH^{Ar}), 125.01 (CH^{Ar}), 119.98 (2C; CH^{Ar}), 82.93 (CCH), 79.16 (C(CH₃)₃), 71.56 (CCH), 66.91 (CHCH₂O), 47.20 (CHCH₂O), 43.19 (**C^α**), 40.22 (**C^ε**), 35.46 (**C^β**), 29.57 (**C^δ**), 28.43 (C(CH₃)₃), 22.66 (**C^γ**).

Boc-Leu[5Tz]Val-chGly[5Tz]Phe-OBzl (40).



Boc-chGly[5Tz]Phe-OBzl (66 mg; 0.13 mmol) is dissolved in DCM/(4 M HCl in dioxane) 1:1 (1 mL) and stirred overnight at rt. After evaporation of the solvent, the crude ammonium salt is used without further purification. Boc-Leu[5Tz]Val-OH (51 mg; 0.14 mmol; 1.1 eq), Oxyma (20 mg; 0.14 mmol; 1.1 eq) and COMU (60 mg; 0.14 mmol; 1.1 eq) are dissolved in DCM (1 mL; dry) under an argon atmosphere, after addition of *sym*-collidine (19 μL; 0.14 mmol; 1.1 eq), the reaction mixture is stirred 10 min for preactivation at rt. The crude ammonium salt is dissolved in DCM (1 mL; dry) and added dropwise to the activated acid mixture, followed by *sym*-collidine

(52 μ L; 0.39 mmol; 3.0 eq). The reaction mixture is left to stir overnight. The solvent is removed under vacuum, the crude peptidotriazolamer purified by preparative HPLC.

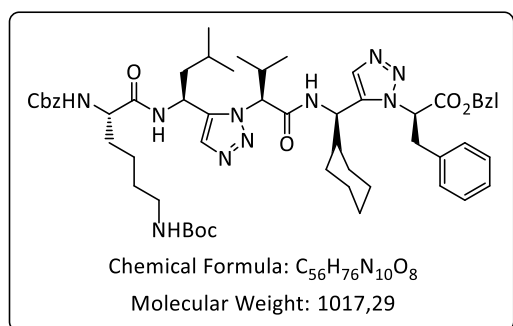
Yield: 46 mg (61 μ mol); 47%. **Analytical RP-HPLC:** t_R = 2.85 min (method 2, 254 nm).

HR-MS (ESI): m/z = 755.4582 $[M+H]^+$ (calc. 755.46029).

1H -NMR (600 MHz, DMSO- d_6): δ [ppm] = 8.36 (m, 1H, chGly3-NH), 7.62 (s, 1H, Tz1-H), 7.55 (s, 1H, Tz2-H), 7.44 (d, 3J = 8.3 Hz, 1H, Leu1-NH), 7.37-7.25 (m, 5H, Ph-H), 7.19-7.13 (m, 3H, Ph-H), 7.09-06 (m, 2H, Ph-H), 5.86 (dd, 3J = 11.5, 4.2 Hz, 1H, Phe4-H $^\alpha$), 5.28 (d, 2J = 12.9 Hz, 1H, O-CHH), 5.10 (d, 2J = 12.9 Hz, 1H, O-CHH), 5.07 (m, 1H, Leu1-H $^\alpha$), 4.81 (d, 3J = 10.6 Hz, 1H, Val2-H $^\alpha$), 4.46 (dd, 3J = 9.0, 9.0 Hz, 1H, chGly-H $^\alpha$), 3.69 (dd, 2J = 13.9, 3J = 4.1 Hz, 1H, Phe4-H $^\beta$), 3.54 (dd, 2J = 13.9, 3J = 11.5 Hz, 1H, Phe4-H $^\beta$), 2.75 (m, 1H, Val2-H $^\beta$), 1.73 (ddd, 2J = 14.0, 3J = 10.6, 4.5 Hz, 1H, Leu1-H $^\beta$), 1.63 (m, 1H, Leu1-H $^\gamma$), 1.44-1.37 (m, 1H, CH $_2$), 1.35 (s, 9H, C(CH $_3$) $_3$), 1.32-1.21 (m, 3H, chGly3-H $^\beta$, Leu1-H $^\beta$, CH $_2$), 1.15-1.09 (m, 1H, CH $_2$), 0.97-0.76 (m, 4H, CH $_2$), 0.91 (d, 3J = 6.6 Hz, 3H, Leu1-H $^\delta$), 0.89 (d, 3J = 6.6 Hz, 3H, Leu1-H $^\delta$), 0.71-0.63 (m, 1H, CH $_2$), 0.67 (d, 3J = 6.4 Hz, 3H, Val2-H $^\gamma$), 0.52-0.39 (m, 1H, CH $_2$), 0.46 (d, 3J = 6.6 Hz, 3H, Val2-H $^\gamma$), 0.00 (m, 1H, CH $_2$).

^{13}C NMR (151 MHz, DMSO- d_6) δ [ppm] = 168.11 (Phe4-C), 166.96 (Val2-C), 155.63 (tBuO-C), 141.47 (Tz1-C), 139.60 (Tz2-C), 136.52 (C Ar), 135.89 (C Ar), 132.36 (Tz1-CH), 131.44 (Tz2-CH), 129.71 (2C, CH Ar), 128.80 (2C, CH Ar), 128.37 (2C, CH Ar), 127.77 (2C, CH Ar), 127.27 (2C, CH Ar), 78.85 (C(CH $_3$) $_3$), 68.09 (Val2-C $^\alpha$), 67.22 (O-CH $_2$), 61.51 (Phe4-C $^\alpha$), 47.37 (chGly3-C $^\alpha$), 44.71 (Leu1-C $^\beta$), 43.19 (Leu1-C $^\alpha$), 37.61 (Phe4-C $^\beta$), 29.65 (Val2-C $^\beta$), 29.41 (CH $_2$), 28.56 (C(CH $_3$) $_3$), 28.18 (CH $_2$), 25.93 (CH $_2$), 25.49 (CH $_2$), 25.43 (CH $_2$), 25.05 (Leu1-C $^\gamma$), 23.61 (chGly3-C $^\beta$), 21.90 (2C, Leu-C $^\delta$), 19.58 (Val2-C $^\gamma$), 19.08 (Val2-C $^\gamma$).

Cbz-Lys(Boc)-Leu[5Tz]/Val-chGly[5Tz]/Phe-OBzl (41).



Boc-Leu[5Tz]/Val-chGly[5Tz]/Phe-OBzl (42 mg; 56 μ mol) is dissolved in DCM/(4 M HCl in dioxane) 1:1 (1 mL) and stirred for 2 h at rt. After evaporation of the solvent, the crude ammonium salt is used without further purification. Cbz-Lys(Boc)-OH (42 mg; 0.11 mmol; 2.0 eq), Oxyma (16 mg; 0.11 mmol; 2.0 eq) and COMU (47 mg;

0.11 mmol; 2.0 eq) are dissolved in DCM (1 mL; dry) under an argon atmosphere, after addition of *sym*-collidine (15 μ L; 0.11 mmol; 2.0 eq), the reaction mixture is stirred 10 min for preactivation at rt. The crude ammonium salt is dissolved in DCM (2 mL; dry) and

7. Experimental section

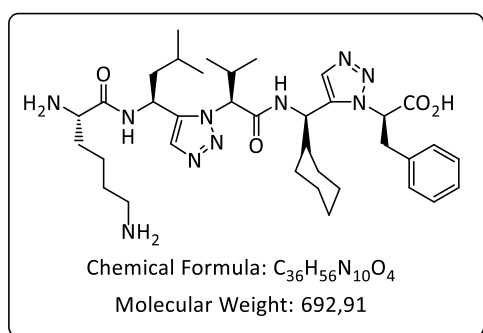
added dropwise to the activated acid mixture, followed by *sym*-collidine (15 μ L; 0.11 mmol; 2.0 eq). The reaction mixture is left to stir overnight. The solvent is removed under vacuum, the crude peptidotriazolamer purified by preparative HPLC.

Yield: 34 mg (33 μ mol); 59%. **Analytical RP-HPLC:** t_R = 3.9 min (method 2, 254 nm).

MS (ESI): m/z = 1039.7 $[M+Na]^+$.

The Peptidotriazolamer was fully characterized after cleavage of the protecting groups.

H-Lys-Leu[5Tz]Val-chGly[5Tz]Phe-OH (42a).



25 mg (25 μ mol) Cbz-Lys(Boc)-Leu[5Tz]Val-chGly[5Tz]Phe-OBzl are dissolved in 4M HCl/DCM (1:1) (1 mL) and stirred 3 h at rt. The solvent is evaporated under vacuum and the residual slurry dissolved in EtOH (2 mL). After addition of Pd/C (2.5 mg; 10 wt%), H_2 (1 atm) is passed through the solution via cannula. The Pd/C

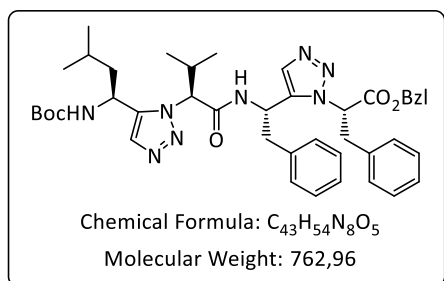
is filtered off over a short plug of silica, which is thoroughly washed with EtOH. The combined filtrate is concentrated under vacuum to obtain the peptidotriazolamer in analytically pure form. **Yield:** 15 mg (22 μ mol); 88%. **Analytical RP-HPLC:** t_R = 2.6 min (method 2, 254 nm). **HR-MS (ESI):** 715.43808 $[M+Na]^+$ (calc. 715.4384).

1H -NMR (600 MHz, MeOH- d_3): δ [ppm] = 9.05 (d, 3J = 7.7 Hz, 1H, Leu2-NH), 8.38 (d, 3J = 9.2 Hz, 1H, chGly4-NH), 7.77 (s, 1H, Tz1-H), 7.54 (s, 1H, Tz2-H), 7.21-7.14 (m, 3H, PhH), 7.09-7.04 (m, 2H, PhH), 5.66 (dd, 3J = 12.1, 3.6 Hz, 1H, Phe5- H^α), 5.46 (m, 1H, Leu2- H^α), 4.84 (d, 3J = 11.1 Hz, 1H, Val3- H^α), 4.44 (dd, 3J = 9.2, 9.2 Hz, 1H, chGly4- H^α), 3.88 (dd, 3J = 6.6, 6.6 Hz, 1H, Lys1- H^α), 3.76 (dd, 2J = 14.0, 3J = 3.5 Hz, 1H, Phe5- H^β), 3.63 (dd, 2J = 14.0, 3J = 12.0 Hz, 1H, Phe5- H^β), 2.89 (dq, 3J = 11.1, 6.7, 6.6 Hz, 1H, Val3- H^β), 2.86-2.81 (m, 2H, Lys1- H^ϵ), 1.90 (m, 1H, Leu2- H^β), 1.80 (m, 1H, Leu2- H^γ), 1.74-1.69 (m, 2H, Lys1- H^β), 1.61-1.55 (m, 2H, Lys1- H^δ), 1.52-1.46 (m, 2H, Leu2- H^β , CH_2), 1.44 (m, 1H, chGly4- H^β), 1.35 (m, 1H, CH_2), 1.32-1.25 (m, 2H, Lys1- H^γ), 1.19 (m, 1H, CH_2), 1.06 (d, 3J = 6.5 Hz, 3H, Leu2- H^δ), 1.01 (d, 3J = 6.7 Hz, 3H, Leu2- H^δ), 0.98 (d, 3J = 6.6 Hz, 3H, Val3- H^γ), 0.97-0.87 (m, 4H, CH_2), 0.81 (m, 1H, CH_2), 0.64 (d, 3J = 6.7 Hz, 3H, Val3- H^γ), 0.51 (m, 1H, CH_2), 0.00 (m, 1H, CH_2).

^{13}C NMR (151 MHz, MeOH- d_3) δ [ppm] = 169.66 (Phe5-C), 168.57 (Lys1-C), 166.84 (Val3-C), 141.17 (Tz1-C), 139.44 (Tz2-C), 136.63 (C^{Ar}), 131.76 (Tz1-CH), 130.70 (Tz2-CH), 128.93 (2C, CH^{Ar}), 128.38 (2C, CH^{Ar}), 126.77 (CH^{Ar}), 69.18 (Val3- C^α), 62.38 (Phe5-C), 52.67 (Lys1- C^α), 47.43 (chGly4- C^α), 43.93 (Leu2- C^β), 42.22 (Leu2- C^α), 40.06 (chGly4- C^β), 39.09 (Lys1- C^ϵ),

37.52 (Phe5- C^β), 30.83 (Lys1- C^β), 29.55 (Val3- C^β), 28.30 (CH_2), 26.71 (Lys1- C^δ), 25.55 (CH_2), 25.10 (CH_2), 24.97 (2C; CH_2), 24.71 (Leu2- C^γ), 22.31 (Leu2- C^δ), 21.59 (Lys1- C^γ), 20.38 (Leu2- C^δ), 18.71 (Val3- C^γ), 18.16 (Val3- C^γ).

Boc-Leu[5Tz]Val-Phe[5Tz]Phe-OBzl (43).



Boc-Phe[5Tz]Phe-OBzl (220 mg; 0.42 mmol) is dissolved in DCM/(4 M HCl in dioxane) 1:1 (5 mL) and stirred for 2 h at rt. After evaporation of the solvent, the crude ammonium salt is used without further purification. Boc-Leu-[5Tz]-Val-OH (164 mg; 0.46 mmol; 1.1 eq; synthesized according to **GP3**),

Oxyrna (1.21 eq; 0.51 mmol; 72 mg) and DIC (1.21 eq; 0.51 mmol; 79 μ L) are dissolved in DCM (3 mL; dry) under an argon atmosphere and stirred 10 min for preactivation. The crude ammonium salt is dissolved in DCM (3 mL; dry) and the activated acid mixture is added dropwise, followed by TMP (10 eq; 4.2 mmol; 555 μ L). The reaction mixture is left to stir overnight. The solvent is removed under vacuum, the residue dissolved in EtOAc and washed with 10% citric acid (2x), water (2x), saturated $NaHCO_3$ (2x), brine and dried over $MgSO_4$. The filtrate is concentrated and the crude peptidotriazolamer purified by column chromatography PE/EtOAc 1:1. **Yield:** 190 mg (0.249 mmol); 59%. R_f (PE/EtOAc 1:1)= 0.57. **HR-MS** (ESI): m/z = 382.2184 [$M+2H$] $^{2+}$ (calc. 382.21813).

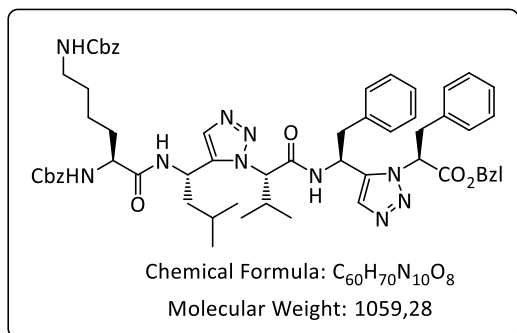
1H -NMR (600 MHz, $DMSO-d_6$): δ [ppm]= 8.87 (m, 1H, Phe3-NH), 7.70 (s, 1H, Tz2-H), 7.57 (s, 1H, Tz1-H), 7.37-7.19 (m, 9H, Ph-H, Boc-NH), 7.01-6.91 (m, 5H, Ph-H), 6.70-6.66 (m, 2H, Ph-H), 5.86 (dd, $^3J=11.0$, 4.5 Hz, 1H, Phe4- H^α), 5.28 (d, $^2J=12.8$ Hz, 1H, O-CHH-), 5.11 (d, $^2J=12.8$ Hz, 1H, O-CHH), 5.09 (m, 1H, Leu1- H^α) 4.73 (d, $^3J=11.2$ Hz, 1H, Val2- H^α), 4.60 (m, 1H, Phe3- H^α), 3.66 (dd, $^2J=13.8$, $^3J=4.5$ Hz, 1H, Phe4- H^β), 3.36 (dd, $^2J=13.8$, $^3J=11.1$ Hz, 1H, Phe4- H^β), 2.77 (dd, $^2J=13.7$, $^3J=10.7$ Hz, 1H, Phe3- H^β), 2.76 (m, 1H, Val2- H^β), 2.22 (dd, $^2J=13.7$, $^3J=4.1$ Hz, 1H, Phe3- H^β), 1.47 (m, 1H, Leu1- H^γ), 1.39 (m, 1H, Leu1- H^β), 1.32 (s, 9H, -C(CH_3) $_3$), 0.85 (d, $^3J=6.6$ Hz, 3H, Leu1- H^δ), 0.82 (d, $^3J=6.7$ Hz, 3H, Leu1- H^δ), 0.71 (m, 1H, Leu1- H^β), 0.61 (d, $^3J=6.5$ Hz, 3H, Val2- H^γ), 0.37 (d, $^3J=6.5$ Hz, 3H, Val2- H^γ).

^{13}C NMR (151 MHz, $DMSO-d_6$): δ [ppm]= 167.93 (Phe4-C), 166.84 (Val2-C), 155.37 ($tBuO$ -C), 141.37 (Tz1-C), 140.27 (Tz2-C), 136.72 (C^{Ar}), 136.43 (C^{Ar}), 135.79 (C^{Ar}), 133.05 (Tz1-CH), 131.76 (Tz2-CH), 129.51 (2C, CH^{Ar}), 129.16 (2C, CH^{Ar}), 128.93 (2C, CH^{Ar}), 128.83 (3C, CH^{Ar}), 128.43 (CH^{Ar}), 128.36 (CH^{Ar}), 127.86 (2C, CH^{Ar}), 127.53 (CH^{Ar}), 126.62 (CH^{Ar}), 78.51 (-C(CH_3) $_3$), 69.52 (Val2- C^α), 67.29 (O- CH_2 -), 61.57 (Phe4- C^α), 44.56 (Leu1- C^β), 43.75 (Phe3-

7. Experimental section

C^α), 42.89 (Leu1- C^α), 39.13 (Phe3- C^β), 38.21 (Phe4- C^β), 29.08 (Val2- C^β), 28.55 ($C(CH_3)_3$), 24.94 (Leu1- C^γ), 23.65 (Leu1- C^δ), 21.73 (Leu1- C^δ), 19.50 (Val2- C^γ), 18.79 (Val2- C^γ).

Z-Lys(Z)-Leu[5Tz]Val-Phe[5Tz]Phe-OBzl (44).



Boc-Leu[5Tz]Val-Phe[5Tz]Phe-OBzl

(107 mg; 0.140 mmol) is dissolved in DCM/(4 M HCl in dioxane) 1:1 (2 mL) and stirred overnight at rt. After evaporation of the solvent, the crude ammonium salt is used without further purification. Z-Lys(Z)-OH (64 mg; 0.15 mmol; 1.1 eq), Oxyma (1.21 eq; 0.17 mmol; 24 mg) and

DIC (1.21 eq; 0.17 mmol; 26 μ L) are dissolved in DCM (1 mL; dry) under an argon atmosphere and stirred 10 min for preactivation. The crude ammonium salt is dissolved in DCM (1 mL; dry) and the activated acid mixture is added dropwise, followed by TMP (10 eq; 1.4 mmol; 185 μ L). The reaction mixture is left to stir overnight. The solvent is removed under vacuum, the residue dissolved in EtOAc and washed with 10% citric acid (2x), water (2x), saturated $NaHCO_3$ (2x), brine and dried over $MgSO_4$. The filtrate is concentrated and the crude peptidotriazolamer purified by column chromatography PE/EtOAc 1:1. **Yield:** 108 mg (0.102 mmol); 73%. **R_f** (PE/EtOAc 1:1)= 0.21.

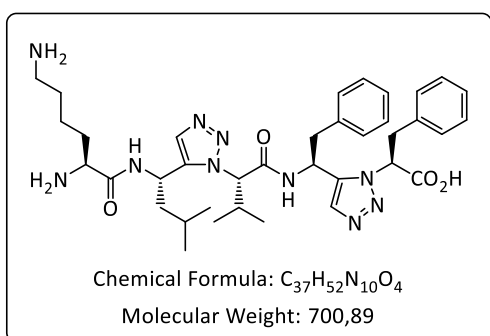
HR-MS (ESI): m/z = 530.2748 [$M+2H$] $^{2+}$ (calc. 530.27618).

1H -NMR (500 MHz, $DMSO-d_6$): δ [ppm]= 8.90 (m, 1H, Phe4-**NH**), 8.39 (Leu2-**NH**), 7.76 (s, 1H, Tz2-**H**), 7.62 (s, 1H, Tz1-**H**), 7.40 (d, $^3J=7.9$ Hz, 1H, Lys1-**NH**), 7.37-7.14 (m, 18H, Ph-**H**), 7.18 (Lys1(Z-**NH**)), 6.99-6.88 (m, 5H, Ph-**H**), 6.57-6.54 (m, 2H, Ph-**H**), 5.89 (dd, $^3J=11.1$, 4.4 Hz, 1H, Phe5-**H $^\alpha$**), 5.27 (m, 1H, Leu2-**H $^\alpha$**), 5.27 (d, $^2J=12.8$ Hz, 1H, Phe5-O-**CHH**), 5.13 (d, $^2J=12.8$ Hz, 1H, Phe5-O-**CHH**), 5.00 (d, $^2J=13.5$ Hz, 4H, Z-**CH $_2$**), 4.77 (d, $^3J=11.0$ Hz, 1H, Val3-**H $^\alpha$**), 4.60 (m, 1H, Phe4-**H $^\alpha$**), 3.92 (m, 1H, Lys1-**H $^\alpha$**), 3.68 (dd, $^2J=13.8$, $^3J=4.4$ Hz, 1H, Phe5-**H $^\beta$**), 3.38 (dd, $^2J=13.8$, $^3J=11.2$ Hz, 1H, Phe5-**H $^\beta$**), 2.92-2.84 (m, 2H, Lys1-**H $^\epsilon$**), 2.76 (dd, $^2J=13.7$, $^3J=10.7$ Hz, 1H, Phe4-**H $^\beta$**), 2.67 (m, 1H, Val3-**H $^\beta$**), 2.20 (dd, $^2J=13.8$, $^3J=4.0$ Hz, 1H, Phe4-**H $^\beta$**), 1.60-1.48 (m, 2H, Leu2-**H $^\beta$** , Leu2-**H $^\gamma$**), 1.44-1.37 (m, 2H, Lys1-**H $^\beta$**), 1.31-1.18 (m, 4H, Lys1-**H $^\gamma$** , Lys1-**H $^\delta$**), 0.84 (d, $^3J=6.5$ Hz, 6H, Leu2-**H $^\delta$**), 0.75 (m, 1H, Leu2-**H $^\beta$**), 0.67 (d, $^3J=6.5$ Hz, 3H, Val3-**H $^\gamma$**), 0.34 (d, $^3J=6.6$ Hz, 3H, Val3-**H $^\gamma$**).

^{13}C -NMR (600 MHz, $DMSO-d_6$): δ [ppm]= 172.33 (Lys1-**C**), 167.95 (Phe5-**C**), 166.43 (Val-**C**), 156.47 (BzlO-**C**), 156.36 (BzlO-**C**), 141.20 (Tz1-**C**), 140.37 (Tz2-**C**), 137.70 (**C Ar**), 137.48 (**C Ar**), 136.75 (Phe4-**C Ar**), 136.47 (Phe5-**C Ar**), 135.79 (**C Ar**), 132.37 (Tz1-**CH**), 131.85 (Tz2-**CH**),

129.49 (CH^{Ar}), 129.10 (CH^{Ar}), 128.93 (CH^{Ar}), 128.84 (2C, CH^{Ar}), 128.78 (3C, CH^{Ar}), 128.44 (CH^{Ar}), 128.23 (CH^{Ar}), 128.17 (CH^{Ar}), 128.13 (CH^{Ar}), 127.86 (CH^{Ar}), 127.52 (CH^{Ar}), 126.55 (CH^{Ar}), 68.70 (Val3-C^α), 67.30 (Phe5-O-CH₂), 61.59 (Phe5-C^α), 54.86 (Lys1-C^α), 44.45 (Leu2-C^β), 43.61 (Phe4-C^α), 41.56 (Leu2-C^α), 40.49 (Lys1-C^ε), 39.12 (Phe4-C^β), 38.19 (Phe5-C^β), 31.71 (Lys1-C^β), 29.47 (2C, Lys1-C^δ, Val3-C^β), 24.78 (Leu2-C^γ), 23.76 (Leu2-C^γ), 23.18 (Lys1-C^γ), Leu2-C^δ), 21.68 (Leu2-C^δ), 19.54 (Val3-C^γ), 18.90 (Val3-C^γ).

H-Lys-Leu[5Tz]Val-Phe[5Tz]Phe-OH (42b).



Prepared according to **GP6**, starting with Z-Lys(Z)-Leu[5Tz]Val-Phe[5Tz]Phe-OBzl (**44**) (103 mg; 97.2 μmol) for 6 h. The product was purified by preparative HPLC.

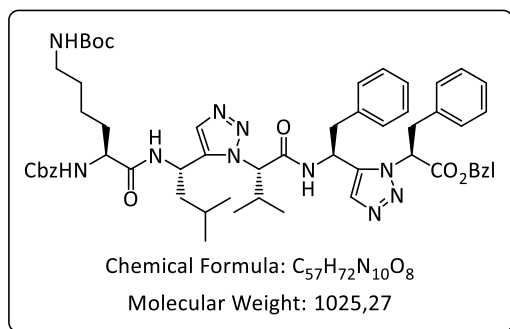
Yield: 51 mg (0.55 mmol); 57%, TFA-salt.

Analytical RP-HPLC: t_R = 3.06 min (method 1, 254 nm).

HR-MS (ESI): *m/z* = 701.4276 [M+H]⁺ (calc. 701.42457).

¹H-NMR (600 MHz, DMSO-*d*₆): δ [ppm] = 9.12 (m, 1H, Phe4-NH), 8.83 (d, ³J = 8.2 Hz, 1H, Leu2-NH), 8.22-8.13 (m, 3H, Lys1-C^αNH₃), 7.80-7.73 (m, 3H, C^εNH₃), 7.71 (s, 1H, Tz2-H), 7.62 (s, 1H, Tz1-H), 7.29-7.18 (m, 3H, Ph-H), 6.99-6.85 (m, 5H, Ph-H), 6.64-6.61 (m, 2H, Ph-H), 5.65 (dd, ³J = 11.8, 4.0 Hz, 1H, Phe5-H^α), 5.43 (m, 1H, Leu-H^α), 4.79 (d, ³J = 11.6 Hz, 1H, Val3-H^α), 4.45 (m, 1H, Phe4-H^α), 3.71 (m, 1H, Lys1-H^α), 3.61 (dd, ²J = 13.8, ³J = 4.0 Hz, 1H, Phe5-H^β), 3.35 (dd, 1H, ²J = 13.8, ³J = 11.8 Hz Phe5-H^β), 2.79-2.72 (m, 2H, Val-H^β, Phe4-H^β), 2.62-2.55 (m, 2H, Lys1-H^ε), 2.22 (dd, ²J = 13.7, ³J = 3.4 Hz, 1H, Phe4-H^β), 1.59-1.47 (m, 3H, Leu-H^γ, Lys1-H^β), 1.43-1.36 (m, 2H, Lys1-H^δ), 1.33-1.15 (m, 2H, Leu2-H^β), 1.13-1.06 (m, 2H, Lys1-H^γ), 0.87 (d, ³J = 6.5 Hz, 3H, Leu-H^δ), 1.19 (m, 1H, Leu2-H^β), 0.81 (d, ³J = 6.7 Hz, 3H, Leu-H^δ), 0.78 (d, ³J = 6.5 Hz, 3H, Val-H^γ), 0.36 (d, ³J = 6.5 Hz, 3H, Val-H^γ).

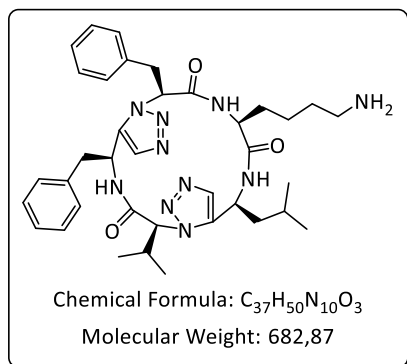
¹³C-NMR (151 MHz, DMSO-*d*₆): δ [ppm] = 169.59 (Phe5-C), 168.27 (Lys1-C), 166.38 (Val3-C), 140.69 (Tz1-C), 140.10 (Tz2-C), 137.03 (C^{Ar}), 136.86 (C^{Ar}), 133.43 (Tz1-CH), 131.68 (Tz2-CH), 129.38 (2C, CH^{Ar}), 129.12 (2C, CH^{Ar}), 128.85 (2C, CH^{Ar}), 128.37 (2C, CH^{Ar}), 127.39 (CH^{Ar}), 126.48 (CH^{Ar}), 70.43 (Val3-C^α), 61.93 (Phe5-C^α), 52.16 (Lys1-C^α), 44.15 (Leu2-C^β), 43.77 (Phe4-C^α), 41.78 (Leu2-C^α), 39.11 (Phe4-C^β), 38.84 (Lys1-C^ε), 38.41 (Phe5-C^β), 30.86 (Lys1-C^β), 28.61 (Val3-C^β), 26.76 (Lys1-C^δ), 24.61 (Leu-C^γ), 23.83 (Leu2-C^δ), 21.49 (Lys1-C^γ), 21.45 (Leu2-C^δ), 19.63 (Val3-C^γ), 19.00 (Val3-C^γ).

Z-Lys(Boc)-Leu-[5Tz]-Val-Phe[5Tz]Phe-OBzl (45).**Boc-Leu[5Tz]Val-Phe[5Tz]Phe-OBzl**

(54 mg; 71 μ mol) is dissolved in DCM/(4 M HCl in dioxane) 1:1 (3 mL) and stirred 2 h at rt. After evaporation of the solvent, the crude ammonium salt is used without further purification. Z-Lys(Boc)-OH (54 mg; 0.14 mmol; 2.0 eq), Oxyma (20 mg; 0.14 mmol; 2.0 eq) and COMU (61 mg;

0.14 mmol; 2.0 eq) are dissolved in DCM (1 mL; dry), after addition of *sym*-collidine (19 μ L; 0.14 mmol; 2.0 eq) the reaction mixture is stirred 10 min for preactivation. The crude ammonium salt is dissolved in DCM (1 mL; dry) and the activated acid mixture is added dropwise, followed by TMP (19 μ L; 0.14 mmol; 2.0 eq). The reaction mixture is left to stir overnight. The solvent is removed under vacuum and the crude product purified by preparative HPLC. **Yield:** 41 mg (40 μ mol); 56%. **Analytical RP-HPLC:** $t_R = 6.96$ min (method 1, 254 nm). **HR-MS** (ESI): $m/z = 1047.54319$ [$M+Na$]⁺ (calc. 1047.5432).

The Peptidotriazolamer was fully characterized after cyclisation and cleavage of the protecting groups.

Cyclo-[Lys-Leu[5Tz]Val-Phe[5Tz]Phe] (42c).**Cbz-Lys(Boc)-Leu[5Tz]Val-Phe[5Tz]Phe-OBzl (45)**

(29 mg; 28 μ mol) is dissolved in MeOH (1 mL), after addition of Pd/C (6 mg; 20 wt%) and TES (45 μ L; 0.28 mmol; 10 eq), the solution is stirred for 20 min at rt. After full conversion of the starting material, the Pd/C is filtered off through a short plug of silica, which is washed with MeOH (3x), the filtrate is concentrated

under vacuum to give H-Lys(Boc)-Leu[5Tz]Val-Phe[5Tz]Phe-OH as a colourless oil.

Analytical RP-HPLC: $t_R = 5.11$ min (method 1, 254 nm).

The crude product is dissolved in DMF / DCM 1:1 (28 mL; 1 mM; dry) and *sym*-collidine (37 μ L; 0.28 mmol; 10 eq) is added, followed by PyBOP (29 mg; 56 μ mol; 2.0 eq), the reaction is left to stir overnight at rt. After full conversion of the linear precursor, H₂O (10 mL) is added and the solvent is removed under vacuum to give cyclo-[Lys(Boc)-Leu[5Tz]Val-Phe[5Tz]Phe] (46) as crude product.

Analytical RP-HPLC: $t_R = 6.14$ min (method 1, 254 nm).

The residual material is dissolved in TFA/H₂O/TIS (95:2.5:2.5) (3 mL) and stirred for 2 h at rt, the TFA is removed by co-evaporation with toluene, the crude product purified by preparative HPLC. **Yield:** 11 mg (14 μmol), TFA-salt; 50% over three steps.

Analytical RP-HPLC: t_R = 4.78 min (method 1, 254 nm).

HR-MS (ESI): m/z = 683.4162 [M+H]⁺ (683.41401).

¹H-NMR (600 MHz, DMSO): δ [ppm] = 7.90 (d, 3J = 7.5 Hz, 3H, Leu2-NH), 7.90 (s, 1H, Tz1-H), 7.69 (m, 1H, Lys1-NH), 7.68 (s, 1H, Tz2-H), 7.28-7.18 (m, 5H, Ph-H), 7.05-7.02 (m, 2H, Ph-H), 7.01 (d, 3J = 9.3 Hz, 1H, Phe4-NH), 6.87-6.85 (m, 2H, Ph-H), 6.68 (m, 1H, Ph-H), 5.23 (dd, 3J = 11.9, 3.6 Hz, 1H, Phe5-H^α), 4.78 (ddd, 3J = 9.7, 9.3, 5.4 Hz, 1H, Phe4-H^α), 4.64 (m, 1H, Leu2-H^α), 4.60 (d, J = 6.1 Hz, 1H, Val3-H^α), 4.31 (m, 1H, Lys1-H^α), 3.71 (dd, 2J = 13.8, 3J = 3.6 Hz, 1H, Phe5-H^β), 3.23 (dd, 2J = 13.8, 3J = 12.0 Hz, 1H, Phe5-H^β), 2.99 (dd, 2J = 14.0, 3J = 9.7 Hz, 1H, Phe4-H^β), 2.80-2.75 (m, Lys1-H^ε), 2.63 (dd, 2J = 14.0, 3J = 5.4 Hz, 1H, Phe4-H^β), 2.48 (qqd, 3J = 6.9, 6.8, 6.1 Hz, 1H, Val3-H^β), 1.83 (m, 1H, Leu2-H^β), 1.75 (m, 1H, Leu2-H^β), 1.58-1.48 (m, 4H, Lys1-H^β, Lys1-H^δ, Leu2-H^γ), 1.36 (m, 1H, Lys1-H^β), 1.32-1.20 (m, 2H, Lys1-H^γ), 0.90 (d, 3J = 6.6 Hz, 3H, Leu2-H^δ), 0.86 (d, 3J = 6.6 Hz, 3H, Leu2-H^δ), 0.49 (d, 3J = 6.9 Hz, 3H, Val3-H^γ), 0.47 (d, 3J = 6.8 Hz, 3H, Val3-H^γ).

¹³C-NMR (151 MHz, DMSO-*d*₆): δ [ppm] = 170.43 (Lys1-C), 166.99 (Phe5-C), 166.44 (Val3-C), 140.10 (Tz2-C), 139.55 (Tz1-C), 137.03 (C^{Ar}), 136.96 (C^{Ar}), 132.73 (Tz1-CH), 132.42 (Tz2-CH), 129.41 (2C, CH^{Ar}), 128.92 (2C, CH^{Ar}), 128.86 (2C, CH^{Ar}), 128.74 (2C, CH^{Ar}), 127.30 (CH^{Ar}), 126.94 (CH^{Ar}), 65.89 (Val3-C^α), 63.15 (Phe5-C^α), 54.55 (Lys1-C^α), 43.29 (Phe4-C^α), 41.84 (Leu2-C^α), 41.54 (Leu2-C^β), 39.09 (Lys1-C^ε), 38.67 (Phe4-C^β), 38.53 (Phe5-C^β), 31.49 (Val3-C^β), 31.04 (Lys1-C^β), 26.79 (Lys1-C^δ), 25.11 (Leu2-C^γ), 22.87 (Leu2-C^δ), 22.52 (Lys1-C^γ), 22.49 (Leu2-C^δ), 19.23 (Val-C^γ), 18.27 (Val-C^γ).

H-KLVFF-OH (42d).

Fmoc-Phe-OH (100 mg; 258 μmol) is loaded onto 2-CTC resin (1.3 eq; 335 μmol; 220 mg; 1.52 mmol/g loading) according to **GP9**. The loading was determined as 0.43 mmol/g (148 μmol; 57%). The peptide was then assembled by standard SPPS and purified by preparative HPLC. **Yield:** 114 mg (129 μmol), TFA-salt; 87%.

Chemical formula: C₃₅H₅₂N₆O₆ (MW = 652.84 g mol⁻¹).

Analytic RP-HPLC: t_R = 6.07 min (method 3, 254 nm).

HR-MS (ESI): m/z = 653.4044 [M+H]⁺ (calc. 653.40211).

H-KLVFF-NH₂ (42e).

Fmoc-Phe-OH (40 mg; 103 μ mol) is loaded onto rink amide resin (206 mg; 103 μ mol; 1.0 eq) according to **GP9**. The loading was determined as 0.42 mmol/g (87 μ mol; 84%). The peptide was then assembled by standard SPPS and purified by preparative HPLC.

Yield: 55 mg (63 μ mol), TFA-salt; 72%.

Chemical formula: C₃₅H₅₃N₇O₅ (MW= 651.85 gmol⁻¹).

Analytic RP-HPLC: t_R= 3.77 min (method 1, 254 nm).

HR-MS (ESI): m/z= 652.4170 [M+H]⁺ (calc. 652.41809).

H-klvff-NH₂ (42f).

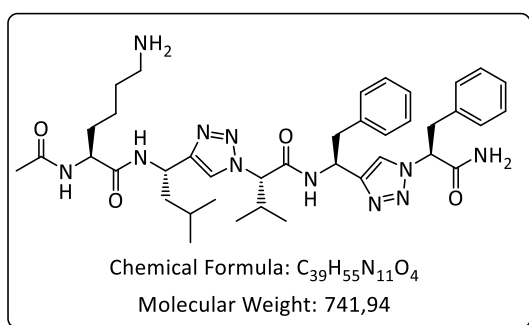
Fmoc-Phe-OH (40 mg; 103 μ mol) is loaded onto rink amide resin (206 mg; 103 μ mol; 1.0 eq) according to **GP9**. The loading was determined as 0.42 mmol/g (87 μ mol; 84%). The peptide was then assembled by standard SPPS and purified by preparative HPLC.

Yield: 55 mg (63 μ mol), TFA-salt; 37%.

Chemical formula: C₃₅H₅₃N₇O₅ (M: 651.85 gmol⁻¹).

Analytic RP-HPLC: t_R= 3.76 min (method 1, 254 nm).

HR-MS (ESI): m/z= 652.4155 [M+H]⁺ (calc. 652.41809).

Ac-Lys-Leu[4Tz]Val-Phe[4Tz]Phe-NH₂ (42g).

Fmoc-Phe[4Tz]Phe-OH (20 mg; 36 μ mol) is loaded onto rink amide resin (83 mg; 0.42 mmol; 1.1 eq) according to **GP9**. The loading was determined as 0.27 mmol/g (22 μ mol; 61%). The peptide was then assembled by standard SPPS and purified by

preparative HPLC. **Yield:** 12 mg (14 μ mol) TFA-salt; 63%. **Analytic RP-HPLC:** t_R= 4.35 min (method 1, 254 nm). **HR-MS (ESI):** m/z= 742.4541 [M+H]⁺ (calc. 742.45112).

¹HNMR (600 MHz; DMSO-*d*₆): δ [ppm] = 9.04 (d, ³J= 8.5 Hz, 1H, Phe4-NH), 8.23 (d, ³J= 8.7 Hz, 1H, Leu2-NH), 8.14 (s, 1H, Tz2-H), 7.98 (d, ³J= 8.3 Hz, 1H, Lys1-NH), 7.92 (s, 1H, CONH₂), 7.79 (s, 1H, Tz1-H), 7.66 (s, 3H, Lys1-NH), 7.46 (s, 1H, CONH₂), 7.24-6.94 (m, 10H, Ph-H), 5.52 (dd, ³J= 10.2, 5.4 Hz, 1H, Phe5-H ^{α}), 5.16 (ddd, ³J= 8.5, 7.8, 6.8 Hz, 1H, Phe4-H ^{α}), 5.04 (td, ³J= 8.6, 6.7 Hz, 1H, Leu2-H ^{α}), 4.91 (d, ³J= 10.1 Hz, 1H, Val3-H ^{α}), 4.24 (td, ³J= 8.3,

5.5 Hz, 1H, Lys1- H^{α}), 3.38 (dd, $^2J= 14.2$, $^3J= 5.4$ Hz, 1H, Phe5- H^{β}), 3.30 (dd, $^2J= 14.2$, $^3J= 10.3$ Hz, 1H, Phe5- H^{β}), 3.12 (dd, $^2J= 13.6$, $^3J= 6.8$ Hz, 1H, Phe4- H^{β}), 2.99 (dd, $^2J= 13.6$, $^3J= 7.8$ Hz, 1H, Phe4- H^{β}), 2.75-2.69 (m, 2H, Lys1- H^{ϵ}), 2.27-2.21 (m, 1H, Val3- H^{β}), 1.84 (s, 3H, H_3C -CO), 1.69-1.64 (m, 2H, Leu2- H^{β}), 1.61-1.52 (m, 2H, Leu2- H^{γ} , Lys1- H^{β}), 1.50-1.43 (3H, Lys1- H^{β} , Lys1- H^{δ}), 1.29-1.17 (m, 2H, Lys1- H^{γ}), 0.90 (d, $^3J= 6.6$ Hz, 3H, Leu- H^{δ}), 0.88 (d, $^3J= 6.6$ Hz, 3H, Leu- H^{δ}), 0.77 (d, $^3J= 6.7$ Hz, 3H, Val3- H^{γ}), 0.56 (d, $^3J= 6.7$ Hz, 3H, Val3- H^{γ}).

$^{13}C\{1H\}$ -NMR (151 MHz, DMSO- d_6): δ [ppm]= 171.44 (Lys1-C), 169.58 (2C; Ac-CO, Phe5-C), 167.12 (Val3-C), 149.61 (Tz1-C), 147.31 (Tz2-C), 137.95 (C^{Ar}), 136.72 (C^{Ar}), 129.46 (2C, CH^{Ar}), 129.29 (2C, CH^{Ar}), 128.69 (2C, CH^{Ar}), 128.35 (2C, CH^{Ar}), 127.17 (CH^{Ar}), 126.51 (CH^{Ar}), 122.10 (Tz2-CH), 120.63 (Tz1-CH), 68.91 (Val3- C^{α}), 64.33 (Phe5- C^{α}), 52.68 (Lys1- C^{α}), 47.27 (Phe4- C^{α}), 44.17 (Leu2- C^{β}), 43.78 (Leu2- C^{α}), 40.52 (Phe4- C^{β}), 39.16 (Lys1- C^{ϵ}), 38.28 (Phe5- C^{β}), 32.06 (Lys1- C^{β}), 31.91 (Val3- C^{β}), 27.18 (Lys1- C^{δ}), 24.65 (Leu2- C^{γ}), 23.32 (Leu- C^{δ}), 22.99 (H_3C -CO), 22.73 (Lys1- C^{γ}), 22.34 (Leu2- C^{δ}), 19.18 (Val3- C^{γ}), 18.84 (Val3- C^{γ}).

H-klvff-OH (42h).

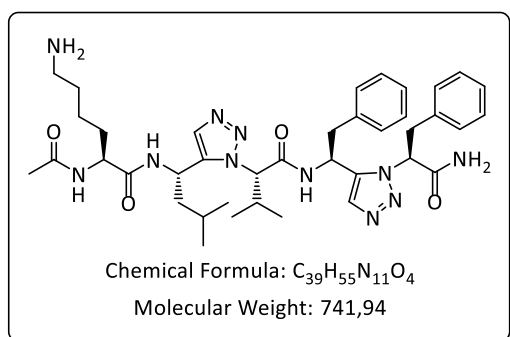
Fmoc-D-Phe-OH (60 mg; 0.15 mmol) is loaded onto 2-CTC resin (1.6 eq; 0.24 mmol; 160 mg; 1.52 mmol/g loading) according to **GP9**. The loading was determined as 0.47 mmol/g (75 μ mol; 50%). The peptide was then assembled by standard SPPS and purified by preparative HPLC. **Yield:** 45 mg (51 μ mol), TFA-salt; 68%.

Chemical formula: $C_{35}H_{52}N_6O_6$ (M: 652.84 $gmol^{-1}$).

Analytic RP-HPLC: $t_R= 3.92$ min (method 1, 254 nm).

HR-MS (ESI): $m/z= 653.4012$ $[M+H]^+$ (calc. 653.40211).

Ac-Lys-Leu[5Tz]Val-Phe[5Tz]Phe-NH₂ (42i).



Fmoc-Phe[5Tz]Phe-OH (50 mg; 89.5 μ mol) is loaded onto rink amide resin (179 mg; 89.5 μ mol; 1.0 eq) according to **GP9**. The loading was determined as 0.42 mmol/g (75 μ mol; 84%). The peptide was then assembled by standard SPPS according to general procedure and purified by preparative HPLC. **Yield:** 24 mg (28 μ mol), TFA-

salt; 37%. **Analytic RP-HPLC:** $t_R= 4.63$ (method 1, 254 nm).

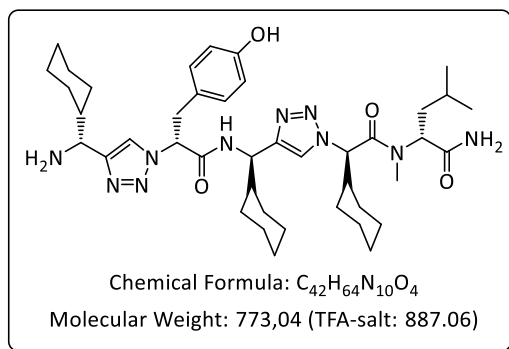
HR-MS (ESI): $m/z= 742.4529$ $[M+H]^+$ (calc. 742.45112).

7. Experimental section

¹H-NMR (600 MHz; DMSO-*d*₆): δ [ppm]= 8.80 (m, 1H, Phe4-NH), 8.45 (m, 1H, Leu2-NH), 7.96 (d, ³J= 8.0 Hz, 1H, Lys1-NH), 7.66 (s, 1H, Tz2-H), 7.63 (s, 1H, Tz1-H), 7.19-6.69 (m, 10H, Ph-H), 5.46 (dd, ³J= 11.1, 4.6 Hz, 1H, Phe5-H^α), 5.19 (m, 1H, Leu2-H^α), 4.87 (m, 1H, Phe4-H^α), 4.81 (d, ³J= 10.7 Hz, 1H, Val3-H^α), 4.15 (td, ³J= 8.5, 5.3 Hz, 1H, Lys1-H^α), 3.52 (dd, ²J= 13.9, ³J= 4.6 Hz, 1H, Phe5-H^β), 3.31 (dd, ²J= 13.9, ³J= 11.1 Hz, 1H, Phe5-H^β), 2.75 (dd, ²J= 13.7, ³J= 10.2 Hz, 1H, Phe4-H^β), 2.69-2.61 (m, 3H, Val3-H^β, Lys1-H^ε), 2.28 (dd, ²J= 13.8, ³J= 4.2 Hz, 1H, Phe4-H^β), 1.83 (s, 3H, Ac-CH₃), 1.57-1.52 (m, 2H, Leu2-H^β, Leu2-H^γ), 1.45-1.32 (m, 4H, Lys1-H^β, Lys1-H^δ), 1.25-1.06 (m, 2H, Lys1-H^γ), 0.90 (m, 1H, Leu2-H^β), 0.83 (d, ³J= 6.9 Hz, 3H, Leu2-H^δ) 0.82 (d, ³J= 6.7 Hz, 3H, Leu2-H^δ), 0.77 (d, ³J= 6.6 Hz, 3H, Val3-H^γ) 0.41 (d, ³J= 6.6 Hz, 3H, Val3-H^γ).

¹³C{¹H}-NMR (151 MHz, DMSO-*d*₆): δ [ppm]= 169.80 (Ac-C), 168.90 (Phe5-C), 166.64 (Val3-C), 141.29 (Tz1-C), 140.12 (Tz2-C), 137.36 (C^{Ar}), 137.08 (C^{Ar}), 132.29 (Tz2-CH), 132.17 (Tz1-CH), 129.35 (2C, CH^{Ar}), 129.25 (2C, CH^{Ar}), 128.72 (2C, CH^{Ar}), 128.44 (CH^{Ar}), 127.13 (CH^{Ar}), 126.62 (CH^{Ar}), 68.24 (Val3-C^α), 63.18 (Phe5-C^α), 52.52 (Lys1-C^α), 44.71 (Phe4-C^α), 44.09 (Leu2-C^β), 41.54 (Leu2-C^α), 39.69 (Phe4-C^β), 39.12 (Lys1-C^ε), 37.88 (Phe5-C^β), 31.57 (Lys1-C^β), 29.43 (Val3-C^β), 27.02 (Lys1-C^δ), 24.80 (Leu2-C^γ), 23.62 (Leu2-C^δ), 22.89 (CH₃-CO), 22.75 (Lys1-C^γ), 21.73 (Leu2-C^δ), 19.73 (Val3-C^γ), 18.99 (Val3-C^γ).

H-D-chGly-[4Tz]-D-Tyr-D-chGly-[4Tz]-D-chGly-D-(NMe)Leu-NH₂ (42j).



Fmoc-D-Leu-OH (27 mg; 75 μmol; 1.5 eq) was loaded onto the rink amide resin (100 mg resin; ~0.5 mmol·g⁻¹) according to **GP9**. The loading was determined as 0.65 mmol·g⁻¹ (65 μmol). The *N*-methylation was performed as described by Chatterjee *et al.*¹⁴⁵ The remaining coupling steps were completed on solid phase, employing

Fmoc-D-chGly-[4Tz]-D-Tyr(^tBu)-OH (**18h**) (1.5 eq; 98 μmol; 61 mg) and Fmoc-D-chGly-[4Tz]-D-chGly-OH (1.5 eq; 98 μmol; 53 mg) (**18i**). The crude peptide was precipitated from Et₂O and purified by preparative HPLC. **Yield:** 8 mg (9 μmol); 14%.

Analytical-HPLC: t_R= 2.80 min (method 2, 254 nm).

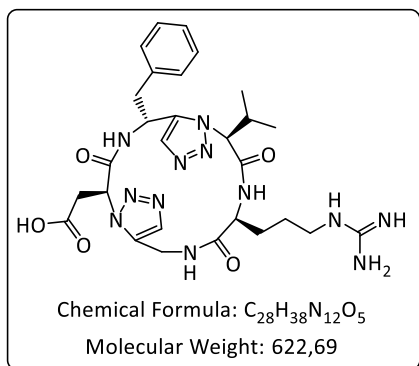
HR-MS (ESI): m/z= 773.5172 [M+H]⁺ (calc. 773.51847).

¹H-NMR (600 MHz, DMSO): δ [ppm]= 8.96 (d, ³J= 9.1 Hz, 1H, chGly3-NH), 8.32 (d, ³J= 5.7 Hz, 3H, chGly1-NH₃), 8.26 (s, 1H, Tz1-H), 7.91 (s, 1H, Tz2-H), 7.32 (s, 1H, Leu5-NH), 7.06 (s, 1H, Leu5-NH), 6.89 (d, ³J= 8.3 Hz, 2H, Tyr2-H^δ), 6.54 (d, ³J= 8.4 Hz, 2H, Tyr2-H^ε),

5.73 (dd, $^3J = 10.3, 5.3$ Hz, 1H, Tyr2- H^α), 5.55 (d, $^3J = 10.1$ Hz, 1H, chGly4- H^α), 4.98 (dd, $^3J = 11.3, 4.9$ Hz, 1H, Leu5- H^α), 4.84 (dd, $^3J = 9.0, 7.2$ Hz, 1H, chGly3- H^α), 4.22 (m, 1H, chGly- H^α), 3.16 (dd, $^2J = 14.5, ^3J = 5.2$ Hz, 1H, Tyr2- H^β), 3.11 (dd, $^2J = 14.6, ^3J = 10.4$ Hz, 1H, Tyr2- H^β), 2.98 (s, 3H, N- CH_3), 2.26 (m, 1H, chGly4- H^β), 1.83-1.68 (m, 6H, CH_2 , chGly1- H^β , chGly3- H^β), 1.67-1.53 (m, 10H, CH_2 , Leu5- H^β , Leu5- H^γ), 1.46 (ddd, $^2J = 14.4, ^3J = 9.9, 4.9$ Hz, 1H, Leu5- H^β), 1.38-0.74 (m, 18H, CH_2), 0.72 (d, $^3J = 6.6$ Hz, 3H, Leu5- H^δ), 0.62 (d, $^3J = 6.5$ Hz, 3H, Leu5- H^δ).

$^{13}C\{^1H\}$ -NMR (151 MHz, DMSO- d_6): δ [ppm] = 172.66 (Leu5-C), 168.51 (chGly4-C), 167.47 (Tyr2-C), 156.61 (Tyr2- C^ζ), 147.00 (Tz2-C), 142.71 (Tz1-C), 130.22 (2C, Tyr2- C^δ), 126.15 (Tyr2- C^γ), 123.51 (Tz1-CH), 121.42 (Tz2-CH), 115.42 (2C, Tyr2- C^ϵ), 64.46 (Tyr2- C^α), 63.83 (chGly4- C^α), 54.53 (Leu5- C^α), 51.98 (chGly1- C^α), 50.60 (chGly3- C^α), 42.05 (chGly3- C^β), 40.92 (chGly1- C^β), 40.40 (chGly4- C^β), 37.43 (Leu5- C^β), 37.41 (Tyr1- C^β), 31.54 (N- CH_3), 29.57 (CH_2), 29.29 (CH_2), 29.05 (CH_2), 28.66 (CH_2), 28.27 (CH_2), 27.83 (2C, CH_2), 26.26 (CH_2), 26.17 (CH_2), 25.93 (2C, CH_2), 25.69 (2C, CH_2), 25.57 (CH_2), 25.53 (CH_2), 24.96 (Leu5- C^γ), 23.52 (Leu5- C^δ), 21.34 (Leu5- C^δ).

Cyclo-[Arg-Gly[5Tz]Asp-D-Phe[5Tz]Val] (48a).



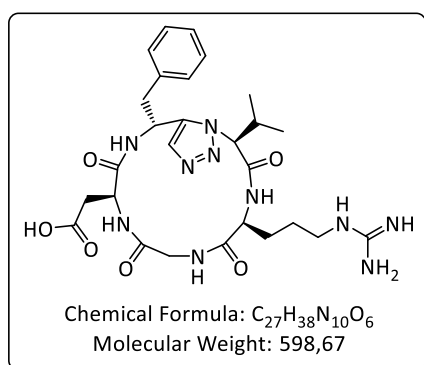
Fmoc-Arg(Pmc)-OH (79 mg; 0.12 mmol) is loaded onto 2-CTC resin (100 mg; 0.15 mmol; 1.3 eq; 1.52 mmol/g loading) according to **GP9**. The loading was determined as 0.58 mmol/g (0.058 mmol; 48%). The peptide was then assembled by standard SPPS and used without further purification after cleavage (20% HFIP in DCM).

Yield: 52 mg (0.054 mmol), 93% crude.

Analytical RP-HPLC: $t_R = 5.14$ min (method 1, 220 nm).

25 mg (26 μ mol) of the linear sequence are dissolved in 26 mL DMF/DCM 1:1, after the addition of *sym*-collidine (34 μ L; 0.26 mmol; 10 eq) and PyBOP (20 mg; 39 μ mol; 1.5 eq) the reaction mixture is left to stir overnight. The solvent is removed under vacuum and the crude peptide dissolved in TFA/TIS/ H_2O (90/5/5) and stirred 2 h at rt. The crude product is concentrated under vacuum and purified by preparative HPLC.

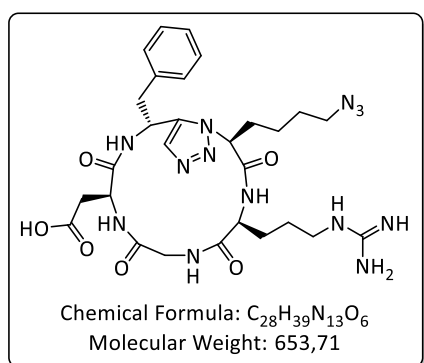
Yield: 8.0 mg (12 μ mol) TFA-salt, 46% over two steps. **Analytical RP-HPLC:** $t_R = 3.60$ (method 1, 220 nm). **HR-MS** (ESI): $m/z = 623.3133$ [$M+H$] $^+$ (calc. 623.31609).

Cyclo-[Arg-Gly-Asp-D-Phe[5Tz]Val] (48b).

Fmoc-Arg(Pmc)-OH (79 mg; 0.12 mmol) is loaded onto 2-CTC resin (100 mg; 0.15 mmol; 1.3 eq; 1.52 mmol/g loading) according to **GP9**. The loading was determined as 0.68 mmol/g (0.068 mmol; 57%). The peptide was then assembled by standard SPPS and used without further purification after cleavage (20% HFIP in DCM). **Yield:** 57 mg (0.061 mmol), 89% crude.

Analytical RP-HPLC: $t_R = 5.16$ min (method 1, 220 nm).

33 mg (31 μ mol) of the linear sequence are dissolved in 31 mL DMF/DCM 1:1, after the addition of *sym*-collidine (41 μ L; 0.31 mmol; 10 eq) and PyBOP (24 mg; 47 μ mol; 1.5 eq) the reaction mixture is left to stir overnight. The solvent is removed under vacuum and the crude peptide dissolved in TFA/thioanisole/EDT/anisole (90:5:3:2) (2mL) and stirred 2 h at rt. The crude product is precipitated from cold Et₂O (20 mL) and purified by preparative HPLC. **Yield:** 8.0 mg (11 μ mol) TFA-salt, 35% over two steps. **Analytical RP-HPLC:** $t_R = 3.42$ min (method 1, 220 nm). **HR-MS (ESI):** $m/z = 599.3054$ [M+H]⁺ (calc. 599.30485).

Cyclo-[Arg-Gly-Asp-D-Phe[5Tz]Lys(N₃)] (48c).

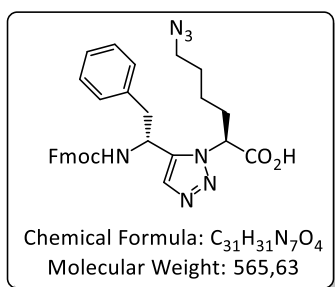
Fmoc-Arg(Pmc)-OH (79 mg; 0.12 mmol) is loaded onto 2-CTC resin (100 mg; 0.15 mmol; 1.3 eq; 1.52 mmol/g loading) according to **GP9**. The loading was determined as 0.84 mmol/g (0.085 mmol; 70%). The peptide was then assembled by standard SPPS and used without further purification after cleavage (DCM/MeOH/AcOH 8:1:1). **Yield:** 89 mg (0.054 mmol),

AcOH salt, quantitative. **Analytical RP-HPLC:** $t_R = 5.33$ min (method 1, 220 nm).

40 mg (38 μ mol) of the linear sequence are dissolved in 38 mL DMF/DCM 1:1, after the addition of *sym*-collidine (56 μ L; 0.42 mmol; 10 eq) and PyBOP (30 mg; 57 μ mol; 1.5 eq) the reaction mixture is left to stir overnight. The solvent is removed under vacuum and the crude peptide dissolved in TFA/thioanisole/EDT/anisole (90:5:3:2) (2mL) and stirred 2 h at rt. The crude product is precipitated from cold Et₂O (20 mL) and purified by preparative HPLC. **Yield:** 3.9 mg (5.1 μ mol) TFA-salt, 13% over two steps.

Analytical RP-HPLC: $t_R = 3.98$ (method 1, 220 nm).

HR-MS (ESI): $m/z = 654.3223$ [M+H]⁺ (calc. 654.32190).

Fmoc-D-Phe[5Tz]Lys(N₃)-OH (53).

Fmoc-D-Phe[5Tz]Lys-OH (52): Prepared according to **GP6** starting from **9t** (0.40 g; 0.52 mmol).

Yield: 0.21 g (0.40 mmol); 77%.

Fmoc-D-Phe[5Tz]Lys(N₃)-OH (53): Tf₂O (0.12 μL; 0.74 mmol; 2.0 eq) and sodium azide (58 mg; 0.89 mmol; 2.4 eq) are suspended in ACN (1 mL) and stirred for 1 h at rt. Fmoc-D-

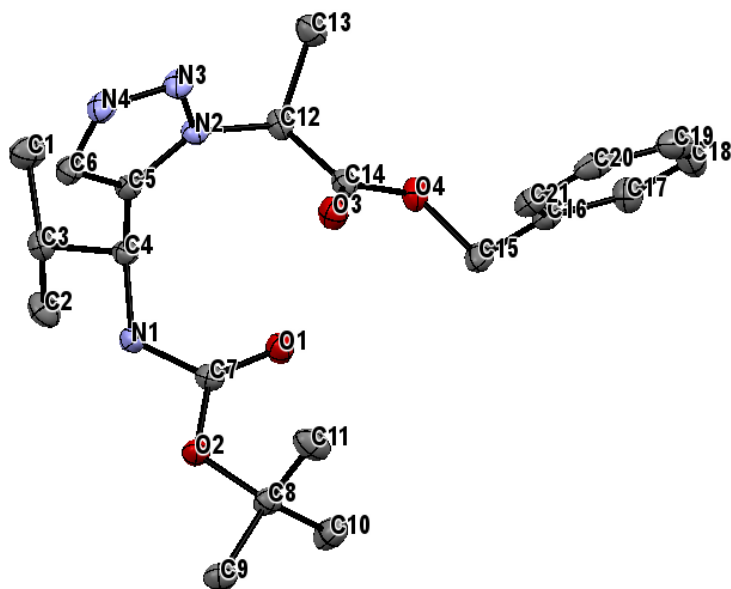
Phe[5Tz]Lys-OH (197 mg; 0.37 mmol) is dissolved in ACN/MeOH 1:1 (1 mL) and added to the reaction mixture above followed by TEA (154 μL; 1.11 mmol; 3.0 eq) and CuSO₄·5H₂O (1 mg; 4 μmol; 1mol%), the reaction mixture is then left to stir over night. The solvent is removed under vacuum and the product purified by column chromatography (PE/EtOAc 2:1 including 1% TFA). **Yield:** 122 mg (0.22 mmol); 59%. **R_f** (PE/EtOAc 1:1 including 1% TFA)= 0.14. **MS (ESI):** *m/z*= 566.3 [M+H]⁺, 588.2 [M+Na]⁺.

¹H-NMR (500 MHz; DMSO-*d*₆): δ [ppm]= 13.46 (s, 1H, CO₂H), 8.07 (d, ³*J*= 8.8 Hz, 1H, NH), 7.90-7.85 (m, 2H, H^{Ar}), 7.78 (s, 1H, Tz-H), 7.58-7.54 (m, 2H, H^{Ar}), 7.44-7.38 (m, 2H, H^{Ar}), 7.33-7.24 (m, 6H, Ph-H, H^{Ar}), 7.20 (m, 1H, Ph-H), 5.34 (dd, ³*J*= 9.8, 4.9 Hz, 1H, Lys-H^α), 4.94 (ddd, ³*J*= 9.4, 8.8, 5.2 Hz, 1H, Phe-H^α), 4.24-4.08 (m, 3H, CH-CH₂-O, CH-CH₂O), 3.18-3.05 (m, 4H, Phe-H^β, Lys-H^β), 2.38-2.19 (m, 2H, Lys-H^β), 1.52-1.36 (m, 2H, Lys-H^δ), 2.24 (m, 1H, Lys-H^γ), 1.07 (m, 1H, Lys-H^γ).

¹³C{¹H}-NMR (151 MHz, DMSO) δ[ppm]= 170.38 (Lys-C), 156.10 (OCON), 144.08 (C^{Ar}), 143.99 (C^{Ar}), 141.12 (C^{Ar}), 141.10 (C^{Ar}), 140.71 (Tz-C), 137.86 (C^{Ar}), 131.80 (Tz-CH), 129.65 (2C; CH^{Ar}), 128.63 (2C; CH^{Ar}), 128.09 (2C; CH^{Ar}), 127.47 (CH^{Ar}), 127.45 (CH^{Ar}), 126.97 (CH^{Ar}), 125.53 (CH^{Ar}), 125.47 (CH^{Ar}), 120.56 (2C; CH^{Ar}), 66.15 (CHCH₂O), 59.98 (Lys-C^α), 50.75 (Lys-C^ε), 46.99 (CHCH₂O), 46.51 (Phe-C^α), 39.56 (Phe-C^β), 30.23 (Lys-C^β), 28.09 (Lys-C^δ), 23.03 (Lys-C^γ).

7.3. X-ray crystal structure analysis

Boc-Val[5Tz]Ala-OBzl (9c)

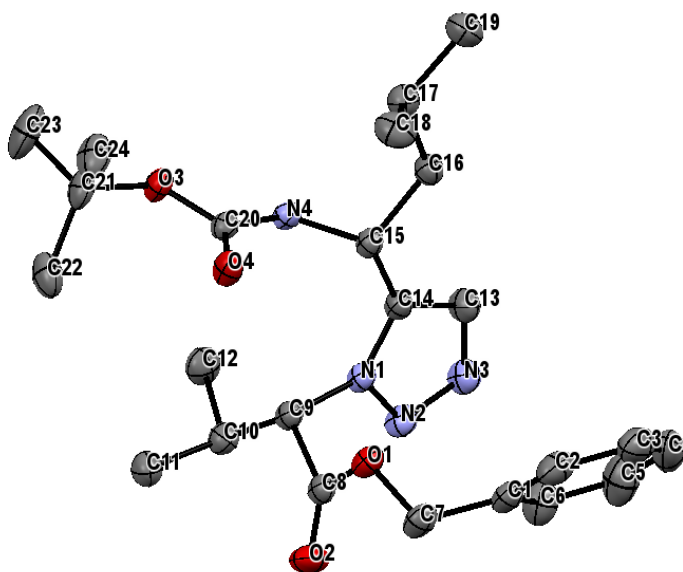
**Table 8.** Crystal data and structure refinement for Boc-Val[5Tz]Ala-OBzl.

Empirical formula	C ₂₁ H ₃₀ N ₄ O ₄ (MW = 402.49 g*mol ⁻¹)
Crystal system, Space group	orthorhombic, P2 ₁ 2 ₁ 2 ₁
Uni cell dimensions	a = 9.48169(7) Å; b = 10.83269(11) Å; c = 21.24183(16) Å α = 90°; β = 90 °; γ = 90°
Volume/Å ³	2181.79(3)
Z	4
ρ _{calc} /mg/mm ³	1.225
μ/mm ⁻¹	0.700
F(000)	864.0
2θ range for data collection	8.324 to 144.202°
Reflections collected	34117
Independent reflections	4299[R(int) = 0.0281]
Data/restraints/parameters	4299/0/273
Final R indexes [I>=2σ (I)]	R ₁ = 0.0226, wR ₂ = 0.0569
Final R indexes [all data]	R ₁ = 0.0236, wR ₂ = 0.0577
Largest diff. peak/hole / e Å ⁻³	0.20/-0.15
Flack parameter	-0.01(4)

Table 9. Fractional Atomic Coordinates ($\times 10^4$) and Equivalent Isotropic Displacement Parameters ($\text{\AA}^2 \times 10^3$). U_{eq} is defined as 1/3 of of the trace of the orthogonalised U_{ij} tensor.

Atom	x	y	z	U(eq)
O1	3002.7(11)	5102.1(10)	1606.7(5)	23.5(2)
O2	4773.2(10)	3710.9(9)	1407.6(4)	20.8(2)
O3	239.7(11)	3658.2(9)	1845.2(5)	24.5(2)
O4	-44.5(10)	5638.7(9)	2155.1(4)	22.0(2)
N1	3567.2(12)	4465.9(11)	616.1(5)	19.0(2)
N2	-70.3(12)	4316.3(10)	608.1(5)	17.8(2)
N3	-947.8(12)	3361.0(11)	493.8(6)	21.7(3)
N4	-311.3(13)	2645.2(12)	85.7(6)	22.4(3)
C1	1638.7(17)	6051.1(16)	-726.8(7)	30.0(4)
C2	4068.9(16)	6413.1(15)	-296.6(8)	27.5(3)
C3	2860.6(15)	5494.5(13)	-357.2(6)	20.3(3)
C4	2389.9(14)	5066.4(13)	302.6(6)	16.7(3)
C5	1148.2(14)	4202.6(13)	275.9(6)	17.4(3)
C6	966.1(15)	3131.5(13)	-58.3(6)	20.4(3)
C7	3704.1(14)	4476.1(12)	1248.1(6)	18.2(3)
C8	5027.6(15)	3354.0(12)	2067.4(6)	20.1(3)
C9	6265.3(16)	2464.0(14)	2003.9(7)	23.9(3)
C10	5437.0(18)	4473.6(15)	2455.3(7)	29.9(3)
C11	3734.9(17)	2697.1(15)	2324.3(8)	28.7(3)
C12	-449.8(14)	5220.1(13)	1089.9(6)	19.6(3)
C13	-2017.6(15)	5542.8(14)	1062.4(7)	25.3(3)
C14	-31.1(14)	4719.4(13)	1736.3(6)	19.5(3)
C15	498.2(15)	5353.7(14)	2784.0(7)	23.5(3)
C16	-628.4(14)	4893.9(13)	3223.9(6)	19.8(3)
C17	-1232.6(16)	5701.7(15)	3653.9(7)	25.5(3)
C18	-2256.4(18)	5288.6(16)	4072.1(7)	31.9(4)
C19	-2682.7(16)	4067.0(17)	4057.5(8)	32.4(4)
C20	-2088.5(17)	3254.7(15)	3630.2(7)	28.5(3)
C21	-1058.0(15)	3661.2(14)	3215.3(7)	23.2(3)

Boc-D-Leu[5Tz]Val-OBzl (9d)

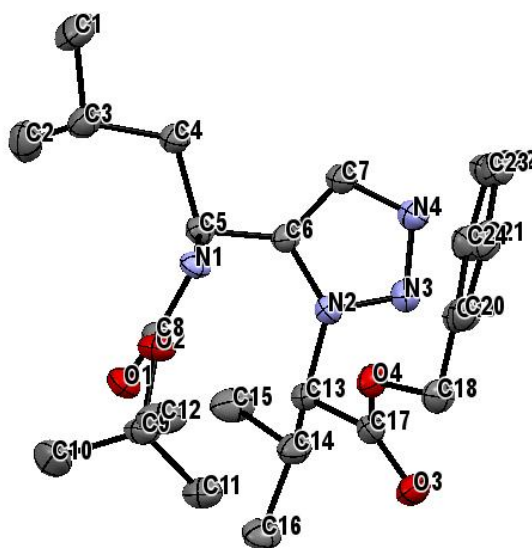
**Table 10.** Crystal data and structure refinement for Boc-D-Leu[5Tz]Val-OBzl.

Empirical formula	C ₂₄ H ₃₆ N ₄ O ₄ (MW = 444.57 g* mol ⁻¹)
Crystal system, Space group	monoclinic, P2 ₁
Unit cell dimensions	a = 9.81156(5) Å; b = 11.41705(6) Å; c = 23.04824(13) Å α = 90 °; β = 90.6203(5) °; γ = 90 °
Volume/Å ³	2581.69(2)
Z	4
ρ _{calc} /mg/mm ³	1.144
μ/mm ⁻¹	0.634
F(000)	960.0
2θ range for data collection	7.672 to 144.25°
Reflections collected	71693
Independent reflections	10148[R(int) = 0.0272]
Data/restraints/parameters	10148/3/610
Final R indexes [I>=2σ (I)]	R ₁ = 0.0268, wR ₂ = 0.0686
Final R indexes [all data]	R ₁ = 0.0272, wR ₂ = 0.0690
Largest diff. peak/hole / e Å ⁻³	0.24/-0.19
Flack parameter	0.00(3)

Table 11. Fractional Atomic Coordinates ($\times 10^4$) and Equivalent Isotropic Displacement Parameters ($\text{\AA}^2 \times 10^3$). U_{eq} is defined as 1/3 of the trace of the orthogonalised U_{ij} tensor.

Atom	x	y	z	U(eq)
O1	4348.0(12)	941.8(10)	3030.5(5)	28.2(3)
O2	6358.3(14)	-12.9(12)	3032.6(6)	39.0(3)
O3	5984.0(12)	5602.1(11)	3693.5(5)	28.5(2)
O4	4789.9(13)	4347.6(11)	3112.0(5)	30.0(3)
N1	5276.0(14)	1561.6(12)	4131.7(6)	23.5(3)
N2	5536.4(15)	583.5(13)	4440.3(6)	28.5(3)
N3	4683.1(16)	575.0(14)	4873.8(6)	32.5(3)
N4	4771.3(14)	4201.5(12)	4095.5(6)	22.6(3)
C1	2522.9(18)	-434.2(15)	3129.7(8)	29.4(4)
C2	1173(2)	-268.3(16)	2975.3(9)	37.8(4)
C3	135(2)	-635.7(19)	3337.6(11)	47.4(5)
C4	454(2)	-1164(2)	3855.8(11)	53.2(6)
C5	1807(3)	-1333(2)	4019.1(10)	55.4(6)
C6	2842(2)	-972(2)	3654.2(9)	41.3(4)
C7	3640(2)	-24.7(16)	2740.5(7)	32.0(4)
C8	5648.6(17)	779.8(14)	3185.2(7)	24.8(3)
C9	6073.9(16)	1758.3(14)	3603.5(7)	23.1(3)
C10	7608.1(18)	1790.4(15)	3728.5(8)	28.7(3)
C11	8363.1(19)	2127.2(18)	3175.9(8)	35.2(4)
C12	7947(2)	2646.6(18)	4217.4(9)	36.9(4)
C13	3885.2(19)	1544.8(16)	4841.0(7)	31.0(4)
C14	4246.3(17)	2190.8(14)	4364.7(7)	24.2(3)
C15	3700.0(16)	3322.1(14)	4118.0(7)	23.2(3)
C16	2490.5(17)	3762.3(15)	4476.6(7)	27.2(3)
C17	1888.7(18)	4936.4(16)	4278.9(8)	30.3(4)
C18	1362(2)	4902(2)	3655.2(8)	40.2(4)
C19	751(2)	5307.7(18)	4689.7(9)	38.5(4)
C20	5144.4(16)	4699.1(14)	3589.7(7)	22.6(3)
C21	6566.1(19)	6265.4(16)	3203.4(8)	33.5(4)
C22	7502(2)	5487(2)	2855.8(9)	42.8(5)
C23	7375(3)	7207(2)	3516.1(12)	56.6(6)
C24	5440(2)	6802.0(19)	2834.4(10)	43.2(5)

Boc-Leu[5Tz]/Val-OBzl (9e)

**Table 12.** Crystal data and structure refinement for Boc-Leu[5Tz]/Val-OBzl.

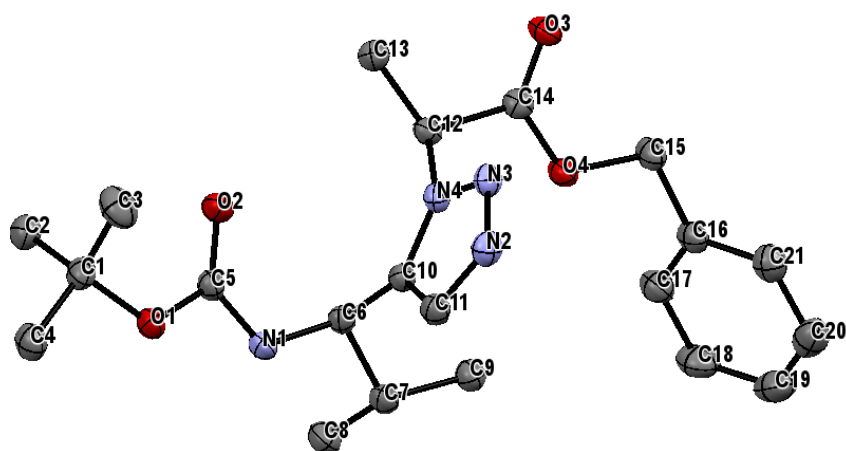
Empirical formula	C ₂₄ H ₃₆ N ₄ O ₄ (MW = 444.57 g* ⁻¹ mol ⁻¹)
Crystal system, Space group	orthorhombic, P2 ₁ 2 ₁ 2 ₁
Uni cell dimensions	a = 10.7988(2) Å; b = 11.15120(19) Å; c = 20.5911(3) Å α = 90°; β = 90°; γ = 90°
Volume/Å ³	2479.58(8)
Z	4
ρ _{calc} /mg/mm ³	1.191
μ/mm ⁻¹	0.660
F(000)	960.0
2θ range for data collection	8.588 to 133.93°
Reflections collected	24888
Independent reflections	4303[R(int) = 0.0585]
Data/restraints/parameters	4303/0/300
Final R indexes [I>=2σ(I)]	R ₁ = 0.0369, wR ₂ = 0.0939
Final R indexes [all data]	R ₁ = 0.0440, wR ₂ = 0.1018
Largest diff. peak/hole / e Å ⁻³	0.16/-0.21
Flack parameter	0.03(13)

7. Experimental section

Table 13. Fractional Atomic Coordinates ($\times 10^4$) and Equivalent Isotropic Displacement Parameters ($\text{\AA}^2 \times 10^3$). U_{eq} is defined as 1/3 of the trace of the orthogonalised U_{ij} tensor.

Atom	x	y	z	U(eq)
O1	5343.8(19)	6195.2(16)	5468.2(9)	31.0(5)
O2	6662.7(17)	4621.5(18)	5627.8(9)	29.9(5)
O3	2640(2)	4463.7(18)	7197.1(9)	35.2(5)
O4	3805.0(19)	3439.5(16)	6481.7(9)	29.5(5)
N1	4990(2)	4352(2)	5025.7(10)	23.2(5)
N2	2310(2)	4383.9(19)	5562.5(10)	24.3(5)
N3	1284(2)	3744(2)	5700.4(11)	28.4(5)
N4	1034(2)	3094(2)	5185.0(11)	28.5(5)
C1	5380(4)	3905(4)	2987.4(15)	49.1(9)
C2	4713(3)	5967(3)	3322.8(16)	42.6(8)
C3	5067(3)	4726(3)	3559.3(13)	32.8(7)
C4	4030(3)	4164(2)	3958.3(13)	27.2(6)
C5	3895(3)	4656(2)	4652.6(12)	23.5(6)
C6	2741(3)	4142(2)	4955.9(12)	23.3(6)
C7	1902(3)	3323(2)	4725.8(13)	27.7(6)
C8	5631(3)	5153(2)	5381.5(13)	24.9(6)
C9	7312(3)	5157(3)	6188.7(13)	30.2(6)
C10	7950(3)	6319(3)	6006.0(17)	47.3(9)
C11	6406(3)	5333(3)	6746.1(14)	36.8(7)
C12	8255(3)	4203(3)	6358.8(16)	43.3(8)
C13	2818(3)	5152(2)	6078.7(12)	25.2(6)
C14	2006(3)	6245(3)	6222.8(13)	30.0(7)
C15	1766(3)	6925(3)	5592.6(15)	40.8(8)
C16	2678(3)	7052(3)	6710.4(14)	35.1(7)
C17	3048(3)	4331(2)	6660.6(12)	26.6(6)
C18	4009(3)	2485(2)	6950.0(14)	33.7(7)
C19	4304(3)	1362(2)	6580.9(13)	29.4(6)
C20	5284(3)	634(3)	6766.8(13)	31.8(7)
C21	5508(3)	-430(3)	6444.1(14)	35.2(7)
C22	4770(3)	-776(3)	5925.1(14)	38.0(7)
C23	3802(3)	-46(3)	5735.9(15)	41.3(8)
C24	3568(3)	1016(3)	6058.9(14)	33.8(7)

Boc-D-Val[5Tz]Ala-OBzl (9f)

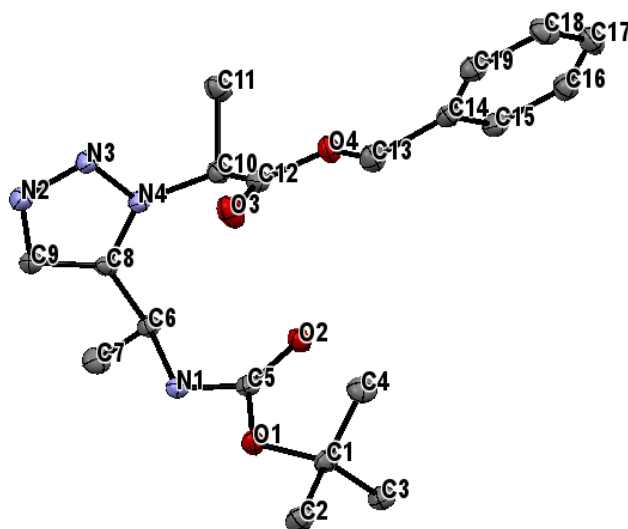
**Table 14.** Crystal data and structure refinement for Boc-D-Val[5Tz]Ala-OBzl.

Empirical formula	C ₂₁ H ₃₀ N ₄ O ₄ (MW = 402.49 g* mol ⁻¹)
Crystal system, Space group	monoclinic, P2 ₁
Unit cell dimensions	a = 10.1473(3) Å; b = 21.6416(5) Å; c = 10.3140(3) Å α = 90°; β = 91.319(3)°; γ = 90°
Volume/Å ³	2264.39(11)
Z	4
ρ _{calc} /mg/mm ³	1.181
μ/mm ⁻¹	0.674
F(000)	864.0
2θ range for data collection	8.576 to 143.984°
Reflections collected	33116
Independent reflections	8856[R(int) = 0.0474]
Data/restraints/parameters	8856/1/535
Final R indexes [I > 2σ(I)]	R ₁ = 0.0396, wR ₂ = 0.0995
Final R indexes [all data]	R ₁ = 0.0416, wR ₂ = 0.1017
Largest diff. peak/hole / e Å ⁻³	0.33/-0.25
Flack parameter	-0.01(9)

7. Experimental section

Table 15. Fractional Atomic Coordinates ($\times 10^4$) and Equivalent Isotropic Displacement Parameters ($\text{\AA}^2 \times 10^3$). U_{eq} is defined as 1/3 of the trace of the orthogonalised U_{ij} tensor.

Atom	x	y	z	U(eq)
O1	993.8(18)	6293.4(8)	4093.8(17)	25.5(4)
O2	2175.8(19)	6268.6(9)	6008.2(18)	29.4(4)
O3	2512.7(19)	5545.4(9)	11592.8(17)	27.4(4)
O4	1536.0(18)	4753.3(8)	10525.2(16)	24.7(4)
N1	974(2)	5443.7(10)	5286(2)	23.6(4)
N2	-1177(2)	5864.7(10)	8719(2)	26.3(4)
N3	-78(2)	5896.6(10)	9403(2)	23.9(4)
N4	867(2)	5628.4(9)	8697.4(19)	20.4(4)
C1	1452(3)	6907.0(12)	3699(3)	25.7(5)
C2	2925(3)	6891.3(13)	3482(3)	30.1(6)
C3	1067(4)	7390.4(15)	4697(3)	39.2(7)
C4	699(3)	7011.7(13)	2434(3)	31.6(6)
C5	1443(2)	6026.3(12)	5200(2)	22.7(5)
C6	1130(2)	5102.6(11)	6498(2)	21.0(5)
C7	640(2)	4434.3(12)	6300(2)	23.9(5)
C8	1466(3)	4100.9(13)	5303(3)	30.2(6)
C9	690(3)	4076.9(12)	7577(2)	26.7(5)
C10	373(2)	5424.2(11)	7544(2)	21.0(5)
C11	-935(3)	5576.6(13)	7578(2)	25.4(5)
C12	2204(2)	5595.7(11)	9257(2)	20.8(5)
C13	2865(3)	6224.3(12)	9293(2)	25.5(5)
C14	2118(2)	5306.1(11)	10607(2)	21.8(5)
C15	1368(3)	4445.2(12)	11760(2)	27.7(5)
C16	694(3)	3836.7(12)	11513(2)	26.3(5)
C17	1241(3)	3401.9(13)	10692(3)	31.7(6)
C18	642(4)	2831.1(14)	10506(3)	40.0(7)
C19	-500(4)	2688.4(15)	11158(3)	42.6(7)
C20	-1051(3)	3119.4(16)	11971(3)	39.7(7)
C21	-462(3)	3694.3(14)	12149(3)	32.4(6)

Boc-Ala[5Tz]Ala-OBzl (9g)**Table 16.** Crystal data and structure refinement for Boc-Ala[5Tz]Ala-OBzl.

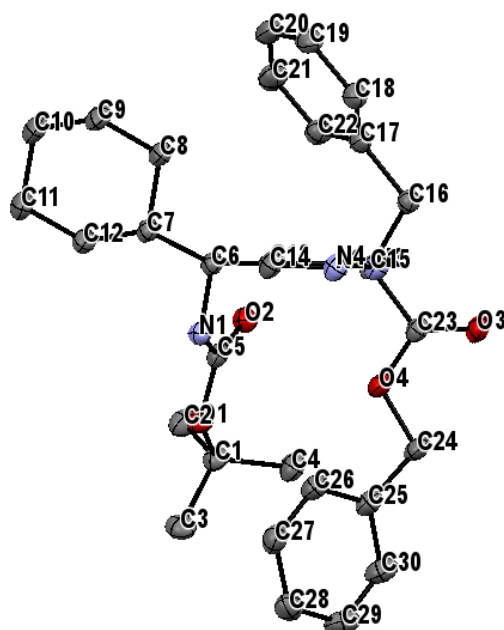
Empirical formula	C ₁₉ H ₂₆ N ₄ O ₄ (MW = 374.44 g*mol ⁻¹)
Crystal system, Space group	orthorhombic, P2 ₁ 2 ₁ 2 ₁
Unit cell dimensions	a = 5.69773(6) Å; b = 9.79814(10) Å; c = 35.5160(4) Å α = 90°; β = 90°; γ = 90°
Volume/Å ³	1982.76(4)
Z	4
ρ _{calc} /mg/mm ³	1.254
μ/mm ⁻¹	0.733
F(000)	800.0
2θ range for data collection	4.976 to 143.986°
Reflections collected	33947
Independent reflections	3868[R(int) = 0.0394]
Data/restraints/parameters	3868/0/349
Final R indexes [I>=2σ (I)]	R ₁ = 0.0243, wR ₂ = 0.0596
Final R indexes [all data]	R ₁ = 0.0252, wR ₂ = 0.0603
Largest diff. peak/hole / e Å ⁻³	0.15/-0.13
Flack parameter	-0.03(6)

7. Experimental section

Table 17. Fractional Atomic Coordinates ($\times 10^4$) and Equivalent Isotropic Displacement Parameters ($\text{\AA}^2 \times 10^3$). U_{eq} is defined as 1/3 of the trace of the orthogonalised U_{ij} tensor.

Atom	<i>x</i>	<i>y</i>	<i>z</i>	<i>U</i> (eq)
O1	4410(2)	7097.6(11)	6443.0(3)	20.4(2)
O2	6549(2)	5295.4(11)	6217.6(3)	20.0(2)
O3	2286(2)	3043.0(13)	6552.2(3)	26.8(3)
O4	4036(2)	1942.1(11)	6073.6(3)	20.0(2)
N1	7015(2)	6137.0(13)	6812.8(3)	16.4(3)
N2	5011(3)	2808.5(13)	7568.4(3)	20.1(3)
N3	4887(2)	2149.2(13)	7248.1(3)	19.5(3)
N4	6174(2)	2857.9(13)	6996.4(3)	16.6(3)
C1	3220(3)	7418.2(15)	6087.7(4)	17.9(3)
C2	1385(3)	8442.9(17)	6215.6(5)	23.0(3)
C3	4970(3)	8067.2(16)	5818.4(4)	21.2(3)
C4	2046(3)	6168.5(18)	5915.5(5)	23.8(3)
C5	6035(3)	6096.8(15)	6467.9(4)	16.5(3)
C6	8550(3)	5049.4(15)	6949.4(4)	16.0(3)
C7	10447(3)	5652.7(18)	7203.3(5)	23.1(3)
C8	7134(3)	3988.7(14)	7155.4(4)	15.5(3)
C9	6377(3)	3931.7(15)	7521.1(4)	18.3(3)
C10	6350(3)	2340.6(16)	6613.0(4)	17.4(3)
C11	7253(3)	866.9(17)	6613.3(5)	22.9(3)
C12	3979(3)	2498.9(15)	6419.6(4)	18.5(3)
C13	1859(3)	2096.3(18)	5863.4(4)	22.7(3)
C14	2084(3)	1348.7(15)	5495.5(4)	18.6(3)
C15	4049(3)	1506.2(16)	5268.1(4)	21.2(3)
C16	4178(3)	834.6(18)	4924.3(5)	23.8(3)
C17	2330(3)	23.1(18)	4802.2(5)	26.5(4)
C18	372(3)	-138.1(18)	5028.3(5)	25.8(3)
C19	251(3)	522.5(17)	5373.9(4)	21.8(3)

Boc-chGly[5Tz]Phe-OBzl (9h)

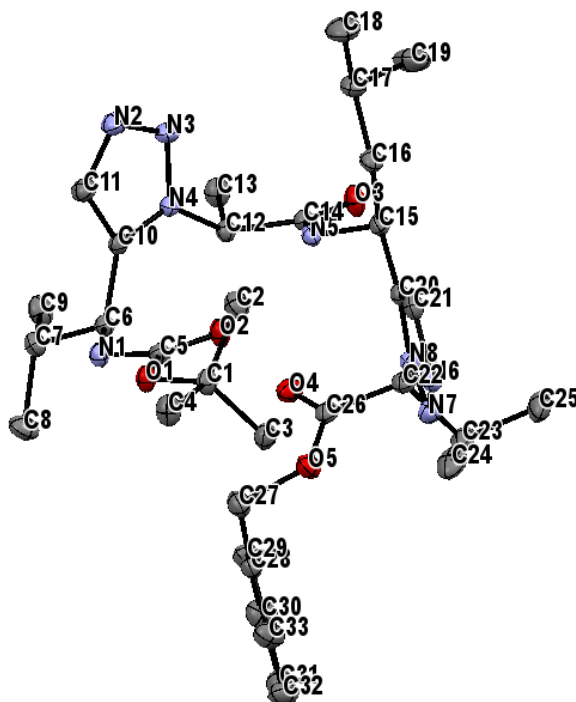
**Table 18.** Crystal data and structure refinement for Boc-chGly[5Tz]Phe-OBzl.

Empirical formula	C ₃₀ H ₃₈ N ₄ O ₄ (MW = 518.66 g*mol ⁻¹)
Crystal system, Space group	orthorhombic, P2 ₁ 2 ₁ 2 ₁
Unit cell dimensions	a = 10.32629(19) Å; b = 12.5469(2) Å; c = 25.1185(4) Å α = 90°; β = 90°; γ = 90°
Volume/Å ³	3254.41(9)
Z	4
ρ _{calc} /mg/mm ³	1.181
μ/mm ⁻¹	0.640
F(000)	1248.0
2θ range for data collection	7.876 to 144°
Reflections collected	58573
Independent reflections	6400[R(int) = 0.0487]
Data/restraints/parameters	6400/0/392
Final R indexes [I>=2σ (I)]	R ₁ = 0.0303, wR ₂ = 0.0753
Final R indexes [all data]	R ₁ = 0.0324, wR ₂ = 0.0770
Largest diff. peak/hole / e Å ⁻³	0.20/-0.17
Flack parameter	-0.10(6)

7. Experimental section

Table 19. Fractional Atomic Coordinates ($\times 10^4$) and Equivalent Isotropic Displacement Parameters ($\text{\AA}^2 \times 10^3$). U_{eq} is defined as 1/3 of of the trace of the orthogonalised U_{ij} tensor.

Atom	x	y	z	U(eq)
O1	1678.5(12)	4074.4(9)	761.8(5)	23.9(3)
O2	2759.6(13)	3767.4(10)	1538.1(5)	24.5(3)
O3	6750.7(14)	5787.7(10)	1299.4(5)	28.8(3)
O4	5150.7(13)	5191.6(9)	766.9(5)	26.7(3)
N1	3141.5(14)	2795.8(11)	787.8(6)	21.8(3)
N2	7250.6(16)	2595.3(12)	341.9(6)	26.7(3)
N3	7259.7(16)	3339.8(12)	709.6(6)	24.6(3)
N4	6162.7(15)	3222.2(11)	995.0(6)	20.5(3)
C1	920.1(18)	4983.7(14)	970.4(7)	24.0(4)
C2	154(2)	4655.8(16)	1459.7(8)	32.3(4)
C3	0(2)	5217.5(16)	512.8(8)	32.5(4)
C4	1811(2)	5919.1(15)	1074.6(8)	30.8(4)
C5	2546.0(17)	3566.1(12)	1068.8(7)	20.9(3)
C6	4116.7(17)	2103.0(13)	1023.6(6)	20.6(3)
C7	3841.0(17)	911.7(13)	918.4(6)	21.6(3)
C8	4762.2(19)	229.6(13)	1253.1(7)	25.7(4)
C9	4543(2)	-963.7(14)	1165.9(8)	30.6(4)
C10	3142(2)	-1263.4(15)	1274.3(9)	35.6(5)
C11	2219(2)	-589.3(15)	939.1(9)	33.3(4)
C12	2439.6(19)	603.5(14)	1033.1(8)	26.8(4)
C13	5434.3(17)	2401.8(13)	811.3(7)	20.7(3)
C14	6149.4(19)	2015.7(14)	394.6(7)	25.5(4)
C15	5891.7(17)	4001.8(13)	1414.7(6)	20.8(3)
C16	6774.5(18)	3860.1(14)	1896.3(7)	23.2(3)
C17	6590.1(18)	2775.8(14)	2146.8(7)	23.9(3)
C18	7456.3(19)	1954.8(15)	2050.2(7)	28.9(4)
C19	7262(2)	952.0(16)	2277.8(8)	34.7(4)
C20	6204(2)	773.2(17)	2598.1(8)	38.3(5)
C21	5323(2)	1579.1(18)	2692.3(8)	36.9(5)
C22	5514(2)	2580.1(16)	2466.5(7)	28.6(4)
C23	6009.7(18)	5104.7(13)	1160.7(7)	22.2(3)
C24	5210(2)	6164.9(14)	459.4(7)	29.7(4)
C25	4384.1(19)	6031.8(14)	-28.6(7)	26.8(4)
C26	4226(2)	5050.3(15)	-275.8(8)	29.5(4)
C27	3538(2)	4977.7(16)	-748.8(8)	33.6(4)
C28	3012(2)	5882.6(18)	-981.5(8)	33.7(4)
C29	3146(2)	6858.5(17)	-730.1(8)	36.9(5)
C30	3821(2)	6927.8(16)	-255.3(8)	34.0(4)

Boc-Val[5Tz]Ala-Leu[5Tz]Val-OBzl (10)**Table 20.** Crystal data and structure refinement for Boc-Val[5Tz]Ala-Leu[5Tz]Val-OBzl.

Empirical formula	$C_{33}H_{50}N_8O_5$ (MW = 638.81 $\text{gm}\cdot\text{mol}^{-1}$)
Crystal system, Space group	orthorhombic, $P2_12_12_1$
Unit cell dimensions	$a = 9.1090(4)$ Å; $b = 15.0895(10)$ Å; $c = 25.6559(16)$ Å $\alpha = 90^\circ$; $\beta = 90^\circ$; $\gamma = 90^\circ$
Volume/Å ³	3526.4(4)
Z	4
ρ_{calc} /mg/mm ³	1.203
μ /mm ⁻¹	0.670
F(000)	1380.0
2 θ range for data collection	6.796 to 143.952°
Reflections collected	68785
Independent reflections	6937[R(int) = 0.0323]
Data/restraints/parameters	6937/0/433
Final R indexes [$I \geq 2\sigma(I)$]	$R_1 = 0.0242$, $wR_2 = 0.0611$
Final R indexes [all data]	$R_1 = 0.0250$, $wR_2 = 0.0617$
Largest diff. peak/hole / e Å ⁻³	0.13/-0.19
Flack parameter	-0.01(3)

7. Experimental section

Table 21. Fractional Atomic Coordinates ($\times 10^4$) and Equivalent Isotropic Displacement Parameters ($\text{\AA}^2 \times 10^3$). U_{eq} is defined as 1/3 of the trace of the orthogonalised U_{ij} tensor.

Atom	x	y	z	U(eq)
O1	4817.4(11)	5646.1(6)	6418.0(4)	18.9(2)
O2	2481.0(11)	5139.6(6)	6299.6(4)	21.4(2)
O3	-2378.9(11)	3753.6(7)	6275.7(4)	24.3(2)
O4	219.9(12)	4364.4(7)	5250.1(4)	23.4(2)
O5	1310.0(11)	5693.4(7)	5148.4(4)	22.0(2)
N1	4439.8(13)	4248.7(8)	6169.6(5)	17.2(2)
N2	2093.9(14)	2835.0(8)	7361.1(5)	22.8(3)
N3	876.9(13)	2817.9(8)	7089.7(4)	20.0(2)
N4	1225.3(12)	3049.8(7)	6593.3(4)	14.8(2)
N5	-427.6(13)	4595.5(7)	6518.3(4)	15.5(2)
N6	86.4(14)	7533.1(8)	6213.0(5)	21.6(2)
N7	-196.3(14)	7124.8(8)	5774.0(5)	21.0(2)
N8	-697.2(13)	6306.3(8)	5895.3(4)	17.1(2)
C1	4323.8(16)	6552.8(9)	6566.2(6)	19.2(3)
C2	3397.9(17)	6509.7(10)	7059.1(6)	25.6(3)
C3	3540.6(16)	6983.9(10)	6108.7(6)	23.2(3)
C4	5763.4(17)	7023.4(10)	6679.1(6)	25.0(3)
C5	3812.8(15)	5028.5(9)	6299.5(5)	16.8(3)
C6	3481.3(14)	3495.3(9)	6060.0(5)	15.6(3)
C7	4367.2(16)	2726.7(9)	5823.0(5)	19.0(3)
C8	5113.5(19)	3008.0(11)	5315.8(6)	28.6(3)
C9	3358.6(17)	1935.1(10)	5727.8(6)	25.6(3)
C10	2685.0(15)	3221.1(8)	6549.1(5)	15.7(3)
C11	3215.7(16)	3077.9(10)	7042.4(5)	20.6(3)
C12	26.5(14)	3095.4(8)	6210.9(5)	16.2(3)
C13	-758.3(16)	2210.4(9)	6168.2(6)	23.6(3)
C14	-1051.7(15)	3849.4(9)	6346.1(5)	16.3(3)
C15	-1261.2(15)	5367.7(9)	6693.8(5)	16.1(3)
C16	-1125.7(16)	5481.1(9)	7288.0(5)	20.0(3)
C17	-1667.4(18)	4700.5(11)	7614.3(6)	25.3(3)
C18	-1381(2)	4887.4(14)	8190.4(6)	39.3(4)
C19	-3289(2)	4506.4(14)	7529.2(7)	38.8(4)
C20	-727.1(15)	6188.5(9)	6422.1(5)	16.1(3)
C21	-226.9(15)	6979.9(9)	6615.9(6)	19.4(3)
C22	-1111.1(16)	5686.3(9)	5481.3(5)	18.7(3)
C23	-1864.8(17)	6168.7(10)	5021.4(5)	23.5(3)
C24	-2211(2)	5511.8(12)	4585.7(6)	34.8(4)
C25	-3265.4(19)	6625.3(12)	5206.7(6)	30.7(4)
C26	216.7(16)	5161.9(9)	5289.4(5)	18.8(3)
C27	2588.9(16)	5265.6(10)	4911.5(6)	24.3(3)
C28	2378.2(15)	5190.1(10)	4332.2(6)	20.7(3)
C29	1709.0(18)	4454.8(10)	4108.9(6)	25.2(3)
C30	1476.0(19)	4420.5(11)	3574.3(6)	29.1(3)
C31	1918.5(18)	5116.9(11)	3260.1(6)	27.9(3)
C32	2603(2)	5845.5(10)	3478.6(6)	29.7(3)
C33	2829.6(18)	5880.9(10)	4013.5(6)	26.9(3)

8. References

- 1 I. Wagner, H. Musso, *Angew. Chem. Int. Ed.*, **1983**, *22*, 816-828.
- 2 V. R. Young, *J. Nutr.*, **1994**, *124(8)*, 1517-1523.
- 3 O. A. C. Petroff, *The Neuroscientist*, **2002**, *8(6)*, 562-573.
- 4 M. V. Rodnina, M. Beringer, W. Wintermeyer, *Trends Biochem. Sci.*, **2007**, *32(1)*, 20-26.
- 5 C. B. Anfinsen, *Biochem J.*, **1972**, *128(4)*, 737-749.
- 6 F. U. Hartl, M. Hayer-Hartl, *Science*, **2002**, *295*, 1852-1858.
- 7 J. M. Berg, J. L. Tymoczko, L. Stryer, *Biochemie*, 7th ed.; Springer: Berlin Heidelberg, 2013.
- 8 L. Pauling, R. B. Corey, *Proc. Natl. Acad. Sci.*, **1951**, *37*, 205-211.
- 9 L. Pauling, R. B. Corey, *Proc. Natl. Acad. Sci.*, **1951**, *37*, 251-256.
- 10 E. J. Milner-White, R. Poet, *Trends Biochem. Sci.*, **1987**, *12*, 189-192.
- 11 K. S. Rotondi, L. M. Gierasch, *Biopolymers*, **2006**, *84(1)*, 13-22.
- 12 M. B. Pepys, *Annu. Rev. Med.*, **2006**, *57*, 223-241.
- 13 N. Sewald, H. -D. Jakubke, *Peptides: Chemistry and Biology*, Wiley: Weinheim, 2002.
- 14 G. N. Ramachandran, C. Ramakrishnan, V. Sasisekharan, *J. Mol. Biol.*, **1963**, 95-99.
- 15 P. J. B. Pereira, A. Bergner, S. Macedo-Ribeiro, R. Huber, G. Matschiner, H. Fritz, C. P. Sommerhoff, W. Bode, *Nature*, **1998**, *392*, 306-310.
- 16 I. C. Sheehan, G. P. Hess, *J. Am. Chem. Soc.*, **1955**, *77*, 1067.
- 17 W. König, R. Geiger, *Chem. Ber.*, **1970**, *103*, 788-798.
- 18 L. A. Carpino, *J. Am. Chem. Soc.*, **1993**, *115*, 4397-4398.
- 19 R. Subirós-Funosas, R. Prohens, R. Barbas, A. El-Faham, F. Albericio, *Chem. Eur. J.*, **2009**, *15*, 9394-9403.
- 20 S.-Y. Han, Y.-A. Kim, *Tetrahedron*, **2004**, *60*, 2447-2467.
- 21 R. B. Merrifield, *J. Am. Chem. Soc.*, **1963**, *85(14)*, 2149.
- 22 B. Marglin, R. B. Merrifield, *J. Am. Chem. Soc.*, **1966**, *88(21)*, 5051-5052.
- 23 R. Behrendt, P. White, J. Offer, *J. Pept. Sci.*, **2016**, *22*, 4-27.
- 24 Y. García-Ramos, M. Paradís-Bas, J. Tulla-Puche, F. Albericio, *J. Pept. Sci.*, **2010**, *16*, 675.
- 25 Y. E. Jad, G. A. Acosta, S. N. Khattab, B. G. de la Torre, T. Govender, H. G. Kruger, A. El-Faham, F. Albericio, *Org. Biomol. Chem.*, **2015**, *13*, 2393-2398.
- 26 R. De Marco, A. Tolomelli, A. Greco, L. Gentilucci, *ACS Sustainable Chem. Eng.*, **2013**, *1*, 566-569.
- 27 J. Gante, *Angew. Chem.*, **1994**, *106*, 1780-1802.
- 28 A. Giannis, T. Kolter, *Angew. Chem.*, **1993**, *105*, 1303-1326.
- 29 I. Avan, D. Hall, A. R. Katritzky, *Chem. Soc. Rev.*, **2014**, *43*, 3575
- 30 I. E. Valverde, T. L. Mindt, *Chimia*, **2013**, *67(4)*, 262-266.
- 31 D. J. Pedersen, A. Abell, *Eur. J. Org. Chem.*, **2011**, 2399-2411.
- 32 R. Huisgen, *Angew. Chem.*, **1963**, *13*, 604-637.
- 33 C. W. Tornoe, C. Christensen, M. Meldal, *J. Org. Chem.*, **2002**, *67*, 3057-3064.
- 34 V. V. Rostovtsev; L. G. Green; V. V. Fokin; K. B. Sharpless, *Angew. Chem. Int. Ed.*, **2002**, *41*, 2596-2599.
- 35 M. Meldal, C. W. Tornoe, *Chem. Rev.*, **2008**, *108*, 2952-3015
- 36 H. C. Kolb, K. B. Sharpless, *Drug Discov Today*, **2003**, *8*, 1128-1137
- 37 L. Zhang, X. Chen, P. Xue, H. H. Y. Sun, I. D. Williams, K. B. Sharpless, V. V. Fokin, G. Jia, *J. Am. Chem. Soc.*, **2005**, *127*, 15998-15999.

8. References

- 38 B. C. Boren, S. Narayan, L. K. Rasmussen, L. Zhang, H. Zhao, Z. Lin, G. Jia, V. V. Fokin, *J. Am. Chem. Soc.*, **2008**, *130*, 8923-8930.
- 39 W. G. Kim, M. E. Kang, J. B. Lee, M. H. Jeon, S. Lee, J. Lee, B. Choi, P. M. S. D. Cal, S. Kang, J.-M. Kee, G. J. L. Bernardes, J.-U. Rohde, W. Choe, S. You Hong, *J. Am. Chem. Soc.*, **2017**, *139*, 12121-12124.
- 40 S. Dey, D. Datta, T. Pathak, *Synlett*, **2011**, *17*, 2521-2524.
- 41 A. El-Awa, M. N. Noshi, X. M. du Jourdin, P. L. Fuchs, *Chem. Rev.*, **2009**, *109*, 2315.
- 42 J. M. Baskin, J. A. Prescher, S. T. Laughlin, N. J. Agard, P. V. Chang, I. A. Miller, A. Lo, J. A. Codelli, C. R. Bertozzi, *PNAS*, **2007**, *43*, 16793-16797.
- 43 A. Massarotti, S. Aprile, V. Mercalli, E. Del Grosso, G. Grosa, G. Sorba, G. C. Tron, *Chem. Med. Chem.*, **2014**, *9(11)*, 2497-2508.
- 44 M. Nahrwold, T. Bogner, S. Eissler, S. Verma, N. Sewald, *Org. Lett.*, **2010**, *12(5)*, 1064-1067.
- 45 A. Tam, U. Arnold, M. B. Soellner, R. T. Raines, *J. Am. Chem. Soc.*, **2007**, *129*, 12670-12671.
- 46 S. I. Lee, S. Y. Park, L. H. Park, I. G. Jung, S. Y. Choi, Y. K. Chung, *J. Org. Chem.*, **2006**, *71*, 91-96.
- 47 M. Wünsch, J. Senger, P. Schultheisz, S. Schwarzbich, K. Schmidtkunz, C. Michalek, M. Klab, S. Goskowitz, P. Borchert, L. Praetorius, W. Sippl, M. Jung, N. Sewald, *Chem. Med. Chem.*, **2017**, *12(24)*, 2044-2053.
- 48 G. Reginato, A. Mordini, F. Messina, A. Degl'Innocenti, G. Poli, *Tetrahedron*, **1996**, *52(33)*, 10985-10996.
- 49 L. Ye, W. He, L. Zhang, *Angew. Chem. Int. Ed.*, **2001**, *50(14)*, 3236-3239.
- 50 D. Habrant, V. Rauhala, A. M. P. Koskinen, *Chem. Soc. Rev.*, **2010**, *39*, 2007-2017.
- 51 E. Ko, J. Liu, L. M. Perez, G. Lu, A. Schaefer, K. Burgess, *J. Am. Chem. Soc.*, **2011**, *133(3)*, 462-477.
- 52 H. D. Dickson, S. C. Smith, K. W. Hinkle, *Tetrahedron Lett.* **2004**, *45*, 5597-5599.
- 53 A. J. Mancuso, S.-L. Huang, D. Swern, *J. Org. Chem.*, **1978**, *43(12)*, 2480-2482.
- 54 J. Jurczak, A. Golebiowski, *Chem. Rev.* **1989**, *89*, 149-164
- 55 K. E. Rittle, C. F. Homnick, G. S. Ponticello, B. E. Evans, *J. Org. Chem.*, **1982**, *47*, 3016-3018
- 56 J. A. Ellman, *Pure and Applied chemistry*, **2003**, *75*, 39-46.
- 57 M. Wakayama, J. A. Ellman, *J. Org. Chem.*, **2009**, *74*, 2646-2650.
- 58 M. T. Robak, M. A. Herbage, J. A. Ellman, *Chem. Rev.*, **2010**, *110*, 3600-3740.
- 59 B. C. Chen, B. Wang, G. Q. Lin, *J. Org. Chem.*, **2010**, *75*, 941-944.
- 60 A. W. Patterson, J. A. Ellman, *J. Org. Chem.*, **2006**, *71*, 7110-7112
- 61 H. Xiao, Y. Huang, F. L. Qing, *Tetrahedron: Assymetry*, **2010**, *21*, 2949-2955
- 62 M. Wünsch, D. Schröder, T. Fröhr, L. Teichmann, S. Hedwig, N. Janson, C. Belu, J. Simon, S. Heidemeyer, P. Holtkamp, J. Rudlof, L. Klemme, A. Hinzmann, B. Neumann, H.-G. Stammer, N. Sewald, *Beilstein J. Org. Chem.* **2017**, *13*, 2428-2441.
- 63 A. Carpita, L. Mannocci, R. Rossi, *Eur. J. Org. Chem.*, **2005**, 1859-1864
- 64 P. B. Alper, S. C. Hung, C. H. Wong, *Tetrahedron Lett.*, **1996**, *37*, 6029-6032.
- 65 J. T. Lundquist, J. C. Pelletier, *Org. Lett.*, **2001**, 781-783
- 66 P. T., Nyffeler, C.-H. Liang, K. M., Koeller, C.-H., Wong, *J. Am. Chem. Soc.*, **2002**, *124*, 10773.
- 67 A. K. Pandiakumar, S. P. Sarma, A. G. Samuelson, *Tetrahedron Lett.*, **2014**, *55*, 2917-2920.
- 68 R. B. Yan, F. Yang, Y. Wu, L. H. Zhang, X. S. Ye, *Tetrahedron Lett.*, **2005**, *46*, 8993-8995.
- 69 E. D. Goddard-Borger, R. V. Stick, *Org. Lett.*, **2007**, *9*, 3797-3800.
- 70 E. D. Goddard-Borger, R. V. Stick, *Org. Lett.*, **2011**, *13*, 2514-2514.
- 71 G. T. Potter, G. C. Jayson, G. J. Miller, J. M. Gardiner, *J. Org. Chem.*, **2016**, *81*, 3443-3446.

- 72 N. Fischer, E. D. Goddard-Borger, R. Greiner, T. M. Klapötke, B. W. Skelton, J. Stierstorfer, *J. Org. Chem.*, **2012**, *77*, 1760-1764.
- 73 S. H. Gellman, *Acc. Chem. Res.*, **1998**, *31*, 173-180.
- 74 J. W. Checco, S. H. Gellman, *Curr. Opin. Struct. Biol.*, **2016**, *39*, 96-105.
- 75 P. Tosovská, P. S. Arora, *Org. Lett.*, **2010**, *12(7)*, 1588-1591.
- 76 B. B. Lao, I. Grishagin, H. Mesallati, T. F. Brewer, B. Z. Olenyuk, P. S. Arora, *PNAS*, **2014**, *111(21)*, 7531-7536.
- 77 A. B. Smith III, T. P. Keenan, R. C. Holcomb, P. A. Sprengeler, M. C. Guzman, J. L. Wood, P. J. Carroll, R. Hirschmann, *J. Am. Chem. Soc.*, **1992**, *114(26)*, 10672-10674.
- 78 N. G. Angelo, P. S. Arora, *J. Am. Chem. Soc.*, **2005**, *127*, 17134-17135.
- 79 N. G. Angelo, P. S. Arora, *J. Org. Chem.*, **2007**, *72*, 7963-7967.
- 80 A. L. Jochim, S. E. Miller, N. G. Angelo, P. S. Arora, *Bioorg. Med. Chem. Lett.*, **2009**, *19*, 6023-6026.
- 81 R. Bone, J. P. Vacca, P. S. Anderson, M. K. Holloway, *J. Am. Chem. Soc.*, **1991**, *113*, 9384-9385.
- 82 I.W. Hamley, *Chem. Rev.*, **2012**, *112*, 5147-5192.
- 83 D. J., Selkoe, *Physiol. Rev.*, **2001**, *81*, 741.
- 84 A. E. Roher, K. C. Palmer, E. C. Yurewicz, M. J. Ball, B. D. Greenberg, *Neurochem.*, **1993**, *61*, 1916.
- 85 M. P. Murphy, H. LeVine III, *J. Alzheimers Dis.*, **2010**, *19(1)*, 311-323.
- 86 C. Priller, T. Bauer, G. Mitteregger, B. Krebs, H. A. Kretschmar, J. Herms, *J. Neurosci.*, **2006**, *26(27)*, 7212-7221.
- 87 K.-H. Sun, G.-H. Sun, Y. Su, C.-I. Chang, M.-J. Chuang, W.-L. Wu, C.-Y. Chu, S.-J. Tang, *Apoptosis*, **2004**, *9*, 833-841.
- 88 S. J. C. Lee, E. Nam, H. J. Lee, M. G. Savelieff, M. H. Lim, *Chem. Soc. Rev.*, **2017**, *46*, 310-323.
- 89 L. O. Tjernberg, J. Näslund, F. Lindqvist, J. Johansson, A. R. Karlström, J. Thyberg, L. Terenius, C. Nordstedt, *J. Biol. Chem.*, **1996**, *271*, 8545-8548.
- 90 A. Hawe, M. Sutter, W. Jiskoot, *Pharm. Res.*, **2008**, *25(7)*, 1487-1499.
- 91 M.R.H. Krebs, E.H.C. Bromley, A.M. Donald, *J. Struct. Biol.*, **2005**, *149*, 30-37.
- 92 N. W. Smith, A. Alonso, C. M. Brown, S. V. Dzyuba, *Biochem. and Biophys. Res. Comm.*, **2010**, *391*, 1455-1458.
- 93 A. Hawe, M. Sutter, W. Jiskoot, *Pharm. Res.*, **2008**, *25*, 1487-1499.
- 94 R. O. Hynes, *Cell*, **2002**, *110*, 673-687
- 95 F. G. Giancotti, E. Ruoslahti, *Science*, **1999**, *285*, 1028-1033.
- 96 C. Mas-Moruno, F. Rechenmacher, H. Kessler, *Anti-Cancer Agents in Medicinal Chemistry*, **2010**, *10*, 753-768.
- 97 M. Barczyk, S. Carracedo, D. Gullberg, *Cell Tissue Res.*, **2010**, *339*, 269-280.
- 98 J. D. Humphries, A. Byron, M. J. Humphries, *J. Cell Sci.*, **2006**, *119*, 3901-3903.
- 99 I. D. Campbell, M. J. Humphries, *Cold Spring Harb Perspect Biol.*, **2011**, 1-14.
- 100 M. A. Arnaout, S. Goodman, J.-P. Xiong, *Curr. Opin. Cell. Biol.*, **2007**, *19(5)*, 495-507.
- 101 C. Mas-Moruno, F. Rechenmacher, H. Kessler, *Anti-Cancer Agents in Medicinal Chemistry*, **2010**, *10(10)*, 753-768.
- 102 A. R. Reynolds, I. R. Hart, A. R. Watson, J. C. Welti, R. G. Silva, S. D. Robinson, G. Da Violante, M. Gourlaouen, M. Salih, M. C. Jones, D. T. Jones, G. Saunders, V. Kostourou, F. Perron-Sierra, J. C. Norman, G. C. Tucker, K. M. Hodivala-Dilke, *Nature*

8. References

- Medicine*, **2009**, *15*(4), 392-400.
- 103 R. Stupp, M. E Hegi, T. Gorlia, S. C. Erridge, J. Perry, Y.-K. Hong, K. D. Aldape, B. Lhermitte, T. Pietsch, D. Grujicic, J. P. Steinbach, W. Wick, R. Tarnawski, D.-H. Nam, P. Hau, A. Weyerbrock, M. J. B. Taphoorn, C.-C. Shen, N. Rao, L. Thurzo, U. Herrlinger, T. Gupta, R.-D. Kortmann, K. Adamska, C. McBain, A. A. Brandes, J. C. Tonn, O. Schnell, T. Wiegel, C.-Y. Kim, L. B. Nabors, D. A. Reardon, M. J. van den Bent, C. Hicking, A. Markivskyy, M. Picard, M. Weller, *The Lancet Oncology*, **2014**, *15*(10), 1100-1108.
- 104 Dissertation, Tanja Fröhr, 2015, University of Bielefeld.
- 105 Masterthesis, Oliver Kracker, 2013, University of Bielefeld.
- 106 J. R. Johansson, E. Hermansson, B. Nordén, N. Kann, T. Beke-Somfai, *Eur. J. Org. Chem.*, **2014**, 2703–2713.
- 107 O. Kracker, J. Góra, J. Krzciuk-Gula, A. Marion, B. Neumann, H.-G. Stammer, A. Nieß, I. Antes, R. Latajka, N. Sewald, *Chem. Eur. J.*, **2018**, *24*, 953-961.
- 108 G. Liu, D. A. Cogan, J. A. Ellman, *J. Am. Chem. Soc.*, **1997**, *119*, 9913-9914.
- 109 G. Liu, D. A. Cogan, T. D. Owens, T. P. Tang, J. A. Ellman, *J. Org. Chem.*, **1999**, *64*, 1278-1284.
- 110 V. R. Arava, L. Gorentla, P. K. Dubey, *Beilstein J. Org. Chem.*, **2011**, *7*, 9-12.
- 111 Y. Basel, A. Hassner, *Synthesis*, **2001**, *4*, 550-552.
- 112 L. A. Carpino, A. El-Faham, *Tetrahedron*, **1999**, *55*, 6813-6830.
- 113 W. S. Horne, C. D. Stout, M. R. Ghadri, *J. Am. Chem. Soc.*, **2003**, *125*, 9372-9376.
- 114 A. Proteau-Gagné, K. Rochon, Mélissa Roy, P.-J. Albert, B. Guérin, L. Gendron, Y. L. Dory, *Bioorg. Med. Chem. Lett.*, **2013**, *23*, 5267-5269.
- 115 A. El-Faham, F. Albericio, *J. Pept. Sci.*, **2010**, *16*(1), 6-9.
- 116 M. A. Fara, J. J. Díaz-Mochón, M. Bradley, *Tetrahedron Letters*, **2006**, *47*, 1011-1014.
- 117 A. Marion, J. Góra, O. Kracker, T. Fröhr, R. Latajka, N. Sewald, I. Antes, *J. Chem. Inf. Model.*, **2018**, *58*(1), 90-110.
- 118 K.-C. Chou, *Analytical Biochemistry*, **2000**, *286*, 1-16.
- 119 S. Müller, B. Liepold, G. J. Roth, H. J. Bestmann, *Synlett*, **1996**, 521-522.
- 120 G. J. Roth, B. Liepold, S. G. Müller, H. J. Bestmann, *Synthesis*, **2004**, 59-62.
- 121 T. H. Jepsen, J. L. Kristensen, *J. Org. Chem.*, **2014**, *79*, 9423-9426.
- 122 W. Doherty, N. Adler, A. Knox, D. Nolan, J. McGouran, A. P. Nikalje, D. Lokwani, A. Sarkate, P. Evans, *Eur. J. Org. Chem.*, **2017**, 175-185
- 123 K. E. Rittle, C. F. Homnick, G. S. Ponticello, B. E. Evans, *J. Org. Chem.*, **1982**, *47*, 3016-3018
- 124 M. T. Reetz, M. W. Drewes, A. Schmitz, *Angew. Chem. Int. Ed.*, **1987**, 1141-1143
- 125 M. T. Reetz, D. Röhrig, *Angew. Chem. Int. Ed.*, **1989**, 1706-1709
- 126 J. F. Dellaria, Jr., R. G. Maki, *Tetrahedron Lett.*, **1986**, 2337-2340
- 127 J. F. Dellaria, Jr., R. G. Maki, H. H. Stein, J. Cohen, D. Whittern, K. Marsh, D. J. Hoffman, J. Plattner, T. J. Perun, *J. Med. Chem.*, **1990**, *33*, 534-542 reference 11b
- 128 M. J. McKennon, A. I. Meyers, *J. Org. Chem.*, **1993**, *58*, 3568-3571
- 129 J. S. Baum, D. A. Shook, H. M. L. Davies, H. D. Smith, *Synthetic Communications*, **1987**, *17*(14), 1709-1716.
- 130 J. Pietruszka, A. Witt, *Synthesis*, **2006**, *24*, 4266-4268.
- 131 H. Lv, J. Shi, B. Wu, Y. Guo, J. Huang, W. Yi, *Org. Biomol. Chem.*, **2017**, *15*, 8054-8058.
- 132 Y. Zhou, Y. Zhang, J. Wang, *Org. Biomol. Chem.*, **2016**, *14*, 10444–10453.
- 133 S.-H. Hwang, M. A. Blaskovich, H.-O. Kim, *The Open Organic Chemistry Journal*, **2008**, *2*, 107-109.

- 134 J. E. Sheppeck II, H. Kar, H. Hong, *Tetrahedron Lett.*, **2000**, *41*, 5329-5333.
- 135 S. V. Jadhav, A. Bandyopadhyay, S. N. Benke, S. M. Mali, H. N. Gopi, *Org. Biomol. Chem.*, **2011**, *9*, 4182-4187.
- 136 E. J. Karppanen, A. M. P. Koskinen, *Molecules*, **2010**, *15*, 6512-6547.
- 137 T. Arai, T. Araya, D. Sasaki, A. Taniguchi, T. Sato, Y. Sohma, M. Kanai, *Angew. Chem. Int. Ed.*, **2014**, *53*, 8236-8239.
- 138 L. A. Carpino, G. Y. Han, *J. Am. Chem. Soc.*, **1970**, *92*, 5748-5749.
- 139 E. Atherton, C. Bury, R. C. Sheppard, B. J. Williams, *Tetrahedron Lett.*, **1979**, *20*, 3041-3042.
- 140 T. Maegawa, Y. Fujiwara, T. Ikawa, H. Hisashi, Y. Monguchi, H. Sajiki, *Amino Acids*, **2009**, *36*, 493-499.
- 141 P. K. Mandal, J. S. McMurray, *J. Org. Chem.*, **2007**, *72*, 6599-6601.
- 142 N. Kokkoni, K. Stott, H. Amijee, J. M. Mason, A. J. Doig, *Biochemistry*, **2006**, *45*, 9906-9918.
- 143 H. Amijee, C. Bate, A. Williams, J. Virdee, R. Jeggo, D. Spanswick, D. I. C. Scopes, J. M. Treherne, S. Mazzitelli, R. Chawner, C. E. Eyers, A. J. Doig, *Biochemistry*, **2012**, *51*, 8338-8352.
- 144 N. N. Chipanina, L. V. Sherstyannikova, I. V. Sterkhova, T. N. Aksamentova, V. K. Turchaninov, B. A. Shainyan, *Russian Journal of General Chemistry*, **2005**, *75(6)*, 876-882.
- 145 J. Chatterjee, B. Laufer, H. Kessler, *Nature Protocols*, **2012**, *7(3)*, 432-444.
- 146 S. Pellegrino, N. Tonali, E. Erba, J. Kaffy, M. Taverna, A. Contini, M. Taylor, D. Allsop, M. L. Gelmia, S. Ongeri, *Chem. Sci.*, **2017**, *8*, 1295-1302.
- 147 C. Soto, E. M. Sigurdsson, L. Morelli, R. A. Kumar, E. N. Castano, B. Frangione, *Nature Med.*, **1998**, *4(7)*, 822-826.
- 148 C. Adessi, C. Soto, *Drug Dev. Res.*, **2002**, *56*, 184-293.
- 149 U. K. Marelli, A. O. Frank, B. Wahl, V. La Pietra, E. Novellino, L. Marinelli, E. Herdtweck, M. Groll, H. Kessler, *Chem. Eur. J.*, **2014**, *20*, 14201-14206.
- 150 M. A. Dechantsreiter, E. Planker, B. Matha, Eb Lohof, G. Hölzemann, A. Jonczyk, S. L. Goodman, H. Kessler, *J. Med. Chem.*, **1999**, *42*, 3033-3040.
- 151 K. Barlos, D. Gatos, J. Kallitsis, G. Papaphotiu, P. Sotiriou, Y. Wenqing, W. Schäfer, *Tetrahedron Lett.*, **1989**, *30(30)*, 3943-3946.
- 152 P. E. Schneggenburger, B. Worbs, U. Diederichsen, *J. Pept. Sci.*, **2010**, *16*, 10-14.
- 153 J. Conradi, S. Huber, K. Gaus, F. Mertink, S. R. Gracia, U. Strijowski, S. Backert, N. Sewald, *Amino Acids*, **2012**, *43*, 219-232.
- 154 T. G. Kapp, F. Rechenmacher, S. Neubauer, O. V. Maltsev, E. A. Cavalcanti-Adam, R. Zarka, U. Reuning, J. Notni, H.-J. Wester, C. Mas-Moruno, J. Spatz, B. Geiger, H. Kessler, *Scientific Reports*, **2017**, *7*, 39805
- 155 H. E. Gottlieb, V. Kotlyar, A. Nudelman, *J. Org. Chem.*, **1997**, *62*, 7512-7515.
- 156 O. V. Dolomanov, L. J. Bourhis, R. J. Gildea, J. A. K. Howard and H. Puschmann, *J. Appl. Cryst.*, **2009**, *42*, 339-341.
- 157 G.M. Sheldrick, *Acta Cryst.*, **2008**, *A64*, 112-122.
- 158 Case, D. A.; Cerutti, D. S.; Cheatham III, T. E.; Darden, T. A.; Duke, R. E.; Giese, T. J.; Gohlke, H.; Goetz, A. W.; Greene, D.; Homeyer, N.; Izadi, S.; Kovalenko, A.; Lee, T. S.; LeGrand, S.; Li, P.; Lin, C.; Liu, J.; Luchko, T.; Luo, R.; Mermelstein, D.; Merz, K. M.; Monard, G.; Nguyen, H.; Omelyan, I.; Onufriev, A.; Pan, F.; Qi, R.; Roe, D. R.; Roitberg, A.; Sagui, C.; Simmerling, C. L.; Botello-Smith, W. M.; Swails, J.; Walker, R. C.; Wang, J.; Wolf, R. M.; Wu, X.; Xiao, L.; York D. M.; Kollman P.A. (2017), AMBER 2016, University of California, San Francisco.

8. References

- 159 Ämmälähti, E.; Bardet, M.; Molko, D.; Cadet, J. *J. Magn. Res. A*, **1996**, *122*, 230–232.
- 160 Loncharich, R. J.; Brooks, B. R.; Pastor, R. W. *Biopolymers*, **1992**, *32*, 523–535.
- 161 Berendsen, H. J. C.; Postma, J. P. M.; van Gunsteren, W. F.; DiNola, A.; Haak, J. R. *J. Chem. Phys.* **1984**, *81*, 3684–3690.
- 162 Fox, T.; Kollman, P. A. *J. Phys. Chem. B*. **1998**, *102*, 8070–8079.
- 163 Horn, H. W.; Swope, W. C.; Pitera, J. W.; Madura, J. D.; Dick, T. J.; Hura, G. L.; Head-Gordon, T. *J. Chem. Phys.* **2004**, *120*, 9665–9678.
- 164 J. Kaffy, D. Brinet, J.-L. Soulier, I. Correia, N. Tonali, K. Fabiana Fera, Y. Iacone, A. R. F. Hoffmann, L. Khemtouriian, B. Crousse, M. Taylor, D. Allsop, M. Taverna, O. Lequin, S. Ongeri, *J. Med. Chem.*, **2016**, *59*, 2025-2040.
- 165 N. Tonali, **2018**, submitted.
- 166 A. O. Frank, E. Otto, C. Mas-Moruno, H. B. Schiller, L. Marinelli, S. Cosconati, A. Bochen, D. Vossmeier, G. Zahn, R. Stragies, E. Novellino, H. Kessler, *Angew. Chem. Int. Ed Engl.*, **2010**, *49*, 9278–9281.
- 167 T. G. Kapp, F. Rechenmacher, S. Neubauer, O. V. Maltsev, E. A. Cavalcanti-Adam, R. Zarka, U. Reuning, J. Notni, H.-J. Wester, C. Mas-Moruno, J. Spatz, B. Geiger, H. Kessler, *Sci. Rep.*, **2017**, *7*, 39805.
- 168 G. Liu, D. A. Cogan, T. D. Owens, T. P. Tang, J. A. Ellman, *J. Org. Chem.*, **1999**, *64*, 1278-1284.
- 169 Novabiochem. Catalog & peptide synthesis handbook. (1999).
- 170 E. T. Kaiser, L. Colescott, C. D. Bossinger, P. I. Cook., *Analytical Biochemistry*, **1970**, *34*(2), 595-598.
- 171 Z. Xu, J. C. DiCesare, P. W. Baures, *J. Comb. Chem.*, **2010**, *12* (2), 248–254.